



REFERENCE ONLY

UNIVERSITY OF LONDON THESIS

Degree PhD

Year 2005

Name of Author DUNCAN, A.J.

COPYRIGHT

This is a thesis accepted for a Higher Degree of the University of London. It is an unpublished typescript and the copyright is held by the author. All persons consulting the thesis must read and abide by the Copyright Declaration below.

COPYRIGHT DECLARATION

I recognise that the copyright of the above-described thesis rests with the author and that no quotation from it or information derived from it may be published without the prior written consent of the author.

LOANS

Theses may not be lent to individuals, but the Senate House Library may lend a copy to approved libraries within the United Kingdom, for consultation solely on the premises of those libraries. Application should be made to: Inter-Library Loans, Senate House Library, Senate House, Malet Street, London WC1E 7HU.

REPRODUCTION

University of London theses may not be reproduced without explicit written permission from the Senate House Library. Enquiries should be addressed to the Theses Section of the Library. Regulations concerning reproduction vary according to the date of acceptance of the thesis and are listed below as guidelines.

- A. Before 1962. Permission granted only upon the prior written consent of the author. (The Senate House Library will provide addresses where possible).
- B. 1962 - 1974. In many cases the author has agreed to permit copying upon completion of a Copyright Declaration.
- C. 1975 - 1988. Most theses may be copied upon completion of a Copyright Declaration.
- D. 1989 onwards. Most theses may be copied.

This thesis comes within category D.



This copy has been deposited in the Library of

UCL



This copy has been deposited in the Senate House Library, Senate House, Malet Street, London WC1E 7HU.

UBIQUINONE STATUS IN NEURONS AND ASTROCYTES:

**THE EFFECTS OF NITROSATIVE
STRESS, LOVASTATIN, AND ~~SHORT~~
~~INTERFERING RNA~~**

Andrew Johnston Duncan

**A thesis submitted as partial fulfillment for the degree of
Doctor of Philosophy in the Faculty of Science, at the
University of London**

April 2005

**Department of Molecular Neuroscience
Division of Neurochemistry
Institute of Neurology
University College London
Queen Square
London WC1N 3BG**

UMI Number: U592007

All rights reserved

INFORMATION TO ALL USERS

The quality of this reproduction is dependent upon the quality of the copy submitted.

In the unlikely event that the author did not send a complete manuscript and there are missing pages, these will be noted. Also, if material had to be removed, a note will indicate the deletion.



UMI U592007

Published by ProQuest LLC 2013. Copyright in the Dissertation held by the Author.
Microform Edition © ProQuest LLC.

All rights reserved. This work is protected against
unauthorized copying under Title 17, United States Code.



ProQuest LLC
789 East Eisenhower Parkway
P.O. Box 1346
Ann Arbor, MI 48106-1346

ABSTRACT

An HPLC method has been established for the determination of ubiquinone (CoQ₉ and CoQ₁₀) levels in biological samples. This necessitated the synthesis of a novel internal standard for CoQ₉ and CoQ₁₀ measurement in rodent tissue. Rat glial cell lines contained CoQ₉ as the predominant ubiquinone isoform; this was CoQ₁₀ in human tissue. Comparison with primary cultures of rat astrocytes showed that these human and rat glial cancer cell lines had relatively less CoQ₉₊₁₀ than primary glial cultures, possibly reflecting a lower dependence of transformed cells upon OXPHOS for ATP generation.

Lovastatin decreased CoQ₉ (but not CoQ₁₀) in primary astrocytes and glial cell lines. Moreover, glial cell lines displayed an approximately 10-fold higher sensitivity to lovastatin or its β -hydroxy acid isoform than primary rat astrocyte cultures.

Cellular CoQ₉ levels did not appear to be limiting for mitochondrial complex II+III activity, thus it is possible that CoQ₁₀ is more intimately involved in OXPHOS than CoQ₉.

Primary cultures of rat astrocytes and neurons contained approximately equal levels of CoQ₉. However CoQ₁₀ levels were significantly higher in neuronal cultures. In contrast to transformed cell lines, the neuron's reliance on mitochondrial OXPHOS to synthesise ATP may manifest as higher cellular availability of CoQ₁₀.

Activation of iNOS in rat primary astrocytes to generate nitric oxide (NO) for 24h did not alter CoQ₉ or CoQ₁₀ levels. Following 36h exposure, activation of iNOS significantly decreased CoQ₉ and CoQ₁₀. An NO-donor decreased astrocyte CoQ₉ and CoQ₁₀ after 24h exposure, while in neurons, both CoQ isoforms were maintained. Additionally 36h exposure of astrocytes to DETA-NO appeared to cause a recovery in the

amount of CoQ₉ and CoQ₁₀, possibly representing a protective effect in response to RNS exposure.

Additionally, preliminary data demonstrated that small interfering RNA (siRNA) may decrease CoQ₉ but not CoQ₁₀ in rat primary astrocytes although not HEK293T cells.

ACKNOWLEDGMENTS

I owe thanks to a number of individuals who have made the period of this work a lot more entertaining and a little less painful. My supervisors Dr. Simon Heales and Professor John Clark have guided, instructed, advised and questioned along the way; their quiet words and vibrant discussions have fostered an interest in mitochondria which would doubtless otherwise have been channeled into less worthy uses of my time.

Members of the Division of Neurochemistry past and present have given their expertise in a number of areas, and invaluable discussions have taken place in a variety of establishments and circumstances. While occasional losses of the powers of recall may have been frustrating for all concerned, their input cannot be underestimated.

I am also very grateful to Dr. Juan Bolaños and his research group at the Universidad de Salamanca, Spain for the opportunity to work in a centre of molecular biological expertise, and for their patience, training and input during and after the practical work of the siRNA study.

The technical excellence of members of the Neurometabolic Unit of the National Hospital, London has been of great help in a number of troubleshooting situations. Thanks are particularly due to Dr. John Land and Dr. Iain Hargreaves for gainful employment in a technical capacity while writing up.

The longsuffering patience, not to mention deep pockets, of Amanda Lam cannot pass without mention. Thank you.

Finally, I owe an immeasurable debt of gratitude to my parents, for their unwavering support in all of my occasionally errant decisions.

I am grateful to the Brain Research Trust for their generous funding to support this project.

CONTENTS

ABSTRACT	2
ACKNOWLEDGEMENTS.....	4
CONTENTS.....	5
LIST OF TABLES AND FIGURES	12
ABBREVIATIONS	17
 1. INTRODUCTION.....	 22
1.1 <i>An introduction to mitochondria</i>	23
1.1.1 Complex I.....	27
1.1.2 Complex II	30
1.1.3 Complex III	31
1.1.4 Complex IV	34
1.1.5 ATP Synthase.....	35
1.2 <i>Other mitochondrial metabolic processes</i>	37
1.2.1 The Krebs cycle.....	37
1.2.2 β -oxidation of fatty acids	42
1.2.3 Ketone body metabolism.....	46
1.2.4 The urea cycle	48
1.2.5 Regulation of the life/death cycle	49
1.3 <i>Oxidative and Nitrosative stress</i>.....	52
1.3.1 ROS and free radicals.....	52
1.3.2 Mitochondrial free radical generation.....	53
1.3.3 Physiological NO generation	54
1.4 <i>Introduction to ubiquinone</i>.....	56
1.4.1 Historical background and nomenclature.....	56
1.4.2 Structure and biosynthesis	57
1.5 <i>Functions of ubiquinone</i>.....	59
1.5.1 CoQ as an antioxidant	60
1.5.2 Electron transfer	61
1.5.3 CoQ as an uncoupling protein co-factor	64
1.6 <i>Human ubiquinone deficiency</i>	65
1.7 <i>Mitochondrial targets in neurological disease</i>	70
1.8 <i>Ubiquinone and neurodegeneration</i>.....	74
1.9 <i>Lovastatin and disruption of CoQ metabolism</i>	76
1.9.1 General pharmacology	76
1.9.2 Statin drugs and neurological disease	78
1.10 <i>Statement of Aims</i>	79
 2. MATERIALS AND METHODS	 80
2.1 <i>Chemicals and Materials</i>	81

2.2 Tissue culture	83
2.2.1 Media and solutions	83
2.2.2 Animals	84
2.2.3 Preparation of astrocyte cultures	84
2.2.4 Preparation of neuron cultures	87
2.2.5 Preparation of cell line cultures	87
2.2.5.1 1321N1 Human astrocytoma cultures	89
2.2.5.2 Rat C6 glioma cultures	89
2.2.6 Cell treatments	90
2.2.6.1 Serum withdrawal	90
2.2.6.2 Cytokine + bacterial lipopolysaccharide treatment	91
2.2.6.3 Lovastatin treatment	91
2.2.6.4 NO donor treatment	93
2.2.6.5 Combination of treatments	93
2.3 Spectrophotometric enzyme analysis	93
2.3.1 NADH:ubiquinone oxidoreductase (Complex I; EC. 1.6.5.3)	93
2.3.2 Succinate dehydrogenase:cytochrome <i>c</i> reductase (Complex II+III; EC. 1.3.5.1 + 1.10.2.2)	94
2.3.3 Cytochrome <i>c</i> oxidase (Complex IV; EC. 1.9.3.1)	95
2.3.3.1 Preparation of reduced cytochrome <i>c</i>	96
2.3.3.2 Measurement of complex IV activity	96
2.3.4 Measurement of citrate synthase activity	97
2.4 Measurement of nitrate and nitrite	98
2.5 Lactate dehydrogenase measurement	100
2.6 Determination of total cellular cholesterol	101
2.7 Determination of protein concentration	104
2.8 Light micrography of cultures	104
2.9 Statistical analysis	104

3. DEVELOPMENT OF AN HPLC METHOD FOR THE DETERMINATION OF CoQ IN BIOLOGICAL MATERIAL OF RODENT ORIGIN	107
3.1 Introduction	108
3.2 Methods	109
3.2.1 Tissue culture	109
3.2.2 Spectrophotometric measurement of ubiquinone standards	109
3.2.3 Reverse phase chromatography coupled to UV detection	109
3.2.4 Synthesis of an internal standard for ubiquinone determination by UV-HPLC	110
3.2.5 Sample preparation for ubiquinone determination by UV-HPLC	113
3.3 Experimental protocol	113
3.3.1 Chromatography and UV absorbance properties of CoQ	113
3.3.2 Validation of the internal standard	114
3.3.3 Determination of CoQ in rat astrocytes using the internal standard	114
3.4 Results	114
3.4.1 Chromatography and UV detection of ubiquinone	114

3.4.2	Development and characterisation of an internal standard	117
3.4.3	Ubiquinone levels in cultured astrocytes	117
3.5	Discussion	123
3.6	Conclusion	125
4.	CoQ₉ AND CoQ₁₀ STATUS OF RAT AND HUMAN BRAIN CELL LINE CULTURES; EFFECTS OF NO, LIPOPOLYSACCHARIDE + γ-INTERFERON & LOVASTATIN EXPOSURE	126
4.1	Introduction	127
4.2	Aims	128
4.3	Methods	128
4.3.1	Tissue culture	128
4.3.2	CoQ measurement by HPLC	128
4.3.3	NO _x determination in cell culture media	130
4.3.4	Protein determination	130
4.4	Experimental protocols	130
4.4.1	Exposure of human 1321N1 and rat C6 cells to lipopolysaccharide + γ -interferon	130
4.4.2	Exposure of rat C6 cells to DETA-NO	130
4.4.3	Exposure of human 1321N1 and rat C6 cells to lovastatin	131
4.4.4	Simultaneous exposure of human 1321N1 and rat C6 cells to lipopolysaccharide + γ -interferon and lovastatin	131
4.4.5	Simultaneous exposure of rat C6 cells to DETA-NO and lovastatin	131
4.4.6	Simultaneous exposure of rat C6 cells to DETA-NO and lipopolysaccharide + γ -interferon	132
4.5	Results	132
4.5.1	CoQ levels in human 1321N1 astrocytoma and rat C6 glioma cells	132
4.5.1.1	Human 1321N1 astrocytoma	132
4.5.1.2	Rat C6 glioma	132
4.5.2	The effect of lipopolysaccharide + γ -interferon on CoQ status of human 1321N1 astrocytoma and rat C6 glioma cells	132
4.5.2.1	Human 1321N1 astrocytoma	132
4.5.2.2	Rat C6 glioma	134
4.5.3	The effect of DETA-NO upon rat C6 glioma cells	134
4.5.4	The effect of lovastatin on human 1321N1 astrocytoma and rat C6 glioma cells	138
4.5.4.1	Human 1321N1 astrocytoma	138
4.5.4.2	Rat C6 glioma	138
4.5.5	The effect of simultaneous exposure of human 1321N1 astrocytoma and rat C6 cells to lipopolysaccharide + γ -interferon and Na-lovastatin	142
4.5.5.1	Human 1321N1 astrocytoma	142
4.5.5.2	Rat C6 glioma	142
4.5.6	The effect of simultaneous exposure of rat C6 cells to DETA-NO and Na-lovastatin	146

4.5.7 The effect of simultaneous exposure of rat C6 cells to lipopolysaccharide + γ -interferon + DETA-NO	146
4.6 Discussion	151
4.7 Conclusion	154
 5. CoQ₉ AND CoQ₁₀ LEVELS IN PRIMARY CULTURES OF RAT ASTROCYTES; EFFECTS OF SERUM WITHDRAWAL	155
5.1 Introduction	156
5.2 Aims	158
5.3 Methods	158
5.3.1 Tissue culture	158
5.3.2 CoQ measurement by HPLC	158
5.3.3 Cholesterol determination	158
5.3.4 Lactate dehydrogenase determination	159
5.3.5 Protein determination	159
5.4 Experimental protocol	159
5.4.1 Determination of CoQ content of Foetal Bovine Serum	159
5.4.2 Determination of cholesterol content of Foetal Bovine Serum	159
5.4.3 Serum withdrawal from astrocyte cultures	160
5.4.4 LDH activity of media from astrocyte cultures	160
5.5 Results	160
5.5.1 Determination of CoQ content of Foetal Bovine Serum	160
5.5.2 Determination of cholesterol content of Foetal Bovine Serum	161
5.5.3 CoQ levels in primary cultures of rat astrocytes	161
5.5.4 The effect of serum withdrawal on cellular CoQ levels	161
5.5.5 The effect of serum withdrawal on media lactate dehydrogenase levels	163
5.5.6 The effect of serum withdrawal on cellular cholesterol levels	163
5.6 Discussion	165
5.7 Conclusion	167
 6. THE EFFECTS OF LOVASTATIN UPON CoQ₉ AND CoQ₁₀ LEVELS IN PRIMARY CULTURES OF RAT ASTROCYTES	169
6.1 Introduction	170
6.2 Aims	172
6.3 Methods	172
6.3.1 Tissue culture	172
6.3.2 CoQ measurement by HPLC	172
6.3.3 ETC enzyme assays	172
6.3.4 Lactate dehydrogenase determination	173
6.3.5 Cholesterol determination	173
6.3.6 Protein determination	173
6.3.7 Astrocyte morphology	173
6.4 Experimental protocol	173
6.4.1 Exposure of astrocyte cultures to lovastatin	173
6.5 Results	174

6.5.1	The effect of lovastatin in the presence of serum	174
6.5.1.1	Ubiquinone and cholesterol status	174
6.5.1.2	Mitochondrial enzyme activity	176
6.5.1.3	LDH release and astrocyte morphology	179
6.5.2	The effect of Na-lovastatin exposure in the presence of serum	179
6.5.2.1	Ubiquinone and cholesterol status	179
6.5.2.2	Mitochondrial enzyme activity	182
6.5.2.3	LDH release	185
6.5.3	The effect of lovastatin exposure in the absence of serum	185
6.5.3.1	Ubiquinone and cholesterol status	185
6.5.3.2	Mitochondrial enzyme activity	187
6.5.3.3	LDH release	187
6.5.4	The effect of Na-lovastatin in the absence of serum	187
6.5.4.1	Ubiquinone and cholesterol status	187
6.5.4.2	Mitochondrial enzyme activity	190
6.5.4.3	LDH release	194
6.6	Discussion	194
6.7	Conclusion	198
7.	CoQ₉ AND CoQ₁₀ LEVELS IN PRIMARY CULTURES OF RAT ASTROCYTES AND NEURONS; EFFECTS OF EXPOSURE TO NITRIC OXIDE	200
7.1	Introduction	201
7.2	Aims	202
7.3	Methods	203
7.3.1	Tissue culture	203
7.3.1.1	Primary astrocyte cultures	203
7.3.1.2	Primary neuron cultures	203
7.3.2	CoQ measurement by HPLC	203
7.3.3	ETC enzyme assays	203
7.3.4	Lactate dehydrogenase determination	204
7.3.5	Measurement of NO _x in culture media	204
7.3.6	Protein determination	204
7.4	Experimental protocol	204
7.4.1	Exposure of astrocyte cultures to LPS + IFN γ	204
7.4.2	Exposure of astrocyte cultures to DETA-NO	205
7.4.3	CoQ status of neuronal cultures and exposure to DETA-NO	205
7.5	Results	205
7.5.1	CoQ status of astrocyte cultures following LPS + IFN γ exposure ...	205
7.5.2	CoQ status of astrocyte cultures following DETA-NO exposure	207
7.5.3	Mitochondrial ETC enzyme activities of astrocytes exposed to NO	210
7.5.4	The effect of LPS+IFN γ and DETA-NO on lactate dehydrogenase levels from primary astrocyte cultures	213
7.5.5	CoQ status of untreated astrocyte and neuron-enriched cultures	213

7.5.6	CoQ status of neuron-enriched cultures following exposure to DETA-NO	213
7.6	Discussion	215
7.7	Conclusion	219
8.	THE USE OF SHORT INTERFERING RNA TO ALTER UBIQUINONE BIOSYNTHESIS IN RAT AND HUMAN CELLS	220
8.1	Introduction	221
8.2	Aims	226
8.3	Methods	227
8.3.1	Tissue culture	227
8.3.2	Small interfering RNA oligonucleotide design	227
8.3.3	Ligation of oligonucleotides into pSuper.gfp/neo, and transformation in bacteria	235
8.3.3.1	Annealing of primers	235
8.3.3.2	Phosphorylation of primers	235
8.3.3.3	Linearisation of pSUPER.gfp/neo, and purification in agarose gel	236
8.3.3.4	Ligation of the primers into pSUPER.gfp/neo, transformation in bacteria and plasmid extraction	237
8.3.4	Transfection of cells with pSuper.gfp/neo and transprenyl transferase knockdown siRNA	240
8.3.5	Imaging of cell cultures for transfection efficiency	240
8.3.6	RNA extraction and isolation from cultures followed by spectrophotometric determination and agarose gel electrophoresis..	240
8.3.7	Reverse Transcription and Polymerase Chain Reaction	242
8.3.7.1	Reverse Transcription	242
8.3.7.2	The Polymerase Chain Reaction	244
8.3.8	Northern Blotting	246
8.3.8.1	Radiolabeling the probe	246
8.3.8.2	RNA electrophoresis	248
8.3.8.3	Sample preparation	248
8.3.8.4	Transfer of RNA to the membrane	249
8.3.8.5	Hybridisation of the membrane and exposure of the film	249
8.3.9	Measurement of ubiquinone levels in transfected cultures	251
8.3.10	Determination of ETC activity in transfected cultures	251
8.4	Experimental protocols	251
8.5	Results	252
8.5.1	Visualising Green Fluorescent Protein as a marker of cellular transfection	252
8.5.2	Confirmation of RT-PCR product as TPTF	252
8.5.3	Northern Blotting for TPTF mRNA	255
8.5.4	Measurement of CoQ in siRNA transfected cultures	255
8.5.4.1	HEK 293T cultures	260
8.5.4.2	Primary astrocyte cultures	260

8.5.5 Determination of ETC enzyme activities in siRNA transfected cultures.....	263
8.5.5.1 HEK 293T cells.....	263
8.5.5.2 Primary astrocytes.....	263
8.6 Discussion	266
8.7 Conclusion	269
 9. GENERAL DISCUSSION, CONCLUSIONS, AND SUGGESTED FURTHER WORK	271
9.1 HPLC Method	272
9.2 Human and rodent cell line responses to lovastatin and iNOS activation	273
9.3 CoQ status of astrocytes and neurons	274
9.4 Cellular dependence on OXPHOS and differences in CoQ₉ and CoQ₁₀ levels	275
9.5 Influence of serum-withdrawal on astrocyte CoQ availability	276
9.6 Influence of lovastatin on CoQ availability	277
9.7 Influence of iNOS and NO on CoQ availability	278
9.8 Differential effects of DETA-NO on astrocytes and neurons	279
9.9 CoQ status and ETC activity	280
9.10 siRNA study	281
9.11 Conclusions and potential implications of research	283
SUGGESTED FUTURE WORK	285
 REFERENCES	288
 APPENDIX I: AN INVESTIGATION INTO A POSSIBLE CASE OF HUMAN UBIQUINONE DEFICIENCY	353
 APPENDIX II: LIST OF PUBLICATIONS	358

LIST OF FIGURES AND TABLES

1. INTRODUCTION

Figure 1.1 <i>Generalised mitochondrial topology</i>	24
Figure 1.2 <i>The mitochondrial electron transport chain</i>	26
Figure 1.3 <i>The structure of ubiquione, ubisemiquinone , and ubiquinol</i>	29
Figure 1.4 <i>Complex III and the protonmotive Q cycle</i>	32
Figure 1.5 <i>The Krebs cycle</i>	39
Figure 1.6 <i>Mitochondrial reducing equivalent shuttle systems</i>	41
Figure 1.7 <i>Mitochondrial β-oxidation of fatty acids</i>	44
Figure 1.8 <i>Ketone body metabolism</i>	47
Figure 1.9 <i>The CoQ₁₀ biosynthetic pathway</i>	58
Figure 1.10 <i>Relationship between the rates of O₂⁻ generation and the amount of CoQ extractable from mitochondria</i>	63
Table 1.1 <i>Muscle ETC enzyme activities with ubiquinone concentration and plasma lactate values</i>	67

2. MATERIALS AND METHODS

Figure 2.1 <i>Phase contrast light micrograph of rat primary astrocyte cultures</i> ...	86
Figure 2.2 <i>Phase contrast light micrograph of rat primary neuron cultures</i>	88
Figure 2.3 <i>The structures of lovastatin and Na-lovastatin</i>	92
Figure 2.4 <i>NO₂⁻ and NO₃⁻ standard calibration curve</i>	99
Figure 2.5 <i>Cholesterol standard calibration curve</i>	103
Figure 2.6 <i>BSA standard calibration curve</i>	105

3. DEVELOPMENT OF AN HPLC METHOD FOR THE DETERMINATION OF CoQ IN BIOLOGICAL MATERIAL OF RODENT ORIGIN

Figure 3.1 <i>Schematic diagram of HPLC apparatus used to determine ubiquinone by reverse-phase HPLC and ultraviolet detection</i>	111
Figure 3.2 <i>The structure of diethoxy-CoQ₁₀</i>	112
Figure 3.3 <i>Wavelength scan of CoQ₉ in ethanol showing maximal absorption at λ= 205 and 275nm</i>	115
Figure 3.4 <i>Wavelength scan of CoQ₁₀ in ethanol showing maximal absorption at λ= 205 and 275nm</i>	116
Figure 3.5 <i>CoQ₉ standard calibration curve</i>	118
Figure 3.6 <i>CoQ₁₀ standard calibration curve</i>	119
Figure 3.7 <i>Chromatogram of 250 nM CoQ₉ and 250 nM CoQ₁₀ standards</i>	120
Figure 3.8 <i>Wavelength scan of diethoxyCoQ₁₀ in ethanol showing maximal absorption at λ= 216 and 280nm</i>	121
Figure 3.9 <i>Typical HPLC chromatogram obtained from analysis of rat astrocytes</i>	122

4. CoQ₉ AND CoQ₁₀ STATUS OF RAT AND HUMAN BRAIN CELL LINE CULTURES; EFFECTS OF NO, LIPOPOLYSACCHARIDE + γ -INTERFERON & LOVASTATIN EXPOSURE

Figure 4.1 Ubiquinone levels in untreated human 1321N1 astrocytoma and rat C6 glioma cultures	133
Figure 4.2 The effect of LPS+IFN γ , and L-NIL treatment upon the CoQ status of human 1321N1 astrocytoma and rat C6 glioma cultures	135
Figure 4.3 The effect of DETA-NO treatment upon levels of NO _x in the media of rat C6 glioma cultures	136
Figure 4.4 Ubiquinone levels in rat C6 glioma cultures treated with DETA-NO	137
Figure 4.5 The effect of lovastatin and its sodium salt (Na-Lovastatin) treatment upon the CoQ status of human 1321N1 astrocytoma cultures	139
Figure 4.6 The effect of lovastatin and its sodium salt (Na-Lovastatin) treatment upon the NO _x levels in the media of human 1321N1 astrocytoma cultures	140
Figure 4.7 The effect of lovastatin and its sodium salt (Na-Lovastatin) treatment upon the CoQ status of rat C6 glioma cultures	141
Figure 4.8 The effect of lovastatin treatment upon levels of NO _x in the media of rat C6 glioma cultures	143
Figure 4.9 The effect of simultaneous exposure of LPS+IFN γ , and the sodium salt of lovastatin upon the CoQ status of human 1321N1 astrocytoma and rat C6 glioma cultures	144
Figure 4.10 The effect of LPS+IFN γ in combination with the sodium salt of lovastatin (Na-Lovastatin) upon the NO _x levels in the media of human 1321N1 astrocytoma and rat C6 glioma cultures	145
Figure 4.11 The effect of DETA-NO in conjunction with Na-lovastatin upon levels of NO _x in the media of rat C6 glioma cultures	147
Figure 4.12 The effect of simultaneous exposure of DETA-NO in conjunction with the sodium salt of lovastatin upon the CoQ status of rat C6 glioma cultures	148
Figure 4.13 The effect of simultaneous exposure of DETA-NO in conjunction with LPS+IFN γ upon the CoQ status of rat C6 glioma cultures	149
Figure 4.14 The effect of DETA-NO in conjunction with LPS+IFN γ upon levels of NO _x in the media of rat C6 glioma cultures	150

5. CoQ₉ AND CoQ₁₀ LEVELS IN PRIMARY CULTURES OF RAT ASTROCYTES; EFFECTS OF SERUM WITHDRAWAL

Figure 5.1 The effect of serum withdrawal upon the CoQ status of primary cultures of rat astrocytes	162
Figure 5.2 The effect of serum withdrawal upon the total cholesterol status of primary cultures of rat astrocytes	164

6. THE EFFECTS OF LOVASTATIN UPON CoQ₉ AND CoQ₁₀ LEVELS IN PRIMARY CULTURES OF RAT ASTROCYTES

Figure 6.1 <i>The effect of lovastatin exposure upon the CoQ status of primary cultures of rat astrocytes</i>	175
Figure 6.2 <i>Cholesterol levels in astrocytes treated with lovastatin</i>	177
Table 6.1 <i>The effect of lovastatin exposure upon the mitochondrial complex activities of primary cultures of rat astrocytes in the presence of serum</i>	178
Table 6.2 <i>The effect of lovastatin exposure upon the mitochondrial complex activities of primary cultures of rat astrocytes in the presence of serum</i>	178
Figure 6.3 <i>Astrocyte morphology in the absence and presence of lovastatin</i>	180
Figure 6.4 <i>The effect of Na-lovastatin exposure upon the CoQ status of primary cultures of rat astrocytes</i>	181
Figure 6.5 <i>Cholesterol levels in astrocytes treated with Na-lovastatin</i>	183
Table 6.3 <i>The effect of Na-lovastatin exposure upon the mitochondrial complex activities of primary cultures of rat astrocytes in the presence of serum</i>	184
Table 6.4 <i>The effect of Na-lovastatin exposure upon the mitochondrial complex activities of primary cultures of rat astrocytes in the presence of serum</i>	184
Figure 6.6 <i>The effect of lovastatin exposure upon the CoQ status of primary cultures of rat astrocytes in the absence of serum</i>	186
Figure 6.7 <i>Cholesterol levels in serum - deprived astrocytes treated with lovastatin</i>	188
Table 6.5 <i>The effect of lovastatin exposure upon the mitochondrial complex activities of primary cultures of rat astrocytes in the absence of serum</i>	189
Table 6.6 <i>The effect of lovastatin exposure upon the mitochondrial complex activities of primary cultures of rat astrocytes in the absence of serum</i>	189
Figure 6.8 <i>The effect of Na-lovastatin exposure upon the CoQ status of primary cultures of rat astrocytes in the absence of serum</i>	191
Figure 6.9 <i>Cholesterol levels in serum - deprived astrocytes treated with Na-lovastatin</i>	192
Table 6.7 <i>The effect of Na-lovastatin exposure upon the mitochondrial complex activities of primary cultures of rat astrocytes in the absence of serum</i>	193
Table 6.8 <i>The effect of Na-lovastatin exposure upon the mitochondrial complex activities of primary cultures of rat astrocytes in the absence of serum</i>	193

7. CoQ₉ AND CoQ₁₀ LEVELS IN PRIMARY CULTURES OF RAT ASTROCYTES AND NEURONS; EFFECTS OF EXPOSURE TO NITRIC OXIDE

Figure 7.1 <i>NO_x levels in culture media from rat primary astrocytes</i>	206
Figure 7.2 <i>The effect of LPS+IFNγ upon the CoQ status of primary cultures of rat astrocytes</i>	208
Figure 7.3 <i>The effect of DETA-NO upon CoQ status of rat primary astrocyte cultures</i>	209

Table 7.1	<i>The effect of LPS+IFNγ exposure upon the mitochondrial complex activities of primary cultures of rat astrocytes</i>	211
Table 7.2	<i>The effect of LPS+IFNγ exposure upon the mitochondrial complex activities of primary cultures of rat astrocytes</i>	211
Table 7.3	<i>The effect of NO exposure upon the mitochondrial complex activities of primary cultures of rat astrocytes</i>	212
Table 7.4	<i>The effect of NO exposure upon the mitochondrial complex activities of primary cultures of rat astrocytes</i>	212
Figure 7.4	<i>CoQ status of rat astrocyte and neuron-enriched rat primary cultures and the effect of DETA-NO</i>	214

8. THE USE OF SHORT INTERFERING RNA TO ALTER UBIQUINONE BIOSYNTHESIS IN RAT AND HUMAN CELLS

Figure 8.1	<i>Schematic diagram of the pSUPER.gfp/neo vector</i>	223
Figure 8.2	<i>Schematic diagram of siRNA mechanism with pSUPER.gfp/neo</i>	224
Figure 8.3	<i>A truncated screenshot of the NCBI "Blast 2 sequences" local alignment tool</i>	229
Figure 8.4	<i>The major homological sequence between mouse and human transprenyl transferase mRNA</i>	231
Figure 8.5	<i>The forward and reverse sequence of the 64-nt primers inserted into the pSUPER.gfp/neo vector system</i>	234
Figure 8.6	<i>Total RNA as extracted from rat astrocytes transfected with pSUPER.gfp/neo and pSUPER.gfp/neo + TPTF</i>	243
Figure 8.7	<i>Selection of primers for the amplification of TPTF cDNA by RT-PCR</i>	245
Figure 8.8	<i>Large scale RT-PCR and gel electrophoresis to make a probe for Northern blotting</i>	247
Figure 8.9	<i>A schematic diagram of the apparatus used to transfer RNA from the gel to the hybridisation membrane</i>	250
Figure 8.10	<i>HEK 293T cells photographed 48h after transfection with pSUPER.gfp/neo</i>	253
Figure 8.11	<i>Rat primary astrocytes photographed 72h after transfection with pSUPER.gfp/neo + TPTF</i>	254
Figure 8.12	<i>Electrophoresis of the astrocyte RT-PCR product</i>	256
Figure 8.13	<i>Astrocyte RT-PCR product following 28 PCR cycles</i>	257
Figure 8.14	<i>Semiquantitative RT-PCR using an increasing number of cycles to aid visualisation of possible TPTF knockdown</i>	258
Figure 8.15	<i>Northern Blot for TPTF mRNA in primary astrocyte and HEK 293T cultures</i>	259
Figure 8.16	<i>Ubiquinone levels in HEK 293T cultures following transfection ...</i>	261
Figure 8.17	<i>Ubiquinone levels in primary astrocyte cultures following transfection</i>	262
Table 8.1	<i>Mitochondrial complex activities in HEK 293T cultures following transfection</i>	264
Table 8.2	<i>Mitochondrial complex activities in primary astrocyte cultures following transfection</i>	265

9. GENERAL DISCUSSION, CONCLUSIONS, AND SUGGESTED FURTHER WORK

Table 9.1 <i>Recovery and variability of HPLC method</i>	273
Table 9.2 <i>CoQ₉ and CoQ₁₀ status of different rat cell types</i>	276
Table 9.3 <i>Preliminary findings examining CoQ₉ and CoQ₁₀ non-synaptic mitochondria from rat brain</i>	285

APPENDIX I: AN INVESTIGATION INTO A POSSIBLE CASE OF HUMAN UBIQUINONE DEFICIENCY

Table A.1 <i>Patient muscle ubiquinone concentration and the paediatric reference range</i>	355
--	-----

ABBREVIATIONS

AD	Alzheimer's Disease
ADP	adenosine diphosphate
AMV	avian myeloblast virus
ANT	adenine nucleotide translocase
ATP	adenosine triphosphate adenine triphosphate
BH ₄	tetrahydrobiopterin
BSA	bovine serum albumin
CIP	calf intestinal alkaline phosphatase
CoA	coenzyme A
CoQ	ubiquinone
CoQH ₂	ubiquinol
CPS	carbamoyl phosphate synthetase
Cs	cyclosporin
CS	citrate synthase
CTP	cytosine triphosphate
CyP-D	cyclophilin-D
DEPC	diethyl pyrocarbonate
DETA-NO	diethylamine NO
DHAP	dihydroxyacetone phosphate
DIV	days in vitro
DMEM	Dulbeccos modified Eagle media
DMQ	demethoxyubiquinone

DMSO	dimethyl sulphoxide
DNA	deoxyribonucleic acid
dsRNA	double-stranded RNA
DTNB	5,5' Dithio-bis(2-nitrobenzoic) acid
EBSS	Earle's balanced salt solution
EC	electrochemical enzyme commission
ECACC	European Collection of Cell Cultures
EDTA	ethylene diamine tetra acetate
ETC	electron transport chain
ETF	electron transport flavoprotein
FAD(H ₂)	flavin adenine dinucleotide (reduced form)
FBS	foetal bovine serum
FMN	flavin mononucleotide
GDP	guanoside diphosphate
GFAP	glial fibrillary acidic protein
GFP	green fluorescent protein
GSH	reduced glutathione
GTP	guanosine triphosphate
HBSS	Hanks Balanced Salts Solution
HD	Huntingdon's disease
HEK	human embryonic kidney
HEPES	N-2-Hydroxyethylpiperazine-N'-2'-ethanesulfonic Acid
HMG	hydroxy-methyl-glutaryl

HPLC	high performance liquid chromatography
IFN γ	interferon gamma
IL-1	interleukin-1
L-BSO	buthionine sulfoximine
LCAD	long chain acyl-CoA dehydrogenase
LCHAD	long chain hydroxyacyl-CoA dehydrogenase
LDH	lactate dehydrogenase
L-NIL	L-N ⁶ -(l-iminoethyl)lysine hydrochloride
LPS	lipopolysaccharide
LS	Leigh's Syndrome
MCAD	medium chain acyl-CoA dehydrogenase
MDH	malate dehydrogenase
MEM	minimum essential medium
MOPS	3-(N-Morpholino)propanesulfonic acid
mRNA	messenger RNA
mtDNA	mitochondrial DNA
NAD(P)(H)	nicotine adenine dinucleotide (phosphate) (reduced form)
NO	nitric oxide
NO ⁺	nitrosonium
NO ⁻	nitroxyl
NOS	nitric oxide synthase
NO _x	total NO ₂ ⁻ + NO ₃ ⁻
-nt	nucleotide

NTP	nucleotide triphosphate
O ₂	molecular oxygen
O ₂ ^{·-}	superoxide
OH [·]	hydroxyl
ONOO ⁻	peroxynitrite
OTC	ornithine transcarbamoylase
OXPPOS	oxidative phosphorylation
PCR	polymerase chain reaction
PD	Parkinson's Disease
PDHC	pyruvate dehydrogenase complex
P _i	inorganic phosphate
PNK	polynucleotide kinase
PT	permeability transition
RISC	RNA-induced silencing complex
RNA	ribonucleic acid
RNAi	RNA interference
RNS	reactive nitrogen species
ROS	reactive oxygen species
RT	reverse transcriptase
SCAD	short chain acyl-CoA dehydrogenase
SDH	succinate dehydrogenase
siRNA	small interfering RNA
SCHAD	short chain hydroxyacyl-CoA dehydrogenase

SDS	sodium dodecyl sulphate
SOD	superoxide dismutase
SSC	sucrose sodium citrate
TE	trypsin/EDTA
TNF α	tumour necrosis factor α
TPTF	transprenyl transferase
TTP	thymine triphosphate
UCP	uncoupling protein
UTP	uracil triphosphate
UV	ultra violet
VDAC	voltage dependant anion channel
VLCAD	very long chain acyl-CoA dehydrogenase

1. INTRODUCTION

1. INTRODUCTION

1.1. *An introduction to mitochondria*

The mitochondrion is an essential organelle in the majority of mammalian cells. While a number of theories exist as to the co-evolution of eukaryotic cells and these intrinsically interesting organelles, the widely-held theory of “endosymbiotic evolution” states that today’s eukaryotic mitochondria evolved as a result of the engulfment of a free-living, aerobic prokaryotic organism by another anaerobic proto-eukaryotic cell (proposed in Margulis, 1981).

To summarise 2 billion years of evolution and the considerable theoretical debate which will not be considered here, mitochondria have become indispensable for higher life. Although far from being their sole function, these organelles are involved in the synthesis of adenosine triphosphate (ATP) from adenosine diphosphate (ADP), a process coupled to the reduction of molecular oxygen to water. In the region of 1 μm in length, these double-membraned, classically “rod-shaped” structures contain a matrix, enclosed within the highly convoluted inner membrane which forms finger-like projections or “cristae” (reviewed in Frey & Manella, 2000). In reality, the diversity of mitochondrial size, shape and motility mean that there is no such thing as a typical mitochondrion. However, general mitochondrial topology is described in Figure 1.1, showing the double-membraned structure, cristae, matrix and the “studding” of ATP synthase on the matrix side of the inner membrane.

The mitochondrial matrix, bounded by the inner membrane, contains a number of soluble (i.e. non-membrane bound) biosynthetic enzymes. Enzymatic

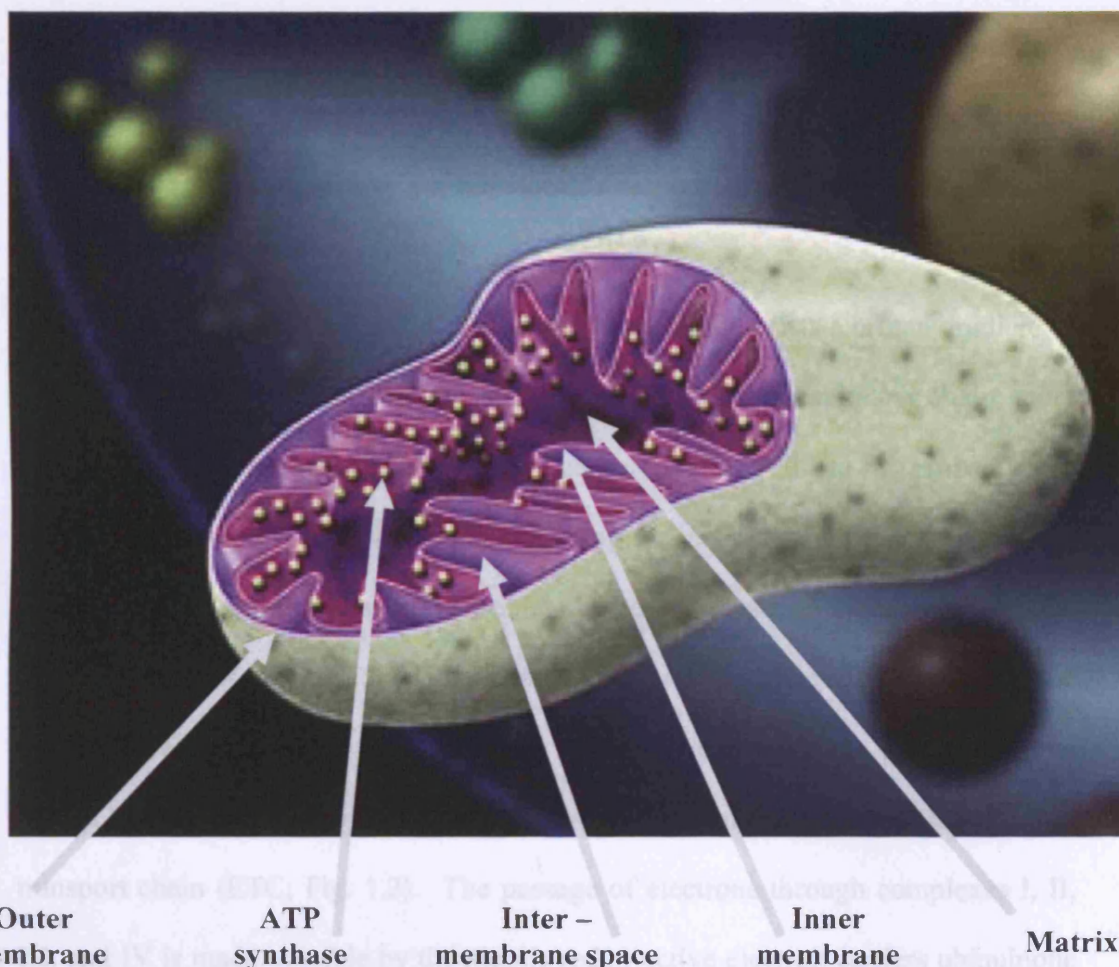


Figure 1.1 Generalised mitochondrial topology

Mitochondria are double-membraned organelles of between $1\mu\text{m}$ and $10\mu\text{m}$ in length. Across the inner membrane exists a proton gradient, maintained by the proton-pumping machinery of the electron transport chain. The inner membrane is highly convoluted, and encloses the matrix. The inner membrane also contains the respiratory complexes and the ATP synthase (visible as a stalked particle on the matrix-side of the inner membrane). The matrix consists of a number of proteins, (including the Krebs cycle and other enzymes) and mitochondrial DNA.

(Image reproduced with permission from BioMedia Associates, Beaufort, USA)

substrates may already be present in the matrix (such as acetyl CoA formed by the pyruvate dehydrogenase complex; PDHC; EC. 1.2.4.1), while others such as fatty acids and pyruvate need a transport mechanism (the carnitine-acylcarnitine translocase and monocarboxylate translocator respectively; reviewed in Heales *et al.*, 2002).

Between the matrix and the inter-membrane space exists a proton gradient of approximately -150 to -170 mV, which is maintained by the respiratory chain, more than 80 polypeptides grouped into protein complexes (termed I to IV) embedded in the inner membrane. Electrons are passed along the chain through the redox centres of the respiratory complexes, while mobile electron carriers traffic electrons between the complexes. Reducing equivalents from NADH and succinate are passed down the chain before finally being used to reduce molecular oxygen (O₂). This functional unit is termed the mitochondrial respiratory chain, or more accurately the electron transport chain (ETC; Fig. 1.2). The passage of electrons through complexes I, II, III, and IV is made possible by the mobile redox-active electron carriers ubiquinone (in the hydrophobic phase of the inner membrane) and cytochrome *c* (in the hydrophilic phase of the inner membrane).

The process of electron transport through the protein complexes is coupled to the pumping of protons from the matrix into the inter-membrane space. The proton gradient is then dissipated through the ATP synthase (complex V) back into the matrix. This catalyses the phosphorylation of ADP to ATP, which can then be shuttled out of the mitochondrion in exchange for ADP by the adenine nucleotide translocase (ANT).

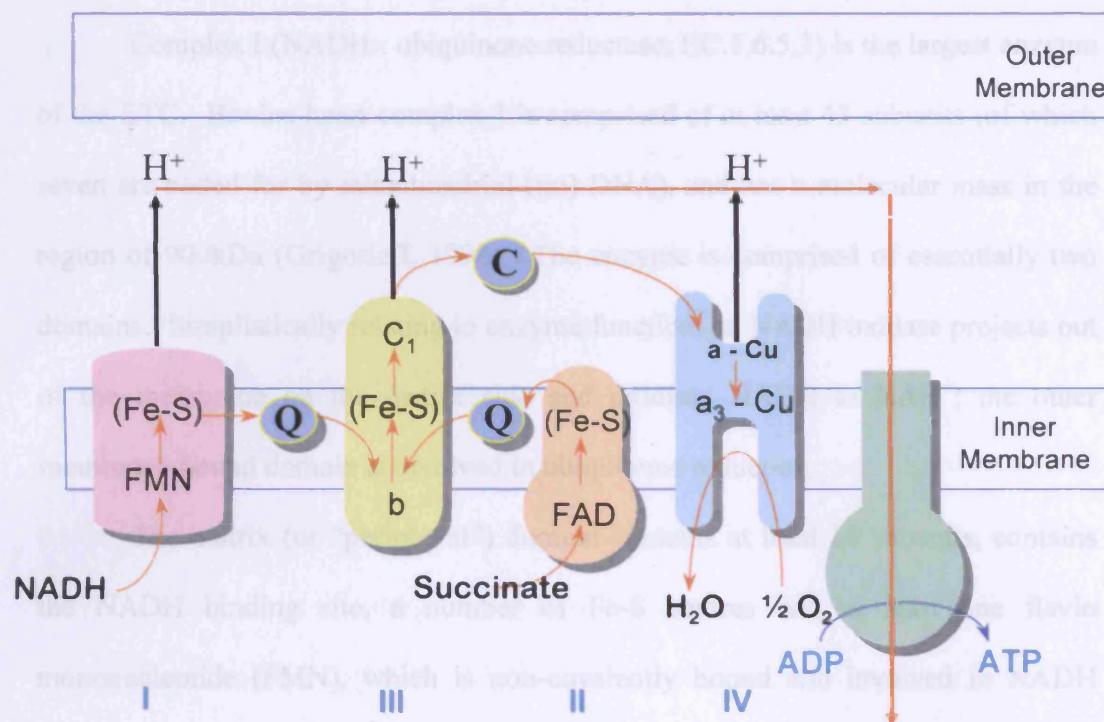


Figure 1.2. The mitochondrial electron transport chain.

The mitochondrial respiratory chain is an assembly of electron carriers grouped into four polypeptide complexes [I (NADH : ubiquinone reductase), II (succinate : ubiquinone reductase), III (ubiquinol : cytochrome *c* reductase), and IV (cytochrome *c* oxidase)]. Complexes I, III, and IV act as oxidation-reduction-driven proton pumps. The flow of electrons from NADH, along the respiratory chain to oxygen is coupled to the pumping of protons across the inner mitochondrial membrane, resulting in the formation of a proton gradient. The flow of protons back into the matrix through the membrane sector of the mitochondrial ATP synthase alters the active site of the enzyme, leading to the synthesis of ATP.

Q = ubiquinone, C = cytochrome *c*. Both act as mobile electron carriers.

1.1.1. Complex I

Complex I (NADH : ubiquinone reductase; EC.1.6.5.3) is the largest enzyme of the ETC. Bovine heart complex I is comprised of at least 43 subunits (of which seven are coded for by mitochondrial (mt) DNA), and has a molecular mass in the region of 900kDa (Grigorieff, 1998). The enzyme is comprised of essentially two domains. Simplistically relating to enzyme function, an NADH oxidase projects out of the membrane on the matrix side and oxidises NADH to NAD⁺; the other membrane-bound domain is involved in ubiquinone reduction.

The matrix (or “peripheral”) domain contains at least 10 subunits, contains the NADH binding site, a number of Fe-S centres and at least one flavin mononucleotide (FMN), which is non-covalently bound and involved in NADH oxidation (reviewed by Friedrich and Böttcher, 2004).

Two ubiquinone binding sites (and at least one reduction site) have been proposed to exist close to one another in the membrane domain of complex I (Tormo and Estornell, 2000); however their exact positions are as yet unknown. Rotenone is a classical and commonly used inhibitor in studies of complex I (Teeter *et al.*, 1969); and one which does not compete with ubiquinone binding (Friedrich *et al.*, 1994). The neurotoxin MPP⁺ binds and inhibits complex I at the ubiquinone binding sites. These studies have suggested that one site is relatively hydrophilic, while one is shielded by a “hydrophobic barrier” on the enzyme (Ramsay *et al.*, 1989, Gluck *et al.*, 1994; reviewed in Miyoshi, 2001). Additionally, an inhibitor-binding domain between these two ubiquinone sites has also been proposed (Tormo and Estornell, 2000).

Due to the complexity and size of complex I, little is known of the mechanism of this enzyme. Electron microscopic analysis has uncovered that the two domains of the complex are arranged in an “L” shape in a number of systems notably bovine heart (Greighoff, 1998), the red bread mould *Neurospora crassa* (Guénebaut *et al.*, 1997), *Yarrowia lipolytica* (Freidrich & Bottcher, 2004) and *Escherichia coli* (Guénebaut *et al.*, 1997; although another “U” shaped conformation has been described in *E.coli* by Freidrich & Bottcher, 2004). The peripheral and membrane domain are believed to be joined by a stalk of approximately 3nm in bovine heart and *E. coli* (Guénebaut *et al.*, 1997 and Grigorieff, 1998) and this may contain the ubiquinone binding sites (Tomo & Estornell, 2000). However, both this measurement, and the angle at which each arm lies have been questioned (reviewed in Freidrich & Bottcher, 2004).

It is understood that as a result of NADH oxidation, complex I transfers four or five protons from the matrix to the inter-membrane space although the mechanism has not been elucidated (reviewed in Heales *et al.*, 2002). The proton-pumping action relies upon complex I's catalysis of the oxidation of NADH to NAD^+ yielding two electrons, which are proposed to reduce the N-2 Fe-S cluster. This then transfers the electrons to ubiquinone (CoQ), reducing it to ubiquinol. CoQ (Fig. 1.3), described in greater depth later in this chapter, is a lipophilic quinone and this substrate-like redox component exists within the inner membrane effectively behaving as a homogenous "pool" (Kröger and Klingenberg, 1973). Electrons are subsequently passed to complex III of the ETC.

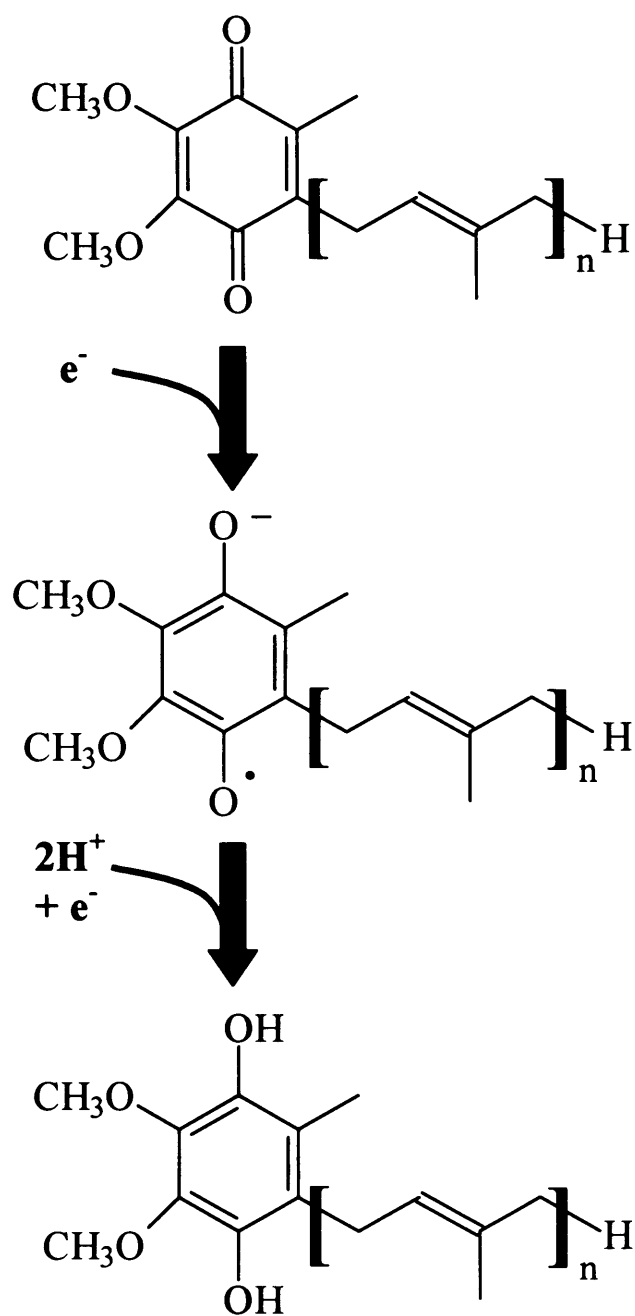


Figure 1.3 The structure of ubiquinone, ubisemiquinone, and ubiquinol

As the lipophilic mobile electron carrier in the ETC, CoQ comprises a six-membered carbon ring, and an isoprenyl tail of n repeating units. The specific homologue is named according to the number of isoprenyl repeats. Predominantly, $n = 9$ in rodents and $n = 10$ in humans. The addition of 1 electron to the oxidised quinone results in partial reduction to ubisemiquinone. Further reduction results in ubiquinol.

1.1.2. Complex II

Complex II (succinate : ubiquinone reductase; EC. 1.3.5.1) is a four-subunit enzyme catalysing the oxidation of succinate from the Krebs cycle to fumarate. The subunits are denoted sdhA to sdhD and uniquely in mammalian ETC enzymes, these are all encoded by nuclear DNA (Hirawake *et al.*, 1999). SdhA and sdhB are hydrophilic, projecting into the matrix, while sdhC and sdhD are membrane-bound (Yankovskaya *et al.*, 2003). Another unique feature among respiratory complexes is that complex II does not act directly as a proton pump *per se*: the electrons stripped from succinate are transferred to ubiquinone to form ubiquinol without actively contributing to the proton gradient. It is also of note that succinate dehydrogenase is additionally an integral enzyme of the Krebs cycle; thus this enzyme provides a direct link from the matrix-contained Krebs cycle to the ETC.

Although very similar to fumarate reductases, the X-ray structure of mammalian mitochondrial complex II has not yet been elucidated. A number of high-resolution X-ray structures for have now been proposed for complex II, based mostly upon membrane-bound menaquinol : fumarate oxidoreductase (QFR) from *E.coli* (Iverson *et al.*, 1999) and *Wolinella succinogenes* (Lancaster *et al.*, 1999). More recently, the structure of anaerobic succinate : ubiquinone reductase which is also analogous to mitochondrial complex II was confirmed in *E. coli* (Horsefield *et al.*, 2003; Yankovskaya *et al.*, 2003), revealing the electron transport pathway from succinate to ubiquinone and the existence of the complex as a tightly packed trimer (Yankovskaya *et al.*, 2003).

As with complex I, a matrix domain is responsible for the catalytic reduction of the substrate, while electron transfer to CoQ occurs within the membrane via generation of ubisemiquinone. It is possible that complex II has 2 CoQ binding sites analogous to complex I, although the finding of Yankovskaya *et al.* (2003) may suggest only a single site in *E. coli*.

A covalently-bound FAD group in subunit A acts as the primary electron acceptor from succinate in complex II, while a number of different Fe-S centres allow electron transport to CoQ. SdhB contains three such clusters [2Fe-2S], [4Fe-4S] and [3Fe-4S] which ultimately pass electrons to ubiquinone. The sdhC and sdhD subunits are anchored within the membrane and contain at least one CoQ binding site in the model of Yankovskaya *et al.* (2003); this is proposed to be different to that of QFR.

1.1.3. Complex III

Complex III (ubiquinol : cytochrome *c* reductase; EC 1.10.2.2) exists as a homodimer and catalyses the oxidation of ubiquinol back to ubiquinone; this is coupled to direct proton pumping across the inner membrane. Comprising 11 subunits of which one is mitochondrially encoded, each monomer has a molecular mass of 240kDa. Complex III spans the membrane, exposed to both the matrix and the inter-membrane space. Electrons from ubiquinol are donated to the hydrophilic carrier cytochrome *c* hydrophilic domain of the inner membrane. Of particular note with the regard to complex III is the “Q cycle” theory (proposed initially by Mitchell, 1975; Figure 1.4). In addition, for the docking site for cytochrome *c*,

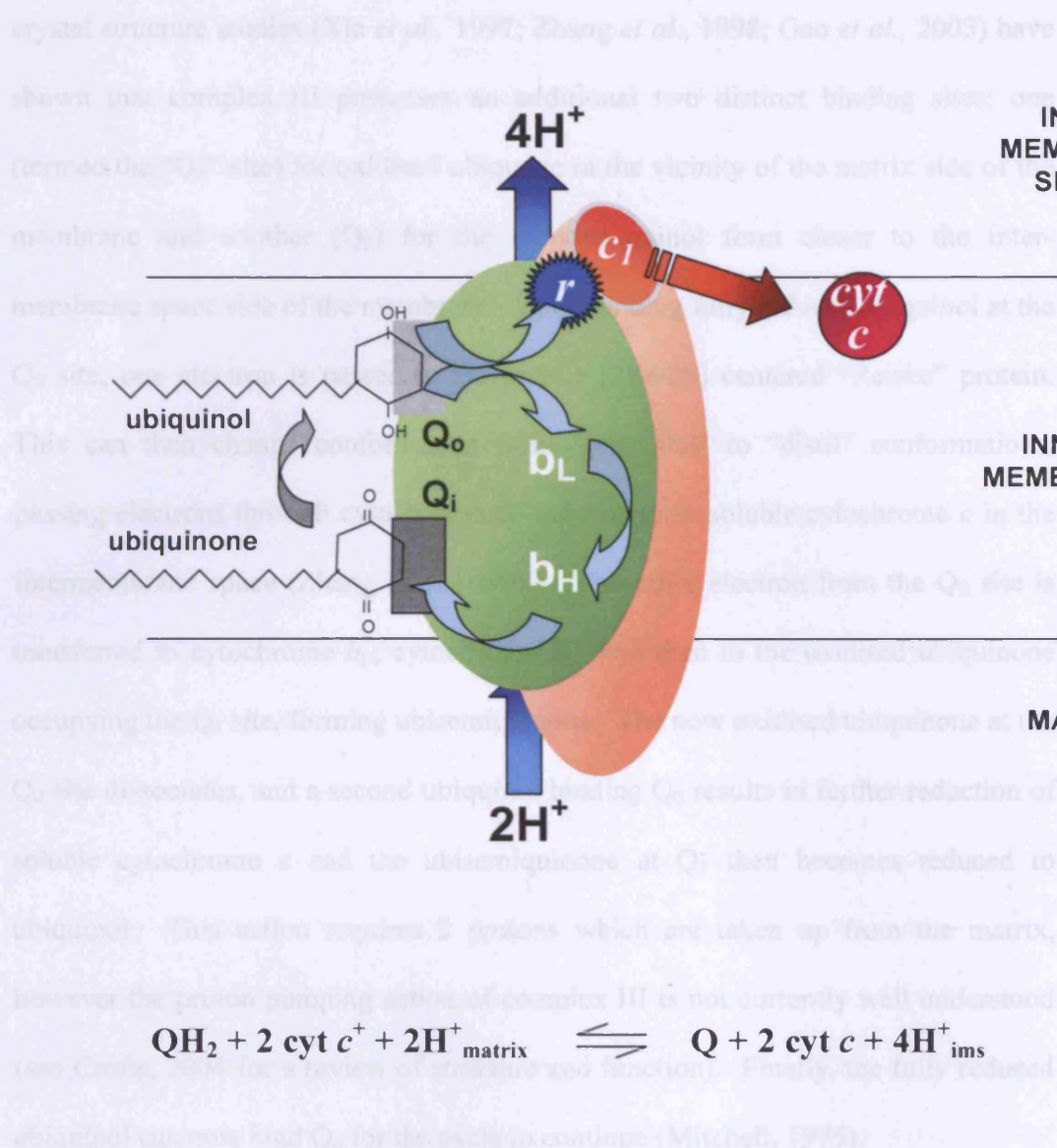


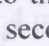



Figure 1.4 Complex III and the protonmotive *Q* cycle

Cytochrome *b* is shown in green; cytochrome c_1 in orange. Initial binding of ubiquinol to the Q_0 site of complex III results in the transfer of one electron (represented in this diagram by ) to the mobile 2Fe-2S Reiske complex () and subsequently cytochrome c_1 (). A second electron is then passed via the b_L and b_H cytochromes to ubiquinone bound to the Q_1 site. This is coupled to the pumping of 2 protons from the matrix to the inter-membrane space (). Following addition of a second electron from another Q_0 -bound ubiquinol, the Q_1 ubiquinone becomes fully reduced. It then dissociates, with the possibility of binding Q_0 . A balanced equation for the process is shown above. (Adapted from Crofts, 2004)

crystal structure studies (Xia *et al.*, 1997; Zhang *et al.*, 1998; Gao *et al.*, 2003) have shown that complex III possesses an additional two distinct binding sites: one (termed the “Q₁” site) for oxidised ubiquone in the vicinity of the matrix side of the membrane and another (Q₀) for the reduced quinol form closer to the inter-membrane space side of the membrane. Upon binding fully reduced ubiquinol at the Q₀ site, one electron is passed to the mobile [2Fe-2S] centered “Reiske” protein. This can then change conformation from “proximal” to “distal” conformations, passing electrons through cytochrome c₁ and finally to soluble cytochrome *c* in the intermembrane space (Zhang *et al.*, 1998). The other electron from the Q₀ site is transferred to cytochrome b_L, cytochrome b_H, and then to the oxidised ubiquinone occupying the Q₁ site, forming ubisemiquinone. The now oxidised ubiquinone at the Q₀ site dissociates, and a second ubiquinol binding Q₀ results in further reduction of soluble cytochrome *c* and the ubisemiquinone at Q₁ then becomes reduced to ubiquinol. This action requires 2 protons which are taken up from the matrix, however the proton pumping action of complex III is not currently well understood (see Crofts, 2004 for a review of structure and function). Finally, the fully reduced ubiquinol can now bind Q₀ for the cycle to continue (Mitchell, 1975).

As each turnover requires two ubiquinol molecules to be oxidised at the Q₀ site, two electrons are available to reduce cytochrome *c* and two to reduce the Q₁ ubiquinone. Subsequently 4 protons are delivered to the inter-membrane space.

1.1.4. Complex IV

Complex IV (cytochrome *c* oxidase; EC. 1.9.3.1) is the terminal member of the ETC proteins and as such binds reduced cytochrome *c*, using the electrons gained to reduce half a molecule of O₂ to water. This reaction also allows the transfer of protons from the matrix to the inter-membrane space. Crystal studies of bovine heart complex IV confirmed a dimerised structure each with 13 subunits and a total molecular mass of 204 kDa (Tsukihara *et al.*, 1996, 1998). Subunits I, II, and III are mitochondrially encoded (Anderson *et al.*, 1981), forming the central core of the protein. The ten remaining subunits are encoded by the nucleus; with likely roles in regulation, stabilisation and assembly of the functional protein (reviewed in Richter and Ludwig, 2003). However, despite an excellent structural understanding of the protein based upon spectroscopic evidence (reviewed in Michel, 1998), mutagenesis studies (Haltia *et al.*, 1989; Witt *et al.*, 1997) and more recent crystallisation data (Yoshikawa *et al.*, 1998), the molecular mechanism of proton translocation and its coupling to the redox steps are still unclear.

The fact that complex IV acts as a proton pump was shown by Wikström (1977), however, the exact mechanism of the transfer of protons to water and the pumping of protons into the inter membrane space remains the topic of debate. Proposed mechanisms have been extensively reviewed (Babcock and Wikström, 1992; Michel, 1998; Richter & Ludwig, 2003). Subunit II is likely to act as the main docking site for cytochrome *c*: two coppers in subunit II (Cu_A) are the first to receive electrons from cytochrome *c*, before these are transferred to the centres of subunit I, viz. the haem cytochrome *a*, and then to the binuclear active site

cytochrome a_3/Cu_B . During the reduction of oxygen at the catalytic site, both metals are reduced after the acceptance of two electrons, a state which allows oxygen binding and the formation of a peroxy intermediate. A further electron allows the formation of water and a ferryl intermediate, while one more electron is required to form a second water molecule and allow the enzyme to revert back to the oxidised state (Han *et al.*, 1990; Babcock and Wilkstrom, 1992). These redox centres are located in the middle of the hydrophobic membrane environment (see Richter & Ludwig, 2003). To reduce O_2 to H_2O requires four protons (from the matrix side), an action which also pumps four additional protons across into the inter-membrane space. The pumping mechanism may yet be shown to involve conformational change at the active site or to occur by a structural change more distal from cytochrome a_3/Cu_B . (reviewed in Richter & Ludwig, 2003)

1.1.5. ATP synthase

The proton motive force, built and maintained by the four complexes, drives ATP synthesis by complex V (F_1F_0 -ATP synthase; EC. 3.6.1.34) (Mitchell, 1961, Mitchell and Moyle, 1969; reviewed in Heales *et al.*, 2002). Complex V binds $\text{ADP} + \text{P}_i$, and proton flux through the complex allows a conformational change of the complex to catalyse the conversion to ATP. Subsequent cleavage of the terminal phosphate group of this molecule liberates energy to drive cellular biochemical functions.

Bovine heart ATP synthase is greater than 500kDA in size, comprises 16 subunits of which two are encoded by the mitochondrial genome, with 2 distinct

domains termed F_1 (matrix subunit) and F_0 (membrane domain) (Abrahams *et al.*, 1994, reviewed in Mueller, 2000). F_1 consists of six alternating (3α & 3β) subunits arranged around a central “stalk” domain. The so-called $(\alpha\beta)_3$ domain is nearly-spherical (8 nm high x 10 nm wide) while the stalk is made up of γ and ϵ (and possibly δ) subunits. Nucleotide binding occurs at the α and β subunit interfaces in the F_1 domain.

The F_0 membrane domain is the site of proton translocation and contains 9 subunits in bovine heart ATP synthase (Abrahams *et al.*, 1994). This domain constitutes the “channel” through which protons flow to re-enter the matrix. It is thought that protonation of an aspartate residue in the F_0 domain causes the rotation of the subunit, and subsequent release of this proton to the cytosol. Crucially, this rotation also mediates ADP phosphorylation.

In order to stop rotation of the F_1 domain during rotation of F_0 and the stalk, there is also a “stator” linking F_1 and F_2 (Ogilvie *et al.*, 1997; Wilkens & Capaldi, 1998). This is believed to anchor the $(\alpha\beta)_3$ domain, inhibiting it from rotating with the γ subunit.

The structures of the β subunits of the F_1 domain have been shown to cycle through conformational changes resulting in “open”, “loose” and “tight” substrate binding. Additionally, the 3β subunits are always each in a different state. The “binding-change mechanism” (Gresser *et al.*, 1982; subsequently reviewed in Boyer, 1997) proposes that the open conformation has a low affinity for either the substrate or product. The loose state allows reversible binding of substrate or product. The tight state is a high affinity state for ADP and P_i , such that ATP formation is

favoured. Following ATP formation in the tight state, it is necessary for another β subunit to be in the loose state and bind ADP and P_i . Thus it is likely that cooperativity exists between the sites (reviewed in Boyer, 1997).

Dissipation of the proton gradient from the inter-membrane space to the matrix through the F_0 domain thus induces a rotational movement in the γ and ϵ subunits of the inner stalk. The δ subunit may form part of an external stator. Rotation induces conformational change and alteration of catalytic activity in the nucleotide binding sites of the $(\alpha\beta)_3$ domain. This allows the phosphorylation of ADP with P_i to form ATP.

1.2. Other mitochondrial metabolic processes

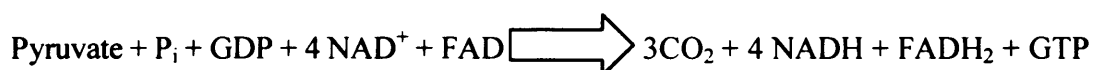
While OXPHOS is crucially important for cellular respiration, mitochondria are involved in a number of other metabolic processes, some of which are described below.

1.2.1. The Krebs cycle

Glycolysis occurring in the cytosol converts glucose to pyruvate and directly generates a net of 2 ATP molecules. 2 NADH molecules per glucose are also fed into the ETC, and could theoretically generate up to 6 ATP molecules via OXPHOS. However, oxidative phosphorylation is not 100% efficient primarily due to proton (and electron) leak, and ATP-dependant processes.

The Krebs cycle was elucidated in 1937 (Krebs and Johnson, 1937, and a review is given in Scheffler, 1999). Pyruvate enters the mitochondrial matrix via the

monocarboxylate translocator and is converted to acetyl-CoA by PDHC. Also called the citric acid cycle and the tricarboxylic acid (TCA) cycle (Fig. 1.5), the Krebs cycle describes the conversion of 6-carbon citrate to oxaloacetate (a 4 carbon molecule) via a number of intermediates: cis-aconitate, isocitrate, α -ketoglutarate, succinyl CoA, succinate, fumarate and malate, and then from oxaloacetate to citrate via condensation with acetyl-CoA. Including the conversion of pyruvate, these reactions may be summarised as:



With each “turn” of the cycle, 2 molecules of CO_2 are liberated (one in the conversion of 6-carbon isocitrate to 5-carbon α -ketoglutarate, another with the conversion of the latter to 4-carbon succinyl-CoA), both of which also reduce NAD^+ to NADH. The reaction of succinyl-CoA to succinate phosphorylates GDP to GTP. Conversion of GTP to ATP is possible by the enzyme nucleoside diphosphokinase (EC. 2.7.4.6). FAD is reduced to FADH_2 in the oxidation of succinate to fumarate; the electrons used to reduce FADH_2 may also be used to reduce CoQ via the electron transport flavoprotein. The final oxidation of malate to oxaloacetate reduces a third molecule of NAD to NADH. These reducing equivalents thus generated act as substrates for the ETC described above.

The 8 major enzymes of the Krebs cycle are shown in Fig. 1.5. All but one are soluble matrix enzymes: succinate dehydrogenase (SDH; EC. 1.3.5.1) reviewed in Yankovskaya *et al.*, 2003) is notable as a membrane-bound exception. Thus SDH

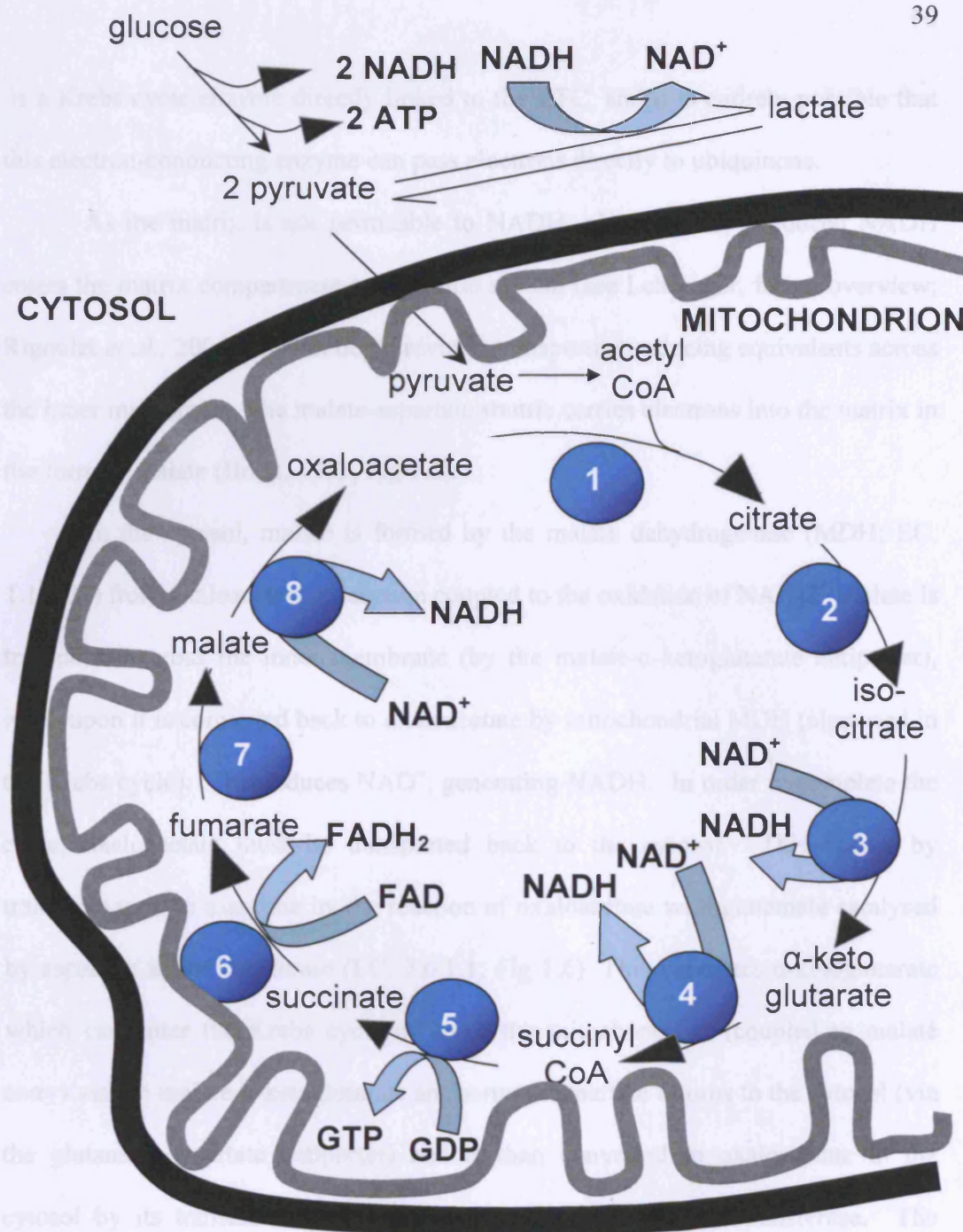


Figure 1.5. The Krebs cycle.

Acetyl CoA may be generated by the action of PDHC on pyruvate, itself generated by glycolysis in the cytosol. The Krebs cycle generates the reducing equivalents NADH and FADH₂ which can then become oxidised by the ETC. Additionally the conversion of succinyl-CoA to succinate liberates GTP, which can be converted to ATP by diphosphonucleotide kinase. Enzymes (●): 1: citrate synthase; 2: aconitase; 3: isocitrate dehydrogenase; 4: α-ketoglutarate dehydrogenase; 5: succinyl CoA synthase; 6: succinate dehydrogenase; 7: fumarase; 8: malate dehydrogenase.

is a Krebs cycle enzyme directly linked to the ETC, and it is entirely possible that this electron-conducting enzyme can pass electrons directly to ubiquinone.

As the matrix is not permeable to NADH, glycolytically produced NADH enters the matrix compartment by a shuttle system (see Lehninger, for an overview; Rigoulet *et al.*, 2004 for an in depth review) transporting reducing equivalents across the inner membrane. The malate-aspartate shuttle carries electrons into the matrix in the form of malate (Borst, 1963; Fig 1.6).

In the cytosol, malate is formed by the malate dehydrogenase (MDH; EC. 1.1.1.37) from oxaloacetate, a reaction coupled to the oxidation of NADH. Malate is transported across the inner membrane (by the malate- α -ketoglutarate antiporter), whereupon it is converted back to oxaloacetate by mitochondrial MDH (also used in the Krebs cycle). This reduces NAD^+ , generating NADH. In order to complete the cycle, oxaloacetate must be transported back to the cytosol. This occurs by transamination to aspartate by the reaction of oxaloacetate with glutamate catalysed by aspartate aminotransferase (EC. 2.6.1.1; Fig 1.6). This generates α -ketoglutarate which can enter the Krebs cycle or leave the mitochondrion (coupled to malate entry) via the malate- α -ketoglutarate antiporter. Aspartate returns to the cytosol (via the glutamate-aspartate antiporter) and is then converted to oxaloacetate in the cytosol by its transamination using a cytosolic aspartate aminotransferase. The overall transport mechanism is governed by the level of NAD^+ / NADH in the matrix; in the presence of high levels of NAD^+ , transport is inhibited.

A second system, the glycerol-phosphate shuttle uses the cytosolic and mitochondrial isoforms of glycerol-3-phosphate dehydrogenase (Glycerol-3-PDH;

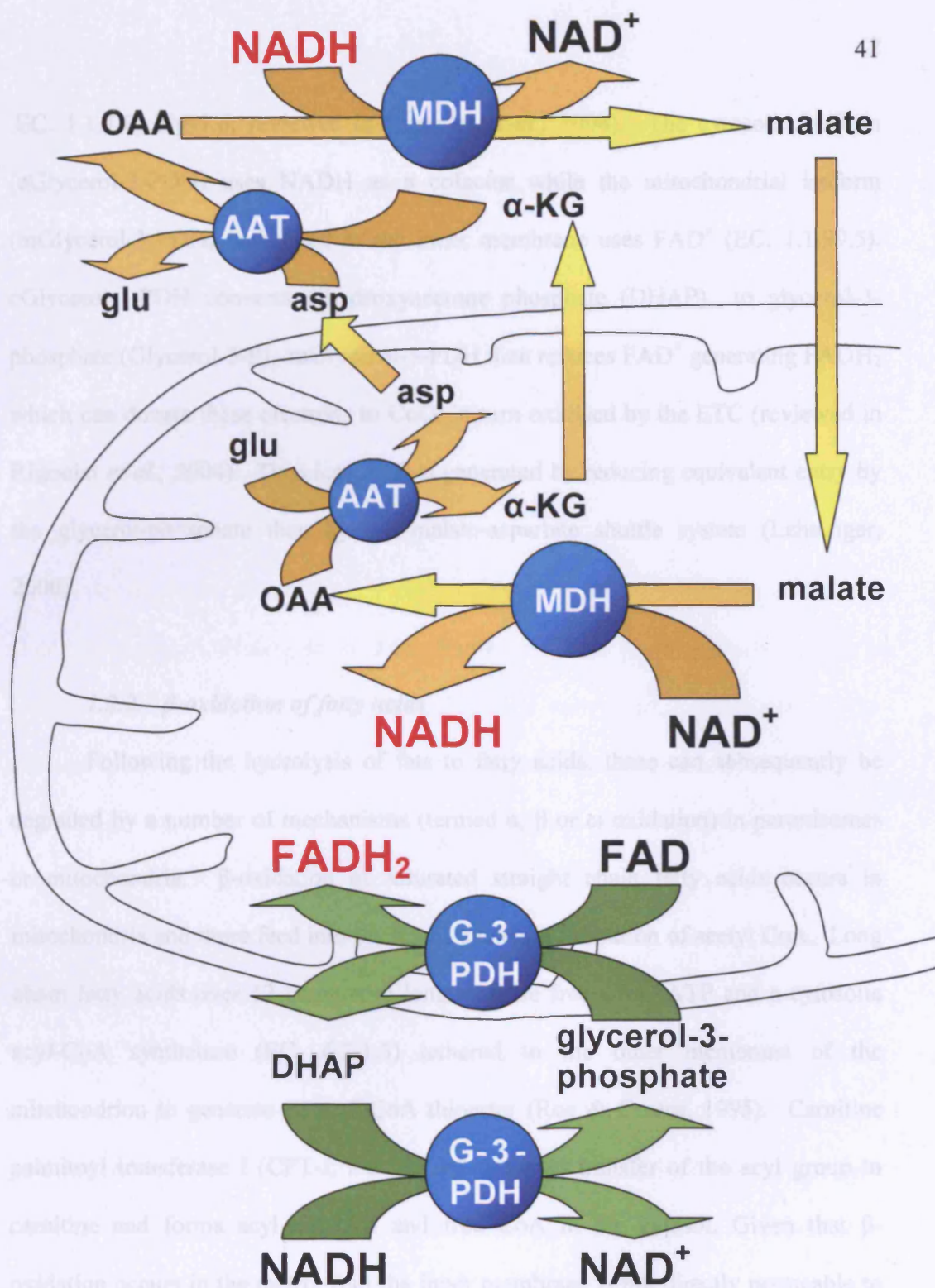


Figure 1.6. Mitochondrial reducing equivalent shuttle systems.

As the inner membrane is not permeable to NAD⁺, NADH, FAD or FADH₂, the electrons must be passed to substrates which can cross the inner membrane. The upper scheme (yellow arrows) depicts the malate-aspartate shuttle for NADH; the lower one (green arrows) the glycerol-phosphate shuttle for FADH₂. Enzymes (●) are MDH: malate dehydrogenase; AAT: aspartate aminotransferase; G-3-PDH: glycerol-3-phosphate dehydrogenase. glu = glutamate; asp = aspartate

EC. 1.1.1.8; Fig 1.6; reviewed in Rigoulet *et al.*, 2004). The cytosolic isoform (cGlycerol-3-PDH) uses NADH as a cofactor while the mitochondrial isoform (mGlycerol-3-PDH) embedded in the inner membrane uses FAD^+ (EC. 1.1.99.5). cGlycerol-3-PDH converts dihydroxyacetone phosphate (DHAP) to glycerol-3-phosphate (Glycerol-3-P). mGlycerol-3-PDH then reduces FAD^+ generating FADH_2 which can donate these electrons to CoQ, in turn oxidised by the ETC (reviewed in Rigoulet *et al.*, 2004). Thus less ATP is generated by reducing equivalent entry by the glycerol-phosphate than by the malate-aspartate shuttle system (Lehninger, 2000).

1.2.2. β -oxidation of fatty acids

Following the hydrolysis of fats to fatty acids, these can subsequently be degraded by a number of mechanisms (termed α , β or ω oxidation) in peroxisomes or mitochondria. β -oxidation of saturated straight chain fatty acids occurs in mitochondria and these feed into the Krebs cycle via formation of acetyl CoA. Long chain fatty acids over 12 carbons in length utilise free CoA, ATP and a cytosolic acyl-CoA synthetase (EC. 6.2.1.3) tethered to the outer membrane of the mitochondrion to generate an acyl-CoA thioester (Roe & Coates, 1995). Carnitine palmitoyl transferase I (CPT-I; EC. 2.3.1.21) allows transfer of the acyl group to carnitine and forms acyl-carnitine and free CoA in the cytosol. Given that β -oxidation occurs in the matrix (but the inner membrane is not directly permeable to long chain fatty acyl-CoA esters) the carnitine-acylcarnitine translocase exists to “shuttle” such molecules into the matrix (reviewed in Brivet *et al.*, 1999). A

permease in the mitochondrial membrane is responsible for the antiporter action. Acyl-carnitine is exchanged for carnitine by the antiporter mechanism described. Once inside the mitochondrion, the esterification reverses (via CPT II), forming acyl-CoA and free carnitine. Carnitine is subsequently exported to the cytosol via the transport mechanism described.

β -oxidation proper involves four enzymatic steps: an initial dehydrogenation, hydration, a further dehydrogenation and finally thiolysis to yield acetyl-CoA (reviewed in Wanders *et al.*, (1999); Fig 1.7).

An acyl-CoA dehydrogenase (EC. 1.3.99.3) eliminates two hydrogen atoms from the acyl-CoA leading to the formation of a double bond between the α & β carbons of the acyl chain; the product is termed enoyl-CoA. 4 isoforms of the enzyme have been identified, each of which is specific with respect to the length of acyl chain which is being saturated. These are the short-chain acyl-CoA dehydrogenase (SCAD; EC. 1.3.99.2), medium-chain acyl-CoA dehydrogenase (MCAD; EC. 1.3.99.3), long-chain acyl-CoA dehydrogenase (LCAD; EC. 1.3.99.13) and the very long-chain acyl-CoA dehydrogenase (VLCAD; EC. 1.3.99.18). The reaction requires FAD as a cofactor and acts to accept electrons from the acyl-CoA molecule, becoming reduced to FADH₂. Subsequently, the latter is re-oxidised to FAD by donation of these electrons to the electron transfer flavoprotein (ETF; Crane and Beinert, 1956). These electrons are used to pass electrons to ETF:ubiquinone oxidoreductase (EC. 1.5.5.1). This then reduces ubiquinone to ubiquinol (Beckmann and Frerman, 1985), which in turn feeds into the ETC as described previously.

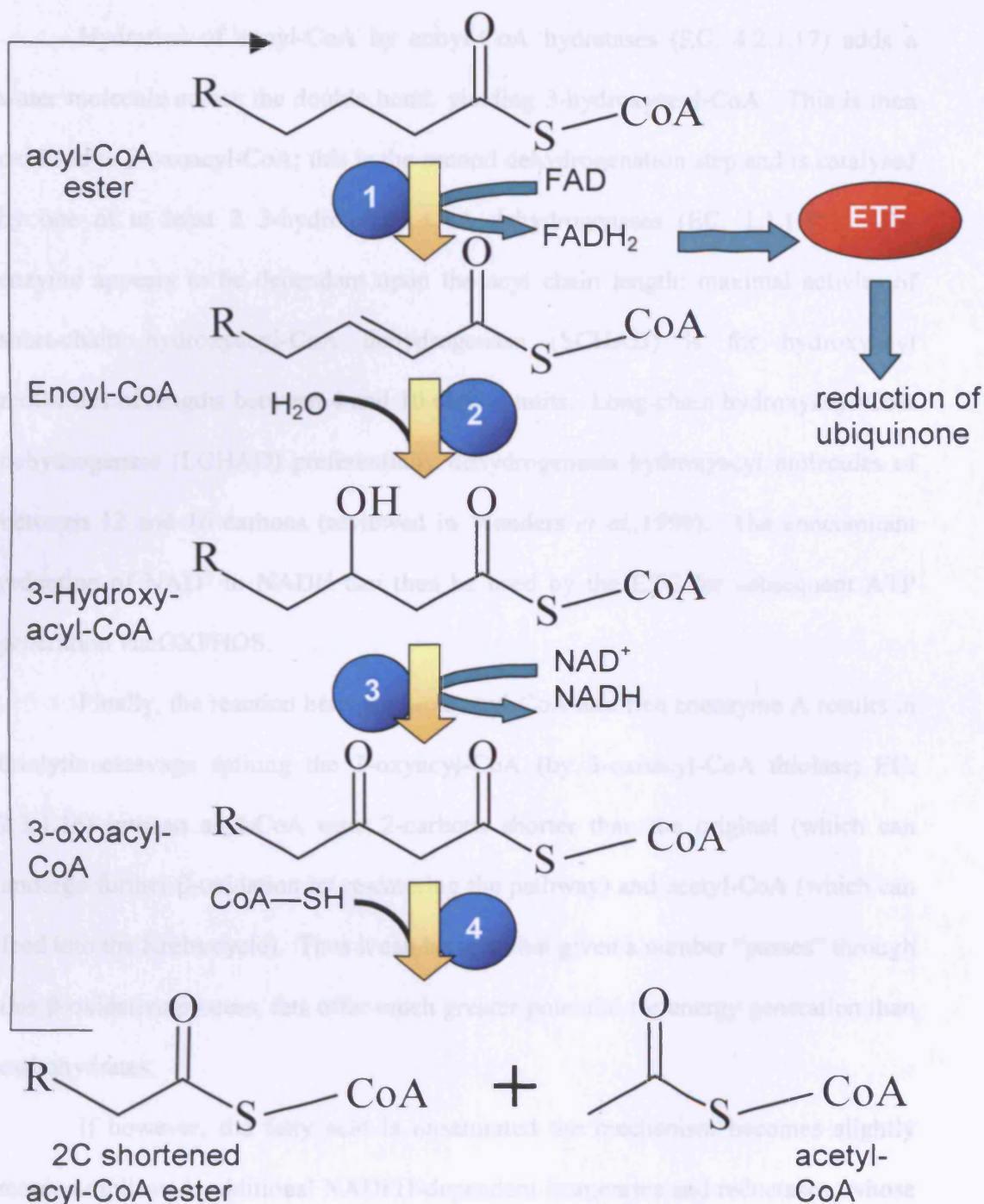


Figure 1.7. Mitochondrial β -oxidation of fatty acids.

Following carnitine shuttling of long chain fatty acids into the mitochondrial matrix, they are shortened as described in the text. This generates NADH, FADH₂ and acetyl CoA. The enzymes involved (signified ●) are 1: acyl-CoA dehydrogenases; 2: enoyl-CoA hydratases; 3: 3-hydroxyacyl-CoA dehydrogenases and 4: thiolases. FADH₂ generated can subsequently reduce the electron transfer flavoprotein (●), which can reduce ubiquinone.

Hydration of enoyl-CoA by enoyl-CoA hydratases (EC. 4.2.1.17) adds a water molecule across the double bond, yielding 3-hydroxyacyl-CoA. This is then oxidised to β -oxoacyl-CoA; this is the second dehydrogenation step and is catalysed by one of at least 2 3-hydroxyacyl-CoA dehydrogenases (EC. 1.1.1.35). The enzyme appears to be dependant upon the acyl chain length: maximal activity of short-chain hydroxyacyl-CoA dehydrogenase (SCHAD) is for hydroxyacyl molecules of lengths between 4 and 10 carbon units. Long-chain hydroxyacyl-CoA dehydrogenase (LCHAD) preferentially dehydrogenates hydroxyacyl molecules of between 12 and 16 carbons (reviewed in Wanders *et al.*, 1999). The concomitant reduction of NAD^+ to NADH can thus be used by the ETC for subsequent ATP generation via OXPHOS.

Finally, the reaction between 3-oxoacyl-CoA and free coenzyme A results in thiolytic cleavage splitting the 3-oxoacyl-CoA (by 3-oxoacyl-CoA thiolase; EC. 2.3.1.16) into an acyl-CoA ester 2-carbons shorter than the original (which can undergo further β -oxidation by re-entering the pathway) and acetyl-CoA (which can feed into the Krebs cycle). Thus it can be seen that given a number “passes” through this β -oxidative process, fats offer much greater potential for energy generation than carbohydrates.

If however, the fatty acid is unsaturated the mechanism becomes slightly more complicated: additional NADPH-dependant isomerases and reductases (whose specificity depends upon the number and positions of the double bonds) are involved. β -oxidation of fatty acids with an odd number of carbons also requires additional steps. The final formation of propionyl-CoA is converted to S-

methylmalonyl-CoA by the addition of one carbon for which ATP hydrolysis is necessary. A racemase converts this isomer to R-methylmalonyl-CoA and a mutase requiring coenzyme B₁₂ as a cofactor forms succinyl-CoA; the latter can enter the Krebs cycle as described previously.

1.2.3. Ketone Body metabolism

“Ketone bodies” is a term describing acetone, acetoacetate and 3-hydroxybutyrate. These metabolites are formed from acetyl-CoA under conditions of starvation when oxaloacetate tends to be diverted away from the Krebs cycle for use in gluconeogenesis (discussed in Girard *et al.*, 1992). In such “overflow” situations, ketone body metabolism becomes a valuable source of succinate and acetyl-CoA for the Krebs cycle, and NADH for OXPHOS (see Mitchell *et al.*, 1995 for a review). Mitochondrial involvement in this pathway comes from the localisation of key enzymes in this organelle in the liver. Two acetyl-CoA molecules condense in the presence of mitochondrial acetoacetyl-CoA thiolase (EC. 2.3.1.9) to form acetoacetyl CoA and free coenzyme A (Fig 1.8). Acetoacetyl-CoA then further condenses with another acetyl-CoA in the presence of 3-hydroxy-3-methylglutaryl-CoA (HMG-CoA) synthase (EC. 2.3.3.10) to form HMG-CoA. The action of HMG-CoA lyase (which is also mitochondrial; EC 4.1.3.4) forms acetoacetate and acetyl-CoA. While the latter can enter the Krebs cycle directly, mitochondrial 3-hydroxybutyrate dehydrogenase (EC. 1.1.1.30) reduces acetoacetate to 3-hydroxybutyrate in the presence of NADH. While the use of ketone bodies as an energy source can occur more readily in high energy dependent tissues such as

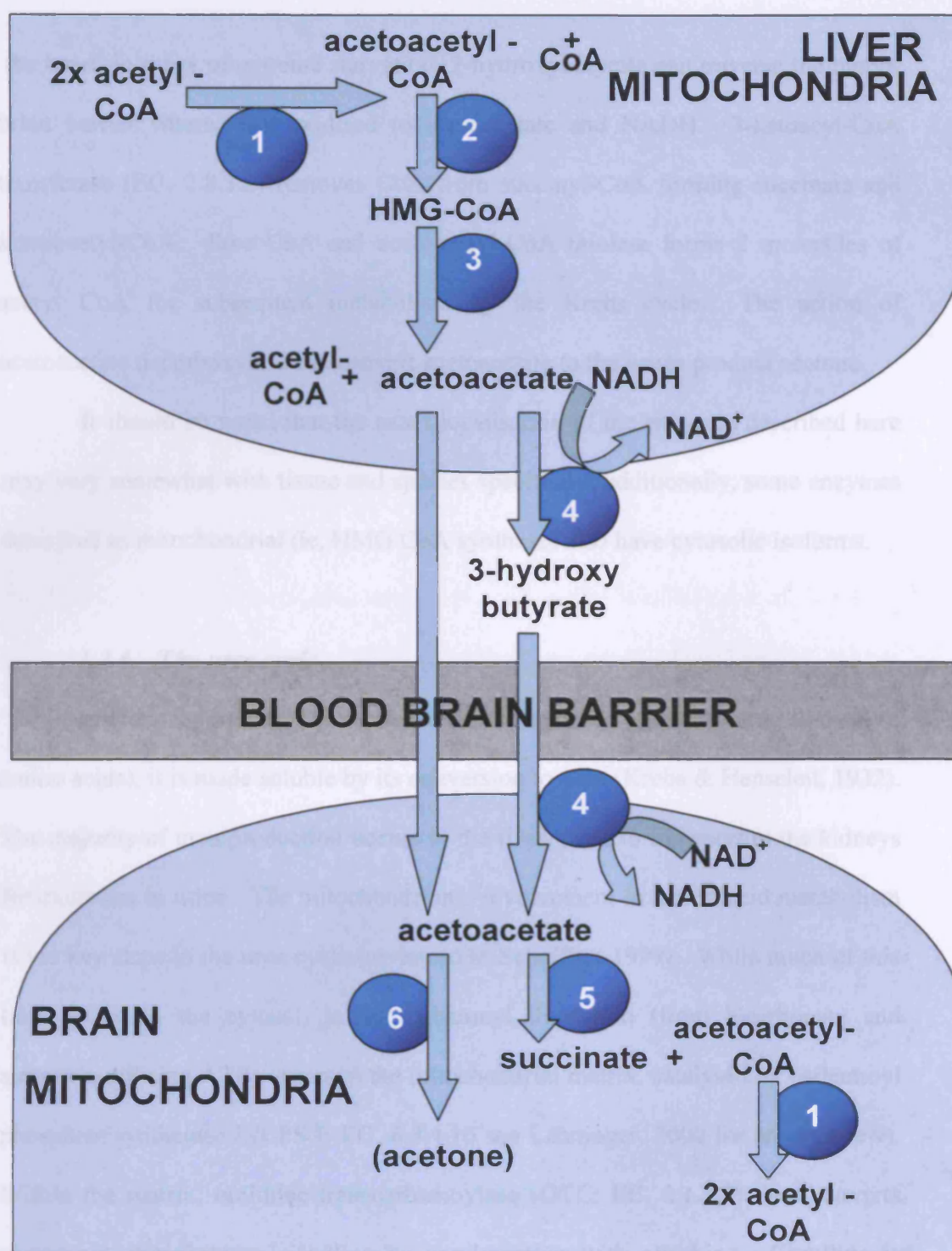


Figure 1.8. Ketone body metabolism.

Ketone bodies are formed predominantly in the liver and transported in the blood as acetoacetate and 3-hydroxybutyrate. Extra-hepatic tissues (including in extreme cases, the brain) can use ketone bodies as a source of acetyl-CoA for the Krebs cycle, succinate can enter the Krebs cycle or the ETC; and NADH can be used substrate for complex I of the ETC. The enzymes (●) are 1: acetoacetyl CoA-thiolase; 2: HMG-CoA synthase; 3: HMG CoA lyase; 4: 3-hydroxybutyrate dehydrogenase; 5: 3-ketoacyltransferase; 6: acetoacetate decarboxylase

the heart, in times of extreme starvation, 3-hydroxybutyrate can traverse the blood-brain barrier where it is oxidised to acetoacetate and NADH. 3-ketoacyl-CoA transferase (EC. 2.8.3.2) removes CoA from succinyl-CoA forming succinate and acetoacetyl-CoA. Free CoA and acetoacetyl-CoA thiolase forms 2 molecules of acetyl CoA for subsequent metabolism by the Krebs cycle. The action of acetoacetate decarboxylase can convert acetoacetate to the waste product acetone.

It should be noted that the exact localisation of the enzymes described here may vary somewhat with tissue and species specificity; additionally, some enzymes described as mitochondrial (ie, HMG CoA synthase) also have cytosolic isoforms.

1.2.4. The urea cycle

In order for animals to excrete excess nitrogen (obtained from metabolism of amino acids), it is made soluble by its conversion to urea (Krebs & Henseleit, 1932). The majority of urea production occurs in the liver, prior to transport to the kidneys for excretion in urine. The mitochondrion's involvement in amino acid metabolism is via key steps in the urea cycle (reviewed in Scheffler, 1999). While much of this takes place in the cytosol, initial carbamoyl formation (from bicarbonate and ammonia utilising ATP) occurs in the mitochondrial matrix, catalysed by carbamoyl phosphate synthetase I (CPS I; EC. 6.3.4.16 see Lehninger, 2000 for an overview). Within the matrix, ornithine transcarbamoylase (OTC; EC, 2.1.3.3) then converts carbamoyl phosphate to citrulline by condensation with ornithine. Citrulline is exported to the cytosol, and following condensation with aspartate by argininosuccinate synthetase (EC. 6.3.4.5) yielding argininosuccinate. The action of

argininosuccinase releases fumarate and arginine; the latter releases urea for excretion following hydrolysis by arginase (EC. 3.5.3.1). The resultant ornithine can then re-enter the mitochondrion, where it condenses with carbamoyl phosphate (catalysed by OTC) to begin the cycle again.

1.2.5. Regulation of the life / death cycle

From existing knowledge of the respiratory function, and their role in generating ATP, mitochondria are essential for eukaryotic life. However, over the last two decades it has become apparent that mitochondria are also intimately involved in the regulation of apoptosis (Luo *et al.*, 1996; Srinivasula *et al.*, 1998) or necrosis (Crompton and Costi, 1988; Nazareth *et al.*, 1991). Additionally CoQ has recently been postulated as having a role in the modulation of mitochondrially mediated mechanisms of cell death.

As mentioned, mitochondria maintain an electrochemical gradient across the inner membrane resulting from proton transport from the matrix to the inter-membrane space. As cells undergo necrosis, this potential is lost, believed to occur as a result of the formation of a pore in the inner membrane; the permeability transition (PT) pore. Potential triggers of pore formation include loss of adenine nucleotides, elevated P_i , increased mitochondrial Ca^{2+} , and oxidative stress. The PT is formed by an association of ANT in the inner membrane with the voltage-dependant anion channel (VDAC) of the outer membrane at sites of contact (reviewed in Crompton, 1999). Cyclophilin D (CyP-D) is generally assumed to be a cyclosporine (Cs)-binding matrix protein, and associates with ANT on the matrix

site (although the physiological function of CyP-D and its role in PT pore formation remains to be completely elucidated; Crompton, 1999). CyP-D confers “Cs A-sensitivity” to the PT pore by blocking the pore following CsA binding (Szabo and Zoratti, 1991; Zoratti and Szabo, 1995). The diameter of the open pore is believed to be in the region of 2-2.5 nm, sufficiently large to allow matrix ions, metabolites proteins of up to 1500 Da to pass through. While transient pore opening, or very brief pore assembly has been proposed to have physiological functions, sustained opening of a number of pores will have hugely detrimental effects upon mitochondrial integrity: OXPHOS will effectively cease, ATP is further depleted due to hydrolysis via reversal of the F_1F_0 ATP synthase, osmotic swelling of the matrix occurs and crucially cytochrome *c* is released to the cytosol. Cytochrome *c* release has been proposed as a key factor in apoptotic death by promotion of caspase activation (Skulachev, 1996; Li *et al.*, 1997). However, apoptosis is an ATP-dependant process (Liu *et al.*, 1996). If the cell is ATP-deficient, necrosis may occur (reviewed in Martinou & Green, 2001).

Bcl-2 are a family of proteins which can be divided into pro- or anti-apoptotic factors. Bcl-2, Bcl-x_L are anti-apoptotic whereas the Bax subfamily (Bax, Bak and Bok) and the BH3 subfamily (including Bid, Bad and Bim) are conversely pro-apoptotic (Martinou and Green, 2001). In a process which is possibly distinct from PT pore formation, Bax proteins are also proposed to insert into the outer membrane, an action inhibited by the anti-apoptotic members. The insertion of such proteins also results in the release of pro-apoptotic factors. Moreover, these proteins may also co-operate either positively or negatively with the PT proteins (Marzo *et*

al., 1998). Whether cells die by apoptosis or necrosis may depend on upon the method mitochondrial disruption, and the cell's "competence" to undergo apoptosis. In this case, cytochrome *c* and ATP participate in the formation of the "apoptosome", a complex which assembles to activate the caspase cascade, and is triggered by cytochrome *c*.

It is possible that insertion of pro-apoptotic Bcl-2 proteins into the outer membrane allows initial maintenance of OXPHOS and thus apoptotic death. On the other hand, pathological opening of the PT pore has been suggested to cause matrix swelling, loss of membrane potential and thus ATP (Martinou and Green, 2001).

Recently, it has also been proposed that ubiquinone analogues may prevent the PT occurring, and thus inhibit cell death (Walter *et al.*, 2000; Armstrong *et al.*, 2003). In addition, an inhibitor of the Q₀ site on complex III inhibited ROS production, PT formation and cell death (Armstrong *et al.*, 2003). While it has been suggested that this is due to the free-radical scavenging ability of CoQ (Armstrong *et al.*, 2003), others propose more direct inhibition of activation by PT pore binding site interactions (Walter *et al.*, 2000; Papucci *et al.*, 2003)

Although a number of theories exist, the involvement of the mitochondrion, pore formation in the outer membrane and cytochrome *c* release is certain. However, the mechanism of cell death, and modulation of PT pore opening and / or formation remains a topic of intense debate.

1.3. Oxidative and nitrosative stress

1.3.1. ROS and free radicals

Free radicals are reactive molecules which exist independently yet contain one unpaired electron. Free radicals occur as byproducts of a number of biological reactions, and occur during phagocytosis by neutrophils and macrophages: oxygen is reduced by NADPH oxidase in lysosomes to destroy invading bacteria. In addition, the cytochrome P₄₅₀ oxygenases also generate radicals (Coon *et al.*, 1973) as can other oxidases such as monoamine oxidase (EC. 1.4.3.4) and xanthine oxidase (EC. 1.17.3.2; discussed in Halliwell and Gutteridge, 1999).

Gain of an electron by O₂ results in the formation of a superoxide radical (O₂^{•-}). O₂^{•-} molecules can pair up and dismutate to form hydrogen peroxide (H₂O₂), a reaction catalysed by superoxide dismutase (SOD; McCord & Fridovitch, 1969; Oury *et al.*, 1992). H₂O₂ can then be fully reduced to water, or partially reduced to the hydroxyl radical (OH[•]). Although H₂O₂, without any unpaired electrons is not strictly a radical, it is included as a reactive oxygen species (ROS). This term is used as an umbrella, covering a number of inter-related species such as O₂^{•-}, H₂O₂, and OH[•]. The hypochlorite ion (OCl⁻), like H₂O₂ also does not contain any unpaired electrons; however given its oxidative ability, it is also included when describing ROS.

Such molecules can have deleterious effects on a number of biological molecules including nucleic acids, cellular lipids, cytoskeletal proteins and enzymes (Halliwell and Gutteridge, 1999).

1.3.2. Mitochondrial free radical generation

Mitochondria, and specifically the ETC, have been implicated as a major source of ROS within the cell (Boveris & Chance, 1973). It has been proposed that between 1 and 3% of electrons passing through the ETC form $O_2^{\cdot -}$ (from Halliwell & Gutteridge, 1999). Thus “electron leak” from respiratory components of the ETC contributes markedly to $O_2^{\cdot -}$ levels in cells (reviewed in Turrens, 2003). Complexes I, II and III in the inner membrane have all been shown to have the ability to reduce oxygen to $O_2^{\cdot -}$ (reviewed in Turrens, 2003), ubiquinol is present in all membranes and may pass single electrons to oxygen, whilst in the outer membrane monoamine oxidase is capable of producing H_2O_2 . Tissue type may also be a factor: while complex III is believed to be responsible for most ROS production in lung and heart mitochondria (Turrens & Boveris 1980; Turrens *et al.*, 1982), in the brain, complex I may be the major source of $O_2^{\cdot -}$ (Barja & Herrero 1998). Additionally, if the ETC begins to become reduced (i.e. inhibition of “downstream” carriers causing electrons to “back-up”; “State 4 respiration”), then $O_2^{\cdot -}$ formation is more likely to occur (Scheffler, 1999; Turrens, 2003).

Complex III is often cited as a major producer of ROS within the mitochondrion (Boveris *et al.*, 1976; Han *et al.*, 2001; Chen *et al.*, 2003). The implication is that following removal of one electron from ubiquinol at the Q_0 site, the resultant semiquinone can become reduced to ubiquinol by passing an electron to O_2 in the aqueous phase thus generating $O_2^{\cdot -}$ (Nohl and Jordan, 1986; Chen *et al.*, 2003).

1.3.3. *Physiological NO generation*

Nitric oxide (NO) is formed in a number of tissues including neural, vascular and immune cells. Its role as a signaling molecule has been implicated in diverse physiological processes such as neurotransmission, memory formation, immune response and vasodilatation (reviewed in Lincoln *et al.*, 1997 and Duncan and Heales, 2005). Formed when the guanidino nitrogen of L-arginine reacts with molecular oxygen in the presence of nitric oxide synthase (NOS EC. 1.14.13.39), various cofactors are necessary including tetrahydrobiopterin (BH₄), FMN and NADPH. NO is also a free radical, and can react with a number of ROS to produce reactive nitrogen species (RNS) such as the nitroxyl and peroxynitrite anion (NO⁻ and ONOO⁻ respectively), nitrosonium cation (NO⁺) and the NO radical itself.

At least three isoforms of NOS are known to exist, denoted NOS I, II, and III. NOS I (nNOS) is found as a cytosolic Ca²⁺-dependant enzyme in central and peripheral neurons (Knowles *et al.*, 1989; Gillespie *et al.*, 1989). Intracellular calcium above approximately 400nM allows Ca²⁺-calmodulin binding of NOS. As Ca²⁺ is very rapidly cleared from the cell, calmodulin dissociates from NOS, allowing tight control over NO production in neurons (Bredt and Snyder, 1990). Given the nature of the molecule, and the products formed in its reaction with ROS, it is unsurprising that inappropriate NO generation by NOS I is implicated in a number of pathologies (reviewed in Lincoln *et al.*, 1997 and Duncan & Heales, 2005)

NOS II (iNOS) is also cytoplasmic, and was initially reported in macrophages (Marletta, *et al.*, 1988; Hibbs *et al.*, 1988) and is now known to exist in

a number of immune cell types including astroglia (Simmons and Murphy 1992). However, under basal conditions this inducible form of NOS is not expressed. Under transcriptional control, (Xie *et al.*, 1993; reviewed by MacMicking *et al.*, 1997) NOS II activity is not Ca^{2+} -dependant; instead it is already bound to calmodulin (Cho *et al.*, 1992). Thus it is able to generate large amounts of NO for much longer periods of time than the other constitutive isoforms: whereas NOS I and NOS III generate picomolar concentrations of NO, NOS II may generate in the nanomolar range (Anggard, 1994). Stimulation of NOS II can be initiated by pro-inflammatory mediators such as bacterial membrane products and endogenous cytokines including γ -interferon ($\text{IFN}\gamma$), interleukin-1 (IL-1), and tumour necrosis factor- α ($\text{TNF}\alpha$) (Bolaños *et al.*, 1994; reviewed in Murphy *et al.*, 1993 and MacMicking *et al.*, 1997).

It is important that NOS II induction occurs with a concomitant increase in the cofactor BH_4 . If BH_4 availability is limiting, NOS II has been proposed to preferentially generate $\text{O}_2^{\cdot -}$. Such a situation would have the potential to generate $\text{ONOO}^{\cdot -}$, a stronger oxidant than either NO or $\text{O}_2^{\cdot -}$ (Consentino *et al.*, 2001).

NOS III is targeted to caveolae, small invaginations in the cell membrane. This isoform is, like NOS I, dependant on Ca^{2+} binding calmodulin and subsequently NOS to allow NO synthesis. The main action of NO thus generated is to act as a vasodilator in smooth muscle, particularly that allowing fine local control of the vasculature such as endothelial cell membranes (for reviews see Moncada *et al.*, 1991 and Alderton *et al.*, 2001). In the endothelial cell, a major activator of NOS III

activity is mechanical shear stress resulting from blood flow within the vessel (Buga *et al.*, 1991).

A novel isoform of NOS has been reported in mitochondria. Mitochondrial NOS (mtNOS) was first proposed a decade ago (Bates *et al.*, 1995, 1996) and was proposed as a physiological regulator of the ETC at the level of complex IV. Later postulated as a splice variant of NOS I rather than a novel NOS isoform (Kanai *et al.*, 2001, 2003), conflictingly mtNOS was found to be reactive to NOS II antibodies, but not those for NOS I or III (Tatoyan & Giulivi, 1998). However, recent works by Lacza *et al.* (2003, 2004) and Tay *et al.*, (2004) have refuted the hypothesis of the presence of physiologically relevant mtNOS in a number of models. Although the subject of a recent review (Haynes *et al.*, 2004), it is likely that until a gene encoding a NOS protein with a mitochondrial targeting sequence is found, the issue will remain unresolved.

1.4. Introduction to Ubiquinone

1.4.1. Historical background and nomenclature

Ubiquinone (also termed Co-enzyme Q; CoQ) describes a series of homologous quinones widely distributed in nature. "Ubiquinone" was first described by Festenstein and co-workers in 1955, who used the term to denote the ubiquitous nature of a molecule found in many tissues. In 1957, Crane *et al.* suggested that "Co-enzyme Q" was a component of the ETC, and the following year Karl Folkers' group determined the structure (Fig. 1.3; Wolf *et al.*, 1958) confirming the findings of Festenstein *et al.*, (1955). However, it was not until 1975 that the IUPAC-IUB

Commission of Biochemical Nomenclature deemed that "ubiquinone" be the official name of the molecule. (IUPAC-IUB, 1975) However, the fact that ubiquinone describes a *series* of quinones means that in fact CoQ with a numerical subscript is probably a more accurate term when describing structural isoforms. Although IUPAC nomenclature does not dictate which molecular mass isoform is being referred to, it does however give insight into the redox state: ubiquinol describes the reduced molecule (CoQH_2), ubiquinone for the oxidised form and ubisemiquinone the intermediate (Fig. 1.3).

1.4.2. Structure and biosynthesis

The molecule can be split into two distinct moieties: a six-membered carbon ring, with 2 delocalised oxygens at positions 1 and 4 (the quinone), and a "tail" section comprising a chain of repeating isoprenyl units. The number of repeats is denoted by the numerical subscript used in the nomenclature of CoQ (i.e. CoQ_9 , CoQ_{10}).

The biosynthetic pathway was originally determined in bacteria and although not fully elucidated, is believed to be similar in mammals. However this assumption must be treated with a degree of caution, as although two mammalian genes involved in biosynthesis have been identified (Vajo *et al.*, 1999; Johanssen and Clarke, 2000) no mammalian enzymes involved in the pathway have as yet been purified or cloned (Dallner and Sindelar, 2000; Turunen *et al.*, 2004). The pathway has two distinct "arms" (Fig. 1.9): the formation of the six-membered benzoquinone ring from tyrosine, and the mevalonate pathway forming the isoprenyl tail from

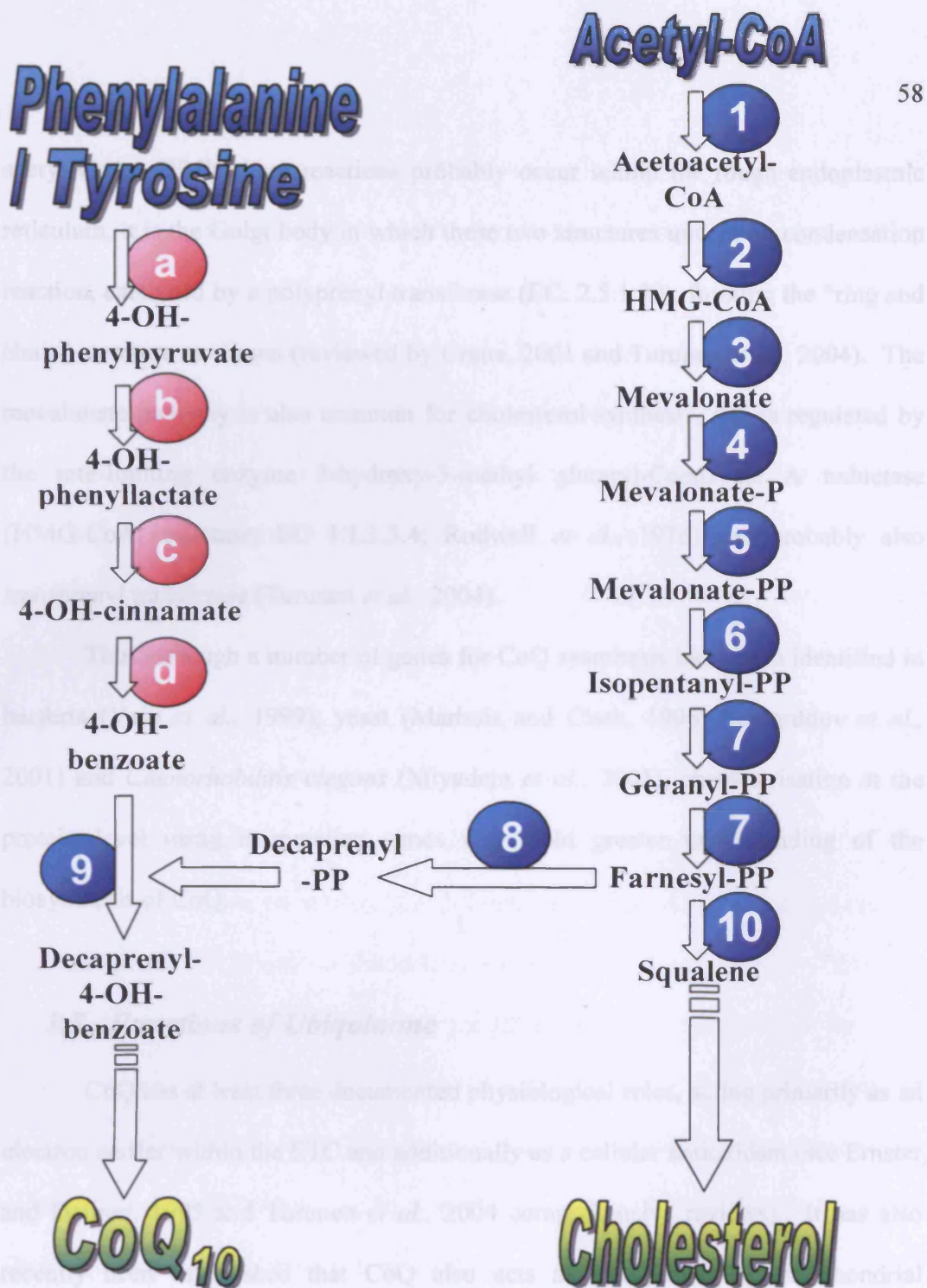


Figure 1.9. The CoQ₁₀ biosynthetic pathway.

The benzoquinone nucleus is derived from tyrosine or phenylalanine; the mevalonate pathway responsible for the synthesis of the isoprenyl side-chain is better understood in mammals. Confirmed enzymes (●) are: 1: acetoacetyl CoA-thiolase; 2: HMG-CoA synthase; 3: HMG-CoA reductase; 4: mevalonate kinase; 5: phosphomevalonate kinase; 6: mevalonate-PP decarboxylase; 7: farnesyl-PP synthase; 8: transprenyl transferase; 9: decaprenyl 4-OH-benzoate transferase; 10: squalene synthetase. Postulated enzymes (●) involved in CoQ synthesis are a: tyrosine transaminase; b: 4-OH-phenyllactate dehydrogenase; c and d represent single or multiple enzymes involved in dehydroxylation and β -oxidation respectively. CoA = coenzyme A; HMG = 3-hydroxy-3-methylglutaryl; PP=pyrophosphate

acetyl CoA. While these reactions probably occur within the rough endoplasmic reticulum, it is the Golgi body in which these two structures undergo a condensation reaction, catalysed by a polyprenyl transferase (EC. 2.5.1.39), forming the "ring and chain" structure as shown (reviewed by Crane, 2001 and Turunen *et al.*, 2004). The mevalonate pathway is also common for cholesterol synthesis, and is regulated by the rate-limiting enzyme 3-hydroxy-3-methyl glutaryl-Coenzyme A reductase (HMG-CoA reductase; EC 1.1.1.3.4; Rodwell *et al.*, 1976) and probably also transprenyl transferase (Turunen *et al.*, 2004).

Thus although a number of genes for CoQ synthesis have been identified in bacteria (Vajo *et al.*, 1999), yeast (Marbois and Clark, 1996; Belogrudov *et al.*, 2001) and *Caenorhabditis elegans* (Miyadera *et al.*, 2001), characterisation at the protein level using mammalian genes will yield greater understanding of the biosynthesis of CoQ.

1.5. Functions of Ubiquinone

CoQ has at least three documented physiological roles, acting primarily as an electron carrier within the ETC and additionally as a cellular antioxidant (see Ernster and Dallner, 1995 and Turunen *et al.*, 2004 comprehensive reviews). It has also recently been established that CoQ also acts as a cofactor for mitochondrial uncoupling proteins (UCPs) (Echtay *et al.*, 2000, 2001).

1.5.1. CoQ as an antioxidant

Although electron transfer takes place within the inner membrane of the mitochondrion, it should be borne in mind that CoQ is found in all cellular membranes. In its fully reduced form ubiquinol, the molecule acts as an antioxidant, protecting cellular lipids, proteins and DNA against the potentially toxic effects of radical damage, usually as a result of nitrosative/oxidative stress. This would appear to be particularly relevant in mitochondria, given that the ETC is a major source of oxidising species (Liu *et al.*, 2002, Chen *et al.*, 2003). Within the past decade, it has also been shown that ubiquinol can reduce tocopheryl radicals and semidehydroascorbate back to α -tocopherol and ascorbate respectively (Constantinescu, *et al.*, 1994, Villalba, *et al.*, 1995). Thus CoQ has a significant secondary antioxidant function which should not be overlooked.

In many tissues, the quinol form predominates, especially the pancreas where none appears to be present in the oxidised form (Åberg *et al.*, 1992). However, variability between tissues is evident as the same study also noted that in the brain only 23% is present as ubiquinol. Given the susceptibility for this organ to damage as a result of oxidative stress, the role of ubiquinone as potential neuroprotective agent continues to be investigated by a number of groups (Beal and Matthews, 1997; Shults *et al.*, 1997; Di Giovanni *et al.*, 2001; Shults *et al.*, 2002)

CoQ short chain homologues are more effective antioxidants than longer chain subtypes *in vitro*, although side chain length of CoQ₅ through CoQ₁₀ may have little effect on reactivity *in vitro* (Kagan *et al.*, 1990). Thus the role of the side chain

may be to modulate hydrophobicity (and thus the position within the membrane) and possibly ETC complex binding.

1.5.2. Electron transfer

The role of CoQ as an electron carrier in the ETC is facilitated by the chemical properties of the molecule: it can diffuse freely within the membrane without "leaking" into the aqueous phase, and easily cycle between redox states. Its lipid nature dictates that ubiquinone binds complex I in a membrane-bound domain. Upon accepting electrons from complex I, a single carbonyl group on the six-membered ring becomes reduced to the O[•] (ubisemiquinone) form. A second electron will further reduce this to ubiquinol. Similarly, complex II reduces ubiquinone to the quinol form, and the carrier subsequently binds to complex III. Upon binding the Q₀ site in its reduced form (and Q₁ in the oxidised state), the electrons are transferred to cytochrome *c*, and ubiquinone re-generated. Electron transfer is directly coupled to the pumping of protons from the matrix to the intra-membrane space (reviewed in Scheffler, 1999).

It is likely that CoQ populates the membrane as a homogeneous "pool" (Kröger and Klingenberg, 1973), although some will remain protein-bound. The model proposed by Kröger and Klingenberg represents a freely diffusible pool, interacting with the complexes as a result of random Brownian collisions. This has recently been challenged by the suggestion of Schägger and Pfiffer (2001) that the ETC may exist as a series of supercomplexes. Subsequently, it may be necessary to reconsider the nature of the CoQ pool (reviewed in Lenaz, 2001).

While it is generally believed that ubiquinones with side chains of differing length probably have the same physiological role, there is a body of evidence accumulating which may suggest the contrary. As a general rule, short-lived animals (such as rodents) utilise CoQ₉ while in longer-lived species CoQ₁₀ predominates (Ramasara, 1985). Given ubisemiquinone's conversion to ubiquinone at complex III can reduce molecular oxygen to superoxide (O₂⁻) (Liu *et al.*, 2002; Chen *et al.*, 2003), Lass and co-workers measured O₂⁻ generation in nine different mammalian species with varying CoQ₉ : CoQ₁₀ ratios (Lass *et al.*, 1997). It was found that the amount of O₂⁻ generated by the ETC of sub-mitochondrial particles was directly correlated to the amount of CoQ₉ and inversely correlated to the amount of CoQ₁₀ (Fig. 1.10). This group also suggested that CoQ₁₀ was a more effective antioxidant than CoQ₉. Thus although the molecular structural differences of the two isoforms are relatively minor, the difference in hydrophobicities may have an effect on the molecule's position in the bilayer, including the inner mitochondrial membrane. The resultant functional differences between CoQ₉ and CoQ₁₀ have been investigated by Edlund *et al.*, 1994. This study infected rat neurons with Sendai virus and mumps virus causing cell death in a large proportion of neurons. It was noted that following viral treatment, ubiquinone levels were lower than in untreated cells. Moreover, CoQ₁₀ depletion was more profound than that of CoQ₉ (Edlund *et al.*, 1994). Addition of CoQ₁₀ but not CoQ₉ conferred protection to those neuronal cultures, resulting in increased cell survival. As oxidative stress is implicated in neuronal death due to viral infection, it is possible that CoQ₁₀ is acting as an antioxidant, whereas CoQ₉ does not. This may support the work of Matsura *et al.*,

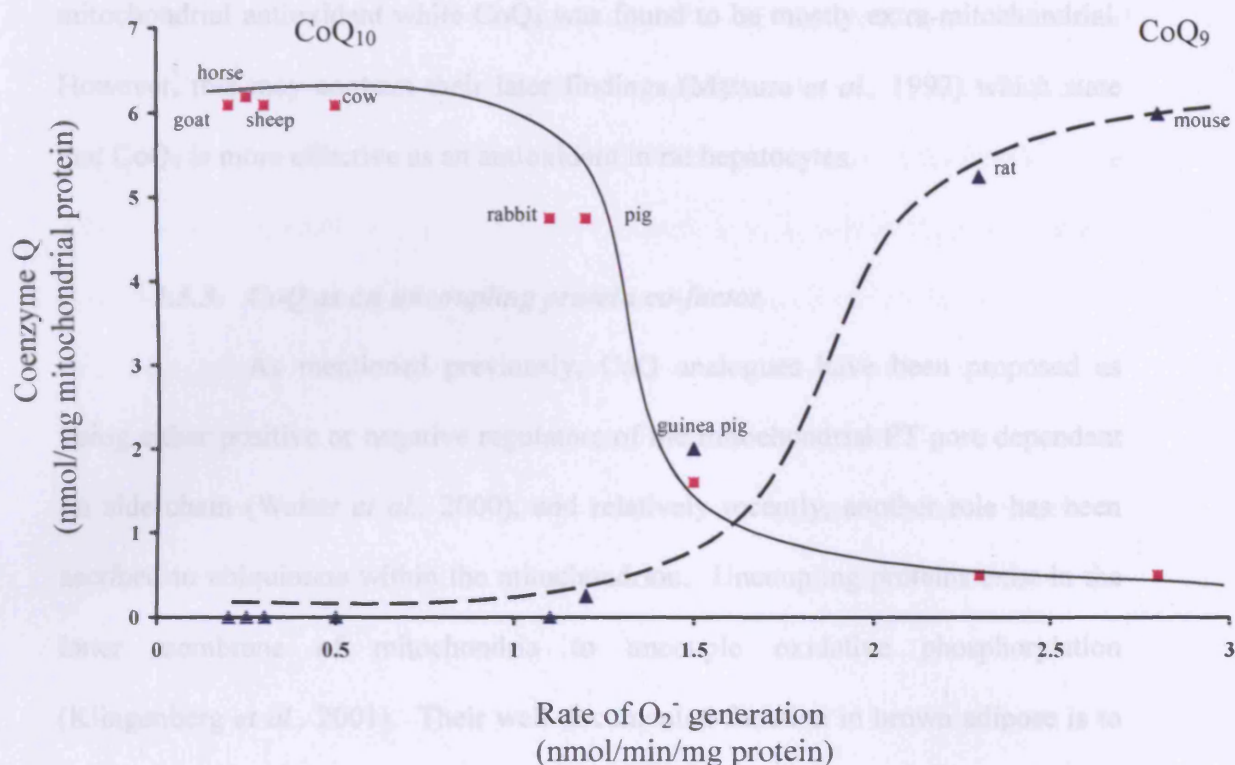


Fig. 1.10. Relationship between the rates of O_2^- generation and the amount of CoQ extractable from mitochondria (from Lass et al., 1997).

Data from studies conducted by Sohal and co-workers lends support to the hypothesised functional differences between CoQ₉ and CoQ₁₀. Here, the rate of O_2^- generation in cardiac sub-mitochondrial particles from nine mammalian species was measured, and plotted against the amount of CoQ₉ (▲) and CoQ₁₀ (■) in that species. This direct correlation between CoQ₉ and the inverse correlation between CoQ₁₀ and O_2^- generation may support a link between the relative abundance of CoQ₁₀ and longevity.

(1991) who postulate that in Japanese white rabbit liver cells CoQ₁₀ acts as a mitochondrial antioxidant while CoQ₉ was found to be mostly extra-mitochondrial. However, this may contrast their later findings (Matsura *et al.*, 1992) which state that CoQ₉ is more effective as an antioxidant in rat hepatocytes.

1.5.3. CoQ as an uncoupling protein co-factor

As mentioned previously, CoQ analogues have been proposed as being either positive or negative regulators of the mitochondrial PT pore dependant on side chain (Walter *et al.*, 2000), and relatively recently, another role has been ascribed to ubiquinone within the mitochondrion. Uncoupling proteins exist in the inner membrane of mitochondria to uncouple oxidative phosphorylation (Klingenberg *et al.*, 2001). Their well-documented function in brown adipose is to allow thermogenesis (reviewed by Kingenberg *et al.*, 2001). Achieved by the “futile” dissipation of the proton gradient rather than flow through the ATP synthase, UCP’s allow the flow of protons back into the matrix, and the conversion of this energy to heat. Thus it is evident that mitochondrial uncoupling must be tightly regulated in order to avoid excessive dissipation of the proton gradient and subsequent inhibition of ATP synthesis. Oxidised CoQ₁₀ has been identified as a cofactor for UCP activation for UCP 1 (Echtay *et al.*, 2000), and subsequently for UCP2 and UCP3 whose primary functions are not yet completely understood (Echtay *et al.*, 2001).

UCP’s have been shown to increase proton conductance in response to superoxide O₂⁻ generation (Echtay *et al.*, 2002a), and this has been shown to occur

from the matrix side (Echtay *et al.*, 2002b). Thus it has been proposed that UCP 2 and UCP3 open at time of excessive mitochondrial ROS generation to either clear intramatrix O_2^- where they may undergo more rapid dismutation due to the lower pH or scavenging by antioxidants (Echtay *et al.*, 2002b) or alternatively by oxidising the ETC to decrease ROS production. UCP2 activation was postulated to occur under conditions in which the ETC was reduced (by KCN-induced inhibition of complex IV); subsequently CoQ will be mostly in the reduced state (Echtay *et al.*, 2002b). While these authors proposed that only oxidised ubiquinone would participate in UCP1 uncoupling (Echtay *et al.*, 2000), later works suggested the quinol form of mitochondrially-targeted CoQ was necessary for uncoupling of UCP2 (Echtay *et al.*, 2002b).

1.6. Human Ubiquinone Deficiency

Having considered some aspects of the physiological roles of ubiquinone, its key role within the ETC is evident. In man, disruption of the ETC leads to defects of mitochondrial respiratory function, leading to a clinical condition termed mitochondrial cytopathy (see Wallace, 1999 for a review). Such dysfunctional mitochondria are usually the result of inborn errors of metabolism, and the arising conditions are considered largely untreatable. However, conditions ascribed to a deficiency in ubiquinone may be amenable to therapeutic intervention following early and accurate diagnosis (Rotig *et al.*, 2000).

Human CoQ₁₀ deficiency can be dominated by myopathic or cerebellar involvement, and usually presents within the first two years of life (Boitier *et al.*,

1998; Ogashara *et al.*, 1989; Rahman *et al.*, 2001; Van Maldergem *et al.*, 2002). Symptoms may include ataxia and dystonia, developmental delay, myopia and visual loss possibly due to retinitis pigmentosa and /or optic nerve atrophy. Renal and cardiac complications may also be evident, and the symptoms associated with most mitochondrial encephalomyopathies are usually progressive. However, mitochondrial encephalomyopathies are usually diagnosed by enzymatic assays following skeletal muscle biopsy to determine activities of the mitochondrial complexes and intermediates (Heales *et al.*, 1995).

In 2001, Rahman and co-workers reported a case of a neonate presenting with ubiquinone deficiency (Rahman *et al.*, 2001). A baby boy presented at 6 hours with "poor feeding, hypothermia and shaking of both arms". Increased peripheral muscle tone was evident, MRI scans demonstrated cerebral and cerebellar atrophy, and peripheral conditions including renal tubulopathy, cardiac hypertrophy and hypokinesia prompted biochemical investigation.

Ubiquinone deficiency in humans can be diagnosed by determination of the CoQ₁₀ concentration of a skeletal muscle biopsy and following determination of the enzymatic activities of the mitochondrial complexes, in particular the combined activity of complexes II+III as this assay relies upon the presence of endogenous ubiquinone (Clark *et al.*, 1994), CoQ₁₀ determination can be achieved by high-performance liquid chromatography (HPLC). The patient values are shown in Table 1.1, and it can be seen that while the activities of the separate complexes are within the reference range, the linked II+III assay in the absence of exogenous ubiquinone (CoQ₁) was undetectable. In the presence of CoQ₁, the value of the complex II+III

Assay	Patient Value	Paediatric reference range
Complex I	0.163	0.104-0.268
Complex II+III	<0.001	0.04-0.204
Complex II+III+CoQ ₁	0.098	0.04-0.204
Complex IV	0.018	0.014-0.340
Complex II	0.151	0.052-0.258
Complex III	0.026	0.008-0.028
CoQ ₁₀ (pmol/ mg protein)	37	140 - 580
Plasma lactate pre-CoQ ₁₀ (mmol/L)	7.6	0.9-1.9
Plasma lactate post-CoQ ₁₀ (mmol/L)	2.5-2.9	0.9-1.9

Table 1.1. Muscle ETC enzyme activities with ubiquinone concentration and plasma lactate values

(From Rahman *et al.*, 2001). Expressed against citrate synthase (CS) activity, these values would suggest a ubiquinone deficiency, given the marked increase in the complex II+III activity in the presence of exogenous ubiquinone (CoQ₁). Plasma lactate values before and after CoQ₁₀ therapy (up to 300 mg/day) are also shown.

assay fell within the existing reference range. Additionally, elevated plasma lactate is not uncommon in patients with suspected ubiquinone deficiency, and as shown in Table 1.1, the lactate concentration as measured from this patient was clearly outside the accepted reference range.

Following administration of oral CoQ₁₀ at 11.5 months, (initially 60 mg/day, increasing to 300 mg/day), lactate levels decreased from 7.6 mmol/L (at the beginning of therapy) to 4.4 mmol/L on day 11, to 2.5 mmol/L by 4 months. Unfortunately, the decrease in lactate concentration was not accompanied by a clinical improvement of symptoms and the patient died at 2 years. Although the observed decrease in plasma lactate may be due to a greater availability of CoQ₁₀ as a result of supplementation, this cannot be confirmed, as consent was not obtained for a post-mortem examination (Rahman *et al.*, 2001).

Although CoQ-deficient states may present within the first few years of life, some adult cases have been documented (Ogashara *et al.*, 1986; Van Maldergem *et al.*, 2002). The latter publication documents the case of 2 sisters, then aged 31 and 34 both having previously been diagnosed with Leigh's Syndrome (LS) as infants and displaying a similar catalogue of clinical symptoms. However, CoQ₁₀ deficiency was not detected. In addition to the developmental delay, increased lactate : pyruvate ratio and basal ganglial lesions indicative of LS, at 4 years, the younger sister displayed ptosis, muscle wasting, spasticity, and required orthopaedic shoes to allow her to walk. She later became deaf and failed to undergo puberty. At 19 years, the only mitochondrial abnormality detected was a mild complex I deficiency in fibroblasts; in skeletal muscle biopsy, complex II+III activity was

normal. At 24 years her general condition worsened, she refused feeding, rapidly began to lose weight and became bedridden. A muscle biopsy was again performed and this time found decreased complex II+III activity. Following addition of exogenous decylubiquinone to the assay reaction mixture, this activity increased eightfold bringing the patient values inside the control range. Moreover, determination of muscle CoQ₁₀ concentration in this patient revealed levels around 5% of the normal mean. Analysis CoQ₁₀ in lymphoblastoid cultures revealed a decrease of around 50% (Van Maldergem *et al.*, 2002).

Administration of exogenous CoQ₁₀ (300 mg/day) at age 24 improved her clinical profile dramatically. Within 15 days muscle abnormalities had decreased, eating resumed and she regained the ability to walk. 7.6kg was gained within 6 months and she underwent puberty at 26 years. By 29 years, the patient had grown 20 cm in height in the 5 years since beginning CoQ₁₀ therapy.

The later biochemical analyses of mitochondrial complex activities of this patient suggested a primary CoQ₁₀ deficiency (Van Maldergem *et al.*, 2002). This was supported by the findings of lowered levels of CoQ₁₀ in both muscle and lymphoblastoid cells. Subsequent oral supplementation with exogenous CoQ₁₀ was clearly beneficial in improving her condition.

When considering the role of mitochondria in the neurodegenerative process, it is unsurprising that these disorders manifest themselves with neurological symptoms. Bearing in mind the neuron's susceptibility to damage following an energy deficit, and CoQ's antioxidant properties, individuals who for whatever reason become CoQ deficient may not only fail to generate sufficient ATP for

normal cellular function, the tissue will also be more readily damaged by oxidising species. Thus supplementation with oral CoQ₁₀ may prove useful not only in the treatment of patients with ubiquinone deficiency, but also certain neurodegenerative conditions associated with oxidative stress and mitochondrial dysfunction.

1.7. Mitochondrial targets in neurological disease

Neurodegenerative diseases, such as Parkinson's Disease (PD) and Alzheimer's Disease (AD), are characterised by a progressive loss of neuronal function in specific brain regions. Although definite mechanisms are only beginning to be elucidated, oxidative/ nitrosative damage has been implicated in the pathology of many neurodegenerative conditions (reviewed in Stewart and Heales, 2003; Duncan and Heales, 2005). For example in PD, elevated levels of nitrosylated proteins have been detected (Good *et al.*, 1998; Giasson *et al.*, 2000). This has been supported by increases in the CSF concentration of NO breakdown products (Quereshi *et al.*, 1998). Post-mortem examination of the brains of patients suffering from AD has also shown elevated levels of protein nitrosylation (Smith *et al.*, 1997). It has been proposed that damage to mitochondria, and in particular the ETC, underlies a component part of neuronal loss in these diseases.

Schapira and co-workers found that complex I activity was decreased in *post-mortem* samples from the substantia nigra of patients with PD (Schapira *et al.*, 1990). A number of other studies have supported these findings (Cleeter *et al.*, 1992; Glinka *et al.*, 1996). Additionally, in the same tissue evidence of NOS activity, NO radicals and nitrotyrosinated protein residues (suggesting ONOO⁻

formation) have all been demonstrated (Hunot *et al.*, 1996; Shergill *et al.*, 1996; Good *et al.*, 1998). However, the susceptibility of complex I to ROS / RNS has itself been a catalyst for scientific debate within the literature. While NO has been reported to inhibit complex I activity in permeabilised hepatocytes (Stadler *et al.*, 1991), and Radi and colleagues reported ONOO⁻-mediated decreased complex I activity in heart mitochondria (Radi *et al.*, 1994; Cassina and Radi, 1996), these findings were not supported by whole cell *in vitro* studies with NO (Bolaños *et al.*, 1994) or ONOO⁻ (Bolaños *et al.*, 1995). These differences may be due to the differing preparations used in these studies. Reviewed by Brown and Borutaite (2004), damage to Fe-S centres in complex I (including removal of iron from and disruption of Fe-S centres) has been proposed to account for complex I inhibition by RNS. S-nitrosation also represents a reversible mechanism of complex I inhibition as reduced thiols (ie. GSH) can reverse such inhibition, as demonstrated in a number of models including isolated heart mitochondria (Jekabsone *et al.*, 2003). ONOO⁻ has also been suggested to induce complex I inhibition in a neural cell line by nitration of tyrosine residues (Yamamoto *et al.*, 2002)

It has been proposed that maintenance of complex I activity in the face of ROS / RNS may be due to glutathione (GSH) availability (Barker *et al.*, 1996; Clementi *et al.*, 1998). GSH reacts favourably with with ROS / RNS; however given a sufficiently high level of oxidative stress upon the cell, it is possible that susceptible proteins such as the ETC may become vulnerable to free radical-mediated attack. In addition loss of GSH from the substantia nigra is proposed to be an early event in PD, preceeding mitochondrial damage (Jenner *et al.*, 1992).

Experimental depletion of GSH with the biosynthetic inhibitor L-buthionine sulfoximine (L-BSO) has revealed that GSH depletion of astrocytes increase the susceptibility of the ETC (particularly at the level of complex I) to ROS / RNS-mediated damage (Barker *et al.*, 1996; Bolaños *et al.*, 1996).

The activities of complex II and complex III are often measured as a linked assay (King *et al.*, 1967), and it has been suggested that this system is susceptible to RNS (and possibly ROS). Culture of astrocytes in the presence of NO has shown decreased activity of complex II+III (Bolaños *et al.*, 1994); this study was subsequently supported by the finding of irreversible complex II+III damage as a result of ONOO⁻ (Bolaños *et al.*, 1996). It is possible that complex II (in particular SDH) is more susceptible to oxidative/ nitrosative stress in cultured brain cells (Radi *et al.*, 1994; Mitrovic *et al.*, 1994) and isolated brain mitochondria (Brookes *et al.*, 1998). Heart sub-mitochondrial particles have been shown as being sensitive to H₂O₂, O₂^{•-} and OH[•] (Zhang *et al.*, 1990); a finding subsequently confirmed with intact brain mitochondria (Gluck *et al.*, 2002).

Loss of complex IV activity has been reported in AD (Kish *et al.*, 1992), and this has been associated with pathogenic β -amyloid generation (Canevari *et al.*, 1999; 2001). AD represents another condition in which inappropriate NO generation and mitochondrial dysfunction have been implicated (Dorheim *et al.*, 1994; Casley *et al.*, 2001; 2002). This complex has been known to be susceptible to the effects of NO for over 60 years (Keilin and Hartree, 1939). Reduced cytochrome a₃ of complex IV can form a nitrosyl-haem centre in the presence of NO (Brudvig, *et al.*, 1980), effectively acting as a competitive inhibitor of the active site. This

increase in the K_m for O_2 (and a concomitant decrease in V_{max}) has the potential to make ATP generation much more sensitive to oxygen tension (Brown and Cooper, 1994; Sharpe and Cooper, 1998). Complex IV inhibition has been demonstrated by NO using a number of models including cultured cells (Bolaños *et al.*, 1994; 1996), isolated mitochondria (Cleeter *et al.*, 1994; Poderoso *et al.*, 1996) and purified enzyme (Sharpe and Cooper, 1998).

Thus inhibition of one or more of the mitochondrial complexes can give rise to an energy deficit. It is now well known that mitochondria display wide variation between cells and cell types, and this is especially true of the heterogeneous mitochondrial population in the brain (Davey *et al.*, 1997). These authors showed that <60% inhibition of complex I in non-synaptic mitochondria will not compromise ATP synthesis whereas synaptic mitochondria can become ATP deficient after only 25% complex I inhibition. Supported by work from the same group published the following year using cultured cells, (Davey *et al.*, 1998) threshold studies using isolated mitochondria from two cell types examined *in vitro* can be useful in gaining insight into the heterogeneity of mitochondrial populations. It is now understood that brain cells which become ATP-compromised will suffer an energy deficit, and if this insult is sufficiently severe and/ or prolonged, the ensuing cellular and mitochondrial damage may give rise to cell death through either the apoptosis or necrosis pathways.

1.8. Ubiquinone and Neurodegeneration

Disruption of CoQ₁₀ metabolism has been implicated in various neurodegenerative diseases including PD (Matsubara *et al.*, 1991; Shults *et al.*, 1997; Götz *et al.*, 2000), Lewy body disease (Molina *et al.*, 2002) and AD (Söderberg *et al.*, 1992). In Kearns-Sayre Syndrome and other encephalomyopathies, altered CoQ₁₀ metabolism has also been implicated (Ogasahara *et al.*, 1986, 1989; Rotig *et al.*, 2000). However a similar number have countered much of the evidence presented, finding no change in endogenous CoQ₁₀ levels. (Beal and Matthews, 1997; Jiminez-Jiminez, *et al.*, 2000; Molina *et al.*, 2000).

It would appear that many different groups have contrasting findings, which may in part be due to the variety of methods for determining ubiquinone concentration. Whether CoQ₁₀ levels are measured in serum (Molina *et al.*, 2000), muscle (Di Giovanni *et al.*, 2001), brain (Söderberg *et al.*, 1992), platelets (Götz *et al.*, 2000) or fibroblasts (Rotig *et al.*, 2000) may influence the findings and interpretation. Oral CoQ₁₀ supplementation has been reported to slow the functional decline in PD (Shults *et al.*, 2002). However, direct evidence of a CoQ₁₀ deficit in the Parkinsonian brain is currently lacking. Additionally, a number of groups have obtained apparently contradictory results with regard to CoQ₉ or CoQ₁₀ entry to the brain following oral supplementation (Matthews *et al.*, 1998; Kwong *et al.*, 2002; Bentinger *et al.*, 2003; Kamzalov *et al.*, 2003; Gomez-Diaz *et al.*, 2003b); thus the reported benefits of CoQ supplementation in neurodegenerative states require further investigation to fully understand the mechanisms involved.

The hypothesis inferring altered CoQ₉ or CoQ₁₀ metabolism in cases of neurodegeneration may however be supported by the work of Bolaños *et al.*, 1994. It was shown in this study that treatment of primary cultures of rat astrocytes with lipopolysaccharide (LPS) and γ -interferon (IFN γ) caused induction of NOS II. The elevated levels of NO subsequently generated led to mitochondrial inhibition, determined by measurement of the activities of the complexes of the ETC. After 18h cytokine exposure, complex IV activity was reduced by 25% compared to control values. After 36h exposure, complex IV exhibited 56% inhibition, and complex II+III activity was reduced by 35%.

The latter phenomenon could be explained by nitrosative/ oxidative damage to the complex II subunit, the complex III subunit, or the intermediate electron carrier (i.e. CoQ). In isolated brain mitochondria, peroxynitrite (ONOO⁻; formed from the reaction of NO with O₂⁻) inhibited complex II activity by 42% (Brookes *et al.*, 1998), and in cultured astrocytes and oligodendrocytes NO was shown to inhibit SDH activity (Mitrovic *et al.*, 1994). However the effects of NO/ONOO⁻ upon CoQ₉ or CoQ₁₀ in intact cells were not evaluated in these studies. NO/ONOO⁻ mediated depletion of CoQ₉ or CoQ₁₀ may have fundamentally important implications for understanding the mitochondrial component of neurological disease, given that in many such conditions, increased NO formation is believed to occur (Dawson *et al.*, 1991; Dawson and Dawson, 1996; Heales *et al.*, 1999; Almeida and Bolaños, 2001).

Reports on the reaction of short chain ubiquinol (CoQ₀ and CoQ₂) with NO and ONOO⁻, such as those by the group of Poderoso (Poderoso *et al.*, 1999;

Schöpfer *et al.*, 2000) suggest that *in vitro*, NO can oxidise ubiquinol to ubisemiquinone and finally to ubiquinone, (Poderoso *et al.*, 1999). A later publication (Schöpfer *et al.*, 2000) describing the reaction with ONOO⁻ suggests that regeneration of the quinone form of the CoQ₀ or CoQ₂ (CoQ₀H₂ and CoQ₂H₂ respectively) may protect mitochondria against nitrosative stress. This group showed that the reactive intermediates formed by ONOO⁻ decaying to NO₃⁻ can be quenched by CoQ₀H₂, which in turn forms ubisemiquinone. Additionally, ONOO⁻ promotes O₂⁻ formation via reduced oxidation of CoQ₀H₂ to the ubisemiquinone and subsequently CoQ₀. The presence of CoQ₀H₂ also protects against ONOO⁻-mediated nitration of tyrosine residues in both mitochondrial membranes, and supplementation of rats with CoQ₁₀ prevents ONOO⁻-mediated mitochondrial respiratory dysfunction (Schöpfer *et al.*, 2000). Thus it is clear that the antioxidant effects of ubiquinols in mitochondrial membranes has the potential to protect against respiratory dysfunction as a result of generation by oxidative and nitrosative radicals. Subsequently, the implications for neurodegenerative disease may suggest that depletion of CoQ₉ or CoQ₁₀ would render the mitochondria of neurones and glia more susceptible to attack by these oxidising species.

1.9. Lovastatin and disruption of CoQ metabolism

1.9.1. General Pharmacology

In the late 1970s, a fungal metabolite was isolated from *Aspergillus terreus* which was to revolutionise the treatment of hypercholesterolaemia. As an inhibitor of the rate-limiting enzyme for cholesterol synthesis, the compound termed ML-

236B (later known as mevinolin or lovastatin) was shown to have hypocholesterolaemic activity in vitro (Endo *et al.*, 1976). Subsequent animal studies confirmed that in dogs (Tsujita *et al.*, 1979) and monkeys (Kuroda *et al.*, 1979) the drug was effective at lowering plasma cholesterol. Similar in structure to HMG-CoA, competitive inhibition of HMG-CoA reductase in hepatocytes results in impairment of *de novo* cholesterol synthesis. This in turn causes an increase in low-density lipoprotein (LDL) clearance of cholesterol from the plasma (Bilheimer *et al.*, 1983; reviewed in Brown & Goldstein, 2004).

Lovastatin is a prodrug; following oral administration, first pass hepatic metabolism results in lactonase enzymes cleaving the molecule's lactone ring by hydrolysis of the ester link. The opened β -hydroxy acid of lovastatin has been shown to have significantly higher HMG-CoA reductase inhibitory activity than the lactone prodrug (Endo *et al.*, 1976; Merck & Co, Inc, 2003).

Inhibition of HMG-CoA reductase by lovastatin is not complete (Merck & Co Inc, 2003), thus mevalonate synthesis is not completely blocked at therapeutic doses. The "flux diversion hypothesis" also states that squalene synthase's relatively low affinity for farnesyl-pyrophosphate (FPP) allows a decrease in the FPP pool to preferentially affect cholesterol (rather than ubiquinone) synthesis. Thus the *cis*- and *trans*-prenyltransferases' higher affinity should theoretically allow dolichol and CoQ₁₀ synthesis to be maintained (Turunen *et al.*, 2004). However studies have demonstrated decreased CoQ₉ and CoQ₁₀ levels in rats (Willis *et al.*, 1990) and CoQ₁₀ in humans (Folkers *et al.*, 1990). Thus it is conceivable that such a

situation may have serious implications of cellular antioxidant status and mitochondrial ETC function.

1.9.2. Statin drugs and neurological disease

Statin drugs have been postulated as being of benefit in a number of neurological conditions (reviewed in Cucchiara and Kasner, 2001) including glioma-type tumours (Prasanna *et al.*, 1996; Soma *et al.*, 1992, 1995), cerebrovascular disease (reviewed in Vaughan and Delanty, 1999), Multiple Sclerosis (Stanislaus *et al.*, 2001) and AD (Jick *et al.*, 2000; Wolozin *et al.*, 2000; Simons *et al.*, 2002). In addition NO generated due to NOS II induction is implicated in a number of neurodegenerative conditions (reviewed in Heales *et al.*, 1999); however, some work has shown that NOS II induction may be inhibited by lovastatin (Pahan *et al.*, 1997; Rattan *et al.*, 2003). Lovastatin has also been shown to inhibit lipid oxidation and increase SOD levels in plasma of orally treated animals (Chen *et al.*, 1997).

Lovastatin has been used in both animal and cell culture models (Nagasawa *et al.*, 2000; Ikeda *et al.*, 2001; Huang *et al.*, 2003) and although conclusive evidence of benefit in neurological disease is lacking, lovastatin is being evaluated by a number of groups for the treatment of neurological diseases (reviewed in Cucchiara and Kasner, 2001).

1.10. Statement of Aims

The aims of this project were to

- a) Establish an HPLC method for the determination of different CoQ homologues in both human and rodent biological material
- b) Determine the CoQ status of glial cell lines, and rat primary astrocyte and neuron-enriched cultures
- c) Investigate modulation of cellular CoQ availability by RNS, potential biosynthetic pharmacological inhibitors and siRNA-mediated biosynthetic enzyme knockdown in a number of cell types including glial cell lines, and rat primary astrocyte and neuron-enriched cultures.
- d) Investigate whether modulation of cellular CoQ availability influences respiratory enzyme activities of the ETC (and specifically the complex II+III assay) *in vitro*.

2. MATERIALS AND METHODS

2. MATERIALS AND METHODS

2.1 Chemicals and Materials

All chemicals, enzymes, coenzymes and reagents were supplied by Sigma-Aldrich (Poole, UK) unless otherwise stated, and were of the highest possible grade:

Antibiotic/antimycotic solution (100x: 10,000 units penicillin, 10mg streptomycin and 25µg amphotericin B per ml), Antimycin A, bovine serum albumin, coenzyme Q₁, coenzyme Q₉, coenzyme Q₁₀, Cytosine β-D-arabinofuranoside hydrochloride, deoxyribonuclease I (Type IV; from bovine pancreas; DNase; EC. 3.1.21.1), Earle's Balanced Salt Solution (with sodium bicarbonate; EBSS), Hanks Balanced Salt Solution (with sodium bicarbonate, without phenol red, calcium chloride and magnesium sulphate; HBSS), L-glutamine, Lipopolysaccharide (from *E. coli* 026:B6; LPS), N6-(1-Iminoethyl)-L-lysine dihydrochloride (L-NIL), Medium 199 (liquid; HEPES modification) Mevinolin (from *aspergillus*; "lovastatin"), Millex GV 0.22µ syringe-driven filters, β-nicotinamide adenine dinucleotide reduced form (disodium salt; NADH), β-nicotinamide adenine dinucleotide phosphate reduced tetrasodium salt (NADPH), poly-D-lysine (lyophilised), poly-L-ornithine (0.01%), rotenone, sodium perchlorate (anhydrous), trypsin-EDTA solution (10x, 0.05% porcine trypsin/ 0.02% EDTA).

Exceptions include the following:

The nitric oxide donor (z)-1-[2-aminoethyl)-N-(2-ammonioethyl) amino] diazen-1-ium-1,2-diolate (DETA-NO) was purchased from Alexis Biochemicals (Nottingham, UK)

Minimal essential medium (MEM; both with and without Phenol Red), Dulbecco's modified Eagle medium (D-MEM; 4.5g glucose/l), foetal bovine serum (FBS; heat inactivated), and all tissue culture plastics were purchased from Invitrogen (Paisley, UK)

γ -interferon (IFN γ) was purchased from Calbiochem (Nottingham, UK)

L-lactate dehydrogenase (from rabbit muscle; LDH; EC. 1.1.1.27), nitrate reductase (from *aspergillus*; EC 1.6.6.2) and oxidised cytochrome *c* (from horse heart) were purchased from Roche Diagnostics (Lewes, UK). The Preciset Cholesterol standard (5.17mM) was purchased from Boehringer Mannheim, now part of Roche (Lewes, UK).

The Total Cholesterol CHOL-H L-type spectrofluorometric assay kit was manufactured by Wako Chemicals and purchased from Alpha Laboratories (Eastleigh, UK).

The BioRad DC Protein Assay Kit was obtained from BioRad, (Hemel Hempstead, UK)

Sephadex G-25M PD-10 desalting columns (elution volume 3.5ml) to remove ascorbate from reduced cytochrome *c* were purchased from Amersham Biosciences (Little Chalfont, UK).

Techsphere ODS 5 μ 150mm HPLC columns and guard columns were purchased from HPLC Technolgy (Welwyn Garden City, UK).

Ethanol and methanol (Hypersolv HPLC grade) perchloric acid (60%) were supplied by VWR (Loughborough, UK).

2.2 Tissue Culture

2.2.1 Media and solutions

Minimum Essential Media (MEM; for astrocytes): MEM supplemented with 10% (v/v) FBS, 2mM L-glutamine, and 1% (v/v) antibiotic antimycotic (100 units/ml penicillin, 100 µg/ml streptomycin and 25 ng/ml amphotericin) solution.

MEM (for neurons): as for astrocytes, with the additional supplementation of 25mM KCl.

Medium 199: supplemented with 10% (v/v) FBS, 2mM L-glutamine, and 1% (v/v) antibiotic antimycotic solution.

D-MEM: supplemented with 10% (v/v) FBS, 2mM L-glutamine, and 1% (v/v) antibiotic antimycotic solution.

EBSS: supplemented with 1% (v/v) antibiotic antimycotic solution.

HBSS: supplemented with 1% (v/v) antibiotic antimycotic solution.

"Solution A": EBSS supplemented with DNase (75 Kunitz units/ml) and BSA (3mg/ml)

"Solution B": "Solution A" supplemented with trypsin (27.5 units/ml) and additional DNase (562.5 Kunitz units/ml)

2.2.2. *Animals*

Pregnant Wistar rats were purchased from A.J. Tuck & Sons (Rayleigh, Essex, UK), and the breeding colony within the Institute of Neurology, UCL, UK. Animals were maintained on a light/dark 12-hour cycle and fed stock laboratory diet and water *ad libitum*. Preparation of rat primary cortical astrocytes required the use of 1-2 day old pups, which were killed by cervical dislocation, while primary neuron culture required the use of foetuses removed on the 17th day of gestation (E17).

2.2.3 *Preparation of astrocyte cultures*

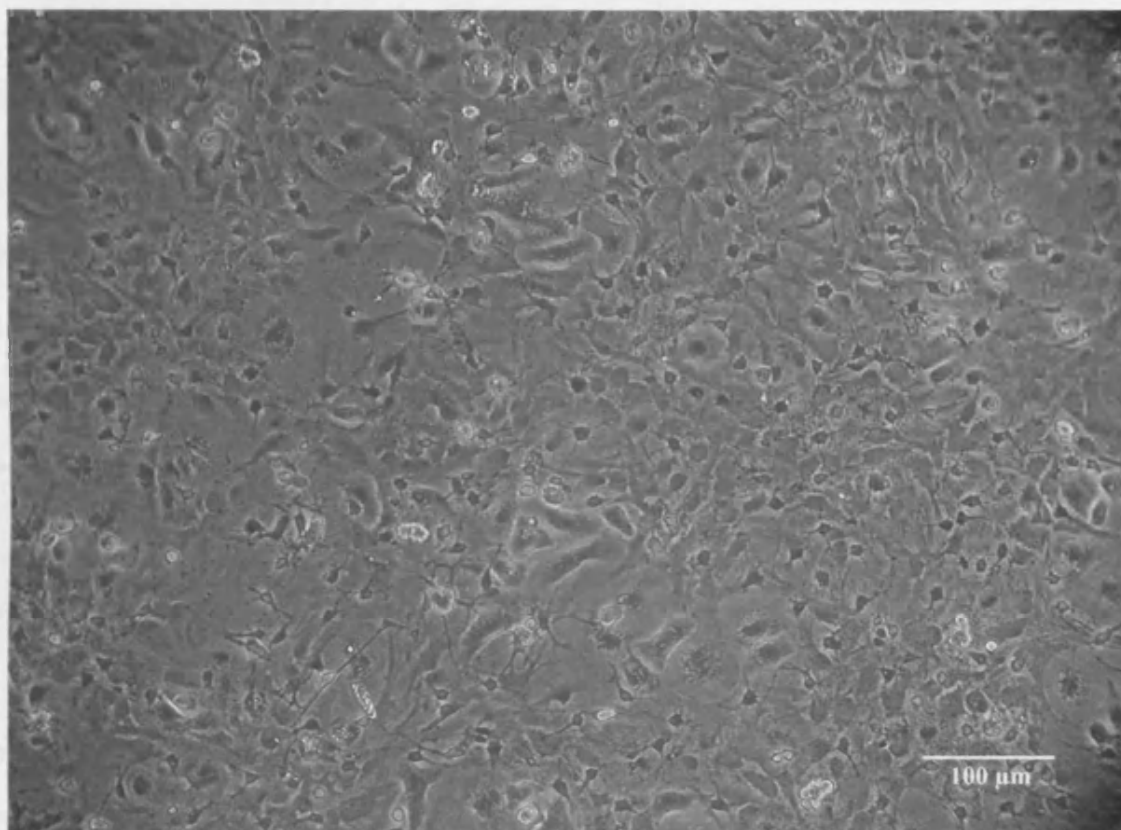
Preparation of rat primary astrocyte cultures followed the method of Tabernero *et al.*, (1993), but with some minor modifications, i.e. lower concentrations of digestive enzymes (DNase and trypsin) and slower spin speeds to increase the yield of viable cells obtained. The animals were decapitated, the cortex carefully removed, and the meninges and blood vessels removed by gently rolling the small pieces of tissue along a piece of clean dry filter paper. The cleaned tissue was then roughly chopped with small, curved edged scissors in EBSS supplemented with DNase (75 Kunitz units/ml) and BSA (3mg/ml). This was termed "Solution A". Then, following mechanical dissociation by aspiration with a P1000 Gilson pipette, the cells were spun at 440 g for 5 mins at 4°C, and the supernatant discarded. The cells were transferred to petri dish and enzymatically

digested with "Solution B" (effectively, this was Solution A supplemented with trypsin (27.5 units/ml) and additional DNase (562.5 Kunitz units/ml) for a maximum of 15 mins at 37°C. The digestion was terminated by the addition of 10% (v/v) FBS. The cell preparation was spun and resuspended in fresh Solution A a further two times to achieve a homogenous suspension. Finally, the cells were resuspended in L-valine based minimum essential media (MEM), supplemented with 10% (v/v) FBS (Invitrogen, Paisley, UK), 2mM L-Glutamine and 1% (v/v) antibiotic/antimycotic before being passed through a 100 μ pore size nylon cell strainer (Becton Dickinson Labware Europe, Le Pont de Claix, France). A monolayer of astrocytes was cultured in 80cm² flasks containing 10ml MEM, and maintained in a humidified incubator (95% air/ 5% CO₂) at 37°C. Media was changed every 3 days, and astrocytes were passaged on the 7th day in vitro (DIV 7), when confluency was reached.

After removal of media, the monolayer was gently washed with HBSS, before incubation with 5 ml trypsin/EDTA solution (0.5% (w/v) trypsin, 0.2% (w/v) EDTA for 5 minutes. Trypsinisation was terminated by the addition of 10% (v/v) FBS, and cells were pelleted by centrifugation at 440 g for 5 mins at 4°C. Following resuspension in MEM, the astrocytes were divided over a larger area and cultured for a further 6 days, with the media changed every 3 days.

At DIV 13, the monolayer was again removed by trypsinisation, pelleted, resuspended and the cells counted using a haemocytometer. Astrocytes were then seeded into poly-lysine coated (10 μ g/ml) 6-well plates at a density of 1x10⁵/cm², in 1 ml medium on the day preceding treatment. Figure 2.1 shows a 20x magnification light microscope image of the cells obtained after plating on day 13.

2.2.4 Preparation of primary cultures



1971), a member of recent University of London School (Mason, 2001; Clasper, 2002; Gregg, 2003; Lane, 2004) and publications from this group (Hollings et al., 1989; Stewart et al., 1990; Stewart et al., 2002a) and others (Taberner et al., 1991; Vignati et al., 1993) have repeatedly found 100% GFAP positivity in astrocyte cultures and 100% positivity for neurofilament in neuronal cultures.

2.2.5 Preparation of cell line cultures

Figure 2.1 Phase contrast light micrograph of rat primary astrocyte cultures. principally

Untreated rat primary astrocytes viewed at x20 magnification on DIV13 of culture showing typical cultured astrocyte morphology at confluence.

2.2.4 Preparation of neuron cultures

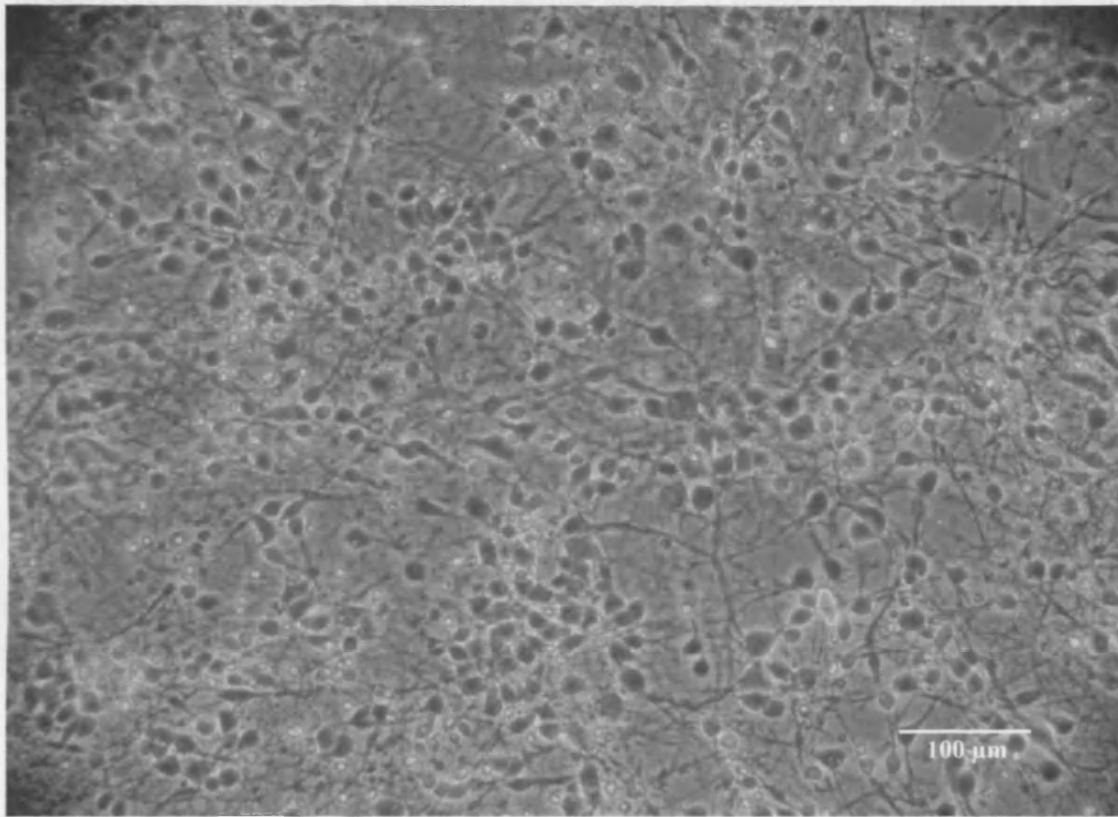
Primary neuron cultures were isolated from Wistar rat E17 foetuses (Bolaños *et al.*, 1995; Vicario *et al.*, 1993). The same basic protocol was followed as for astrocyte preparation, except that the MEM was additionally supplemented with 25mM KCl, and on the day the preparation was performed, neurons were plated directly onto poly-ornithine coated (10µg/ml) 6-well plates (2.5×10^5 cells/cm² in 1.5 ml media). On DIV 3, the media was changed to one supplemented with cytosine arabinofuranoside (1mM) to inhibit DNA synthesis in proliferating cells. Experiments were performed on DIV 6-7.

Figure 2.2 shows a typical 20x magnification light microscope image of the cells on DIV 6.

These cells have been previously characterised in this laboratory with regard to purity, i.e. immunohistochemical staining against green fibrillary acidic protein (GFAP; Bignami *et al.*, 1972) in astrocytes and neurofilament in neurones (Dahl and Bignami, 1977). A number of recent University of London theses (Stone, 2001; Casley, 2002; Gegg, 2003; Lam, 2004) and publications from this group (Bolaños *et al.*, 1995; Stewart *et al.*, 1998; Stewart *et al.*, 2002a) and others (Tabanero *et al.*, 1993; Vicario *et al.*, 1993) have repeatedly found >90% GFAP positivity in astrocyte cultures and >85% positivity for neurofilament in neuronal cultures.

2.2.5 Preparation of cell line cultures

While CoQ₉ is the predominant ubiquinone in rodents, humans utilise principally CoQ₁₀. In order to further investigate this homologue in the human brain, it was necessary



The (CCIN) human astrocytoma line (ECACC No. 9603042) derives from primary human glioma cultures (Portier and Bachelard, 1958; Macintosh et al., 1972; Foster and Portier, 1977) and is well characterized (Delouis, 1993; Simeoni et al., 1998). These cells were grown in Dulbecco's Modified Eagle Media (DMEM; 4500mg glucose/l) supplemented with 10% (v/v) FCS, 2mM L-Glutamine and 1% (v/v) antibiotic/antimycotic.

2.2.3.1. Rat C6 glioma cultures

The rat C6 glioma line (ECACC No. 90090409) originates from a rat glioblastoma

Figure 2.2 Phase contrast light micrograph of rat primary neuron cultures.

Untreated rat primary neurons viewed at x20 magnification on DIV6 of culture showing typical cultured neuron morphology at confluence.

1998 for review). These cells were routinely grown in supplemented media 199 (M199)

to use a human cell line as a readily available source of human cells. However, because of possible metabolic and biochemical differences between primary cultures and immortalised cell lines, a rodent cell line was also studied. These cell lines, originally derived from rat and human brain tumours were originally purchased from the European Collection of Cell Cultures (ECACC; Porton Down, UK) and stored in liquid nitrogen until use. Cell line recovery, following removal from liquid nitrogen, required rapid defrosting at 37°C for a maximum of 2 minutes. The cells (frozen in FBS: media: DMSO at a ratio of 5:3:2) were transferred to a 25cm² tissue culture flask and supplemented with 5 ml of the appropriate media. 4 hours later, once the cells had become adherent, the media was changed, and the cells split when confluent.

2.2.5.1. Human 1321N1 astrocytoma cultures

The 1321N1 human astrocytoma line (ECACC No. 86030402.) derives from primary human glioma cultures, (Ponten and MacIntyre, 1968; MacIntyre *et al.*, 1972; Foster and Perkins 1977) and is well characterised (Brismar, 1995; Stewart *et al.*, 1998). These cells were grown in Dulbecco's Modified Eagle Media (DMEM; 4500mg glucose/l) supplemented with 10% (v/v) FBS, 2mM L-Glutamine and 1% (v/v) antibiotic/antimycotic.

2.2.5.2. Rat C6 glioma cultures

The rat C6 glioma line (ECACC No. 92090409) originates from a rat glial tumour induced by N-nitromethylurea (Breda *et al.*, 1968) and has been widely used for various cell biology studies (Feinstein *et al.*, 1994; Cao and Reith (2002) or Brismar, 1995; Barth, 1998 for reviews). These cells were routinely grown in supplemented media 199 (M199),

which consisted of N-2-hydroxypiperazine-N-2-ethanesulphonic acid (HEPES)-buffered M199 containing 10% (v/v) FBS, 2mM L-Glutamine and 1% (v/v) antibiotic/antimycotic.

Both cell lines were passaged every 3-4 days, (1:6 split), and seeded into 6-well plates at a density of $1 \times 10^5/\text{cm}^2$ on the day preceding treatment.

2.2.6 Cell treatments

Cells were usually treated in 6-well well plates. Media was removed, the monolayer gently washed with HBSS, and fresh media added containing the necessary supplements for the specific treatment. After either 24 or 36 hours, the medium was removed, and usually saved and stored at -80°C for later determination of nitrate and nitrite concentration. Cells were then washed with HBSS, trypsinised, and gently scraped using a plastic cell scraper, then pelleted by centrifugation at 400g for 5 minutes. Following removal of the supernatant cells were snap frozen in liquid nitrogen before being stored at -80°C until assay. In the case of LDH measurement, a sample of culture media (typically 50 μl) was removed before lysis of the cells with Triton X-100 (0.1% v/v). Cells and remaining media were then removed, snap frozen in liquid nitrogen and stored at -80°C until assay.

2.2.6.1 Serum withdrawal

In order to examine the effects of serum withdrawal upon cellular CoQ levels, some cells were cultured in MEM without FBS for up to 36h. In addition where noted, some treatments were also carried out in the presence and in the absence of FBS.

2.2.6.2 Cytokine + bacterial lipopolysaccharide treatment

Using a protocol based on that of Bolaños *et al.*, (1994), cells were treated with LPS (1 µg/ ml) and IFN γ (100 U/ml) \pm the NOS inhibitor L-NIL; (100µM; Moore *et al.*, 1994)

2.2.6.3 Lovastatin treatment

Mevinolin (also known as lovastatin) is a member of the statin class of drugs, used clinically to inhibit HMG-CoA reductase the rate limiting enzyme in the cholesterol biosynthetic (mevalonate) pathway (Alberts *et al.*, 1980). This fungal metabolite is inactive in its prodrug form, although cleavage of the lactone ring to a 5 carbon chain as performed in-vivo by lactonase enzymes, converts the prodrug to its bioactive isoform (Endo *et al.*, 1976, Gerson *et al.*, 1989).

In some experiments lovastatin was dissolved in ethanol, and added to the media at 1% v/v. It was used at a final concentration of 10µM or 100µM. However, due to the lack of evidence in the literature of the expression of lactonases in cultures, and the fact that lovastatin was found to be a more effective inhibitor of HMG-CoA reductase as a sodium salt (the β -hydroxy acid; Endo *et al.*, 1976), the prodrug was also converted to the sodium salt (as shown in Fig 2.3) by alkaline hydrolysis by dissolution in ethanol containing 1M NaOH (Endo *et al.*, 1976). Thus the sodium salt of lovastatin was also added to the culture media at a final concentration of 10µM or 100µM.

Controls for these experiments were the vehicle (ethanol or 1M NaOH in ethanol) added to the culture media at 1% (v/v)

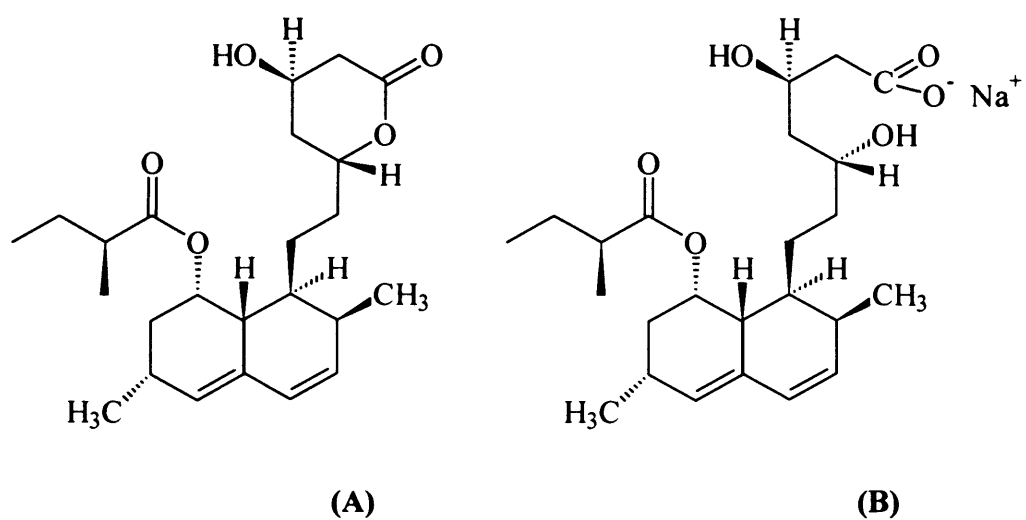


Figure 2.3. The structures of lovastatin and Na-lovastatin.

The natural lactone form of lovastatin (A), was used to generate Na-lovastatin (B), following alkaline hydrolysis, as described in section 2.2.6.3

2.2.6.4 NO Donor treatment

(z)-1-[2-aminoethyl)-N-(2-ammonioethyl) amino] diazen-1-ium-1,2-diolate (DETA-NO) is a slow-release NO donor (Seccia *et al.*, 1996). A 500 μ M solution of DETA-NO gives sustained release of approximately 1 μ M NO for 24h in astrocyte and neuron MEM (Gegg *et al.*, 2003).

Controls for these experiments used degraded DETA-NO. As the half life of this compound is in the region of 8h (Seccia *et al.*, 1996), a stock solution of 100mM was allowed to degrade for 7 days. Thus the compound had passed 21 half lives, at this time point released minimal amounts of NO.

2.2.6.5 Combination of treatments

In some experiments combinations of the treatments described above were used to evaluate the effects of the induction of iNOS in conjunction with lovastatin treatment.

2.3. Spectrophotometric ETC Enzyme assays

2.3.1. NADH:ubiquinone oxidoreductase (Complex I; EC. 1.6.5.3)

Complex I catalyses the oxidation of NADH to NAD⁺. Thus, electrons are transferred from NADH to ubiquinone (which becomes reduced to ubiquinol). Subsequently, these electrons are passed to complex III. The activity of complex I was determined by the method of Ragan *et al.*, (1987) using a Uvikon XL spectrophotometer running at 30°C (NorthStar Scientific Ltd, Bedford, UK) as the rotenone-sensitive decrease in NADH (340nm). The sample was three times freeze-thawed (using liquid N₂), and divided into separate aliquots for each spectrophotometric assay described here. 20 μ l was

added to a cuvette with final concentrations of 20mM phosphate buffer (20mM KH_2PO_4 , 20mM K_2PO_4 , 8mM MgCl_2 , pH 7.2), 2.5 mg/ml BSA, 0.15mM NADH and 1mM KCN. Contents were mixed, and placed in the spectrophotometer for 2 mins to reach 30°C. The final volume in the cuvette was 1ml. Addition of 50 μM ubiquinone (CoQ_1) started oxidation of NADH, and this was followed for 5 mins. Using the Beer-Lambert Law ($\text{Abs} = \epsilon c l$; ϵ = NADH extinction co-efficient = $6.81 \times 10^3 \text{ M}^{-1} \text{ cm}^{-1}$; c = [NADH]; l = path length = 1 for all calculations) the activity of NADH oxidase in the sample could be calculated. After approximately 5 mins, 20 μM rotenone (a specific complex I inhibitor) was added to inhibit the complex I-dependant component, thus allowing calculation of NADH oxidation due solely to complex I; thus complex I activity.

Activity was expressed against the protein content of the sample as nmol/min/mg. All sample cuvettes were run against a "blank", containing sample and all substrates and reagents except CoQ_1 . Complex I was proportional to protein between 5 and 25 μg protein ($R^2 = 0.994$)

2.3.2. Succinate dehydrogenase:cytochrome c reductase (Complex II+III; EC. 1.3.5.1 + 1.10.2.2)

In the ETC, succinate is oxidised by complex II. As a result of this oxidation, ubiquinone becomes reduced upon accepting electrons from the Fe-S centres of complex II, and subsequently becomes oxidised upon donation of electrons to the cytochrome *b* of complex III. This leads to reduction of the hydrophilic electron carrier cytochrome *c*. Thus the activities of complex II and complex III are often measured as the complex II+III linked assay (King *et al.*, 1967); an assay which appears to be dependant upon endogenous

ubiquinone availability (Rahman *et al.*, 2001). The linked activities of complex II+III are followed as the succinate-dependant antimycin A-sensitive reduction of cytochrome *c* (King *et al.*, 1967) at 550nm using a Uvikon XL spectrophotometer running at 30°C (NorthStar Scientific Ltd, Bedford, UK). The sample (of volume 20µL) was three times freeze-thawed (using liquid N₂), and added to a cuvette with final concentrations of 100mM phosphate buffer (100mM KH₂PO₄, 100mM K₂PO₄, pH 7.4), 0.3mM EDTA 1mM KCN and 0.1 mM cytochrome *c*. Contents were mixed, and placed in the spectrophotometer for 2 mins to reach 30°C. The final volume in the cuvette was 1ml. Addition of 20mM succinate started oxidation of NADH, and this was followed for 5 mins. Taking the extinction coefficient of cytochrome *c* at 550 nm as $19.2 \times 10^3 \text{ M}^{-1} \text{ cm}^{-1}$, the rate of reduction of cytochrome *c* could be calculated. After approximately 5 mins, 10µM antimycin A (an inhibitor of complex III) was added to inhibit the reduction of cytochrome *c* due solely to the activity of complex III. Thus calculation of the linked activity of complex II+III was possible.

Activity was expressed against the protein content of the sample as nmol/min/mg. All sample cuvettes were run against a "blank", containing sample and all substrates and reagents except succinate. Complex II+III was proportional to protein between 5 and 25 µg protein ($R^2 = 0.986$)

2.3.3. Cytochrome *c* oxidase (Complex IV; EC. 1.9.3.1)

As previously described, complex III passes electrons to reduce oxidised cytochrome *c*. Reduced cytochrome *c* then transfers electrons to cytochrome *c* oxidase (complex IV). Determination of complex IV activity used the method of Wharton and

Tzagoloff (1967), in which the oxidation of reduced cytochrome *c* is followed at 550 nm. Thus it was necessary to prepare freshly reduced cytochrome *c* for use in this assay.

2.3.3.1 Preparation of reduced cytochrome *c*

Ascorbate crystals were added in excess to cytochrome *c* (0.8mM; horse heart). The reduction resulted in a colour change from dark to light red. It was then necessary to perform a gel filtration to remove the ascorbate from the solution. This was performed using a Sepharex PD₁₀ gel filtration column previously equilibrated by washing with approximately 50ml of 10mM phosphate buffer (10mM K₂PO₄, 10 mM KH₂PO₄, pH 7.0). In order to determine the concentration of reduced cytochrome *c*, a 1:20 solution was made, and 1ml added to 2 cuvettes. These were placed in the reference and sample carriers in a Uvikon XL spectrophotometer, and "zeroed" at an absorbance of 550nm. 1mM ferricyanide was then added to the reference cuvette to fully oxidise the reference and allow determination of the concentration of reduced cytochrome *c*. The extinction coefficient of reduced cytochrome *c* for this calculation was $19.2 \times 10^3 \text{ M}^{-1} \text{ cm}^{-1}$

2.3.3.2 Measurement of Complex IV activity

Oxidation of cytochrome *c* was monitored at 550nm at 30°C using a Uvikon XL spectrophotometer. In both sample and reference cuvettes, a final concentration of 50µM reduced cytochrome *c* was added to 10mM phosphate buffer (10mM K₂PO₄, 10 mM KH₂PO₄, pH 7.0). The sample was "zeroed" against the reference, and ferricyanide added to the reference to oxidise the cytochrome *c*. At this point, absorbance increased to approximately 1.0. 20µl of sample (previously 3 times freeze-thawed) was added to the

sample cuvette and the resultant oxidation of cytochrome c followed for 5 mins. As this is a first-order reaction highly dependant upon cytochrome c concentration, activity of complex IV was expressed as the first-order rate constant k per minute per mg of protein ($k \text{ min}^{-1} \text{ mg}^{-1}$), and was determined by noting the highest absorbance following sample addition (t_0), and every subsequent minute thereafter for 3 mins (t_1 , t_2 , and t_3). Calculation of k necessitated the use of a plot of the natural log of absorbance at the 4 points against time. The mean of the slope of the line at t_1 , t_2 and t_3 gave the rate constant, which was then expressed as $k \text{ min}^{-1} \text{ ml}^{-1}$. This was then balanced against the protein concentration of the solution, thus the expression of activity as $k \text{ min}^{-1} \text{ mg protein}^{-1}$. Complex IV activity was shown to be linear between 5 and 25 μg protein ($R^2 = 0.989$)

2.3.4. Measurement of citrate synthase activity (EC. 4.1.3.7)

Citrate synthase (CS) is a mitochondrial matrix enzyme which catalyses the condensation of oxaloacetate and acetyl CoA resulting in the formation of citrate and free CoA. Measurement of citrate synthase was used as an index of mitochondrial enrichment within a given sample. Rate of production of CoA was detected by its reaction with 5,5' Dithio-bis(2-nitrobenzoic) acid (DTNB) (Shepherd & Garland, 1969) which was followed at 412nm at 30°C using a Uvikon XL spectrophotometer. 20 μl of sample (previously three times freeze-thawed) was mixed in a cuvette containing 100mM Tris, 0.1% (v/v) Triton X-100, 0.1mM acetyl CoA and 0.2mM DTNB. Addition of 0.2mM oxaloacetate started the reaction, and this was monitored for 5 mins. Samples were measured in conjunction with a reference blank, which contained all reagents and substrates save oxaloacetate, and the

extinction co-efficient of DTNB ($13.6 \times 10^6 \text{ M}^{-1} \text{ cm}^{-1}$) was used to calculate activity. Citrate synthase activity was linear between 5 and 25 μg protein ($R^2 = 0.998$)

2.4 Measurement of nitrate and nitrite

In this study, the measurement of nitrate and nitrite (NO_x ; the stable breakdown products of reactive nitrogen species) was used as an index of NO generation (Ignarro *et al.*, 1993). In this instance, any NO_3^- present in the culture media was reduced to NO_2^- by incubation with nitrate reductase (E.C.1.6.6.2; 0.1 U/mL; Roche, Lewes, UK) in the presence of NADPH (100 μM) and FAD (5 μM) for 15mins at 37°C. As excess NADPH would interfere with the final colourimetric stage in the assay, this was oxidised by addition of lactate dehydrogenase (LDH; E.C.1.1.1.27; 100 U/mL) and sodium pyruvate (100mM). This allowed the measurement of NO_2^- (representing total $\text{NO}_2^- + \text{NO}_3^-$) by the assay based on the Greiss reaction (Green *et al.*, 1982). Using the method of Green and co-workers, the formation of a pink diazo product from the clear colourless solution of phenol red free cell culture medium was enabled by the addition of equal quantities of 0.1% naphthaethylenediamine dihydrochloride, and 1% sulphanilamide/ 5% H_3PO_4 . Conducting the reaction in a 96-well plate allowed higher throughput and ensured consistent results, and a SPECTRAmax Plus 96-well Plate Reader (Molecular Devices, Wokingham, UK) was used to read absorbance of the reaction mixture at 540 nm.

The method was validated by titrating standard curves of NaNO_2 and NaNO_3 (Fig. 2.4), showing both linearity to 100 μM and almost complete oxidation of nitrate to nitrite.

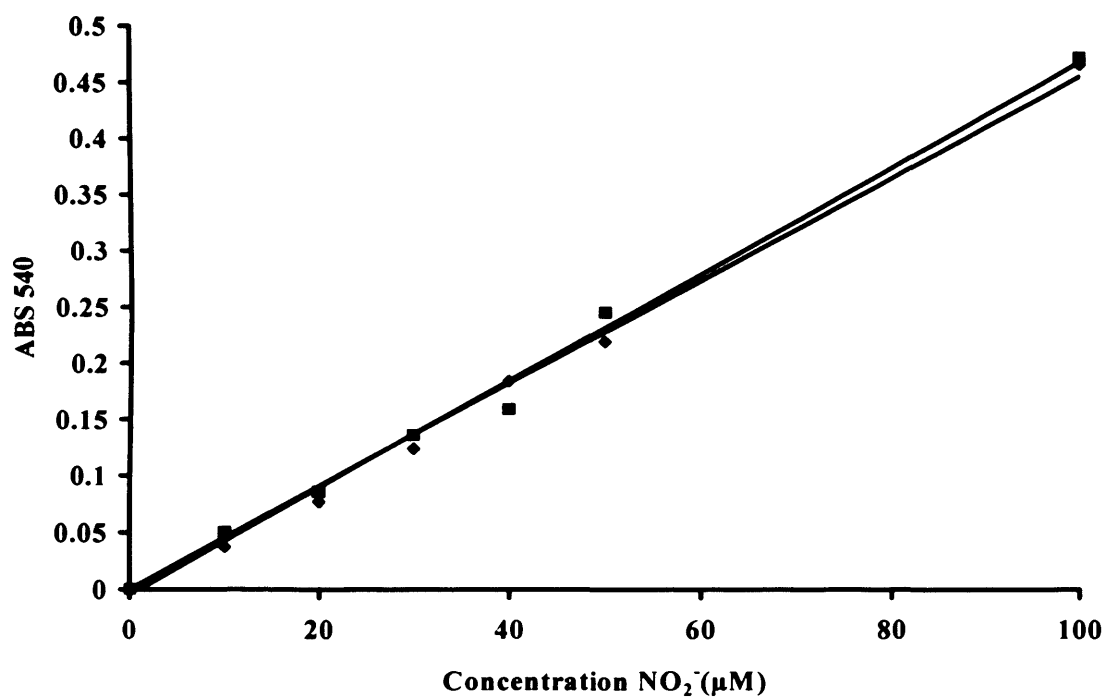


Figure 2.4. *NO₂⁻ and NO₃⁻ standard calibration curve.*

NO₂⁻ (◆) and NO₃⁻ (■) standards (the latter reduced to NO₂⁻) were used in the determination of in cell culture medium. Absorbance at 540nm is plotted against concentration of the standard, showing linearity and conversion of NO₃⁻ to NO₂⁻

2.5 Lactate dehydrogenase measurement

As an index of plasma membrane integrity, LDH was measured in the cell culture media. This is often used as an estimate of cell viability (Koh & Choi, 1987, Bolaños *et al.*, 1995). This was determined using a Uvikon XL spectrophotometer after the method of Vassault (1983). During the harvest of cells, 50 μ l of media was removed. Following the addition of 0.1% (v/v) Triton X-100 which resulted in complete cell lysis, the remaining media and cell lysate was removed, centrifuged to pellet any solid material and stored at -80°C. LDH assay buffer (100mM KH_2PO_4 , 100mM K_2HPO_4 , 170mM pyruvate, pH7.5) was added to reference and sample cuvettes. 0.16 mM NADH was added to both, while the absorbance was monitored at 340nm. As it was necessary to measure LDH in the culture media both before and after lysis, 2 sample cuvettes were used: one containing 33 μ l of media from unlysed cells, and one containing 33 μ l of cell lysate. Thus (using an extinction co-efficient of $6.22 \times 10^3 \text{M}^{-1} \text{cm}^{-1}$), a percentage of total LDH released into the media was calculated:

$$\% \text{ LDH release} = \frac{\text{LDH activity in culture media}}{\text{Total LDH activity (lysed cells + media)}}$$

The determination of the LDH activity of FBS was carried out in order to account for the relative contribution of this serum supplement in the culture media. In this case, a “theoretical maximal LDH activity” was calculated by measuring the LDH activity of a number of lysed cultures grown in the presence of FBS. The following calculation was used:

$$\% \text{ LDH contribution from FBS} = \frac{\text{LDH activity of 10\% FBS in cell-free media}}{\text{LDH activity of lysed cells in FBS-supplemented media}}$$

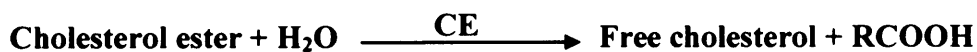
2.6 Determination of total cellular cholesterol

Inhibitors of HMG CoA reductase (such as the statin class of drugs) have been described as inhibiting synthesis of products of the mevalonate pathway including CoQ and cholesterol (Folkers *et al.*, 1990; Alberts *et al.*, 1980). In order to further understand the mechanism of action, cholesterol levels were determined as they relate to ubiquinone status.

Cholesterol determination was carried out by means of the Wako Chemicals Total Cholesterol CHOL-H L-type spectrofluorometric assay kit (Alpha Laboratories, Eastleigh, UK). This 2 reagent diagnostic kit provides a highly reproducible method with which to measure total cholesterol in human serum (Richmond, 1973). As this method has not been validated by the manufacturer for use in cultured cells, it was necessary to do so by way of a series of spiking experiments. Cell homogenates were divided into separate aliquots and a known concentration of cholesterol standard was added to half of them. By comparison of spiked and unspiked standards, a recovery of $96 \pm 3 \%$ was calculated.

Reagent "R1" consists of a buffered solution of N-(2-hydroxy-3-sulfopropyl)-3,5-dimethoxy aniline sodium salt (HDAOS) and cholesterol esterase (CE). The latter hydrolyses any cholesterol esters present in the sample to free cholesterol (EQ1).

EQ1:



The second reagent (R2) is a buffered solution of cholesterol oxidase (CO), peroxidase (POD) and 4-aminoantipyrine. CO reacts with the total free cholesterol, forming cholest-4-en-3-one and hydrogen peroxide (H_2O_2 ; EQ2). H_2O_2 causes 4-aminoantipyrine to undergo

a quantitative oxidative condensation reaction with HDAOS, catalysed by peroxidase and resulting in the formation of a blue pigment (EQ3).

EQ2:



EQ3:



Cell pellets were resuspended in 200 μl isolation buffer (320 mM sucrose, 1 mM EDTA, 10 mM Tris; pH 7.4), and 100 μl undiluted homogenate transferred to an eppendorf tube. 675 μl of R1 was added and the mixture vortexed and incubated for 10 mins at 37°C. Addition of 225 μl of R2 followed by vortexing and incubation for a further 10 mins at 37°C allowed formation of the blue reaction product. Absorbance was measured at 600nm on a Uvikon XL spectrophotometer (NorthStar Scientific Ltd, Bedford, UK). A standard curve for cholesterol showing linearity in the range measured is shown in Fig. 2.5 ($R^2 = 0.998$). This was prepared in isolation buffer using the Preciset water-soluble cholesterol standard solution (5.17 mM) purchased from Boehringer Mannheim Biochemicals UK; now part of Roche Diagnostics (Lewes, UK).

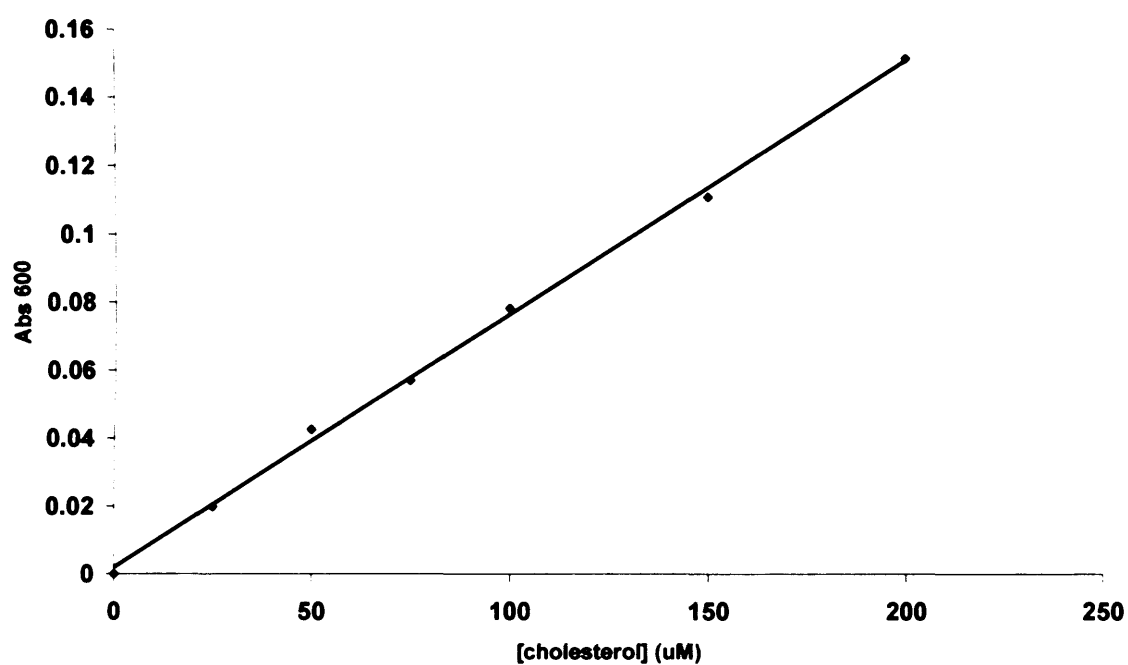


Figure 2.5. Cholesterol standard calibration curve

A serial dilution of Preciset cholesterol standard was made in the range shown. Following the protocol as described in the text, absorbance at 600nm was determined and plotted against standard concentration showing linearity.

2.7 Determination of protein concentration

All biochemical investigations carried out were expressed against a cellular protein baseline. The amount of protein in tissue samples was determined by the method of Lowry *et al.*, (1951), using the BioRad DC protein assay kit BioRad (BioRad, Hemel Hempstead, UK). This kit consists of the two reagents, conveniently pre-mixed and ready for use. Solution A consists of alkaline copper tartrate, and solution B is Folin-Ciocalteu reagent. . The colour development is mainly due to copper binding to primarily tryptophan and tyrosine (although additionally cysteine, cystine and histidine) residues. Subsequent copper-mediated reduction of the Folin reagent results in a characteristic blue species. Samples were typically diluted 1/20 , 100 μ l Solution A was added, 800 μ l solution B added and the mixture thoroughly vortexed. Absorbance was measured at 750 nm, again using the SpectraMax spectrophotometer. Fig. 2.6 shows the linearity of the standard curve, prepared with a 0.2 mg/mL solution of bovine serum albumin (BSA) in isolation buffer.

2.8 Light micrography of cultures

Photographs of cell cultures were obtained using a Nikon 950 CoolPix digital camera and Nikon TMS light microscope.

2.9 Statistical Analysis

Results are presented as mean \pm the standard error of the mean. *n* represents the number of independent experiments. While comparisons between two groups were analysed using an unpaired Student's t-test, multiple comparisons were made by one-way

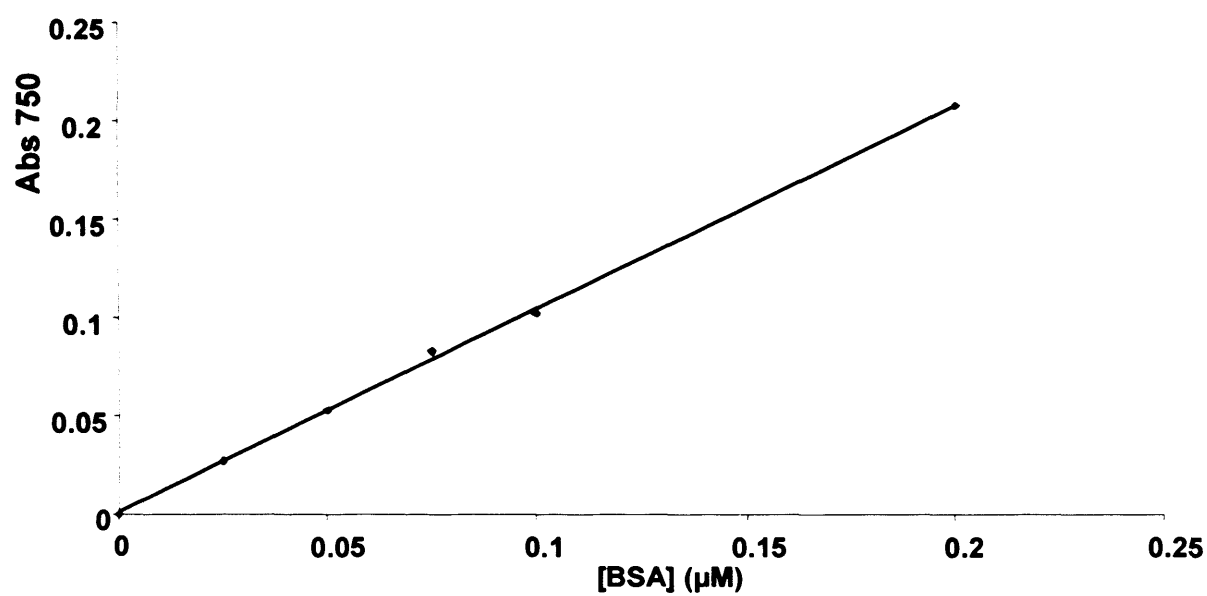


Figure 2.6. BSA standard calibration curve

A serial dilution of 0.2 mg/ml BSA as used in the determination of protein cell samples. Absorbance at 750nm is plotted against concentration of protein, showing linearity.

ANOVA followed by a least significant difference multiple range test. Where expressed as ratios (such as complex activity expressed as a ratio to citrate synthase, or percentages), data were first transformed to yield a normal distribution prior to the appropriate analyses were performed: $= \arcsin \sqrt{(\text{ratio})}$. (Gegg *et al.*, 2003; $\arcsin = \sin^{-1}$)

In all cases, $p < 0.05$ was considered statistically significant. Statistics were performed using the Statgraphics program. (Rockville, Maryland, USA)

3. DEVELOPMENT OF AN HPLC METHOD FOR THE DETERMINATION OF CoQ IN BIOLOGICAL MATERIAL OF RODENT ORIGIN

3. DEVELOPMENT OF AN HPLC METHOD FOR THE DETERMINATION OF CoQ IN BIOLOGICAL MATERIAL OF RODENT ORIGIN

3.1. Introduction

CoQ₉ and CoQ₁₀ levels in both rodent and human samples are of interest to both research and clinical disciplines. It is therefore essential that a reliable method for determination of CoQ derivatives in such tissues is available. While reduced ubiquinone (ubiquinol) can be detected using reverse-phase HPLC with electrochemical (EC) detection, oxidised ubiquinone is amenable to HPLC followed by ultraviolet (UV) detection (Takada *et al.*, 1982).

CoQ, as a hydrophobic component of lipid membranes, requires organic extraction from cellular homogenate. As such extraction can result in losses, in order to consolidate such losses, an internal standard must be added to tissue homogenate prior to solvent extraction. Existing HPLC methods for the determination of ubiquinone in tissues have used various alternative CoQ homologues as internal standards (Ogashara *et al.*, 1989; Boitier *et al.*, 1998). However, because most organisms' tissues contain at least small amounts of CoQ isoforms not predominant for that species, (Åberg *et al.*, 1992, Dalner & Sindelar, 2000), it may be preferable to use an internal standard which is not found in nature. Studies involving clinical determination of human ubiquinone levels have previously used CoQ₉ as an internal standard (Ogashara *et al.*, 1989), but this could be complicated by the presence of small amounts of this homologue in human samples due to dietary intake. Additionally, the predominance of CoQ₉ as the major homologue in rodents precludes its use as an internal standard when analysing the ubiquinone content of tissue of rodent origin. This chapter describes the development of a reverse-phase HPLC method using UV detection and a non-physiological diethoxy

analogue of CoQ₁₀ which can be used as an internal standard in the measurement of tissues where either CoQ₉ or CoQ₁₀ predominate.

3.2 Methods

3.2.1. Tissue Culture

Primary astrocytes were cultured as described in section 2.2

3.2.2. Spectrophotometric measurement of ubiquinone standards

The oxidised forms of CoQ₉ and CoQ₁₀ absorb UV light maximally at 275 nm (Okamoto *et al.* 1985). In order to confirm this, ubiquinone was dissolved in ethanol and a wavelength scan of absorbance from 200 to 400 nm performed using a Uvikon XL spectrophotometer. The Beer-Lambert Law, given molar extinction coefficients of $14.7 \times 10^3 \text{ M}^{-1} \text{ cm}^{-1}$ and $14.6 \times 10^3 \text{ M}^{-1} \text{ cm}^{-1}$ for CoQ₉ and CoQ₁₀ respectively, allowed determination of the concentration of ubiquinone standards. Stock solutions dissolved in ethanol were stored at -80°C until required. Oxidised ubiquinone standards appeared to be unaffected by freezing and storage, as determined by spectrophotometry. In addition, the fully oxidised state of CoQ in the standard was confirmed by addition of the oxidising agent hexacyanoferrate (Okamoto *et al.*, 1985).

3.2.3. Reverse phase chromatography coupled to UV detection

The reverse-phase HPLC employed was based on the methods of Takada *et al.* (1982) and Boitier *et al.* (1998), utilising a C18 column (150mm x 4mm; ODS 5 μ ; Techsphere; HPLC Technology, Welwyn Garden City, UK.) preceded by a Techsphere ODS 5 μ guard column. A Jasco (Great Dunmow, UK) UV-975 Intelligent UV-Vis

detector measured absorbance at 275nm. The mobile phase consisted of 7:3 ethanol:methanol, with 33 mM HClO₄ and 57mM NaClO₄, and samples were injected into a 50µl loop through a Rheodyne injector (Thermo Separation Products, Hemel Hempstead, UK.). A Jasco PU-1580 pump (flow rate: 0.7 ml/min), Jasco DG-1580-53 degasser and ChromJet (Thermo Separation Products, Hemel Hempstead, UK.) integrator completed the HPLC hardware. A schematic diagram of the apparatus is shown in Fig. 3.1.

3.2.4. Synthesis of an internal standard used for ubiquinone determination by UV- HPLC

Using modifications of the methods of Edlund, (1988) and Eaton *et al.* (2000), a diethoxy analogue of CoQ₁₀ (Fig. 3.2) was synthesised. CoQ₁₀ (100 mg) was dissolved in 1ml hexane, and sonicated to ensure dissolution. This solution was then dissolved in 4ml dry ethanol and transferred to a separating funnel. The substitution of the methoxy groups with ethoxy groups was catalysed with the addition of NaOH in ethanol (1M; 100 µl). After 20 mins, the addition of glacial acetic acid (1M; 100 µl) acidified the mixture and terminated the reaction. 10 ml of hexane was added, and the reaction mixture was twice washed with 10 ml H₂O. The aqueous layer was run off, leaving the solvent, which was then dried with excess Na₂SO₄. Approximately 2ml of the resultant yellow, oily liquid was removed and centrifuged at 19,000g for 3 mins to check for and remove any particles. Supernatant was then aliquotted and stored at -80°C. This neat mixture was diluted by approximately 1 : 8000 when added to samples for use as an internal standard

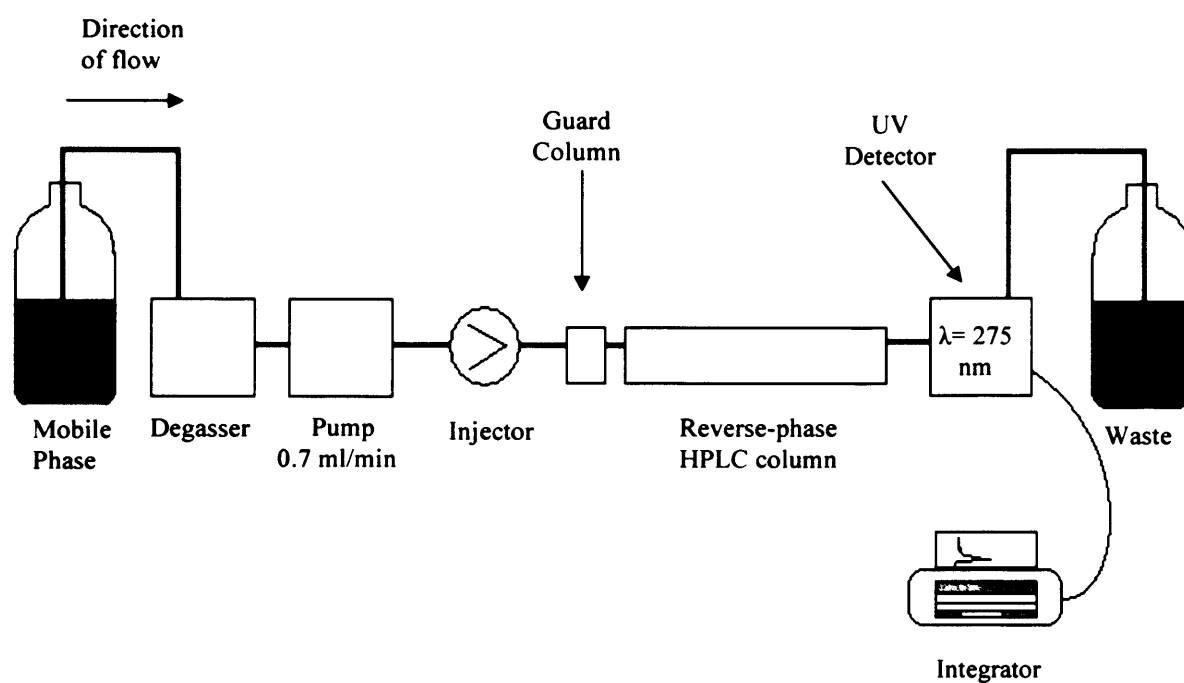


Figure 3.1. Schematic diagram of HPLC apparatus used to determine ubiquinone by reverse-phase HPLC and ultraviolet detection.

3.2.5. Sample preparation for ubiquinone determination by UV-HPLC

Rat primary astrocytes were harvested as described in section 2.2.6, and the pellet resuspended in 200 µl ice-cold isolation medium (320 mM sucrose, 1 mM EDTA, 10 mM Tris; pH 7.4). 40 µl was removed for protein determination, and 20 µl of internal standard added to the remaining 160 µl. Following thorough vortexing to distribute the internal standard, disruption of the mitochondrial membrane was achieved by freeze-thawing three times using liquid nitrogen and a 37°C water bath. 600 µl of extraction medium (hexane:ethanol; 5:2) was added to the tissue homogenate, and the mixture was vortexed again before centrifugation at 16,000 g for 4 mins. The solvent layer was removed and saved, another 600 µl of extraction medium added to the homogenate and the extraction process repeated a further two times. Subsequently, approximately 1000 µl of supernatant organic solvent was obtained, in which was dissolved the endogenous CoQ₉ and CoQ₁₀. This was then dried under a stream of nitrogen gas and the residue reconstituted in 160µl ethanol. This was passed through a Millex 0.22µ syringe-driven filter to remove protein and cellular debris directly before injection onto the column. In some cases, hexacyanoferrate was added to the extract immediately prior to filtration in order to ascertain that CoQ was fully oxidised when extracted by this method (Okamoto *et al.*, 1985).

3.3. Experimental protocol

3.3.1. Chromatography and UV absorbance properties of CoQ

Following confirmation of absorption spectra maxima of CoQ₉ and CoQ₁₀ at 275nm, concentrations were calculated using the Beer Lambert Law. These standards were then combined in known concentrations. This mixture was then resolved by HPLC into 2 peaks showing CoQ₉ and CoQ₁₀.

3.3.2. Validation of the internal standard

Validation experiments in which a known amount of internal standard was subjected to three times freeze-thawing, followed by extraction, reconstitution and filtering steps were performed. As the internal standard's UV-HPLC properties were unchanged following these procedures, rat brain homogenate was prepared (10% w/v) in ice-cold isolation buffer (320 mM sucrose, 1 mM EDTA, 10 mM Tris; pH 7.4), and the CoQ₉ concentration of this homogenate determined (using CoQ₁₀ as an internal standard). The homogenate was then divided into six parts, and internal standard added to all. In addition, three of the six samples also had 50% of the original amount of CoQ₉ added. Ubiquinone was then extracted from these samples, and the concentration measured by HPLC analysis as described in the previous section. These allowed determination of a percentage recovery, and comparison with existing methods using other CoQ analogues as internal standards.

3.3.3. Determination of CoQ in rat astrocytes using the internal standard

Internal standard was added to rat astrocytes prior to freeze-thawing and solvent extraction as described in Section 3.2.5. These samples were then analysed by UV-HPLC as described in section 3.2.2.

3.4. Results

3.4.1. Chromatography and UV detection of ubiquinone

The absorption of UV light by CoQ₉ and CoQ₁₀ in the range 200 nm - 400 nm was measured. This is shown in figures 3.3 & 3.4 respectively. In addition to a peak at 275 nm a stronger peak was evident at 205 nm. However, due to the absorbance of a

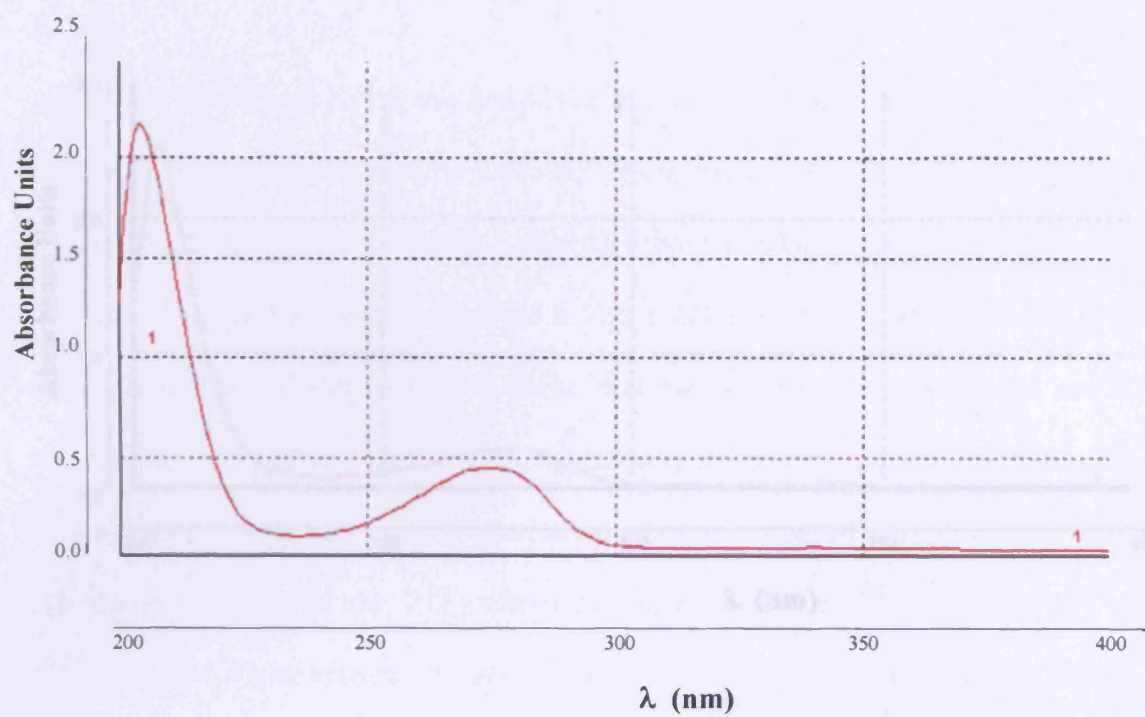


Figure 3.3. Wavelength scan of CoQ₉ in ethanol showing maximal absorption at $\lambda=205$ and 275nm.

number of molecules at this wavelength, determination of ubiquinol was carried out at 275nm.

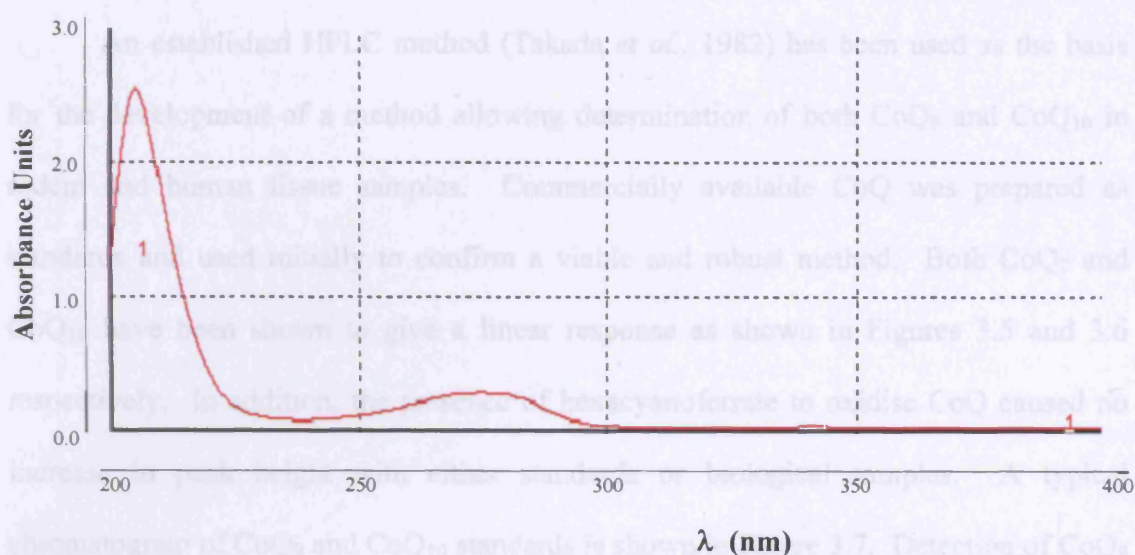


Figure 3.4. Wavelength scan of CoQ₁₀ in ethanol showing maximal absorption at $\lambda=205$ and 275nm.

3.4.3. Ubiquinone levels in cultured astrocytes

Following extraction as described in section 3.2.3, detection of both CoQ₉ and CoQ₁₀ in the extract was possible (Fig 3.8). Cellular CoQ levels were calculated by measuring the peak height of the extract, and comparing it to the standard. The concentration of CoQ in the extract was divided by the percentage recovery of the

number of molecules at this wavelength, determination of ubiquinone was carried out at 275nm.

An established HPLC method (Takada *et al.*, 1982) has been used as the basis for the development of a method allowing determination of both CoQ₉ and CoQ₁₀ in rodent and human tissue samples. Commercially available CoQ was prepared as standards and used initially to confirm a viable and robust method. Both CoQ₉ and CoQ₁₀ have been shown to give a linear response as shown in Figures 3.5 and 3.6 respectively. In addition, the presence of hexacyanoferrate to oxidise CoQ caused no increase in peak height with either standards or biological samples. A typical chromatogram of CoQ₉ and CoQ₁₀ standards is shown in Figure 3.7. Detection of CoQ₉ and CoQ₁₀ was linear between 50 and 1000 nM. $R^2 = 0.999$ for both CoQ₉ and CoQ₁₀.

3.4.2. Development and characterisation of an internal standard

Synthesis of diethoxy-CoQ₁₀ as an internal standard allowed the calculation of and compensation for losses occurring as a result of solvent extractions. A spectral scan between 200 - 400 nm is shown in Figure 3.8. Addition of the internal standard to biological samples before the extraction did not interfere with the existing CoQ chromatography (Fig. 3.9). Spiking experiments resulted in a calculated recovery of $107 \pm 2\%$.

3.4.3. Ubiquinone levels in cultured astrocytes

Following extraction as described in section 3.2.5, detection of both CoQ₉ and CoQ₁₀ in the extract was possible (Fig 3.8). Cellular CoQ levels were calculated by measuring the peak height of the extract, and comparing it to the standard. The concentration of CoQ in the extract was divided by the percentage recovery of the

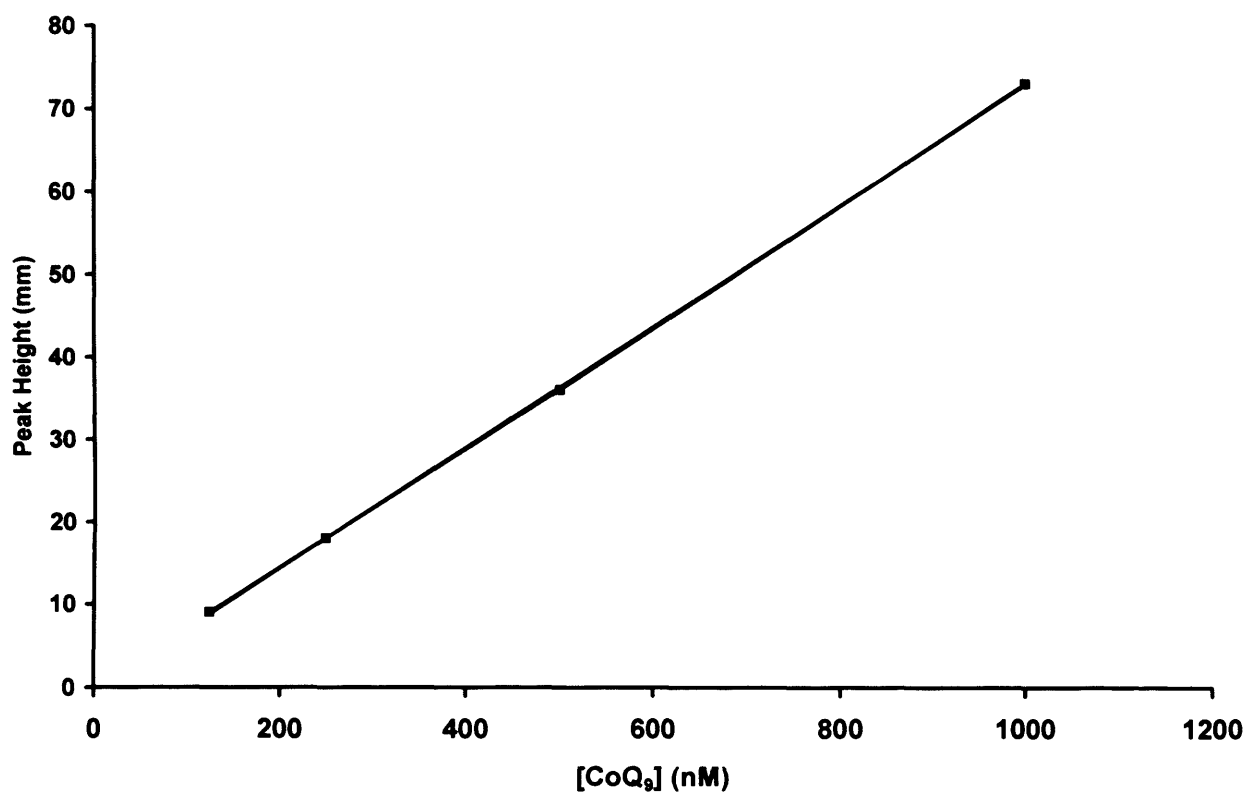


Figure 3.5. CoQ₉ standard calibration curve.

Detector settings were as follows:

Absorption λ = 275 nm

Range = 0.005

Response speed = standard

Mode = normal

Integrator settings were as follows:

Chart speed = 0.25 cm/sec

Attenuation = 16

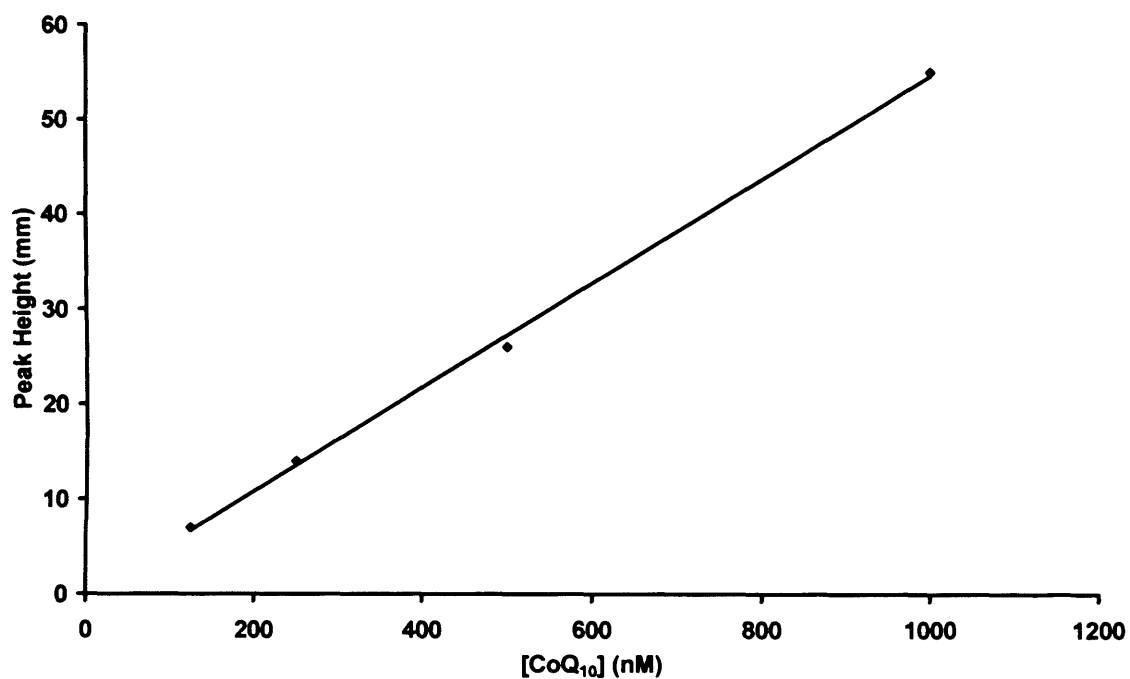


Figure 3.6. CoQ₁₀ standard calibration curve.

Detector settings were as follows:

Absorption λ = 275 nm

Range = 0.005

Response speed = standard

Mode = normal

Integrator settings were as follows:

Chart speed = 0.25 cm/sec

Attenuation = 16

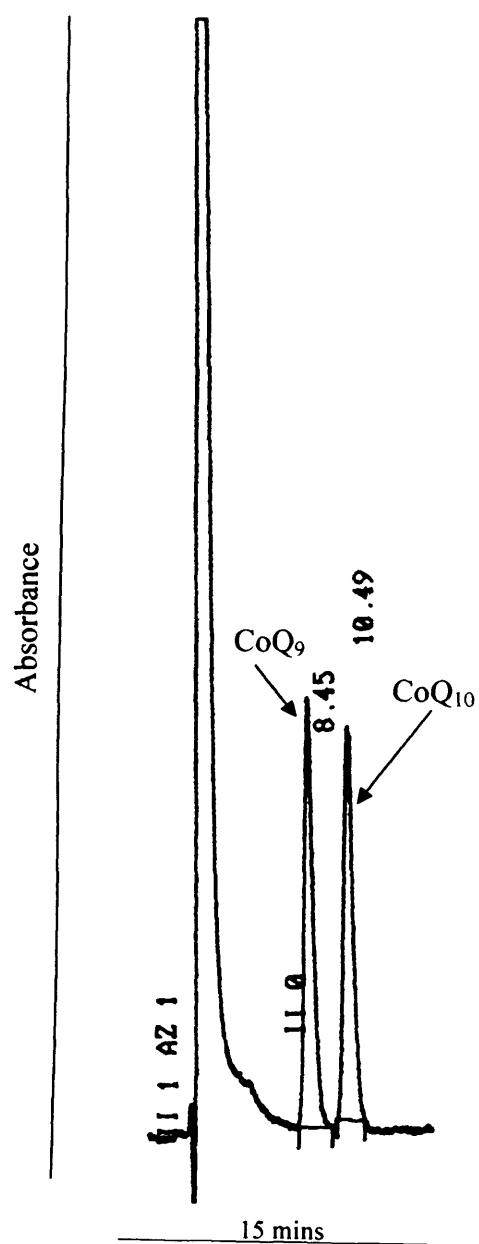


Figure 3.7. Chromatogram of 250 nM CoQ₉ and 250 nM CoQ₁₀ standards.

Settings as described previously except attenuation = 4.

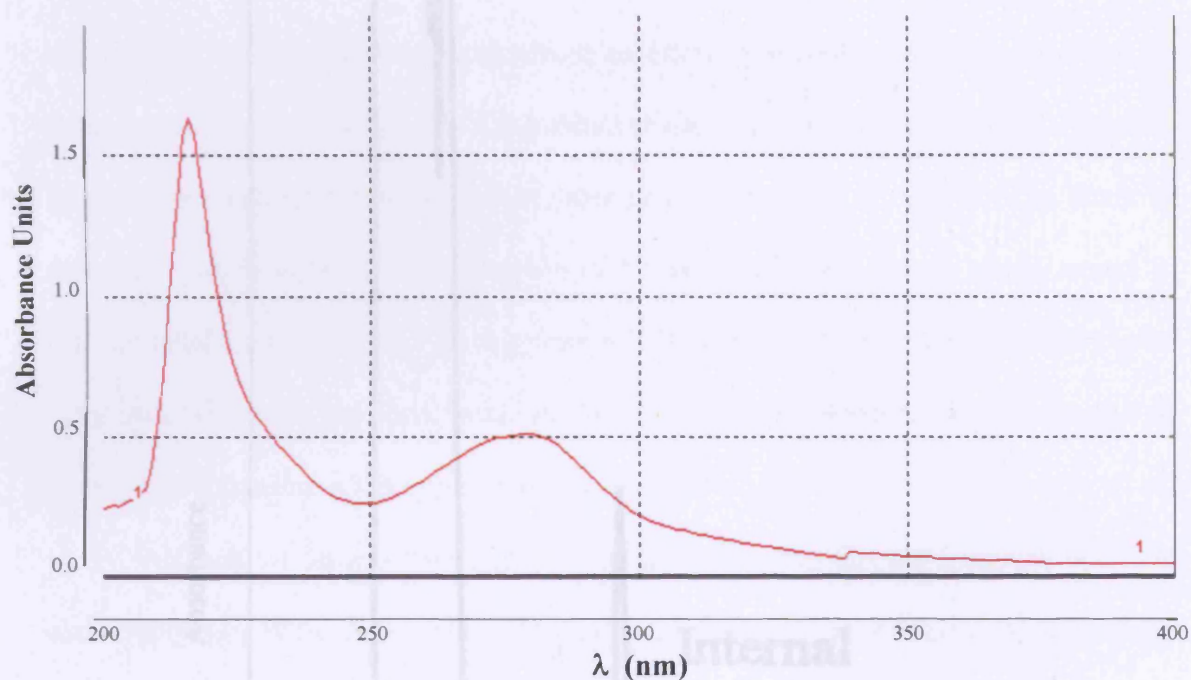


Figure 3.8. Wavelength scan of diethoxyCoQ₁₀ in ethanol showing maximal absorption at $\lambda = 216$ and 280nm .

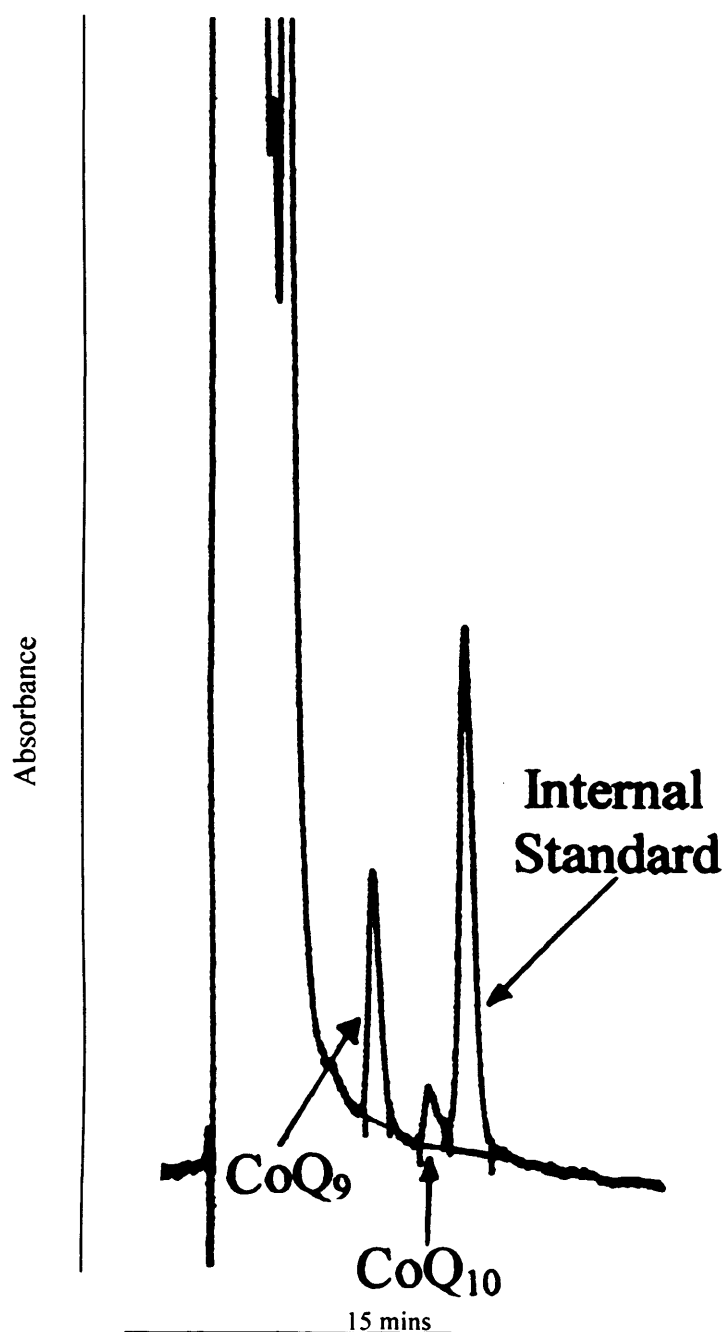


Figure 3.9. Typical HPLC chromatogram obtained from analysis of rat astrocytes.

Settings as described previously, except integrator attenuation is in this case = 4. This figure shows CoQ₉ and CoQ₁₀ as extracted from rat primary astrocytes, with the internal standard.

internal standard. Finally, this concentration (in nmol/l) was expressed against a protein baseline (pmol CoQ/ mg protein). CoQ₉ levels in these astrocytes was calculated as 174.2 ± 10.8 pmol CoQ₉ /mg protein. CoQ₁₀ was less abundant at 37.9 ± 1.6 pmol /mg protein (n = 12 independent cell culture preparations for both observations). Variability was calculated as 6.5%, observed when a single astrocyte homogenate was extracted and CoQ determined 3 times. Additionally, 3 separate astrocyte preparations resulted in an inter-assay variability of 4.8%. The limit of detection was found to be in the region of 5 nM CoQ in the extract, which relates to cellular levels in the pmol range/ mg protein. The extraction process yielded CoQ in its fully oxidised state, as there was no increase in CoQ detected when exposed to hexacyanoferrate immediately prior to analysis.

Although a large solvent front was observed, this did not interfere with the chromatography of CoQ₉ or CoQ₁₀. If ubiquinone homologues of molecular mass lower than that of CoQ₉ were to be considered, this may prove problematic.

3.5 Discussion

Previously, CoQ₉ has been routinely used as an internal standard in clinical determination of human ubiquinone levels. However, this is clearly unsuitable for species in which this homologue is the predominant isoform. Appendix I describes the analysis of a human sample using the diethoxy internal standard. A muscle biopsy received by the Neurometabolic Unit of the National Hospital for Neurology and Neurosurgery, London, UK for analysis. This case of suspected ubiquinone deficiency was analysed using the internal standard described here.

As rodents utilise primarily CoQ₉, and CoQ₁₀ accounts for approximately 18% of the total ubiquinone extracted from rat primary astrocytes, an alternative internal

standard was necessary. The modification of CoQ₁₀ to its diethoxy analogue caused an increase in retention time on this HPLC system when compared to CoQ₁₀ itself. Initial experiments had shown diethoxy-CoQ₁₀ to be stable, and subsequent spiking experiments using tissue homogenates gave a recovery of close to 100%. Time has shown that this internal standard does not revert back to CoQ₁₀ in measurable amounts when stored at -80°C and handled with the same precautions as ubiquinone. The internal standard has been used previously to assess the ubiquinone content of human plasma (Eaton *et al.*, 2000) but not in rodent tissue.

Edlund *et al.* (1994) calculated the CoQ₉ level in cultures of rat dorsal root ganglion neurons as 680 pmol/ mg, and CoQ₁₀ levels in the region of 400 pmol/ mg. However, the findings of Kamzalov, *et al.* (2003) describing CoQ levels in homogenate of rat brain report CoQ₉ levels of 200 pmol/ mg protein with CoQ₁₀ present at approximately 100 pmol/ mg. Albano *et al.* (2002) measured CoQ₉ and CoQ₁₀ in rat foetal mixed cultures, and report levels of approximately 250 pmol/ mg protein for each homologue. Thus it can difficult to make comparisons to previous findings for a number of reasons: the results described here, are from monocultures of neonatal rat primary astrocytes expressed against a protein baseline. The literature databases yield no publications discussing CoQ levels in rat astrocyte cultures. Differences may occur as a result of *in vivo* experiments compared to *ex vivo* cell culture techniques. Species differences will alter the ratio of CoQ₉: CoQ₁₀, and possibly the amount of total CoQ. Finally, it is possible that a failure to use, or differences in, internal standards could account for some of the variability of CoQ levels encountered when searching the literature.

3.6 Conclusion

It was necessary to develop this HPLC method to measure CoQ₉ and CoQ₁₀ in biological material of rodent origin with a novel internal standard as the use of other CoQ homologues may affect results obtained. This method has employed an internal standard which is not a naturally-occurring CoQ homologue. Thus the peak obtained are distinct from those of the analytes. The method is highly reproducible with a low co-efficient of deviation and excellent recovery.

In addition, this internal standard can also be used in the determination of CoQ₁₀ in human samples, which may contain small but measurable amounts of CoQ₉. As described in subsequent chapters, this HPLC method has been used in to determine CoQ levels in a number of neural cell types exposed to various potentially oxidative and nitrosative stresses. It has also been used to determine the amount of CoQ₁₀ in human muscle biopsy samples (Appendix I). As ubiquinone has been postulated as being neuroprotective (Edlund *et al.*, 1994; Matthews *et al.*, 1998; Cammer, 2002) and alterations in ubiquinone metabolism have been described in some neurodegenerative conditions, (Söderberg *et al.*, 1992; Shults *et al.*, 1997; Molina *et al.*, 2002) this method can be used to elucidate whether CoQ₉ or CoQ₁₀ levels are altered in response to oxidative/ nitrosative stimuli in brain cell culture models of oxidative and nitrosative stress.

**4. CoQ₉ AND CoQ₁₀ STATUS OF RAT AND
HUMAN BRAIN CELL LINE CULTURES;
EFFECTS OF NO, LIPOPOLYSACCHARIDE
+ γ -INTERFERON & LOVASTATIN
EXPOSURE**

4. CoQ₉ AND CoQ₁₀ STATUS OF RAT AND HUMAN BRAIN CELL LINE CULTURES; EFFECTS OF NO, LIPOPOLYSACCHARIDE + γ -INTERFERON & LOVASTATIN EXPOSURE

4.1. Introduction

CoQ₉ is the predominant ubiquinone homologue in rodents. In humans, a higher molecular mass isoform with 10 repeating units forming its polyprenyl tail is the most abundant CoQ molecule (Ramasara, 1985). Most mammals have a small percentage of a second isoform comprising their total ubiquinone (reviewed in Szkopinska, 2000). CoQ₉ and CoQ₁₀ were initially assumed to perform the same physiological role in different species. Thus, in earlier studies, little attention was paid to potential physiological differences between the different molecular mass homologues. However the ratio of CoQ₉ : CoQ₁₀ varies between species and tissues examined, and it has subsequently been proposed that separate isoforms may be employed in differing physiological roles. The findings of Matsura *et al.* (1991), supported by the findings of Battino *et al.* (1995 and 2001) suggest that CoQ₁₀ acts as an electron carrier in the ETC, while CoQ₉ may be expected to function primarily as an antioxidant (Matsura *et al.*, 1991). Lass *et al.*, (1997) reported that CoQ₁₀ generated less superoxide than CoQ₉, and subsequent studies raised the possibility of this being due to a lower degree of mitochondrial protein binding of CoQ₉ (Lass and Sohal, 1999).

Additionally, the role of CoQ₁₀ in the human brain has provoked much discussion within the literature. Putative neuroprotective actions of CoQ₁₀ towards cultured cells (Edlund *et al.*, 1994; Cammer 2002; Sandu *et al.*, 2003), or as a therapy for diseases such as PD (Shults *et al.*, 2002), HD (Huntingdon Study Group, 2001), and animal

models of ALS (described in Beal, 1999) and cerebral ischemia (Ostrowski, 2000) have increased interest in CoQ₁₀ as a human therapeutic agent.

In order to further investigate this homologue using human brain cells, it was necessary to use a human neural cell line. This chapter describes investigations carried out using the human-derived 1321N1 astrocytoma cell line. Cultures were exposed to a number of treatments by supplementation of their culture media.

For comparison, data derived from the human cell line were compared to those obtained from the rat C6 glioma cell line.

Lovastatin inhibits HMG-CoA reductase, the rate-limiting enzyme for cholesterol synthesis (Alberts *et al.*, 1980). Due to commonality between the biosynthetic pathways for cholesterol and CoQ, statin drugs are also proposed to potentially inhibit CoQ₉ and CoQ₁₀ synthesis leading to decreased CoQ₉ and CoQ₁₀ levels in rats (Willis *et al.*, 1990) and serum CoQ₁₀ in humans (Folkers *et al.*, 1990).

A combination of lipopolysaccharide and γ -interferon (LPS+IFN γ) induces iNOS in astrocytes (Galea *et al.*, 1992; Bolaños *et al.*, 1994) and some astrocyte-derived cell lines (Feinstein *et al.*, 1994). The C6 glioma line is reported to be capable of inducing iNOS when treated for 24h with LPS+IFN γ (Feinstein *et al.*, 1994). CoQ is reported to be susceptible to attack by NO or its metabolites (Kalen *et al.*, 1989; Schopfer *et al.*, 2000). Thus the effects of NO and lovastatin upon CoQ₉ and CoQ₁₀ status were examined in these cultures. In addition, lovastatin is proposed to induce cytokine-mediated iNOS expression in rat and human brain transformed cell lines (Rattan *et al.*, 2003), thus combinations treatments examined the effects of NO production in lovastatin-treated cultures.

4.2. Aims

- To determine the basal levels of CoQ₉ and CoQ₁₀ in rat C6 glioma and human 1321N1 astrocytoma cultures.
- To examine the effects of lovastatin (in both the prodrug and active isoform) upon such cultures
- To examine the effects of iNOS induction / exogenous NO on these cells, and the effects of lovastatin upon iNOS-mediated NO generation.

4.3. Methods

4.3.1. Tissue culture

1321N1 human astrocytoma cells (ECACC no. 86030402) were recovered from cryostat liquid nitrogen storage as described in section 2.2.5. Culture conditions were maintained as per section 2.2.5.1. Rat C6 glioma cultures (ECACC no. 92090409) were also investigated, and cultured as described in sections 2.2.5. and 2.2.5.2. Cultures were exposed to a range of treatments for 24h in the absence of serum and the cells collected as a pellet as described in sections 2.2.6.

4.3.2. CoQ measurement by HPLC

Following extraction of cellular lipids as described in section 3.2.5, the concentrations of CoQ₉ and CoQ₁₀ were measured by reverse-phase UV-HPLC as described in section 3.2.3.

4.3.3. NO_x determination in tissue culture media

The concentration of nitrate+nitrite (NO_x) in the cell culture medium was determined as an index of NO generation as per section 2.4.

4.3.4. Protein determination

All measurements were expressed against a protein baseline. Protein content of samples was determined by the method of Lowry *et al.* (1951) as in section 2.7.

4.4. Experimental protocols

4.4.1. Exposure of human 1321N1 and rat C6 cells to lipopolysaccharide + γ -interferon

Human 1321N1 and rat C6 cultures were exposed to media supplemented with LPS (1 μ g/ml) and IFN γ (100 U/ml) for 24h and the cellular CoQ levels measured. L-N6-(1-iminoethyl)lysine hydrochloride (L-NIL) is an inhibitor of iNOS (Moore *et al.*, 1994), and in some cases this was used in conjunction with LPS+IFN γ . In order to determine whether LPS+IFN γ elicited NO generation in these cultures, NO_x concentration in the media was determined.

4.4.2. Exposure of rat C6 cells to DETA-NO

Following experiments in which both cell lines were exposed to LPS+IFN γ , the nitric oxide donor DETA-NO (500 μ M) was used to expose the rat-derived cell line to exogenously generated NO. NO generation was confirmed by the measurement in the cell culture media of NO_x. In some cases, DETA-NO was allowed to degrade for at least 7 days at 37°C, and was used as a negative control where appropriate.

4.4.3. Exposure of human 1321N1 and rat C6 cells to lovastatin

Lovastatin is an inhibitor of HMG Co-A reductase (Alberts *et al.*, 1980). It has been reported that lactonase enzymes increase the efficacy of lovastatin *in vivo* (Endo, 1976; Gerson *et al.*, 1989). As expression of such lactonases in these cells was unconfirmed, the lactone ring was cleaved by conversion of lovastatin to its sodium salt (Na-lovastatin; Endo *et al.*, 1976). Thus lovastatin (10 μ M) was added to cell culture media in both the natural lactone form and as Na-lovastatin (see figure 2.3 for structures). In order to measure whether iNOS was induced in response to either the treatment or the appropriate controls (ethanol (1% (v/v)) for the lactone or 1M NaOH in ethanol (1% (v/v) for the sodium salt), NO_x concentration in the cell culture media was determined.

4.4.4. Simultaneous exposure of human 1321N1 and rat C6 cells to lipopolysaccharide + γ -interferon and lovastatin

Both cell types were exposed to media supplemented with Na-lovastatin (10 μ M) in addition to LPS+IFN γ used at the concentrations described previously. Media were collected and NO_x measured to evaluate the effects of lovastatin upon NO generation in these cells.

4.4.5. Simultaneous exposure of rat C6 cells to DETA-NO and lovastatin

Rat C6 cultures were exposed to media supplemented with both DETA-NO (500 μ M) and Na-lovastatin (10 μ M). NO_x was also measured in the cell culture media in order to confirm generation of NO by the NO donor.

4.4.6. Simultaneous exposure of rat C6 cells to DETA-NO and lipopolysaccharide + γ -interferon

The dual insult of exogenous NO generation by DETA-NO (500 μ M) combined with LPS and IFN γ (as previous concentrations) was examined to determine the effect upon CoQ levels and resultant NO generation in the cell culture media.

4.5. Results

4.5.1. CoQ levels in human 1321N1 astrocytoma and rat C6 glioma cells

4.5.1.1. Human 1321N1 astrocytoma

The predominating ubiquinone homologue was found to be CoQ₁₀ (33.8 ± 7.6 pmol/ mg protein). CoQ₉ accounted for approximately 9% of the total (3.3 ± 1.6 pmol/ mg protein; Fig 4.1A).

4.5.1.2. Rat C6 glioma

In contrast to the human cell line, in these rat-derived cultures CoQ₉ was found to be the most abundant isoform (114.3 ± 15.7 pmol/ mg protein). In this case, CoQ₁₀ accounted for approximately 13% of the total cellular CoQ (17.8 ± 3.3 pmol/ mg protein; Fig 4.1B).

4.5.2. The effect of lipopolysaccharide + γ -interferon on CoQ status of human 1321N1 astrocytoma and rat C6 glioma cells

4.5.2.1. Human 1321N1 astrocytoma

Exposure of 1321N1 cultures to LPS+IFN γ for 24h did not significantly alter the amount of either CoQ₉ or CoQ₁₀ detected in these cells (CoQ₉: control = 3.3 ± 1.6 pmol/ mg protein; LPS+IFN γ = 3.7 ± 3.1 pmol/ mg protein; CoQ₁₀: control = 33.8 ± 7.6

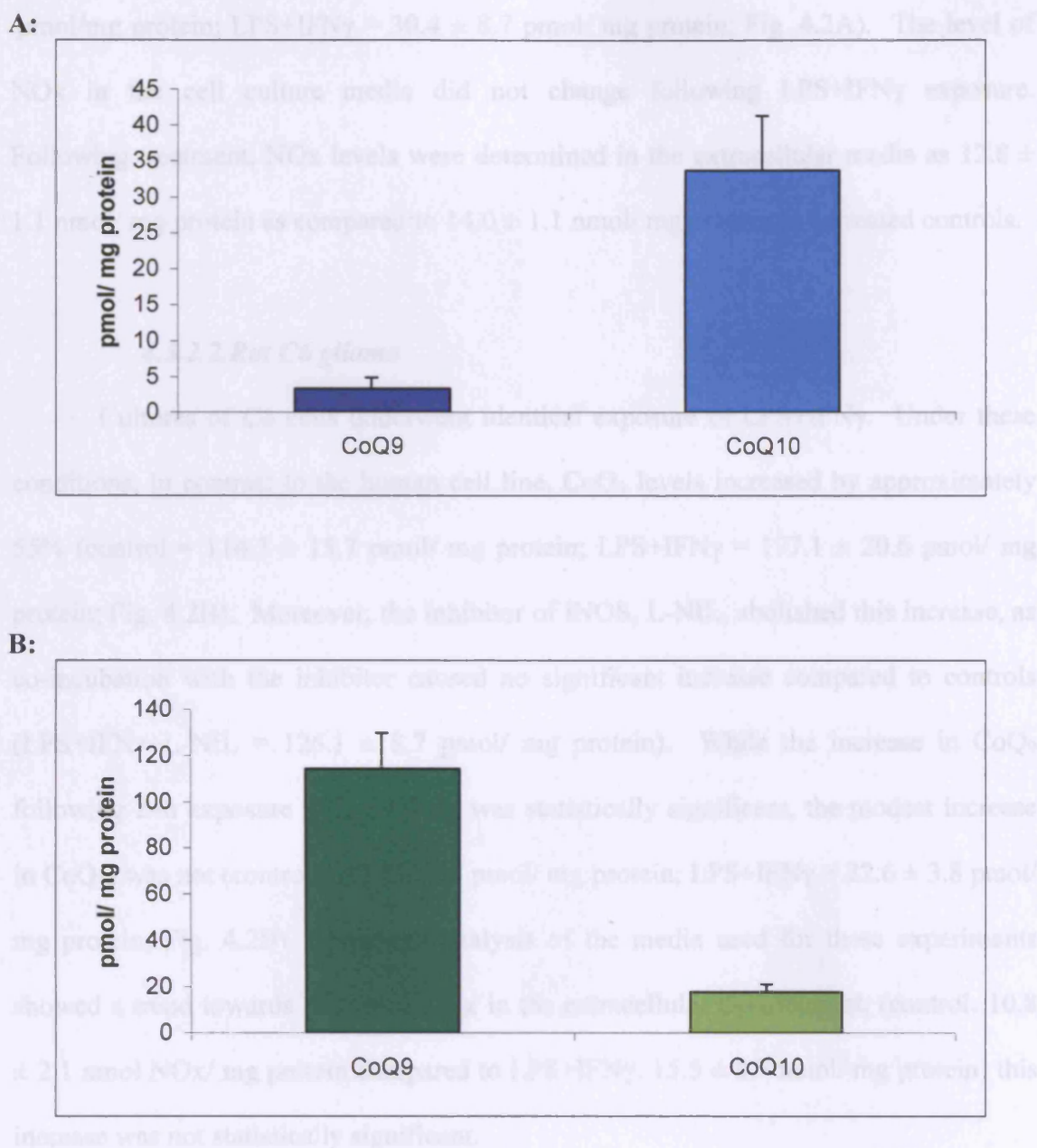


Figure 4.1. Ubiquinone levels in untreated human 1321N1 astrocytoma and rat C6 glioma cultures.

Human 1321N1 astrocytoma (**A**) and rat C6 glioma cells (**B**) were grown for 24h in 6-well culture plates without FBS as described in sections 2.2.4 and 2.2.5. Data are mean \pm SEM values of five independent culture preparations.

pmol/mg protein; LPS+IFN γ = 30.4 ± 8.7 pmol/ mg protein; Fig. 4.2A). The level of NO $_x$ in the cell culture media did not change following LPS+IFN γ exposure. Following treatment, NO $_x$ levels were determined in the extracellular media as 12.8 ± 1.1 nmol/ mg protein as compared to 14.0 ± 1.1 nmol/ mg protein in untreated controls.

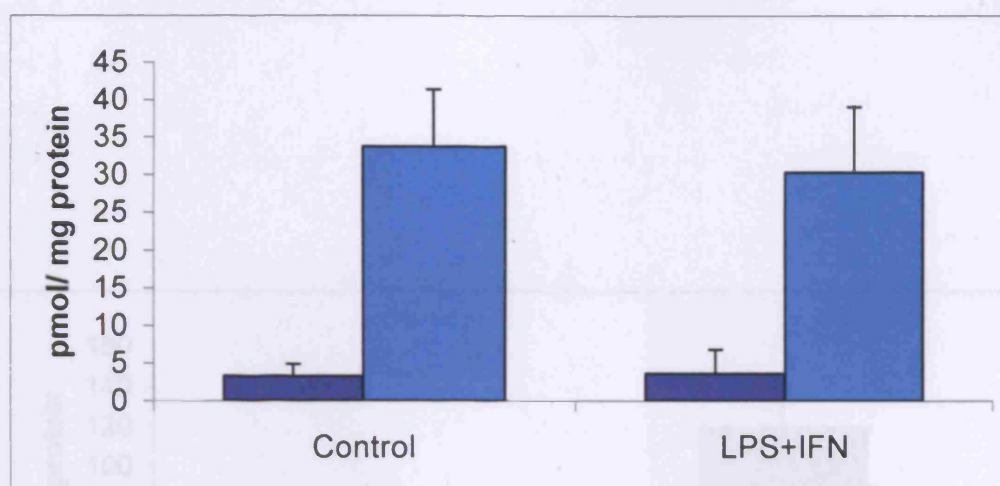
4.5.2.2. Rat C6 glioma

Cultures of C6 cells underwent identical exposure of LPS+IFN γ . Under these conditions, in contrast to the human cell line, CoQ $_9$ levels increased by approximately 55% (control = 114.3 ± 15.7 pmol/ mg protein; LPS+IFN γ = 177.1 ± 20.6 pmol/ mg protein; Fig. 4.2B). Moreover, the inhibitor of iNOS, L-NIL, abolished this increase, as co-incubation with the inhibitor caused no significant increase compared to controls (LPS+IFN γ +L-NIL = 126.1 ± 8.7 pmol/ mg protein). While the increase in CoQ $_9$ following 24h exposure to LPS+IFN γ was statistically significant, the modest increase in CoQ $_{10}$ was not (control = 17.8 ± 3.3 pmol/ mg protein; LPS+IFN γ = 22.6 ± 3.8 pmol/ mg protein; Fig. 4.2B). Although analysis of the media used for these experiments showed a trend towards increased NO $_x$ in the extracellular environment, (control: 10.8 ± 2.1 nmol NO $_x$ / mg protein compared to LPS+IFN γ : 15.5 ± 0.7 nmol/ mg protein) this increase was not statistically significant.

4.5.3. The effect of DETA-NO on CoQ status of rat C6 glioma cells

The NO donor DETA-NO increased NO $_x$ in the cell culture media by approximately 11-fold (untreated control = 10.8 ± 2.1 nmol/ mg protein; DETA-NO = 119.4 ± 18.2 nmol/ mg protein Fig. 4.3). No significant change was observed against control values for either CoQ $_9$ (control = 99.1 ± 7.8 pmol/ mg protein; DETA-NO = 88.5 ± 2.2 pmol/ mg protein; Fig 4.4) or CoQ $_{10}$ (control = 16.4 ± 2.1 pmol/ mg protein;

A:



B:

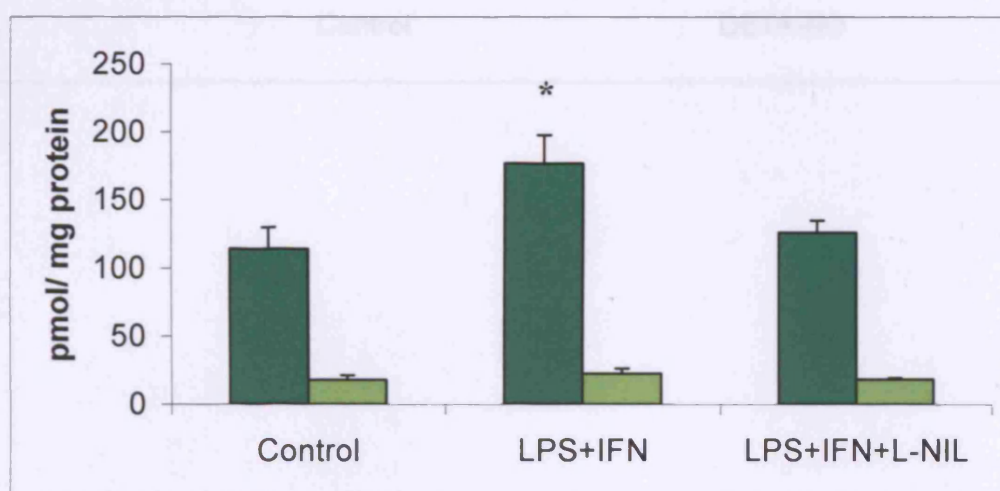


Figure 4.2. The effect of LPS+IFN γ , and L-NIL treatment upon the CoQ status of human 1321N1 astrocytoma and rat C6 glioma cultures.

A: Human 1321N1 astrocytoma cells were incubated for 24h in 6-well culture plates in the absence (control) or presence of LPS + IFN γ (1 μ g/ml; 100 U/ml, respectively) as indicated. ■ = CoQ₉; ■ = CoQ₁₀. Data are mean \pm SEM values of four to five independent culture preparations.

B: Rat C6 glioma cells were incubated for 24h in 6-well culture plates in the absence (control) or presence of LPS + IFN γ (1 μ g/ml; 100 U/ml, respectively). L-NIL (100 μ M) was included as indicated. ■ = CoQ₉; ■ = CoQ₁₀. Data are mean \pm SEM values of four to five independent culture preparations. * signifies $p < 0.05$ analysed by one-way ANOVA.

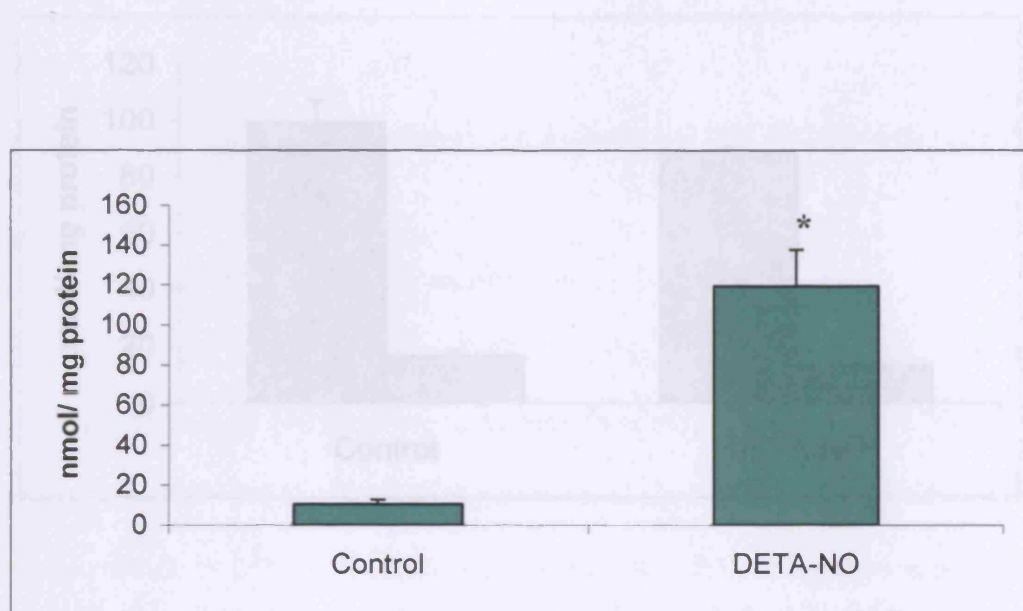


Figure 4.4. Ubiquinone levels in rat C6 glioma cultures treated with DETA-NO.

Figure 4.3. The effect of DETA-NO treatment upon levels of NOx in the media of rat C6 glioma cultures.

Rat C6 glioma cells were grown for 24h in 6-well culture plates without FBS in the absence (control) or presence of DETA-NO (500 μ M) as indicated. ■ = Control, ▨ = DETA-NO.

Rat C6 glioma cells (■) were incubated for 24h in 6-well culture plates in the absence (control) or presence of DETA-NO (500 μ M). Cell culture medium was collected and analysed as described in section 2.4. Data are mean \pm SEM values of four to six independent culture preparations. * signifies $p < 0.05$ analysed by one-way ANOVA.

DETA-NO = 13.1 ± 0.6 pmol/ mg protein; Fig. 4.4). This despite having confirmed generation of NO, levels of CoQ₉ or CoQ₁₀ as measured under these conditions were not significantly different (Fig. 4.4).

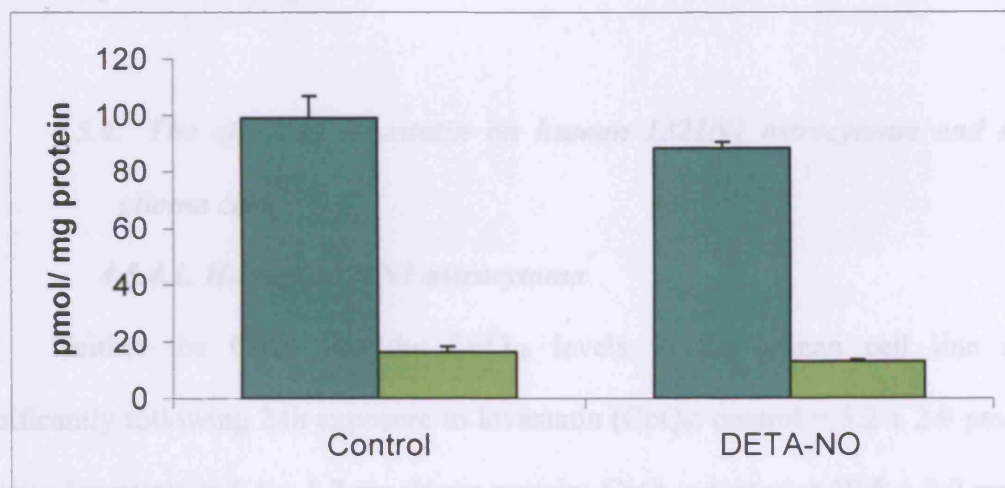


Figure 4.4. Ubiquinone levels in rat C6 glioma cultures treated with DETA-NO.

Rat C6 glioma cells were grown for 24h in 6-well culture plates without FBS in the absence (control) or presence of DETA-NO (500 μ M) as indicated. ■ = CoQ₉; ■ = CoQ₁₀. Data are mean \pm SEM values of four to six independent culture preparations.

In response to 24h exposure to lovastatin, CoQ₉ status of rat C6 cultures decreased by 33% (control = 105.9 ± 10.3 pmol/ mg protein; lovastatin = 71.2 ± 7.3 pmol/ mg protein; Fig. 4.7A). The sodium salt of lovastatin had a similar effect (control

DETA-NO = 13.1 ± 0.6 pmol/ mg protein; Fig. 4.4). . Thus despite having confirmed generation of NO, levels of CoQ₉ or CoQ₁₀ as measured under these conditions were not significantly different. (Fig. 4.4).

4.5.4. The effect of lovastatin on human 1321N1 astrocytoma and rat C6 glioma cells

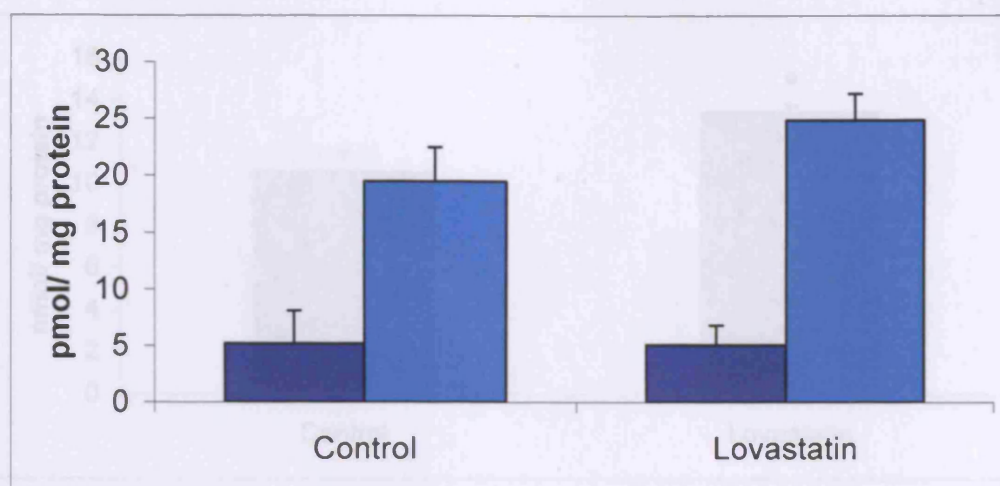
4.5.4.1. Human 1321N1 astrocytoma

Neither the CoQ₉ nor the CoQ₁₀ levels in the human cell line altered significantly following 24h exposure to lovastatin (CoQ₉: control = 5.2 ± 2.9 pmol/ mg protein; lovastatin = 5.1 ± 1.7 pmol/ mg protein; CoQ₁₀: control = 19.5 ± 3.0 pmol/mg protein; lovastatin = 24.9 ± 2.3 pmol/ mg protein; Fig. 4.5A). This treatment resulted in a modest increase of NO_x in the cell culture media and in this case statistical significance was achieved (control = 10.6 ± 1.0 nmol/ mg protein; lovastatin = 13.4 ± 0.3 nmol/ mg protein Fig. 4.6A). Na-lovastatin caused a statistically significant decrease in the amount of cellular CoQ₉ (control = 8.7 ± 1.2 pmol/ mg protein; Na-lovastatin = 1.7 ± 1.1 pmol/ mg protein; Fig. 4.5B) but not CoQ₁₀ (control = 24.4 ± 2.3 pmol/ mg protein; Na-lovastatin = 29.5 ± 6.0 pmol/ mg protein; Fig. 4.5B). Under these conditions however, the amount of NO_x in the cell culture media did not change (control = 12.0 ± 0.5 nmol/ mg protein; Na-lovastatin = 12.8 ± 1.1 nmol/ mg protein; Fig. 4.6B)

4.5.4.2. Rat C6 glioma

In response to 24h exposure to lovastatin, CoQ₉ status of rat C6 cultures decreased by 33% (control = 105.9 ± 10.5 pmol/ mg protein; lovastatin = 71.2 ± 7.8 pmol/ mg protein Fig. 4.7A). The sodium salt of lovastatin had a similar effect (control

A:



B:

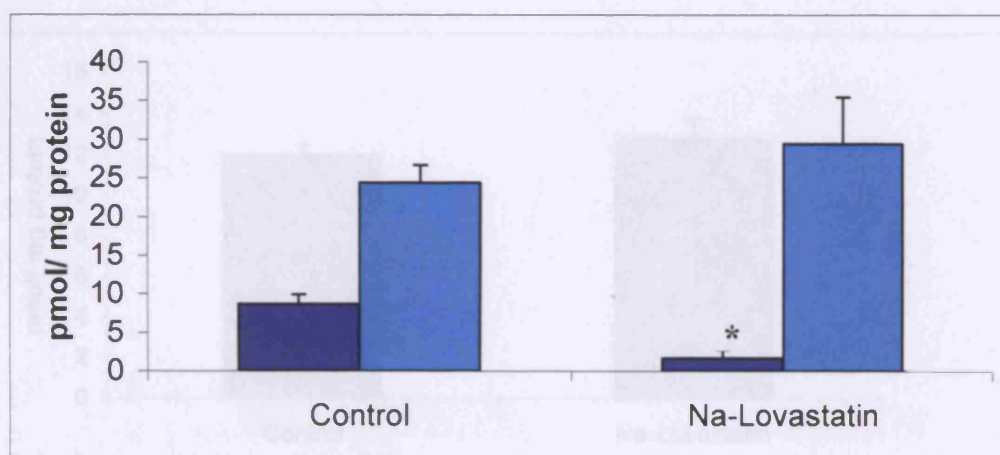


Figure 4.5. The effect of lovastatin and its sodium salt (Na-Lovastatin) treatment upon the CoQ status of human 1321N1 astrocytoma cultures.

A: Human 1321N1 astrocytoma cells were incubated for 24h in 6-well culture plates in ethanol (1% (v/v); control) or lovastatin (10 μ M) as indicated. ■ = CoQ₉; ■ = CoQ₁₀. Data are mean \pm SEM values of three to five independent culture preparations.

B: Human 1321N1 astrocytoma cells were incubated for 24h in 6-well culture plates in 1M NaOH in ethanol (1% (v/v); control) or Na-lovastatin (10 μ M) as indicated. ■ = CoQ₉; ■ = CoQ₁₀. Data are mean \pm SEM values of three to five independent culture preparations. * signifies $p < 0.05$ analysed by one-way ANOVA.

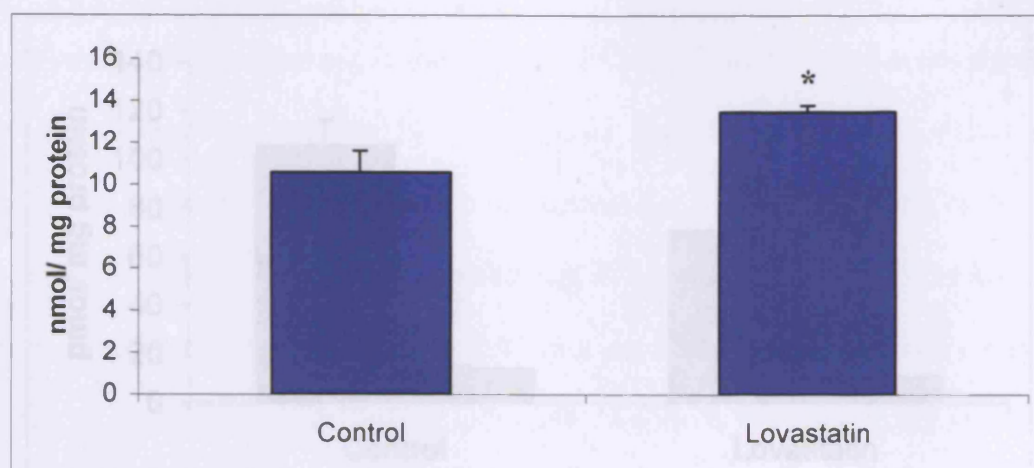
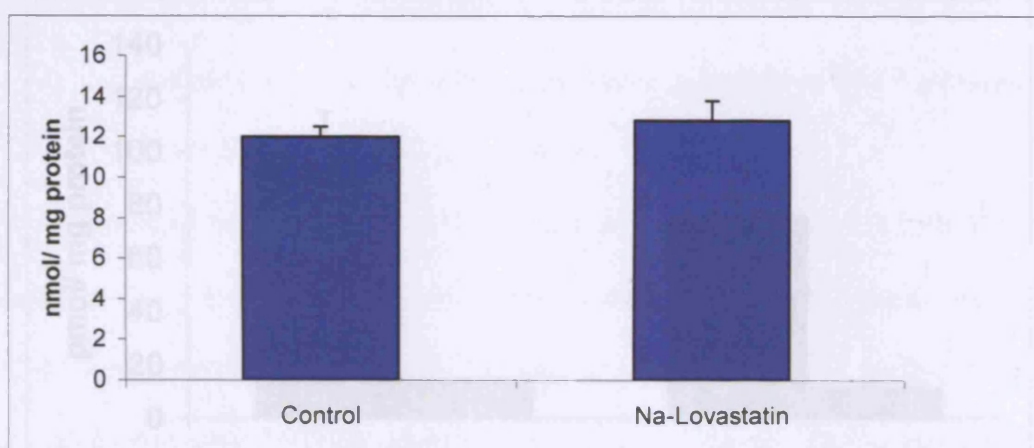
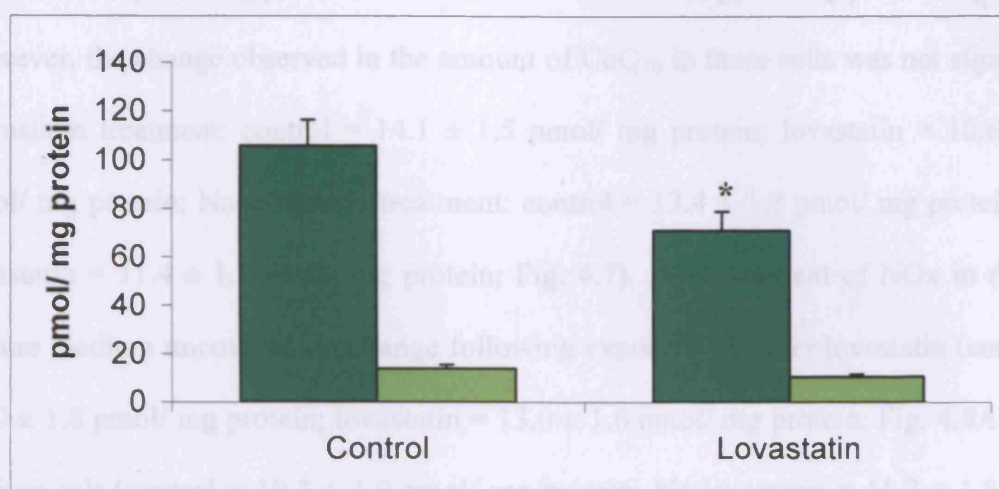
A:**B:**

Figure 4.6. The effect of lovastatin and its sodium salt (Na-Lovastatin) treatment upon the NOx levels in the media of human 1321N1 astrocytoma cultures.

A: Human 1321N1 astrocytoma cells were incubated for 24h in 6-well culture plates in ethanol (1% (v/v) control) or lovastatin (10 μ M) as indicated. Data are mean \pm SEM values of three to four independent culture preparations. * signifies $p < 0.05$ analysed by one-way ANOVA.

B: Human 1321N1 astrocytoma cells were incubated for 24h in 6-well culture plates in 1M NaOH in ethanol (1% (v/v); control) or the sodium salt of lovastatin (10 μ M) as indicated. Data are mean \pm SEM values of three to four independent culture preparations.

A: 106.0 ± 9.2 pmol/ mg protein; Na-lovastatin = 75.7 ± 7.0 pmol/ mg protein (Fig. 4.7B).



B:

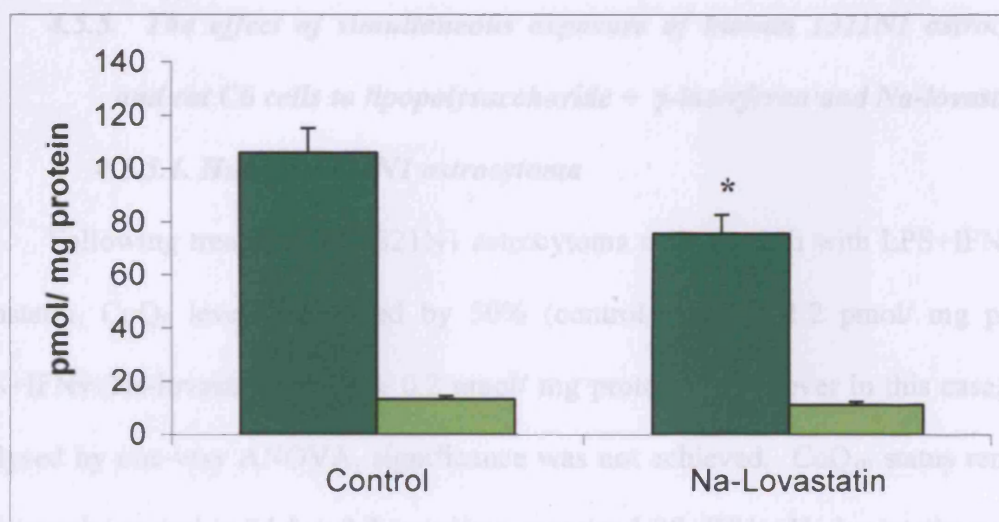


Figure 4.7. The effect of lovastatin and its sodium salt (Na-Lovastatin) treatment upon the CoQ status of rat C6 glioma cultures.

A: Rat C6 glioma cells were incubated for 24h in 6-well culture plates in ethanol (1% (v/v); control) or lovastatin (10 μ M) as indicated. ■ = CoQ₉; ■ = CoQ₁₀. Data are mean \pm SEM values of three to five independent culture preparations. * signifies $p < 0.05$ analysed by one-way ANOVA.

B: Human 1321N1 astrocytoma cells were incubated for 24h in 6-well culture plates in 1M NaOH in ethanol (1% (v/v); control) or Na-lovastatin (10 μ M) as indicated. ■ = CoQ₉; ■ = CoQ₁₀. Data are mean \pm SEM values of three to five independent culture preparations. * signifies $p < 0.05$ analysed by one-way ANOVA.

= 106.0 ± 9.2 pmol/ mg protein; Na-lovastatin = 75.7 ± 7.0 pmol/ mg protein Fig. 4.7B). However, the change observed in the amount of CoQ₁₀ in these cells was not significant (lovastatin treatment: control = 14.1 ± 1.5 pmol/ mg protein; lovastatin = 10.6 ± 1.0 pmol/ mg protein; Na-lovastatin treatment: control = 13.4 ± 1.3 pmol/ mg protein; Na-lovastatin = 11.4 ± 1.1 pmol/ mg protein; Fig. 4.7). Measurement of NO_x in the cell culture medium uncovered no change following exposure to either lovastatin (control = 12.0 ± 1.8 pmol/ mg protein; lovastatin = 13.0 ± 1.6 nmol/ mg protein; Fig. 4.8A) or its sodium salt (control = 10.3 ± 1.0 pmol/ mg protein; Na-lovastatin = 11.7 ± 1.0 nmol/ mg protein; Fig. 4.8B).

4.5.5. The effect of simultaneous exposure of human 1321N1 astrocytoma and rat C6 cells to lipopolysaccharide + γ -interferon and Na-lovastatin

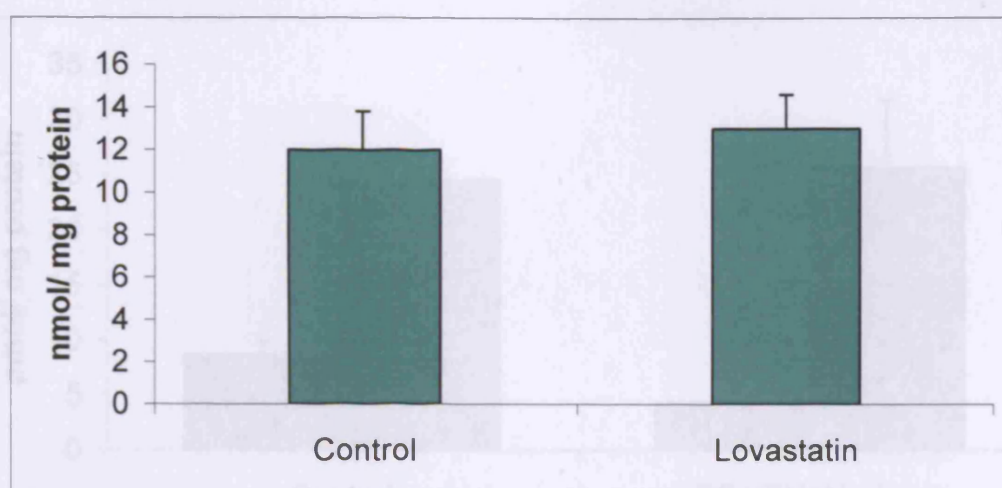
4.5.5.1. Human 1321N1 astrocytoma

Following treatment of 1321N1 astrocytoma cells for 24h with LPS+IFN γ +Na-lovastatin, CoQ₉ levels decreased by 50% (control = 8.7 ± 1.2 pmol/ mg protein; LPS+IFN γ +Na-lovastatin = 4.4 ± 0.2 pmol/ mg protein). However in this case, when analysed by one-way ANOVA, significance was not achieved. CoQ₁₀ status remained unchanged (control = 24.5 ± 2.3 pmol/mg protein; LPS+IFN γ +Na-lovastatin = 25.6 ± 6.2 pmol/ mg protein; Fig. 4.9A). In addition, the levels of NO_x were not significantly affected (control = 12.0 ± 0.5 nmol/ mg protein; LPS+IFN γ +Na-lovastatin = 10.3 ± 0.5 nmol/ mg protein; Fig. 4.10A).

4.5.5.2. Rat C6 Glioma

Exposure of rat C6 cultures to LPS+IFN γ +Na-lovastatin caused a decrease of approximately 37% in CoQ₉ levels when compared to controls (control = 106.0 ± 9.2

A:



B:

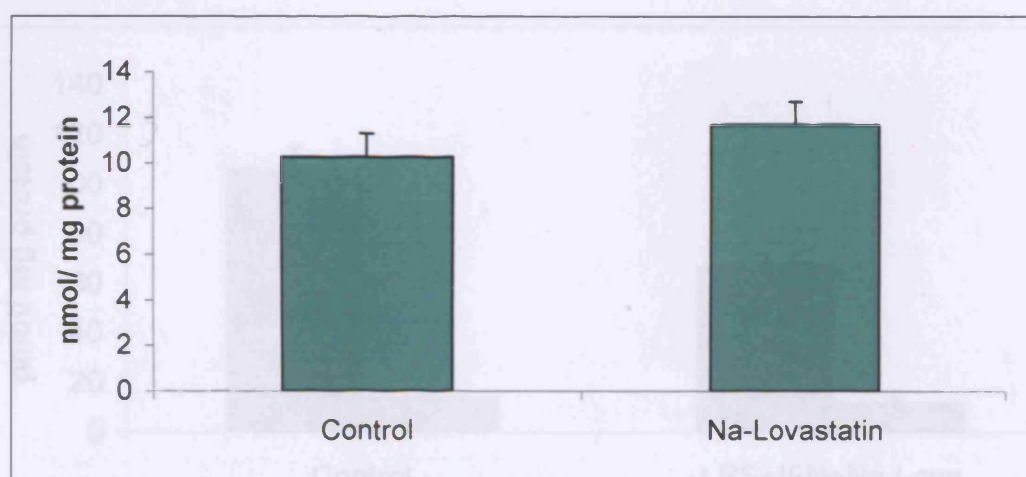
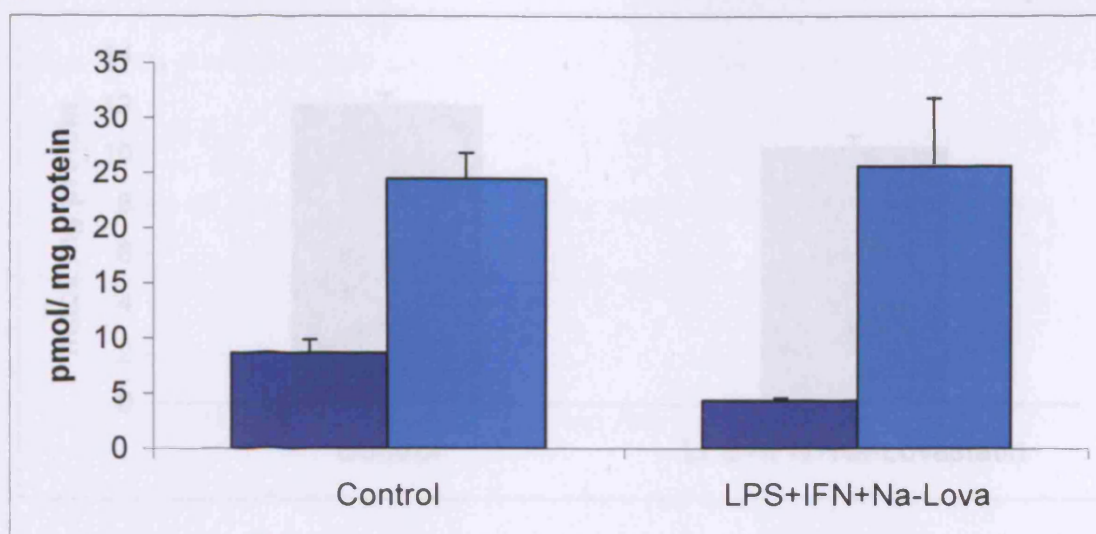


Figure 4.8. The effect of lovastatin treatment upon levels of NOx in the media of rat C6 glioma cultures.

Rat C6 glioma cells were incubated for 24h in 6-well culture plates, either
A: In the presence of the ethanol (1% (v/v) control) or lovastatin (10 μ M), or

B: In the presence of 1M NaOH in ethanol (1% (v/v); control) or Na-lovastatin (10 μ M). Culture medium was collected and used for NOx analysis as described in section 2.4. Data are mean \pm SEM values of five independent culture preparations..

A:



B:

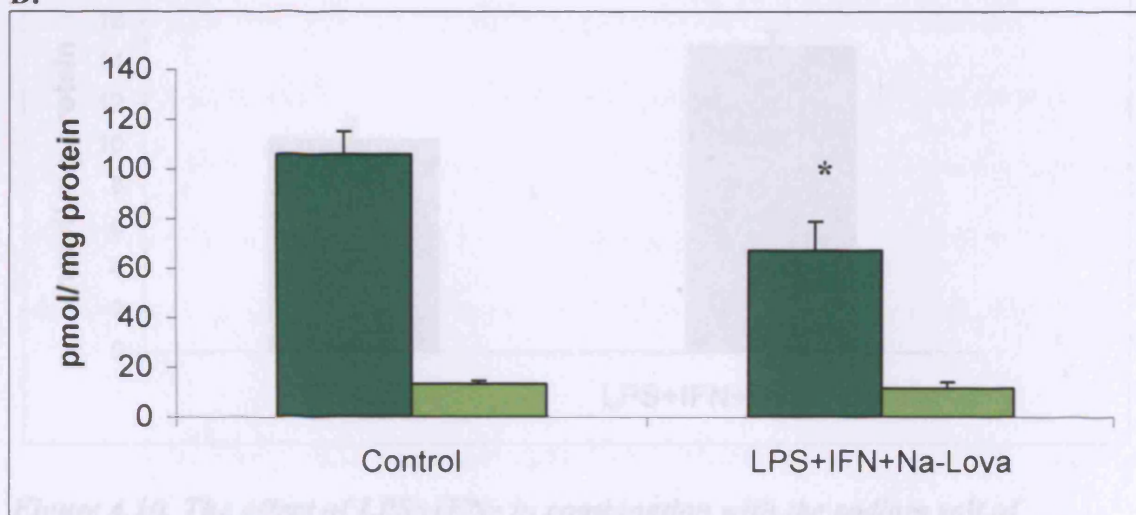


Figure 4.9. The effect of simultaneous exposure of LPS+IFN γ , and the sodium salt of lovastatin upon the CoQ status of human 1321N1 astrocytoma and rat C6 glioma cultures.

A: Human 1321N1 astrocytoma cells were incubated for 24h in 6-well culture plates in the presence of 1M NaOH in ethanol (1% (v/v); control) or LPS+IFN γ as previously, with the addition of Na-lovastatin as indicated. ■ = CoQ₉; ■ = CoQ₁₀. Data are mean \pm SEM values of three to four independent culture preparations.

B: Rat C6 glioma cells were incubated for 24h in 6-well culture plates in the presence of 1M NaOH in ethanol (1% (v/v); control) or LPS+IFN γ as previously, with the addition of Na-lovastatin as indicated. ■ = CoQ₉; ■ = CoQ₁₀. Data are mean \pm SEM values of five to six independent culture preparations. * signifies $p < 0.05$ analysed by one-way ANOVA.

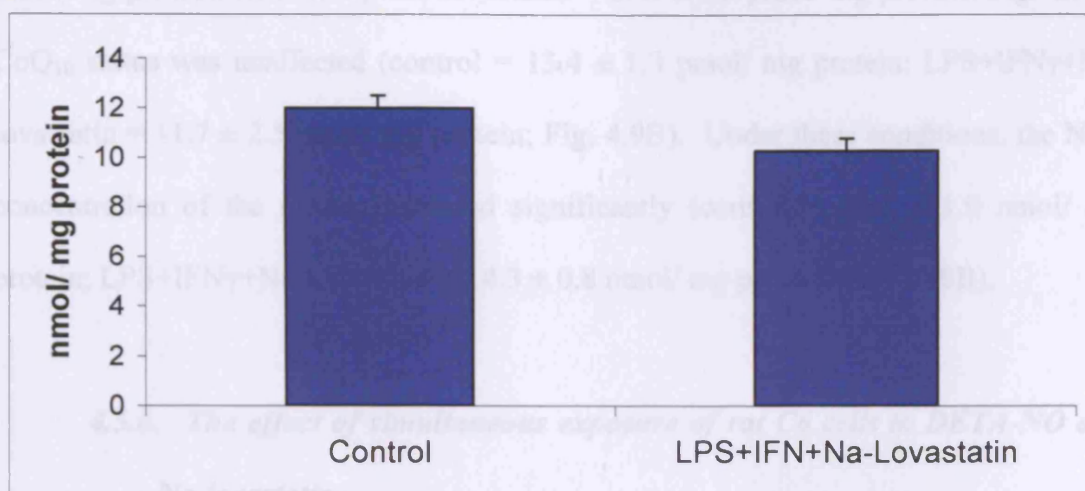
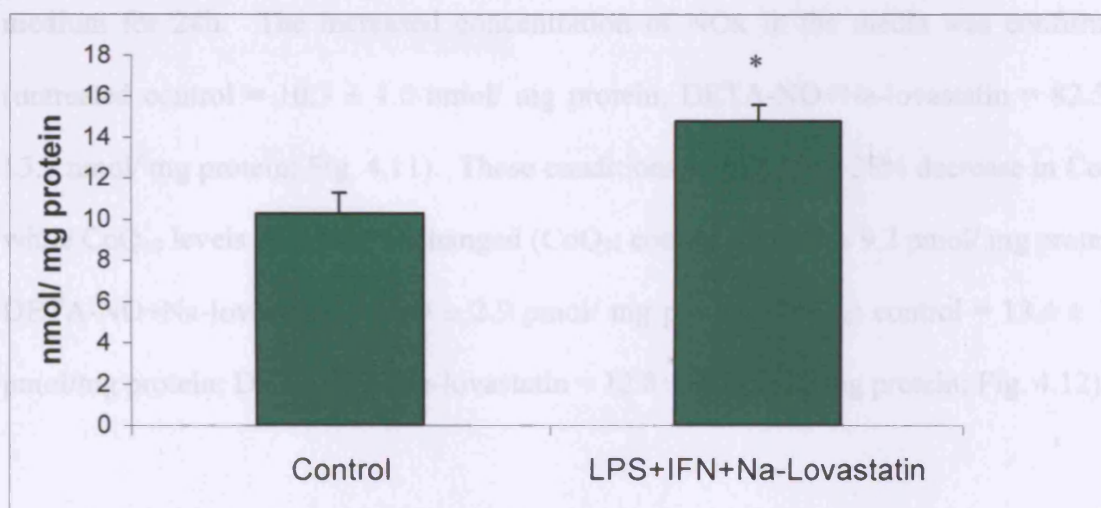
A:**B:**

Figure 4.10. The effect of LPS+IFN γ in combination with the sodium salt of lovastatin (Na-Lovastatin) upon the NO $_x$ levels in the media of human 1321N1 astrocytoma and rat C6 glioma cultures.

A: Human 1321N1 astrocytoma cells were incubated for 24h in 6-well culture plates in the presence of 1% 1M NaOH in ethanol or LPS+IFN γ as previously but with the addition of Na-lovastatin (10 μ M). Culture medium was collected and used for NO $_x$ analysis as described in section 2.4. Data are mean \pm SEM values of three to four independent culture preparations.

B: Rat C6 glioma cells were incubated for 24h in 6-well culture plates in the presence of 1M NaOH in ethanol (1% (v/v); control) or LPS+IFN γ as previously but with the addition Na-lovastatin (10 μ M). Culture medium was collected and used for NO $_x$ analysis as described in section 2.4. as indicated. Data are mean \pm SEM values of three to four independent culture preparations. * signifies $p < 0.05$ analysed by one-way ANOVA.

pmol/ mg protein; LPS+IFN γ +Na-lovastatin = 67.4 ± 1.6 pmol/ mg protein; Fig. 4.9B). CoQ₁₀ status was unaffected (control = 13.4 ± 1.3 pmol/ mg protein; LPS+IFN γ +Na-lovastatin = 11.7 ± 2.5 pmol/ mg protein; Fig. 4.9B). Under these conditions, the NO_x concentration of the media increased significantly (control = 10.3 ± 1.0 nmol/ mg protein; LPS+IFN γ +Na-lovastatin = 14.3 ± 0.8 nmol/ mg protein; Fig. 4.10B).

4.5.6. The effect of simultaneous exposure of rat C6 cells to DETA-NO and Na-lovastatin

DETA-NO in combination with Na-lovastatin was added to the C6 cell culture medium for 24h. The increased concentration of NO_x in the media was confirmed (untreated control = 10.3 ± 1.0 nmol/ mg protein; DETA-NO+Na-lovastatin = 82.5 ± 13.2 nmol/ mg protein; Fig. 4.11). These conditions resulted in a 38% decrease in CoQ₉ while CoQ₁₀ levels remained unchanged (CoQ₉: control = 106.0 ± 9.2 pmol/ mg protein; DETA-NO+Na-lovastatin = 65.9 ± 2.9 pmol/ mg protein; CoQ₁₀: control = 13.4 ± 1.3 pmol/mg protein; DETA-NO+Na-lovastatin = 12.8 ± 0.7 pmol/ mg protein; Fig. 4.12).

4.5.7. The effect of simultaneous exposure of rat C6 cells to lipopolysaccharide + γ -interferon + DETA-NO

The combination of LPS + IFN γ in conjunction with exogenous NO generation did not significantly alter CoQ₁₀ levels, however CoQ₉ decreased by 29% (CoQ₉: control = 99.1 ± 7.8 pmol/ mg protein; LPS+IFN γ +DETA-NO = 70.5 ± 2.7 pmol/ mg protein; CoQ₁₀: control = 16.4 ± 2.1 pmol/mg protein; LPS+IFN γ +DETA-NO = 13.3 ± 0.7 pmol/ mg protein; Fig. 4.13). NO_x in the media, was no greater than that from DETA-NO alone (untreated control = 10.8 ± 2.1 nmol/ mg protein; DETA-NO = 119.4 ± 18.2 nmol/ mg protein; LPS+IFN γ +DETA-NO = 118.2 ± 18.6 nmol/ mg protein; Fig 4.14)

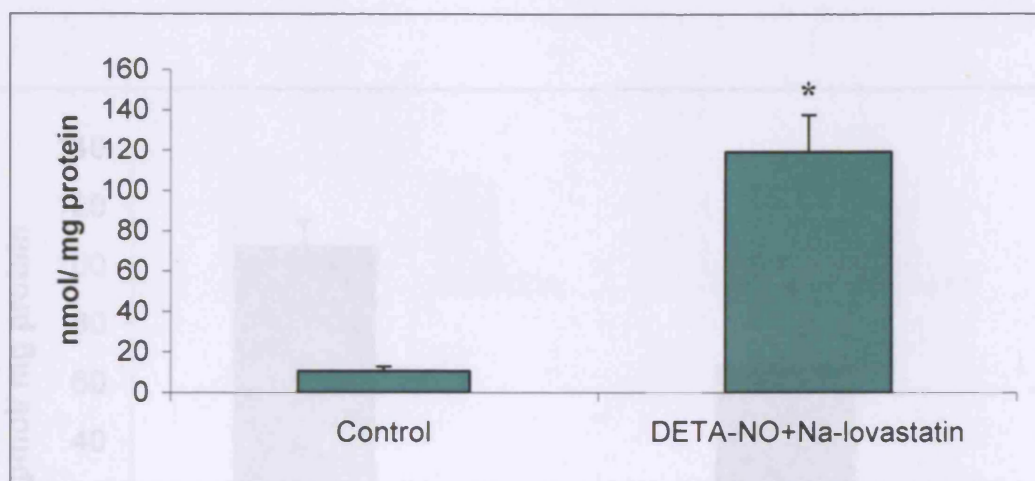


Figure 4.11. The effect of DETA-NO in conjunction with Na-lovastatin upon levels of NOx in the media of rat C6 glioma cultures.

Figure 4.12. The effect of simultaneous exposure of DETA-NO in conjunction with the 10

Rat C6 glioma cells (■) were incubated for 24h in 6-well culture plates in the presence of 1M NaOH in ethanol (1% (v/v); control) or DETA-NO (500μM) with Na-lovastatin (10μM). Cell culture media was removed for analysis of NOx. Data are mean ± SEM values of five to six different culture preparations. * signifies $p < 0.05$ analysed by one-way ANOVA.

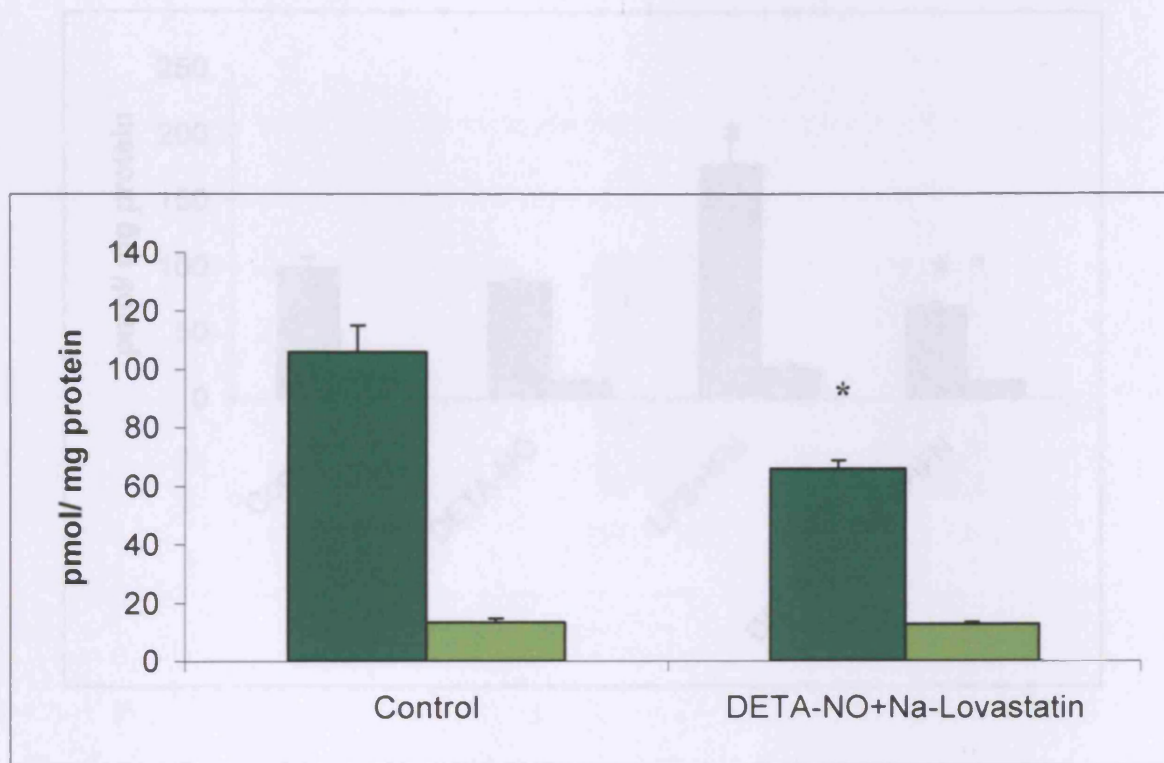


Figure 4.12. The effect of simultaneous exposure of DETA-NO in conjunction with LPS+IFN γ upon the CoQ status of rat C6 glioma cultures.

Figure 4.12. The effect of simultaneous exposure of DETA-NO in conjunction with the sodium salt of lovastatin upon the CoQ status of rat C6 glioma cultures.

Rat C6 glioma cells were incubated for 24h in 6-well culture plates in the presence of 1M NaOH in ethanol (1% (v/v); control) or DETA-NO (500 μ M) in conjunction with Na-lovastatin (10 μ M). ■ = CoQ₉; ■ = CoQ₁₀. Data are mean \pm SEM values of five to six different culture preparations. * signifies $p < 0.05$ analysed by one-way ANOVA

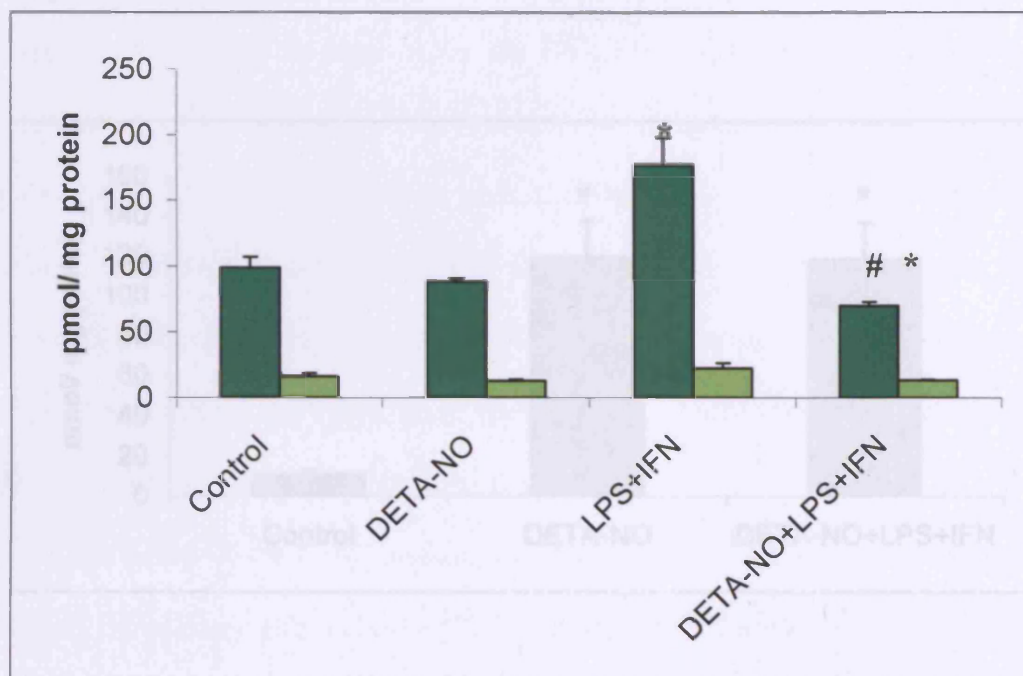


Figure 4.13. The effect of simultaneous exposure of DETA-NO in conjunction with LPS+IFN γ upon the CoQ status of rat C6 glioma cultures.

Rat C6 glioma cells were incubated for 24h in 6-well culture plates in the presence of degraded DETA-NO (control) or fresh DETA-NO (500 μ M) in conjunction with LPS+IFN γ (concentrations as previously). ■ = CoQ₉; □ = CoQ₁₀. Data are mean \pm SEM values of five to six independent culture preparations. * signifies $p < 0.05$ as analysed by one-way ANOVA compared to control values. # signifies $p < 0.05$ as analysed by one-way ANOVA compared to values for LPS+IFN γ .

4.6 Discussion

In human cells CoQ₁₀ predominates; in the 1321NI astrocytoma cultures CoQ₉ accounted for approximately 9% of the total ubiquinone. Conversely, CoQ₁₀ comprised approximately 13% of the total in the rat C6 glioma cultures. With regard to total

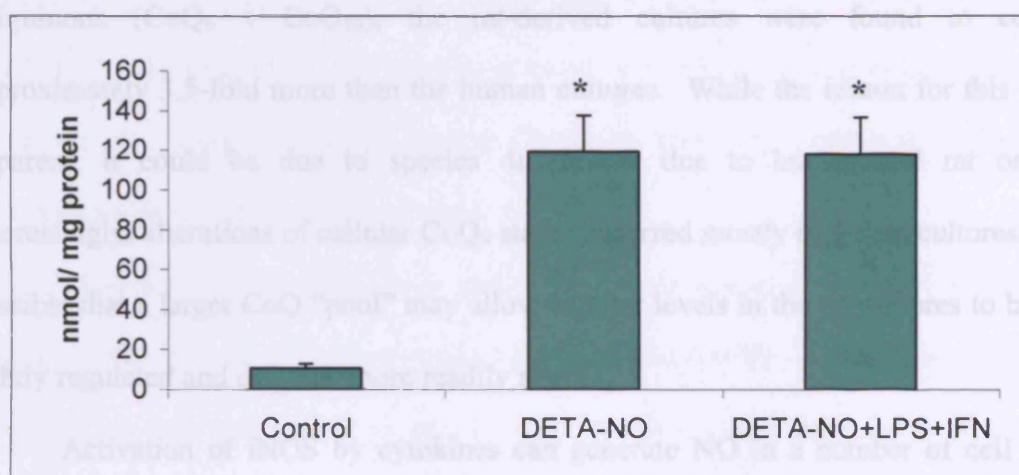


Figure 4.14. The effect of DETA-NO in conjunction with LPS+IFN γ upon levels of NOx in the media of rat C6 glioma cultures.

Rat C6 glioma cells (■) were incubated for 24h in 6-well culture plates in the absence (control) or presence of DETA-NO(500 μ M) and LPS+IFN γ (used as previously). Data are mean \pm SEM values of five to six independent culture preparations. * signifies $p < 0.05$ as analysed by one-way ANOVA.

4.6. Discussion

In human cells CoQ₁₀ predominates; in the 1321N1 astrocytoma cultures CoQ₉ accounted for approximately 9% of the total ubiquinone. Conversely, CoQ₁₀ comprised approximately 13% of the total in the rat C6 glioma cultures. With regard to total ubiquinone (CoQ₉ + CoQ₁₀), the rat-derived cultures were found to contain approximately 3.5-fold more than the human cultures. While the reason for this is not apparent, it could be due to species differences due to human and rat origins. Interestingly, alterations of cellular CoQ₉ status occurred mostly in the rat cultures. It is possible that a larger CoQ “pool” may allow cellular levels in the rat cultures to be less tightly regulated and can thus more readily altered.

Activation of iNOS by cytokines can generate NO in a number of cell types including rat primary glial cultures (Galea *et al.*, 1992; Bolaños *et al.*, 1994), rat C6 glioma cells (Feinstein *et al.*, 1994) and certain astrocytoma lines (Vigne *et al.*, 1993; Mollace *et al.*, 1993). However the specific stimuli required for NO generation, can vary between cell types; for example in C6 cells, NO generation was substantially increased by co-incubation with tumour necrosis factor- α (TNF α ; Feinstein *et al.*, 1994).

Following treatment with LPS+IFN γ , no change was observed in cellular levels of either CoQ₉ or CoQ₁₀ or media NO_x from the human astrocytoma cells. However, although rat C6 glioma cells did not increase NO_x under the same conditions (in agreement with Feinstein *et al.*, 1994) a 55% increase in the amount of CoQ₉ was observed. Moreover, co-incubation of these cultures with L-NIL abolished this increase suggesting the involvement of iNOS, but not NO. The presence of DETA-NO did not alter cellular CoQ levels; however DETA-NO in conjunction with LPS+IFN γ appeared to inhibit the LPS+IFN γ -mediated increase in CoQ₉, reducing CoQ₉ levels to a value significantly below control levels.

Under conditions where either L-arginine (L-arg) or tetrahydrobiopterin (BH₄) are limiting, it has been proposed that iNOS may preferentially generate superoxide (O₂⁻ Heinzl *et al.*, 1992; Consentino *et al.*, 2001). Given that there is no detectable increase in NO_x in the cell culture media, these findings raise the possibility that iNOS-generated O₂⁻ rather than NO could mediate such an increase in CoQ₉ in rat cells. In addition, it is conceivable that inclusion of exogenous NO could scavenge O₂⁻ forming the potentially more deleterious species ONOO⁻. This may explain the subsequent decrease in CoQ₉ under these conditions.

Lovastatin can inhibit CoQ₉ and CoQ₁₀ synthesis as a result of HMG-CoA reductase inhibition in cell culture models (Maltese and Aprille, 1985), humans (Folkers *et al.*, 1990) and rats (Willis *et al.*, 1990). In this study a decrease in CoQ₉ was observed following exposure of the human cell line to Na-lovastatin, but not the prodrug form. In contrast to the human cell line, the rat glioma cultures showed profound decreases in CoQ₉ levels following treatment with both lovastatin and Na-lovastatin respectively. These findings would suggest that the β-hydroxy acid form of lovastatin can be used to decrease cellular CoQ₉ status after 24h incubation of rodent and human-derived cells. In both cell types, CoQ₁₀ appears to be preserved.

Studies by Yamamoto *et al.* (1989) and Gomez-Diaz *et al.* (2003b) have proposed that an interconversion may exist between CoQ₉ and CoQ₁₀. If this were the case, it is also conceivable that if the period of exposure were increased, following CoQ₉ depletion, CoQ₁₀ levels would subsequently begin to fall. A similar effect may be seen if CoQ₁₀ were directly synthesised from CoQ₉ (i.e. by the addition of a single isoprenyl unit), as proposed by Yamamoto *et al.* (1989) using perfused rat heart preparations.

These data would also imply that rodent cells are capable of converting the prodrug to the active isoform. Lactonase activity conferred by paraoxonase-like enzymes have been described in rat liver microsomes (Ozols, 1999); it is conceivable that the rat C6 glioma cell line may possess a similar enzyme which could convert lovastatin to the β -hydroxy form.

Inclusion of LPS+IFN γ with Na-lovastatin in the media of both cell types did not have a different effect compared to the statin alone. However, under these conditions, the increase in CoQ $_9$ obtained when rat glioma cultures were treated with LPS+IFN γ alone was abolished, thus it is possible that Na-lovastatin decreased CoQ $_9$ via biosynthetic inhibition while blocking any iNOS / O $_2^-$ -mediated increase in CoQ.

Conflicting reports in the literature suggest that lovastatin may augment (Ikeda *et al.*, 2001; Rattan *et al.*, 2003) or inhibit (Pahan *et al.*, 1997; Huang *et al.*, 2003) iNOS induction. These studies examined a diverse range of cell types: neonatal rat cardiac myocytes (Ikeda *et al.*, 2001) C6 glioma, T98G and A172 human astrocytoma, neuroblastoma and immortalised rat astrocytes (Rattan *et al.*, 2003), rat primary astrocytes (Pahan *et al.*, 1997), and murine macrophages (Huang *et al.*, 2003). Although in the current study, the human cells exposed to the natural lactone form of lovastatin alone elicited an increase in the amount of NO $_x$ in the cell culture media, this was not reflected with Na-lovastatin. Neither was it consistent with the rat cell line exposed to either form of lovastatin.

The simultaneous inclusion of LPS+IFN γ with Na-lovastatin in the media of the human cell line failed to alter NO generation. However in the rat-derived cultures, the presence of Na-lovastatin caused an increase in NO $_x$ in the media of almost 40%. This statin-mediated increase in the apparent sensitivity of iNOS has been previously described by Ikeda *et al.* (2001) and Rattan *et al.*, (2003). Thus it is evident that

metabolic differences existing between various cell types and species can have profound effects upon cellular responses, in particular lovastatin metabolism and the mechanism by which iNOS is induced.

While exogenous NO alone did not significantly decrease CoQ₉ or CoQ₁₀ in rat C6 glioma cultures, the inclusion of Na-lovastatin with DETA-NO elicited a decrease in CoQ₉ greater than that which occurred in response to Na-lovastatin alone. Thus it may be the case that inhibition of CoQ biosynthesis at the level of HMG Co-A reductase is more profound in the presence of NO possibly as a result of increased turnover.

4.7. Conclusion

These data would suggest that the rat glioma cultures are capable of metabolising the prodrug lovastatin to the active β -hydroxy acid form; while human astrocytoma cells cannot. It is conceivable that this may be due to the presence of a lactonase enzyme in the rat cells, possibly absent in the human cells.

In addition, although human 1321N1 astrocytoma cells contain less total ubiquinone, they may conserve both their CoQ₉ and CoQ₁₀ status in response to treatments causing profound alterations in CoQ₉ status in rat C6 glioma cells. Although CoQ₉ predominates in the rat, and CoQ₁₀ is more abundant in the human, CoQ₉ levels (particularly in the rat-derived cell line) appeared more susceptible to manipulation.

As all but one of the effects manifest as alterations in CoQ₉ status, it is possible to hypothesise that the experimental conditions used here generally influence only CoQ₉ metabolism, but not CoQ₁₀. This could suggest a "sparing effect" in that CoQ₁₀ levels are maintained at the expense of CoQ₉.

**5. CoQ₉ AND CoQ₁₀ LEVELS IN PRIMARY
CULTURES OF RAT ASTROCYTES;
EFFECTS OF SERUM WITHDRAWAL**

5. CoQ₉ AND CoQ₁₀ LEVELS IN PRIMARY CULTURES OF RAT ASTROCYTES; THE EFFECTS OF SERUM WITHDRAWAL

5.1. Introduction

Previous studies have detected small but significant amounts of CoQ₁₀ in rodent-derived tissue (Edlund *et al.*, 1994; Lass & Sohal 1999; Tang *et al.*, 2004). However, reports in the literature are currently lacking with respect to CoQ₉ and CoQ₁₀ levels in primary cultures of rat cortical astrocytes. Primarily, this chapter evaluates the ubiquinone status of these cells, and describes the effects of removal of serum from the cell culture medium for up to 36h prior to harvest.

Serum is a complex mixture of numerous biomolecules. Foetal bovine serum (FBS) is commonly used in cell culture media as a source of anti-apoptotic, hormonal and growth factors, attachment and spreading factors, binding proteins, enzymes, lipoproteins, antioxidants and minerals. Usually, optimum cell growth requires serum in the culture medium between 5 to 20% (v/v) (Maurer, 1986). It has been widely accepted that unless supplemented with the necessary growth, survival and other extracellular factors, cell populations may begin to undergo a number of responses including programmed cell death unless continuously signalled not to either by neighbouring cells, or factors within the culture medium (Raff *et al.*, 1983; Ishizaki *et al.*, 1995). Thus although not all mechanisms are yet understood, serum withdrawal has been used to induce apoptosis, oxidative stress and affect expression of numerous cellular proteins (Ishizaki *et al.*, 1995; Palazzotti *et al.*, 1999; Koshimura *et al.*, 2000; Rössler *et al.*, 2004).

Although the composition of sera used to supplement cultures has not been fully elucidated, FBS is known to be a source of exogenous CoQ (although the CoQ

homologue was not specified; Maltese & Aprille 1985) and cholesterol (Quesney-Huneeus *et al.*, 1979). It is also possible that proteins present in FBS such as bovine serum albumin could affect cellular uptake of compounds from the culture media (Maranga *et al.*, 2002; Selleri *et al.*, 2003; Mundy *et al.*, 2004). Previous chapters have involved supplementation of the culture media with lovastatin in serum-free media to avoid effects resulting from the presence of CoQ in the serum; subsequent chapters will involve supplementation with lovastatin in the presence of serum. However, this drug binds plasma proteins such as albumin *in vivo*, and its cellular uptake involves a carrier-mediated system (Nagasawa *et al.*, 2000). The effects of simvastatin (a close structural analogue of lovastatin) have been shown to decrease with increasing concentration of FBS in the culture media (Kikuchi *et al.*, 1997). It is possible that protein-bound lovastatin may be unable to enter cells resulting in decreased bioavailability or lower efficacy in this cell culture model. Alternatively, the binding of lovastatin to albumin in FBS could conceivably facilitate entry to the cells. Thus it is necessary to investigate serum withdrawal in these cells prior to the use of lovastatin in order to control for any cellular effects due to incubation in the absence of serum.

CoQ₉ and CoQ₁₀ synthesis involves the mevalonate pathway, another end product of which is cholesterol (Turunen *et al.*, 2004; see also figure 1.9). Acetyl CoA is converted to farnesyl pyrophosphate, a common substrate for the synthesis of both CoQ and cholesterol. The rate limiting enzyme (HMG CoA reductase) is thus believed common for both cholesterol and CoQ homologues (reviewed in Dallner and Sindelar, 2000 and Turunen *et al.*, 2002). However, as the latter stages of CoQ₉ and CoQ₁₀ synthesis in mammals are not well characterised, the relationship between relative amounts of these molecules in rat primary astrocytes was investigated.

5.2.Aims

- To determine the levels of CoQ₉, CoQ₁₀ and cholesterol in FBS
- To determine the levels of CoQ₉, CoQ₁₀ and cholesterol in primary cultures of rat cortical astrocytes.
- To investigate the effects of serum withdrawal for up to 36h upon the cellular levels of CoQ₉, CoQ₁₀ and cholesterol.

5.3.Methods

5.3.1. Tissue culture

Primary cultures of rat astrocytes were prepared and maintained as described in section 2.2.3. On DIV 14, cells were subcultured in 6-well plates for 24h or 36h in the presence or absence of serum and the cells collected as a pellet as described in sections 2.2.6.

5.3.2. CoQ measurement by HPLC

Cellular lipids were extracted as described in section 3.2.5, and the concentrations of CoQ₉ and CoQ₁₀ were measured by reverse-phase UV-HPLC as in section 3.2.3.

5.3.3. Cholesterol determination

Determination of total cellular cholesterol in the cell pellet was carried out by spectrophotometry. This is described in section 2.6.

5.3.4. *Lactate dehydrogenase determination*

As an index of cell stress, LDH release from the astrocyte cultures was measured after 36h growth in 6 well plates, and expressed as a percentage of the total LDH activity of the culture following complete lysis using Triton X-100 (0.1% v/v). This is described in section 2.5. In order to account for LDH present in FBS supplements (Haslam *et al.*, 1999), the LDH activity of FBS itself was measured in cell-free culture systems and these values subtracted from total LDH activities of serum-containing cultures

5.3.5. *Protein determination*

For those findings expressed against a protein baseline, the protein content of samples was determined by the method of Lowry *et al.* (1951) as in section 2.7.

5.4. *Experimental protocol*

5.4.1. *Determination of CoQ content of Foetal Bovine Serum*

Lipid extraction was performed (similar to that described in section 3.2.5) by the addition of 600 μ l of hexane/ethanol (5:2) to 160 μ l of FBS. This was vigorously vortexed, centrifuged at 16,000g, and the non-polar supernatant removed. This was repeated twice more, the supernatants pooled and evaporated to dryness under a stream of nitrogen gas. The lipids extracted were resuspended in ethanol (160 μ l), and passed through a 0.22 μ filter prior to injection into the HPLC system.

5.4.2. *Determination of cholesterol content of Foetal Bovine Serum*

As per section 2.6, 100 μ l of FBS (10%, v/v) was added to 675 μ l of reagent 1 (R1) from the CHOL-H L-type spectrofluorometric assay kit (Alpha Laboratories,

Eastleigh, UK). Following incubation for 10 mins at 37°C, 225 µl of R2 was added, the mixture vortexed and incubated as previously. Subsequently, the total cholesterol content of FBS was determined by spectrophotometric measurement at 604 nm. In order to ensure concurrent results across batches, 3 separate batches of serum were used.

5.4.3. Serum withdrawal from astrocyte cultures

Primary cultures of rat astrocytes were plated and maintained in media supplemented with FBS (10% v/v) and media without FBS for either 24h or 36h. Cellular CoQ and cholesterol levels were measured as described.

5.4.4. LDH activity of media from astrocyte cultures

Following removal of 50 µl of culture media, Triton X-100 (0.1%; v/v) was used to lyse the cells. The LDH activity of these samples was determined and the viability of the culture expressed as a “percentage leakage” as previously described in section 2.5.

Additionally, the LDH activity of FBS was determined and expressed as a percentage of the theoretical maximum. The theoretical maximum was obtained by determining the mean of the activity of the cultures following lysis.

5.5. Results

5.5.1. CoQ concentration of Foetal Bovine Serum

Lipid extraction of FBS followed by HPLC analysis resulted in the determination of the concentration of ubiquinone in FBS as $\text{CoQ}_9 = 253.1 \pm 7.6 \text{ nM}$ and $\text{CoQ}_{10} = 54.6 \pm 3.2 \text{ nM}$. This was determined by separate observations on 3 batches of serum.

5.5.2. Cholesterol concentration of Foetal Bovine Serum

Cholesterol content of FBS was measured as in section 2.6. This was determined using 3 separate batches of serum (in duplicate) as $805.8 \pm 26.9 \mu\text{M}$.

5.5.3. CoQ levels in primary cultures of rat astrocytes

Figure 5.1A shows that basal levels in rat primary astrocytes cultured in the presence of FBS for 24h were determined as $\text{CoQ}_9 = 173.6 \pm 19.1 \text{ pmol/ mg protein}$; $\text{CoQ}_{10} = 35.4 \pm 2.7 \text{ pmol/ mg protein}$ (Fig 5.1A). The same cells under similar conditions, but with incubation time extended to 36h in the presence of FBS, were found to have slightly higher cellular CoQ_9 and CoQ_{10} levels of $\text{CoQ}_9 = 183.1 \pm 16.4 \text{ pmol/ mg protein}$ and $\text{CoQ}_{10} = 41.2 \pm 4.4 \text{ pmol/mg}$ (Fig 5.1A). This was not significantly different to the CoQ_9 or CoQ_{10} levels after 24h.

5.5.4. The effect of serum withdrawal on cellular CoQ levels

Cells cultured in the absence of serum for 24h did not contain significantly different amounts of CoQ_9 or CoQ_{10} to those cultured in media supplemented with FBS ($\text{CoQ}_9 = 174.2 \pm 10.8 \text{ pmol/ mg protein}$; $\text{CoQ}_{10} = 37.9 \pm 1.6 \text{ pmol/ mg protein}$; Fig 5.1B).

However, extension of the period of serum withdrawal to 36h gave rise to a statistically significant ($p < 0.05$) increase in CoQ_9 (23%) and CoQ_{10} (18%) when compared to the cells cultured for 24h in the absence of FBS ($\text{CoQ}_9 = 214.8 \pm 6.8 \text{ pmol/ mg protein}$; $\text{CoQ}_{10} = 44.9 \pm 3.2 \text{ pmol/ mg protein}$; Fig 5.1B).

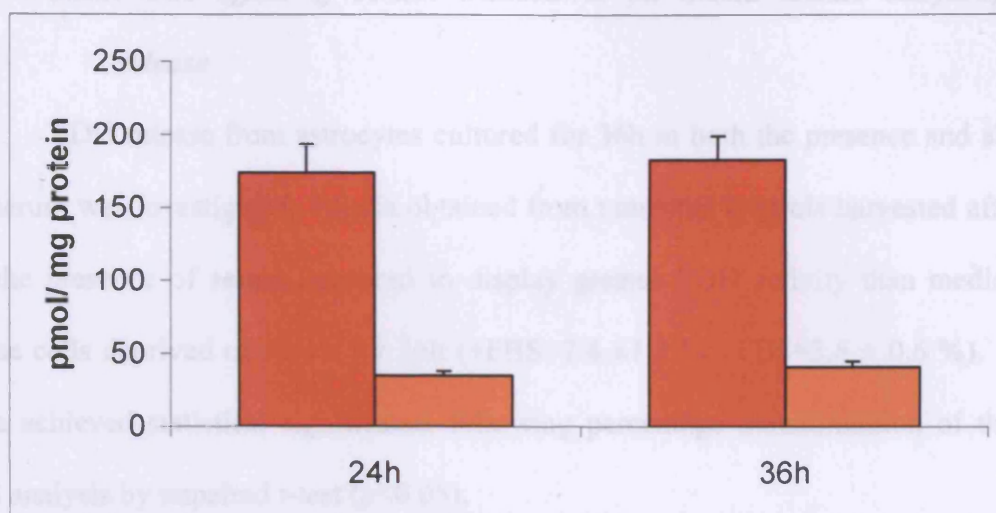
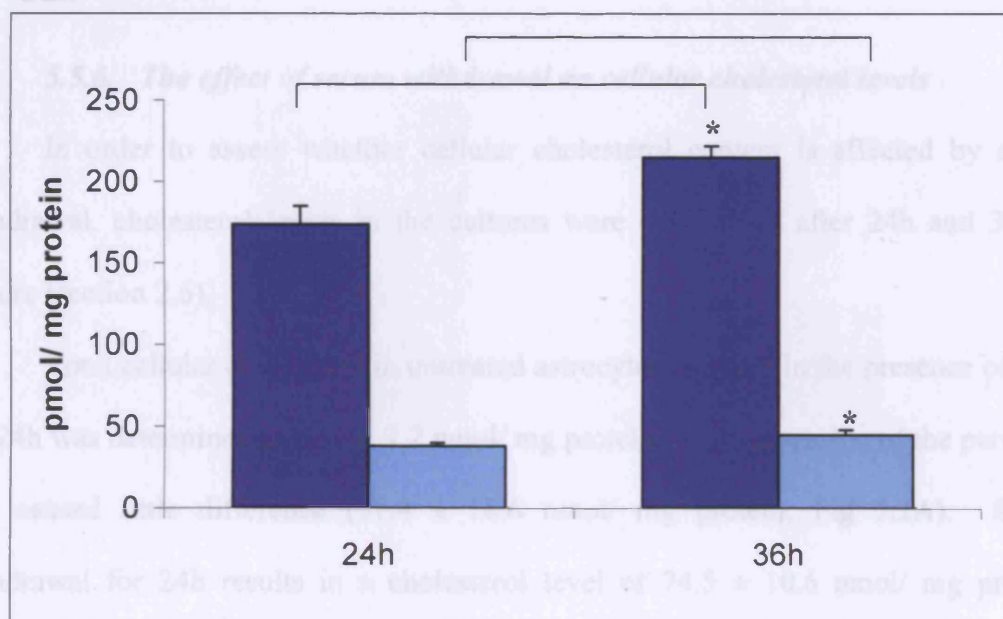
A: + FBS**B: - FBS**

Figure 5.1. The effect of serum withdrawal upon the CoQ status of primary cultures of rat astrocytes.

A: Rat astrocytes cells were incubated in the presence of FBS (10% v/v) for 24h or 36h in 6-well culture plates as indicated. ■ = CoQ₉; ■ = CoQ₁₀. Data are mean ± SEM values of between six and twelve independent culture preparations.

B: Rat astrocytes cells were incubated in the absence of FBS for 24h or 36h in 6-well culture plates as indicated. ■ = CoQ₉; ■ = CoQ₁₀. Data are mean ± SEM values of between six and ten independent culture preparations (* signifies p < 0.05).

5.5.5. The effect of serum withdrawal on media lactate dehydrogenase release

LDH release from astrocytes cultured for 36h in both the presence and absence of serum was investigated. Media obtained from untreated controls harvested after 36h in the presence of serum appeared to display greater LDH activity than media from those cells deprived of serum for 36h (+FBS=7.4 \pm 1.3 %; -FBS=3.6 \pm 0.6 %). These data achieved statistical significance following percentage transformation of the data and analysis by unpaired t-test ($p < 0.05$).

The mean LDH activity of 3 batches of FBS (10% v/v) was equal to 6.5 \pm 0.8% of the total lysed (cells + serum-supplemented media) value.

5.5.6. The effect of serum withdrawal on cellular cholesterol levels

In order to assess whether cellular cholesterol content is affected by serum withdrawal, cholesterol levels in the cultures were determined after 24h and 36h in culture (section 2.6).

Total cellular cholesterol in untreated astrocytes cultured in the presence of FBS for 24h was determined as 62.0 \pm 7.2 nmol/ mg protein, while extension of the period to 36h caused little difference (57.4 \pm 18.6 nmol/ mg protein; Fig 5.2A). Serum withdrawal for 24h results in a cholesterol level of 74.5 \pm 10.6 nmol/ mg protein, however, extension of withdrawal to 36h results in a statistically significant decrease of around 66% (36h withdrawal: 26.8 \pm 5.0 nmol/ mg protein; $p < 0.01$; 5.2B).

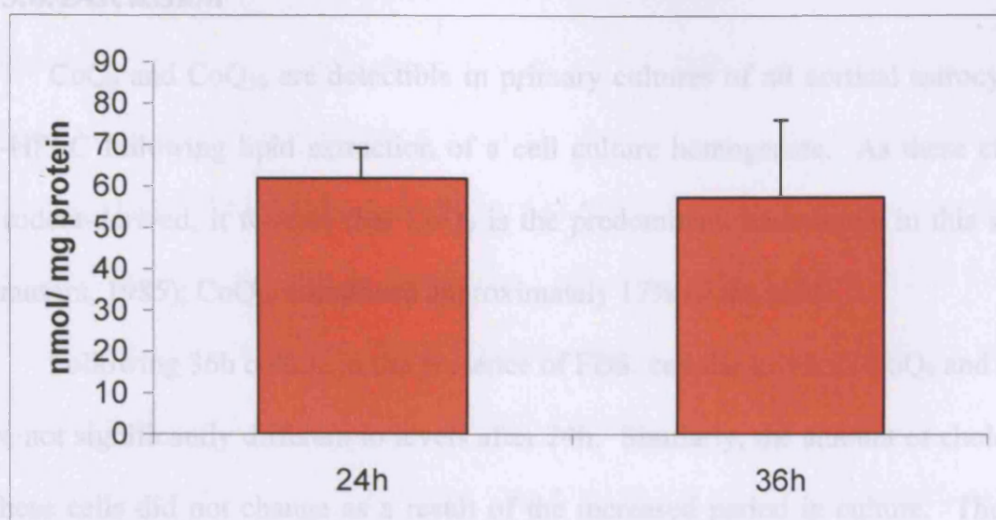
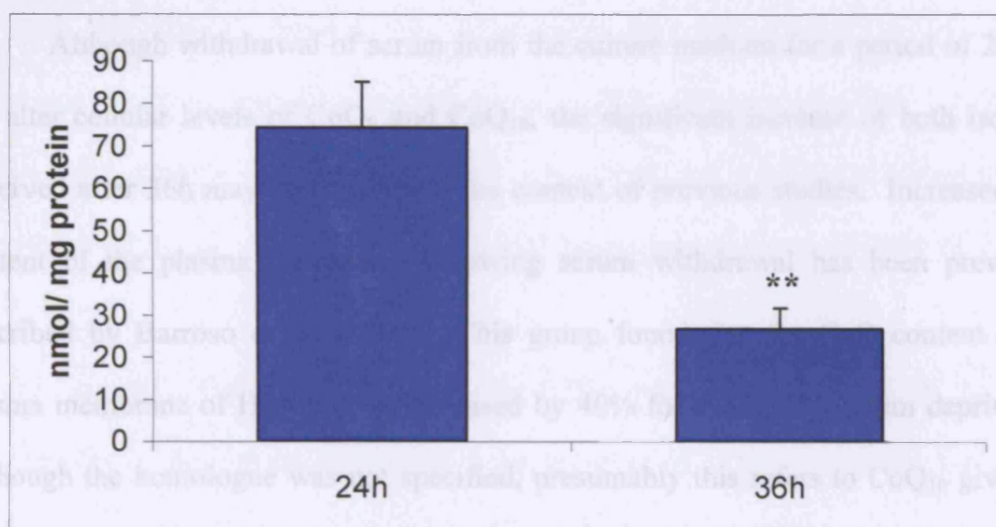
A: + FBS**B: - FBS**

Figure 5.2. The effect of serum withdrawal upon the total cholesterol status of primary cultures of rat astrocytes.

A: Rat astrocytes cells were incubated in the presence of FBS (10% v/v) for 24h or 36h in 6-well culture plates as indicated. Data are mean \pm SEM values of three to four independent culture preparations.

B: Rat astrocytes cells were incubated in the absence of FBS for 24h or 36h in 6-well culture plates as indicated. Data are mean \pm SEM values of three to four independent culture preparations (** signifies $p < 0.01$).

5.6. Discussion

CoQ₉ and CoQ₁₀ are detectable in primary cultures of rat cortical astrocytes by UV-HPLC following lipid extraction of a cell culture homogenate. As these cultures are rodent-derived, it follows that CoQ₉ is the predominant homologue in this species (Ramasara, 1985); CoQ₁₀ comprised approximately 17% of the total.

Following 36h culture in the presence of FBS, cellular levels of CoQ₉ and CoQ₁₀ were not significantly different to levels after 24h. Similarly, the amount of cholesterol in these cells did not change as a result of the increased period in culture. Thus it is clear that given the presence of FBS in the cell culture media, these products of the mevalonate pathway are not affected by their time in culture for up to 36h.

Although withdrawal of serum from the culture medium for a period of 24h did not alter cellular levels of CoQ₉ and CoQ₁₀, the significant increase of both isoforms observed after 36h may be clarified in the context of previous studies. Increased CoQ content of the plasma membrane following serum withdrawal has been previously described by Barroso *et al.* (1997). This group found that the CoQ content of the plasma membrane of HL-60 cells increased by 40% following 48h serum deprivation. Although the homologue was not specified, presumably this refers to CoQ₁₀ given the human source of the cell line. It was proposed by the authors that this may represent a stress response induced by serum withdrawal. Additionally, it has been noted that the substitution of FBS in primary astrocyte cultures with lipoprotein-depleted serum resulted in an approximately two-fold increase in both HMG-CoA reductase activity and sterol synthesis (Langan *et al.*, 1987). Such a mechanism may account for the milder increase observed with these whole-cell primary astrocyte preparations after 36h serum-withdrawal.

24h serum withdrawal resulted in a slight increase in cellular levels of total cholesterol. However, extension of the period of withdrawal to 36h resulted in profound depletion of cellular cholesterol to approximately 66% of the 24h serum-withdrawn group. It has not been determined as to whether this is due to the withdrawal of exogenous cholesterol *per se* (present in FBS) or another component (i.e. loss of a precursor compound) in serum. It may additionally be due to as yet unknown inherent metabolic alterations as a result of serum withdrawal.

These findings show that serum supplementation of the cell culture media is necessary in order to maintain cholesterol, but not CoQ₉ or CoQ₁₀ status, in astrocytes. It is possible that this reflects the requirement of an exogenous source of cholesterol, but not CoQ₉ or CoQ₁₀. Indeed, this requirement may be reflected by the relative concentrations of cholesterol and CoQ found in FBS. When considering a 10% (v/v) FBS-supplementation of cell culture media, these represent a cholesterol concentration of approximately 80 μ M, while CoQ₉ would be present at approximately 25nM, and CoQ₁₀ at 5nM.

Analysis of the activity of media LDH would initially suggest increased permeability of the plasma membrane in the presence of serum. However, the greater LDH activity of media from cells cultured in the presence of FBS may be explained by LDH within sera (Haslam *et al.*, 1999). A 10% (v/v) solution of FBS contained $6.5 \pm 0.8\%$ of the total LDH activity of the lysed cells and media. Thus it is likely that the higher LDH activity observed in the serum-supplemented cultures is not the result of increased membrane permeability, but instead reflects the LDH activity of the serum. It is therefore necessary to take into account the contribution from FBS when considering the amount of LDH in culture media. The difference between the serum-supplemented cultures ($7.4 \pm 1.3\%$) and the contribution from FBS alone ($6.5 \pm 0.8\%$) would suggest

that LDH release from the cytoplasm of those cultures was in the region of 0.9%. Given that in the absence of serum, LDH in the cell culture media was $3.6\% \pm 0.6\%$, these data would suggest that the presence of FBS in the culture media was beneficial with regard to cellular viability, and that the absence of serum for 36h increased release of cytoplasmic LDH.

5.7. Conclusion

This chapter has shown that it is possible to detect the major and minor homologues of CoQ in primary cultures of rat cortical astrocytes. As such, this system can be employed to study factors influencing CoQ₉ and CoQ₁₀ metabolism.

Given that these cells are rodent-derived, CoQ₉ was found to predominate. Following 24h serum withdrawal, no change was evident in cellular levels of CoQ₉ or CoQ₁₀. Neither did cholesterol levels alter significantly. Thus it is feasible to culture these cells for 24h without serum and not affect CoQ₉ or CoQ₁₀ metabolism. Subsequently, drugs such as lovastatin which may be highly bound to serum proteins can be evaluated in the absence of potential effects due to removal of serum for up to 24h.

36h culture in the absence of serum resulted in significantly increased levels of CoQ₉ and CoQ₁₀ while cholesterol levels were profoundly decreased. These differential effects may suggest that the requirements for the maintenance of cellular levels of these two molecules are different. It is possible that primary astrocyte cultures require the presence of exogenous cholesterol (or precursors) from serum-supplemented media to maintain cellular levels. While removal of serum has been reported to increase the activity of HMG-CoA reductase (Langan *et al.*, 1987), the half life of CoQ turnover has been calculated as approximately 40-fold higher than that of cholesterol in rat brain

tissue (Andersson *et al.* 1990). Thus following inhibition of cholesterol synthesis resulting from serum withdrawal, induction of HMG-CoA reductase activity may be more apparent with regard to CoQ₉ or CoQ₁₀ levels than total cholesterol.

6. THE EFFECTS OF LOVASTATIN UPON CoQ₉ AND CoQ₁₀ LEVELS IN PRIMARY CULTURES OF RAT ASTROCYTES

6. THE EFFECTS OF LOVASTATIN UPON CoQ₉ AND CoQ₁₀ LEVELS IN PRIMARY CULTURES OF RAT ASTROCYTES

6.1. Introduction

Lovastatin inhibits HMG-CoA reductase in a number of models (Alberts *et al.*, 1980; Maltese & Aprille, 1985, Folkers *et al.*, 1990). A large body of work over more than two decades exists within the literature relating to the effects of lovastatin; in addition this drug appears to be widely-used in a number of cell culture models (Pahan *et al.*, 1997; Laufts *et al.*, 1998; Nagasawa *et al.*, 2000; Ikeda *et al.*, 2001; Huang *et al.*, 2003). The drug is well characterised, and its lipophilic properties mean that while it is necessary to first dissolve it in ethanol before its addition to aqueous media, it could readily cross hydrophobic barriers such as the plasma membrane and the blood-brain barrier (Tsuji *et al.*, 1993; Merck & Co. Inc. 2003).

Lovastatin is predominantly bound to plasma proteins such as albumin *in vivo* (Merck & Co. Inc. 2003). Thus, it is highly likely that it would bind similar proteins in FBS-supplemented cell culture media. Such a situation has previously been reported to lower the bioavailability of some compounds added to cell cultures (Maranga, *et al.*, 2002; Selleri *et al.*, 2003; Mundy *et al.*, 2004); it is therefore conceivable that the bioavailability of lovastatin may be decreased by the use of FBS in the culture media. While the β -hydroxy acid form has been proposed to enter bovine brain capillary endothelial cells via the monocarboxylic acid transporter (Tsuji *et al.*, 1993), and rat mesangial cells by way of a carrier-mediated mechanism (Nagasawa *et al.*, 2000), the prodrug form may enter by non-specific diffusion (Nagasawa *et al.*, 2000). However albumin is known to bind and transport multiple bioactive substances (Peters, 1985). Thus rather than decrease bioavailability, it is also possible that the entry of lovastatin to

cells could be facilitated by albumin carriage, following binding to proteins in FBS. Alternatively, while lactonase activity in FBS has not been described, lactone hydrolysing enzymes have been described in other mammalian sera (Roth *et al.*, 1967; Teiber *et al.*, 2003). Subsequently, results obtained following addition of lovastatin to the culture media may be altered by the presence or absence of serum in the media.

As discussed in previous chapters, HMG-CoA reductase inhibition is conferred by its *in vivo* conversion to its β -hydroxy acid (such as the sodium salt of lovastatin; here denoted Na-lovastatin) by cleavage of the lactone ring (Endo *et al.*, 1976). This is shown in Figure 2.3.

As the ability of astrocytes to metabolise lovastatin to this β -hydroxy acid isoform was unknown, both lovastatin and Na-lovastatin were added to cultures in the presence or absence of serum. Lovastatin has been reported to decrease total ubiquinone (CoQ₉₊₁₀) levels in cultured murine neuroblastoma cells, following addition to the cell culture media (Maltese & Aprille, 1985). Given the commonality of the CoQ₉, CoQ₁₀ and cholesterol biosynthetic pathways, the status of these compounds was determined in order to address the effect of lovastatin and Na-lovastatin on primary astrocyte cultures.

As this study examines cellular, rather than mitochondrial CoQ levels, in order to gain insight into the function of CoQ₉ and CoQ₁₀ within the ETC, the activities of the mitochondrial reparatory chain were determined. It has been suggested that the activity of complex II+III may be dependant upon the endogenous level of CoQ₉ or CoQ₁₀ in the inner mitochondrial membrane (Clark *et al.*, 1994; Rahman *et al.*, 2001). This hypothesis is further supported by the work of Fernández-Ayala *et al* (2005) which found that supplementation of human promyelocytic HL-60 cells with CoQ₁₀ increases levels in mitochondria, and that this lead to increased complex II+III activity.

6.2.Aims

- To investigate the effects of lovastatin and Na-lovastatin upon cellular levels of CoQ₉, CoQ₁₀ and cholesterol in rat primary astrocytes.
- To examine the effects of serum withdrawal in conjunction with the addition of lovastatin and Na-lovastatin
- To ascertain whether alterations in cellular CoQ status influence the complex II+III activity *in vitro*.

6.3.Methods

6.3.1. Tissue culture

Primary cultures of rat astrocytes were prepared and maintained in culture as described in section 2.2.3. Cultures were exposed to a number of culture conditions for 24h or 36h in the presence or absence of serum and the cells collected as a pellet as described in sections 2.2.6.

6.3.2. CoQ measurement by HPLC

Cellular lipids were extracted as described in section 3.2.5, and the concentrations of CoQ₉ and CoQ₁₀ were measured by reverse-phase UV-HPLC as in section 3.2.3.

6.3.3. ETC enzyme assays

The activities of the enzymes of the respiratory chain were assayed in the samples as described in section 2.3

6.3.4. Lactate dehydrogenase determination

As an index of cell stress, LDH release from the astrocyte cultures was measured after 36h growth in 6 well plates, and expressed as a percentage of the total LDH activity of the culture as described in section 2.5. Previously, it has been observed that FBS in culture media is responsible for a proportion of total LDH activity. Thus activity attributable to FBS was subtracted from the activity of each sample of culture media containing FBS prior to calculation (section 2.5).

6.3.5. Cholesterol determination

Determination of total cellular cholesterol was carried out as described in section 2.6.

6.3.6. Protein determination

For those findings expressed against a protein baseline, the protein content of samples was determined by the method of Lowry *et al.* (1951) as in section 2.7.

6.3.7. Astrocyte morphology

Cells were photographed as described in section 2.8, using a Nikon CoolPix 950 digital camera and Nikon TMS phase contrast light microscope.

6.4. Experimental protocol

6.4.1. Exposure of astrocyte cultures to lovastatin

Primary cultures of rat astrocytes were exposed to media containing lovastatin for 24h or 36h. The β -hydroxy acid of lovastatin ("Na-lovastatin") was generated from the lactone form by dissolution in 1M NaOH in ethanol. Nucleophilic attack of the β

carbon and subsequent alkaline hydrolysis resulted in formation of Na-lovastatin. While absolute quantification of the concentration of Na-lovastatin was not obtained, this established method of conversion has been used by a number of groups previously (Endo *et al.*, 1976; Alberts *et al.*, 1980; Maltese & Aprille, 1985), and was shown to have greater inhibitory activity of HMG-CoA reductase by Endo *et al.* (1976) and in the manufacturer's product monograph (Merck and Co. Inc., 2003)

Both lovastatin and Na-lovastatin were added to the media in two concentrations; either 10 μ M or 100 μ M. FBS (10% v/v) was added to the media in some experiments, while in others, cells were deprived of serum for up to 36h before being harvested. In control experiments, only the appropriate vehicle was added without lovastatin, as described in section 2.2.6.3. In the case of lovastatin, the control vehicle is ethanol (present at 1% (v/v) in the cell culture media), while Na-Lovastatin used NaOH in ethanol (10mM; 1% (v/v) final concentration). A 1% (v/v) solution of ethanol amounts to an absolute concentration of 171mM.

6.5. Results

6.5.1. The effect of lovastatin exposure in the presence of serum

6.5.1.1. Ubiquinone and cholesterol status

Cultured with FBS, exposure of astrocytes for 24h to 10 μ M lovastatin did not alter levels of either CoQ₉ or CoQ₁₀ in the presence of FBS (10% v/v; control: CoQ₉ = 202.8 \pm 18.4 pmol/ mg protein; CoQ₁₀ = 40.3 \pm 3.0 pmol/ mg protein; 10 μ M lovastatin: CoQ₉ = 198.8 \pm 31.8 pmol/ mg protein; CoQ₁₀ = 42.1 \pm 5.3 pmol/ mg protein; Fig 6.1A). 100 μ M lovastatin caused a statistically significant decrease in cellular CoQ₉ status of 52% in cells cultured in the presence of FBS (p <0.05). In contrast, CoQ₁₀

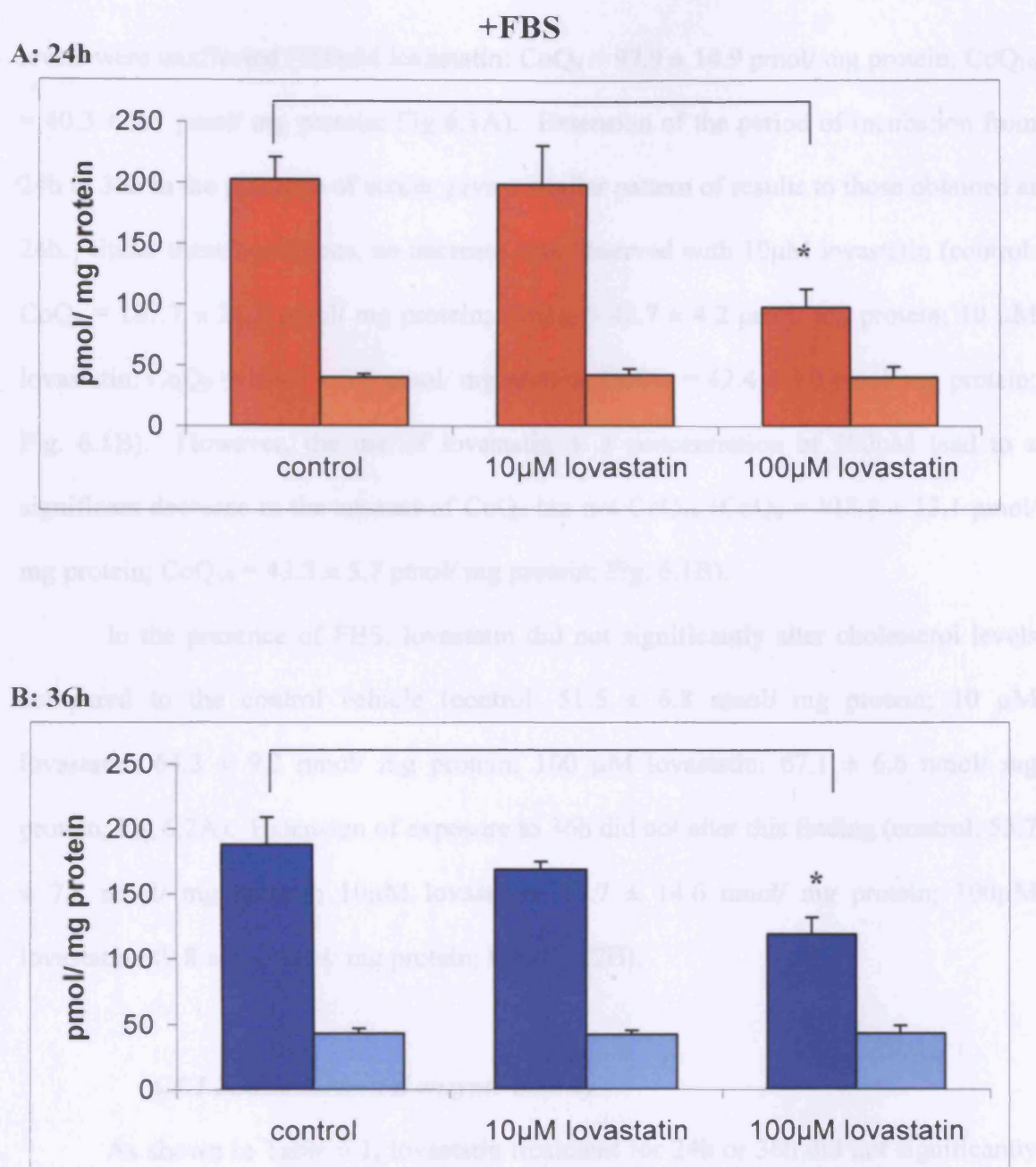


Figure 6.1. The effect of lovastatin exposure upon the CoQ status of primary cultures of rat astrocytes.

A: Rat astrocytes cells were incubated for 24h in 6-well culture plates in the presence of lovastatin (10µM or 100µM) and FBS (10% v/v) as indicated (■ = CoQ₉; ■ = CoQ₁₀). Data are mean ± SEM values of five to seven independent culture preparations.

B: Rat astrocytes cells were incubated for 36h in 6-well culture plates in the presence of lovastatin (10 or 100µM) and FBS (10% v/v) as indicated (■ = CoQ₉; ■ = CoQ₁₀). Data are mean ± SEM values of four to six independent culture preparations. * signifies $p \leq 0.05$, analysed by one-way ANOVA.

levels were unaffected (100 μ M lovastatin: CoQ₉ = 97.9 ± 14.9 pmol/ mg protein; CoQ₁₀ = 40.3 ± 9.1 pmol/ mg protein; Fig 6.1A). Extension of the period of incubation from 24h to 36h in the presence of serum gave a similar pattern of results to those obtained at 24h. Under these conditions, no decrease was observed with 10 μ M lovastatin (control: CoQ₉ = 187.7 ± 21.2 pmol/ mg protein; CoQ₁₀ = 42.7 ± 4.2 pmol/ mg protein; 10 μ M lovastatin: CoQ₉ = 169.1 ± 5.9 pmol/ mg protein; CoQ₁₀ = 42.4 ± 3.0 pmol/ mg protein; Fig. 6.1B). However, the use of lovastatin at a concentration of 100 μ M lead to a significant decrease in the amount of CoQ₉ but not CoQ₁₀ (CoQ₉ = 118.8 ± 13.1 pmol/ mg protein; CoQ₁₀ = 43.3 ± 5.7 pmol/ mg protein; Fig. 6.1B).

In the presence of FBS, lovastatin did not significantly alter cholesterol levels compared to the control vehicle (control: 51.5 ± 6.8 nmol/ mg protein; 10 μ M lovastatin: 64.3 ± 9.2 nmol/ mg protein; 100 μ M lovastatin: 67.1 ± 6.6 nmol/ mg protein; Fig 6.2A). Extension of exposure to 36h did not alter this finding (control: 53.7 ± 7.8 nmol/ mg protein; 10 μ M lovastatin: 65.7 ± 14.6 nmol/ mg protein; 100 μ M lovastatin: 49.8 ± 5.4 nmol/ mg protein; Figure 6.2B).

6.5.1.2.Mitochondrial enzyme activity

As shown in Table 6.1, lovastatin treatment for 24h or 36h did not significantly affect CS activity. The activities of the enzymes of the ETC were not affected by lovastatin treatment at either 10 μ M or 100 μ M for up to 36h expressed against a protein baseline.

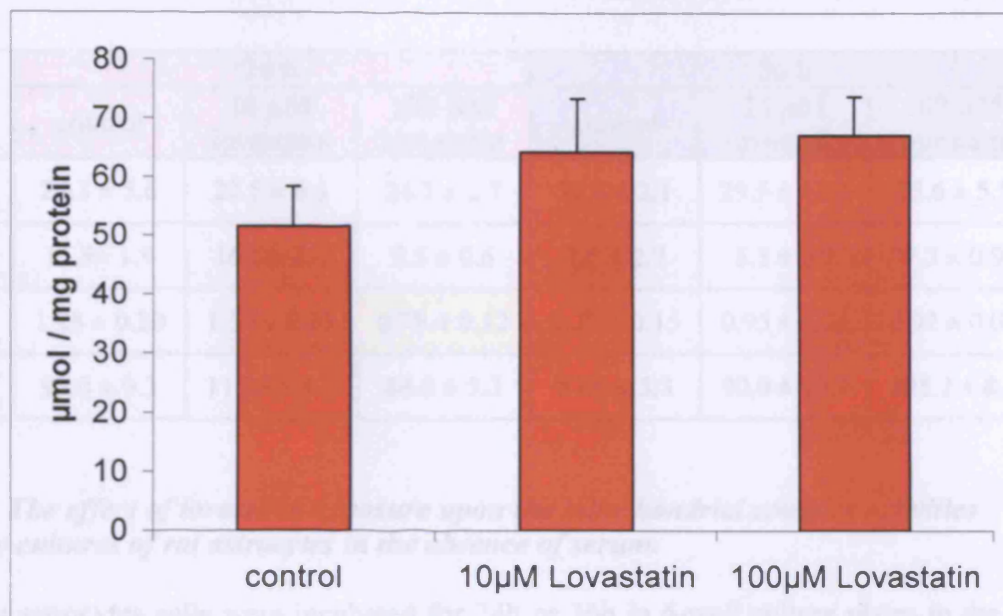
Table 6.2 reports the activities of the ETC enzymes expressed as a ratio of CS. It can be seen that against a ratio of CS activity, complex IV activity decreased by 26% following 36h incubation with 100 μ M lovastatin. This was the only observed decrease; all other activities were not significantly different from their control values.

A: 24h

+FBS

24h

36h



B: 36h

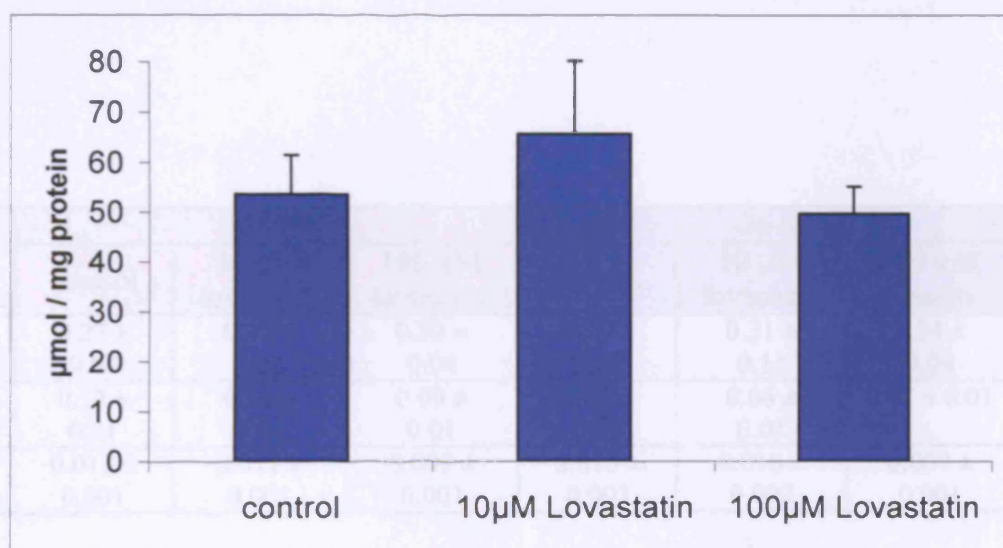


Figure 6.2. Cholesterol levels in astrocytes treated with lovastatin

Rat astrocytes were incubated for 24h (■) or 36h (■) in 6-well culture plates in the presence of FBS (10% v/v). Cell culture media was supplemented as indicated, and cells harvested following 24h or 36h incubation. Data are mean \pm SEM values of three to four independent culture preparations expressed against a protein baseline.

6.5.1.3. LDH release and astrocyte morphology

As an index of membrane integrity, staining weight and cell viability, LDH

	24 h			36 h		
	control	10 μ M lovastatin	100 μ M lovastatin	control	10 μ M lovastatin	100 μ M lovastatin
Cx I (nmol/min/mg)	24.3 \pm 5.6	21.5 \pm 6.5	24.7 \pm 2.7	22.4 \pm 2.1	29.5 \pm 11.2	25.6 \pm 5.5
Cx II+III (nmol/min/mg)	11.9 \pm 1.9	16.6 \pm 2.1	7.5 \pm 0.6	7.6 \pm 2.7	5.3 \pm 0.5	7.3 \pm 0.9
Cx IV (k/min/mg)	1.28 \pm 0.20	1.39 \pm 0.07	0.78 \pm 0.12	1.29 \pm 0.15	0.95 \pm 0.34	0.92 \pm 0.07
CS (nmol/min/mg)	98.0 \pm 9.3	117.0 \pm 4.1	84.0 \pm 5.3	87.0 \pm 5.3	90.0 \pm 10.4	105.2 \pm 8.5

Table 6.5. The effect of lovastatin exposure upon the mitochondrial complex activities of primary cultures of rat astrocytes in the absence of serum.

Rat astrocytes cells were incubated for 24h or 36h in 6-well culture plates in the presence of Na-lovastatin (10 μ M or 100 μ M). Mitochondrial complex activity was determined as described. Data are mean \pm SEM values of three to four independent culture preparations, expressed against a protein baseline. Yellow highlighting represents a statistically significant difference compared to control values ($p < 0.05$).

6.5.2. The effect of Na-lovastatin exposure in the presence of serum

	24 h			36 h		
	control	10 μ M lovastatin	100 μ M lovastatin	control	10 μ M lovastatin	100 μ M lovastatin
Cx I	0.27 \pm 0.09	0.19 \pm 0.06	0.30 \pm 0.04	0.26 \pm 0.02	0.31 \pm 0.11	0.24 \pm 0.04
Cx II+III	0.12 \pm 0.01	0.14 \pm 0.02	0.09 \pm 0.01	0.09 \pm 0.03	0.06 \pm 0.01	0.07 \pm 0.01
Cx IV (k/nmol)	0.013 \pm 0.001	0.012 \pm 0.001	0.009 \pm 0.001	0.015 \pm 0.003	0.010 \pm 0.002	0.009 \pm 0.001

protein; Fig 6.44). Moreover, increasing the concentration of Na-lovastatin to 100 μ M

Table 6.6. The effect of lovastatin exposure upon the mitochondrial complex activities of primary cultures of rat astrocytes in the absence of serum.

Complex activities were determined as described above, and expressed as a ratio of citrate synthase activity.

6.5.1.3. LDH release and astrocyte morphology

As an index of membrane integrity, gaining insight into cell viability, LDH activity in the cell culture media was determined. The inclusion of ethanol (1%) in the culture medium resulted in 3.7% greater release than the untreated controls (untreated control: $0.9 \pm 0.6\%$; ethanol vehicle: $4.6 \pm 1.3\%$). However, lovastatin appears to increase this in a statistically significant manner by approximately an additional 5% and 9% for 10 μM and 100 μM lovastatin respectively (10 μM : $9.2 \pm 2.1\%$; 100 μM : $13.6 \pm 2.2\%$).

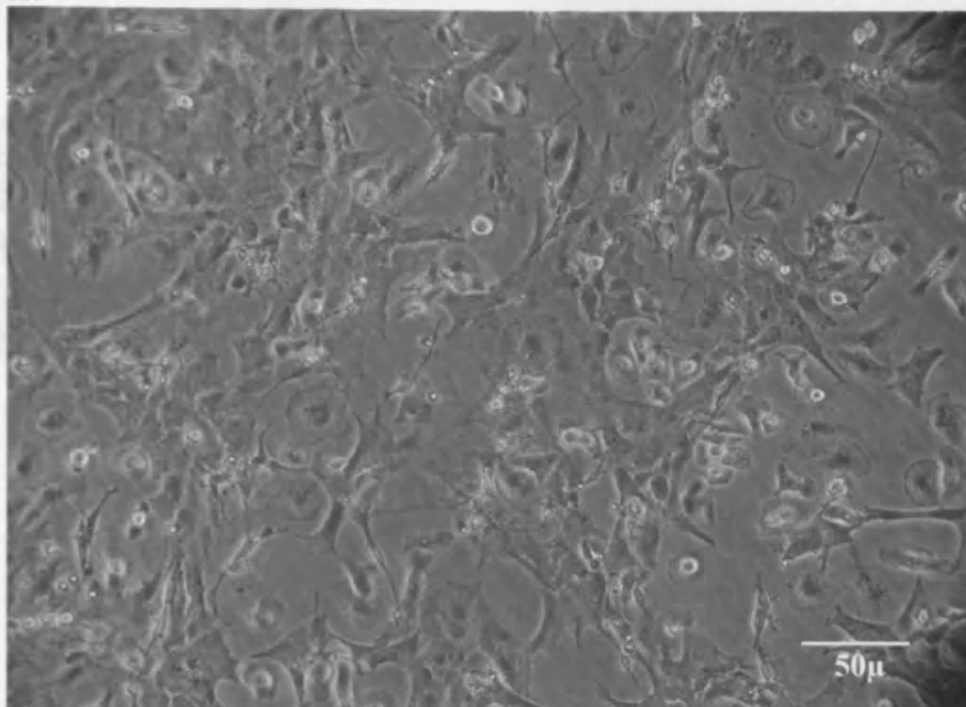
Typical polygonal *in-vitro* astrocyte morphology is shown in figure 6.3A, in contrast to the stellation observed in the majority of cells treated with lovastatin (100 μM ; Fig. 6.3B). No changes were observed in astrocyte morphology following serum withdrawal or the addition of control vehicles; stellation occurred following 10 μM or 100 μM lovastatin exposure for 24 or 36h.

6.5.2. The effect of Na-lovastatin exposure in the presence of serum

6.5.2.1. Ubiquinone and cholesterol status

The sodium salt of lovastatin (Na-lovastatin; 10 μM) did not change the amount of either CoQ₉ or CoQ₁₀ extracted from rat astrocytes in the presence of FBS (control: CoQ₉ = 153.3 ± 14.2 pmol/ mg protein; CoQ₁₀ = 34.5 ± 4.1 pmol/ mg protein; 10 μM Na-lovastatin: CoQ₉ = 159.9 ± 22.6 pmol/ mg protein; CoQ₁₀ = 38.3 ± 4.8 pmol/ mg protein; Fig 6.4A). However, increasing the concentration of Na-lovastatin to 100 μM elicited a statistically significant ($p = 0.05$) decrease of 31% in CoQ₉ levels (100 μM Na-lovastatin: CoQ₉ = 106.6 ± 14.0 pmol/ mg protein; CoQ₁₀ = 33.3 ± 5.5 pmol/ mg protein; Fig 6.4A). CoQ₁₀ levels did not change significantly.

A:



B:

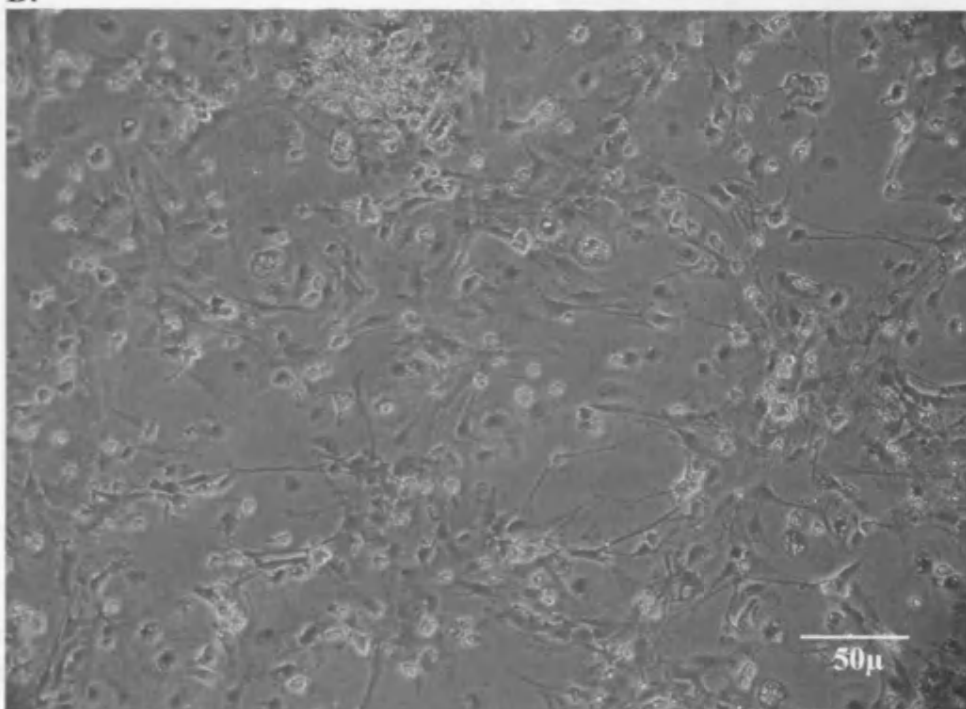


Figure 6.3. Astrocyte morphology in the absence and presence of lovastatin

Light micrographs (x 40 magnification) showing typical polygonal astrocyte morphology in vitro (A) and stellation following incubation with lovastatin for 36h (B). Following serum withdrawal for up to 36h, no changes in morphology were evident. Stellation occurred as a result of treatment with 10 μ M or 100 μ M lovastatin or Na-lovastatin in the presence or absence of serum.

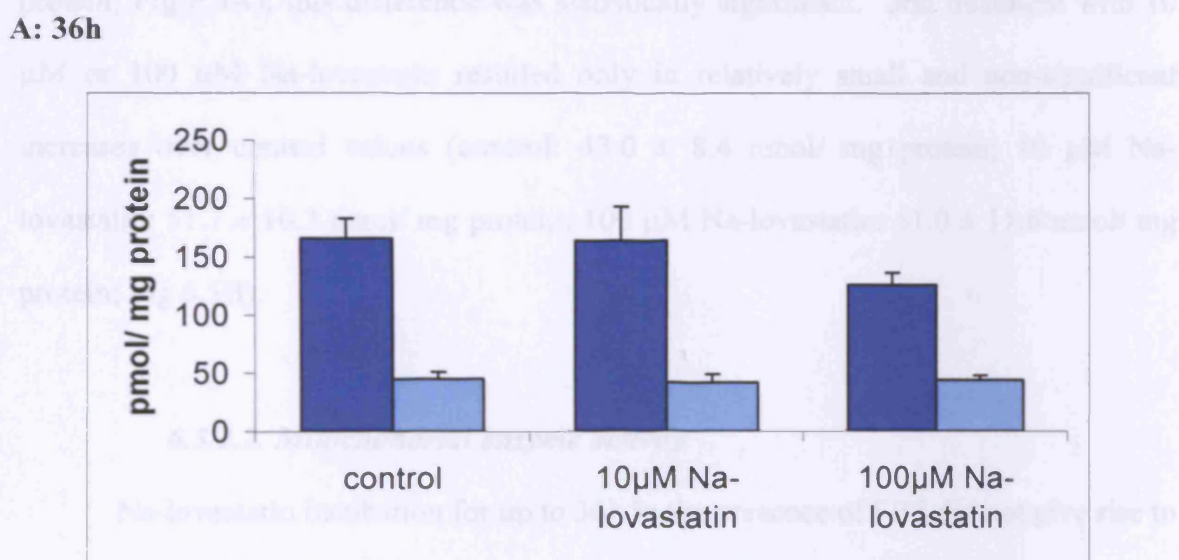
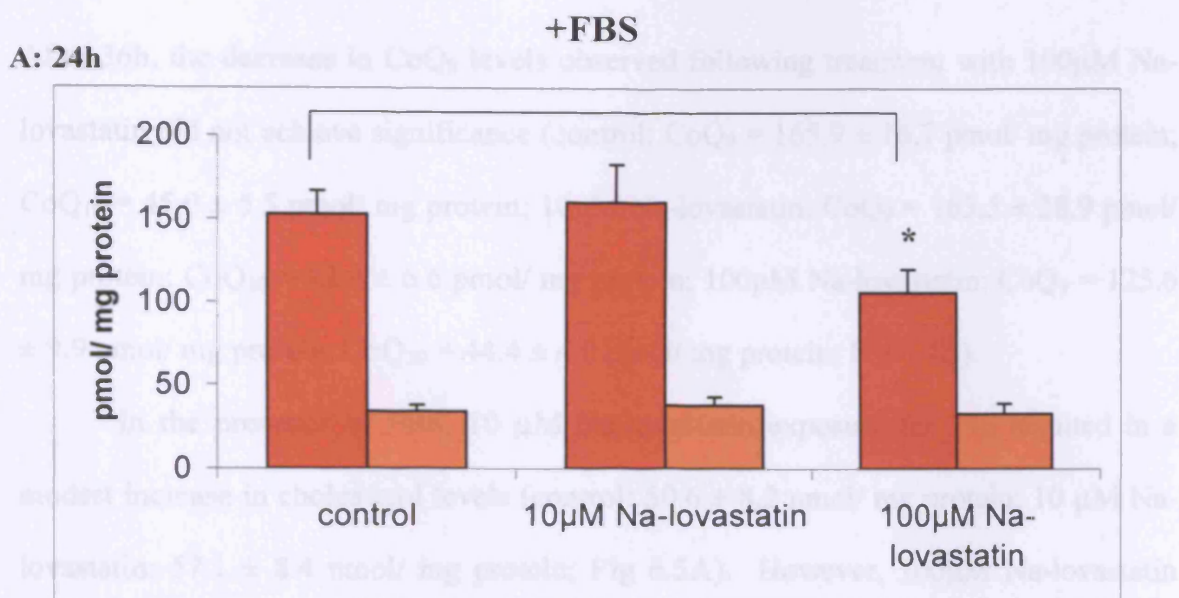


Figure 6.4. The effect of Na-lovastatin exposure upon the CoQ status of primary cultures of rat astrocytes.

A: Rat astrocytes cells were incubated for 24h in 6-well culture plates in the presence of Na-lovastatin (10 µM or 100 µM) and FBS (10% v/v) as indicated (■ = CoQ₉; □ = CoQ₁₀). Data are mean ± SEM values of eight independent culture preparations.

B: Rat astrocytes cells were incubated for 36h in 6-well culture plates in the presence of Na-lovastatin (10 or 100µM) and tFBS (10% v/v) as indicated (■ = CoQ₉; □ = CoQ₁₀). Data are mean ± SEM values of four to six independent culture preparations.

After 36h, the decrease in CoQ₉ levels observed following treatment with 100µM Na-lovastatin did not achieve significance (control: CoQ₉ = 165.9 ± 16.7 pmol/ mg protein; CoQ₁₀ = 45.0 ± 5.5 pmol/ mg protein; 10µM Na-lovastatin: CoQ₉ = 163.5 ± 28.9 pmol/ mg protein; CoQ₁₀ = 42.0 ± 6.6 pmol/ mg protein; 100µM Na-lovastatin: CoQ₉ = 125.6 ± 9.9 pmol/ mg protein; CoQ₁₀ = 44.4 ± 4.0 pmol/ mg protein; Fig 6.4B).

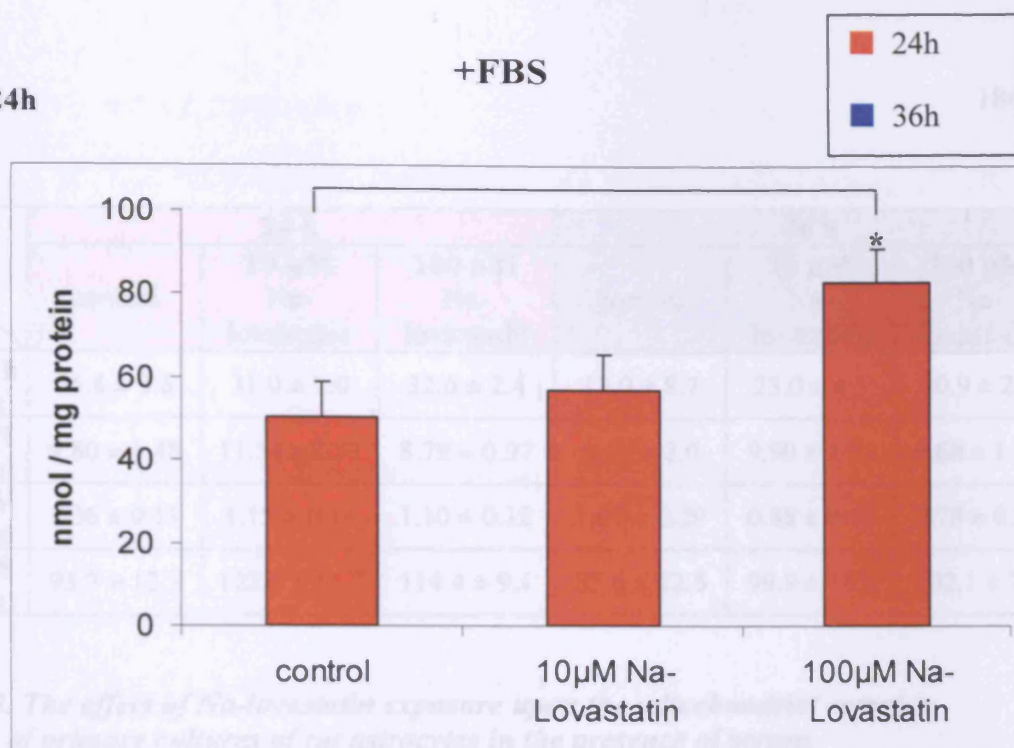
In the presence of FBS, 10 µM Na-lovastatin exposure for 24h resulted in a modest increase in cholesterol levels (control: 50.6 ± 8.2 nmol/ mg protein; 10 µM Na-lovastatin: 57.1 ± 8.4 nmol/ mg protein; Fig 6.5A). However, 100µM Na-lovastatin exposure resulted in a 64% increase in the amount of cholesterol in these cultures when compared to their appropriate control (100 µM Na-lovastatin: 83.2 ± 7.6 nmol/ mg protein; Fig 6.5A); this difference was statistically significant. 36h treatment with 10 µM or 100 µM Na-lovastatin resulted only in relatively small and non-significant increases over control values (control: 43.0 ± 8.4 nmol/ mg protein; 10 µM Na-lovastatin: 51.7 ± 10.3 nmol/ mg protein; 100 µM Na-lovastatin: 61.0 ± 11.6 nmol/ mg protein; Fig 6.5B).

6.5.2.2. Mitochondrial enzyme activity

Na-lovastatin incubation for up to 36h in the presence of FBS did not give rise to statistically significant differences in the activities of citrate synthase or the respiratory enzymes as shown in tables 6.3 and 6.4.

A: 24h

+FBS



B: 36h

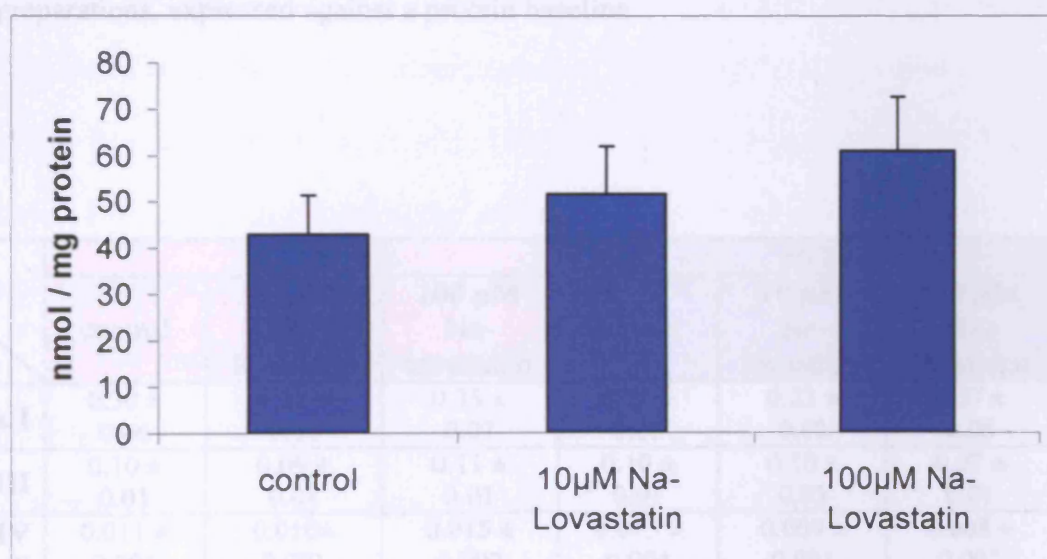


Figure 6.5. Cholesterol levels in astrocytes treated with Na-lovastatin

Rat astrocytes were incubated for 24h (■) or 36h (■) in 6-well culture plates in the presence of FBS (10% v/v). Cell culture media was supplemented as indicated, and cells harvested following 24h or 36h incubation. Data are mean \pm SEM values of three to four independent culture preparations expressed against a protein baseline.

	24 h			36 h		
	control	10 μ M Na-lovastatin	100 μ M Na-lovastatin	control	10 μ M Na-lovastatin	100 μ M Na-lovastatin
Cx I (nmol/min/mg)	25.8 \pm 3.6	31.0 \pm 7.0	32.6 \pm 2.4	19.0 \pm 8.7	23.0 \pm 4.5	30.9 \pm 2.4
Cx II+III (nmol/min/mg)	9.80 \pm 1.48	11.54 \pm 2.57	8.79 \pm 0.97	8.17 \pm 2.0	9.90 \pm 2.92	6.68 \pm 1.14
Cx IV (k/min/mg)	1.36 \pm 0.11	1.15 \pm 0.14	1.10 \pm 0.12	1.07 \pm 0.29	0.88 \pm 0.17	0.78 \pm 0.24
CS (nmol/min/mg)	93.7 \pm 12.3	122.8 \pm 11.7	114.4 \pm 9.1	83.6 \pm 22.5	99.9 \pm 14.3	102.1 \pm 7.6

Table 6.3. The effect of Na-lovastatin exposure upon the mitochondrial complex activities of primary cultures of rat astrocytes in the presence of serum.

Rat astrocytes cells were incubated for 24h or 36h in 6-well culture plates in the presence of Na-lovastatin (10 μ M or 100 μ M) and FBS (10% v/v). Mitochondrial complex activity was determined as described. Data are mean \pm SEM values of three independent culture preparations, expressed against a protein baseline.

	24 h			36 h		
	control	10 μ M Na-lovastatin	100 μ M Na-lovastatin	control	10 μ M Na-lovastatin	100 μ M Na-lovastatin
Cx I	0.30 \pm 0.06	0.27 \pm 0.08	0.35 \pm 0.07	0.21 \pm 0.05	0.23 \pm 0.02	0.37 \pm 0.08
Cx II+III	0.10 \pm 0.01	0.09 \pm 0.01	0.11 \pm 0.01	0.10 \pm 0.01	0.10 \pm 0.03	0.07 \pm 0.01
Cx IV (k/nmol)	0.011 \pm 0.001	0.010 \pm 0.001	0.015 \pm 0.002	0.013 \pm 0.004	0.009 \pm 0.001	0.008 \pm 0.002

Table 6.4. The effect of Na-lovastatin exposure upon the mitochondrial complex activities of primary cultures of rat astrocytes in the presence of serum.

Complex activities were determined as described in the table above, and expressed as a ratio of citrate synthase activity.

6.5.2.3. LDH release

10 μM Na-lovastatin increased LDH release in the region of 5% of the maximum above controls (vehicle: $5.0 \pm 1.2\%$; 10 μM lovastatin: $10.4 \pm 3.0\%$). This was not statistically significant. 100 μM Na-lovastatin caused LDH release approximately 10% of the maximum above control levels ($14.6 \pm 5.4\%$); this was statistically significantly different compared to control vehicle values.

6.5.3. The effect of lovastatin exposure in the absence of serum

6.5.3.1. Ubiquinone and cholesterol status

CoQ₉ and CoQ₁₀ levels were determined as previously, but astrocytes were cultured for 24h or 36h in the absence of serum. Following 24h culture under these conditions with the natural lactone form of lovastatin, CoQ₉ and CoQ₁₀ levels were found not to be significantly different (control: CoQ₉ = 173.3 ± 23.6 pmol/ mg protein; CoQ₁₀ = 36.0 ± 3.5 pmol/ mg protein; 10 μM lovastatin: CoQ₉ = 193.3 ± 24.7 pmol/ mg protein; CoQ₁₀ = 41 ± 5.3 pmol/ mg protein; 100 μM lovastatin: CoQ₉ = 142.3 ± 21.2 pmol/ mg protein; CoQ₁₀ = 48.9 ± 8.6 pmol/ mg protein; Fig 6.6A).

The same experimental conditions maintained for 36h again resulted in no significant difference in the CoQ₉ status of these cultures (control: CoQ₉ = 224.8 ± 22.7 pmol/ mg protein; 10 μM lovastatin: CoQ₉ = 258.2 ± 26.6 pmol/ mg protein; 100 μM lovastatin: 227.6 ± 3.5 pmol/ mg protein; Fig. 6.6B). However, it was observed that 36h exposure of the 100 μM lovastatin caused a statistically significant increase in the amount of CoQ₁₀ (control: CoQ₁₀ = 51.9 ± 3.1 pmol/ mg protein; 10 μM lovastatin: CoQ₁₀ = 59.8 ± 5.1 pmol/ mg protein; 100 μM lovastatin: CoQ₁₀ = 80.0 ± 8.3 pmol/ mg protein; Fig 6.6B).

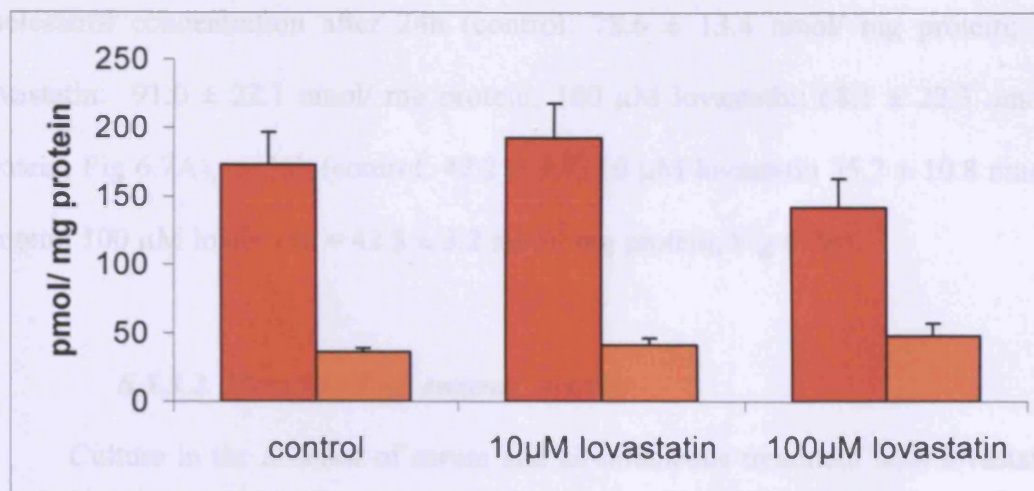
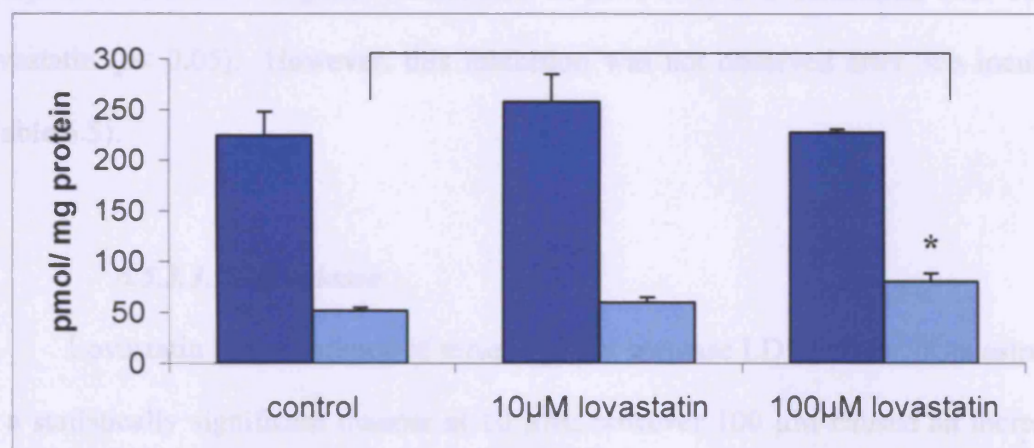
-FBS**A: 24h****B: 36h**

Figure 6.6. The effect of lovastatin exposure upon the CoQ status of primary cultures of rat astrocytes in the absence of serum.

A: Rat astrocytes cells were incubated for 24h in 6-well culture plates in the presence of lovastatin (10 µM or 100µM) but in the absence of FBS as indicated (■ = CoQ₉; ■ = CoQ₁₀). Data are mean ± SEM values of six to seven independent culture preparations.

B: Rat astrocytes cells were incubated for 36h in 6-well culture plates in the presence of lovastatin (10 or 100µM) but in the absence of FBS as indicated (■ = CoQ₉; ■ = CoQ₁₀). Data are mean ± SEM values of four to eight independent culture preparations. * signifies $p \leq 0.05$, analysed by one-way ANOVA

These conditions did not cause statistically significant differences in cellular cholesterol concentration after 24h (control: 78.6 ± 13.4 nmol/ mg protein; 10 μ M lovastatin: 91.0 ± 22.1 nmol/ mg protein; 100 μ M lovastatin: 68.1 ± 22.3 nmol/ mg protein; Fig 6.7A), or 36h (control: 42.2 ± 9.7 ; 10 μ M lovastatin 35.7 ± 10.8 nmol/ mg protein; 100 μ M lovastatin = 42.8 ± 3.2 nmol/ mg protein; Fig 6.7B).

6.5.3.2. Mitochondrial enzyme activity

Culture in the absence of serum and simultaneous treatment with lovastatin for 24h did not profoundly affect CS activity, and no significant differences in ETC enzyme activities were observed when compared to controls (Table 6.6). Against protein, complex IV showed a significant decrease of 39% after 24h incubation with 100 μ M lovastatin ($p < 0.05$). However, this inhibition was not observed after 36h incubation (Table 6.5).

6.5.3.3.LDH release

Lovastatin in the absence of serum did not increase LDH release from astrocytes in a statistically significant manner at 10 μ M; however 100 μ M caused an increase in release of approximately 10% of the maxamal value (vehicle: $6.0 \pm 3.2\%$; 10 μ M lovavatin: $12.6 \pm 2.9\%$; 100 μ M lovastatin: $17.5 \pm 6.4\%$). The latter was statistically significant.

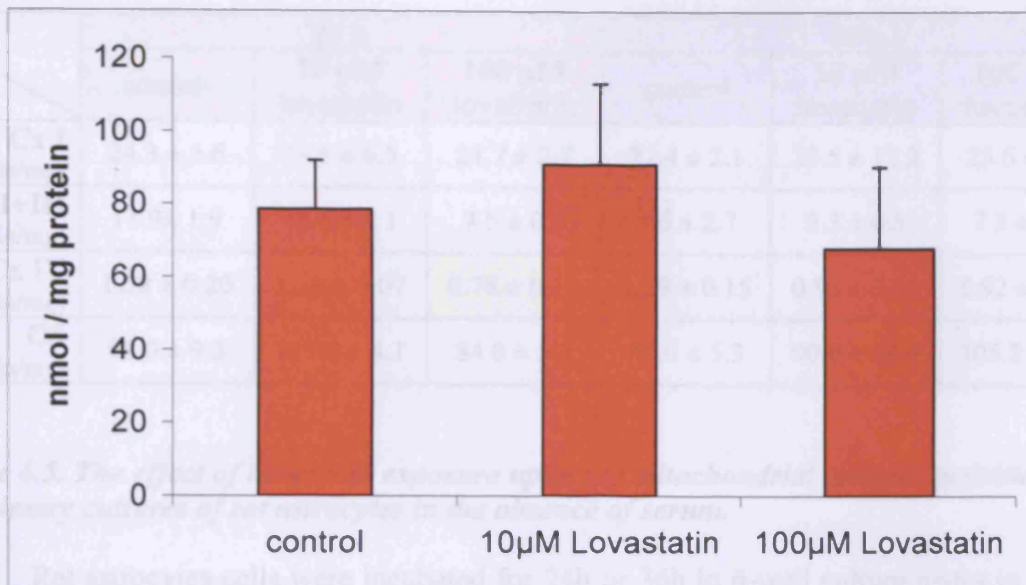
6.5.4. The effect of Na-lovastatin exposure in the absence of serum

6.5.4.1. Ubiquinone and cholesterol status

Exclusion of FBS and simultaneous supplementation of culture media with 10 μ M Na-lovastatin did not profoundly alter the amount of CoQ₉ or COQ₁₀ extracted from

A: 24 h -FBS

-FBS



B: 36 h -FBS

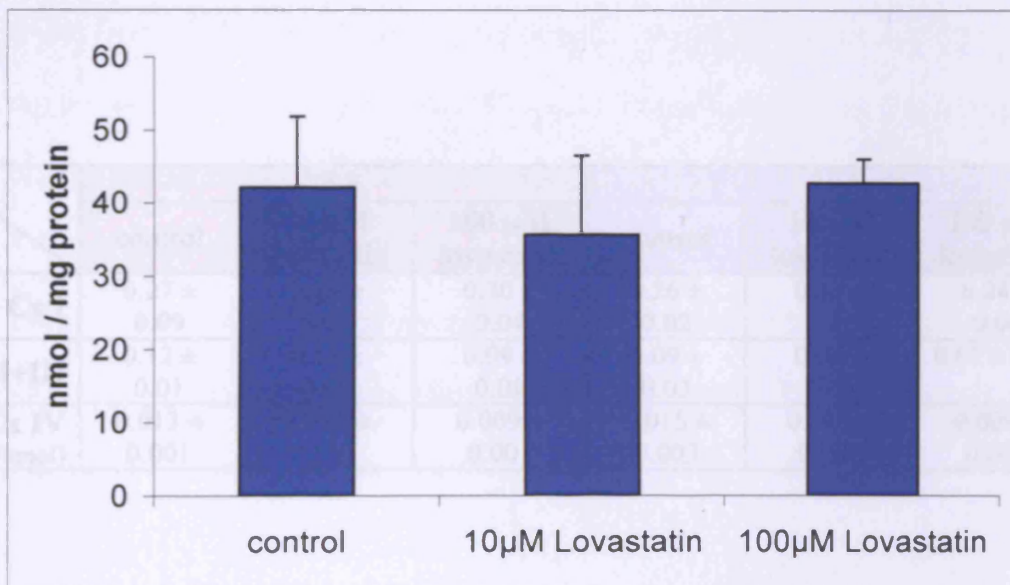


Figure 6.7. Cholesterol levels in serum - deprived astrocytes treated with lovastatin

Rat astrocytes were incubated for 24h (■), or 36h (■) in 6-well culture plates in the absence of FBS as indicated. Cell culture media was supplemented as indicated, and cells harvested following 24h or 36h incubation. Data are mean \pm SEM values of three to four independent culture preparations expressed against a protein baseline.

	24 h			36 h		
	control	10 μ M lovastatin	100 μ M lovastatin	control	10 μ M lovastatin	100 μ M lovastatin
Cx I (nmol/min/mg)	24.3 \pm 5.6	21.5 \pm 6.5	24.7 \pm 2.7	22.4 \pm 2.1	29.5 \pm 11.2	25.6 \pm 5.5
Cx II+III (nmol/min/mg)	11.9 \pm 1.9	16.6 \pm 2.1	7.5 \pm 0.6	7.6 \pm 2.7	5.3 \pm 0.5	7.3 \pm 0.9
Cx IV (k/min/mg)	1.28 \pm 0.20	1.39 \pm 0.07	0.78 \pm 0.12	1.29 \pm 0.15	0.95 \pm 0.34	0.92 \pm 0.07
CS (nmol/min/mg)	98.0 \pm 9.3	117.0 \pm 4.1	84.0 \pm 5.3	87.0 \pm 5.3	90.0 \pm 10.4	105.2 \pm 8.5

Table 6.5. The effect of lovastatin exposure upon the mitochondrial complex activities of primary cultures of rat astrocytes in the absence of serum.

Rat astrocytes cells were incubated for 24h or 36h in 6-well culture plates in the presence of Na-lovastatin (10 μ M or 100 μ M). Mitochondrial complex activity was determined as described. Data are mean \pm SEM values of three to four independent culture preparations, expressed against a protein baseline. Yellow highlighting represents a statistically significant difference compared to control values ($p < 0.05$).

	24 h			36 h		
	control	10 μ M lovastatin	100 μ M lovastatin	control	10 μ M lovastatin	100 μ M lovastatin
Cx I	0.27 \pm 0.09	0.19 \pm 0.06	0.30 \pm 0.04	0.26 \pm 0.02	0.31 \pm 0.11	0.24 \pm 0.04
Cx II+III	0.12 \pm 0.01	0.14 \pm 0.02	0.09 \pm 0.01	0.09 \pm 0.03	0.06 \pm 0.01	0.07 \pm 0.01
Cx IV (k/nmol)	0.013 \pm 0.001	0.012 \pm 0.001	0.009 \pm 0.001	0.015 \pm 0.003	0.010 \pm 0.002	0.009 \pm 0.001

Table 6.6. The effect of lovastatin exposure upon the mitochondrial complex activities of primary cultures of rat astrocytes in the absence of serum.

Complex activities were determined as described above, and expressed as a ratio of citrate synthase activity.

these cultures (control: CoQ₉ = 159.8 ± 16.1 pmol/ mg protein; CoQ₁₀ = 39.3 ± 5.1 pmol/ mg protein; 10 µM Na-lovastatin: CoQ₉ = 167.2 ± 15.7 pmol/ mg protein; CoQ₁₀ = 45.5 ± 7.1 pmol/ mg protein; Fig 6.8A). With 100µM Na-lovastatin, a decrease observed in CoQ₉ levels did not achieve statistical significance; neither were CoQ₁₀ levels altered (100µM Na-lovastatin: CoQ₉ = 117.5 ± 30.2 pmol/ mg protein; CoQ₁₀ = 37.8 ± 9.2 pmol/ mg protein; Fig 6.8A).

Similarly, 36h incubation did not elicit statistically significant changes in CoQ₉ or CoQ₁₀ status, although CoQ₉ and CoQ₁₀ levels were generally higher when compared to those cultures grown in the presence of serum (control: CoQ₉ = 249.2 ± 41.2 pmol/ mg protein; CoQ₁₀ = 56.9 ± 6.5 pmol/ mg protein; 10µM Na-lovastatin: CoQ₉ = 253.6 ± 30.9 pmol/ mg protein; CoQ₁₀ = 63.0 ± 6.7 pmol/ mg protein; 100µM lovastatin: CoQ₉ = 178.0 ± 28.2 pmol/ mg protein; CoQ₁₀ = 59.4 ± 11.4 pmol/ mg protein; Fig 6.8B).

With regard to cholesterol, 24h exposure did not significantly alter cellular levels (control: 72.7 ± 10.4 nmol/ mg protein; 10 µM Na-lovastatin: 75.9 ± 12.3 nmol/ mg protein; 100 µM Na-lovastatin: 83.3 ± 13.2 nmol/ mg protein; Fig 6.9A). While no change was observed following 36h exposure to 10 µM Na-lovastatin (control: 35.2 ± 5.4 nmol/ mg protein; 10 µM Na-lovastatin: 35.9 ± 3.5 nmol/ mg protein; Fig 6.9B) 100µM Na-lovastatin in the absence of serum resulted in an approximate doubling of total cellular cholesterol after 36h (100µM Na-lovastatin: 72.0 ± 6.5 nmol/ mg protein; Fig 6.9B), and this result was statistically significant ($p < 0.05$).

6.5.4.2. Mitochondrial enzyme activity

As shown in tables 6.7 and 6.8, Na-lovastatin incubation during 24h or 36h culture without FBS did not lead to statistically significant alterations in CS or ETC enzyme activity against either protein or CS.

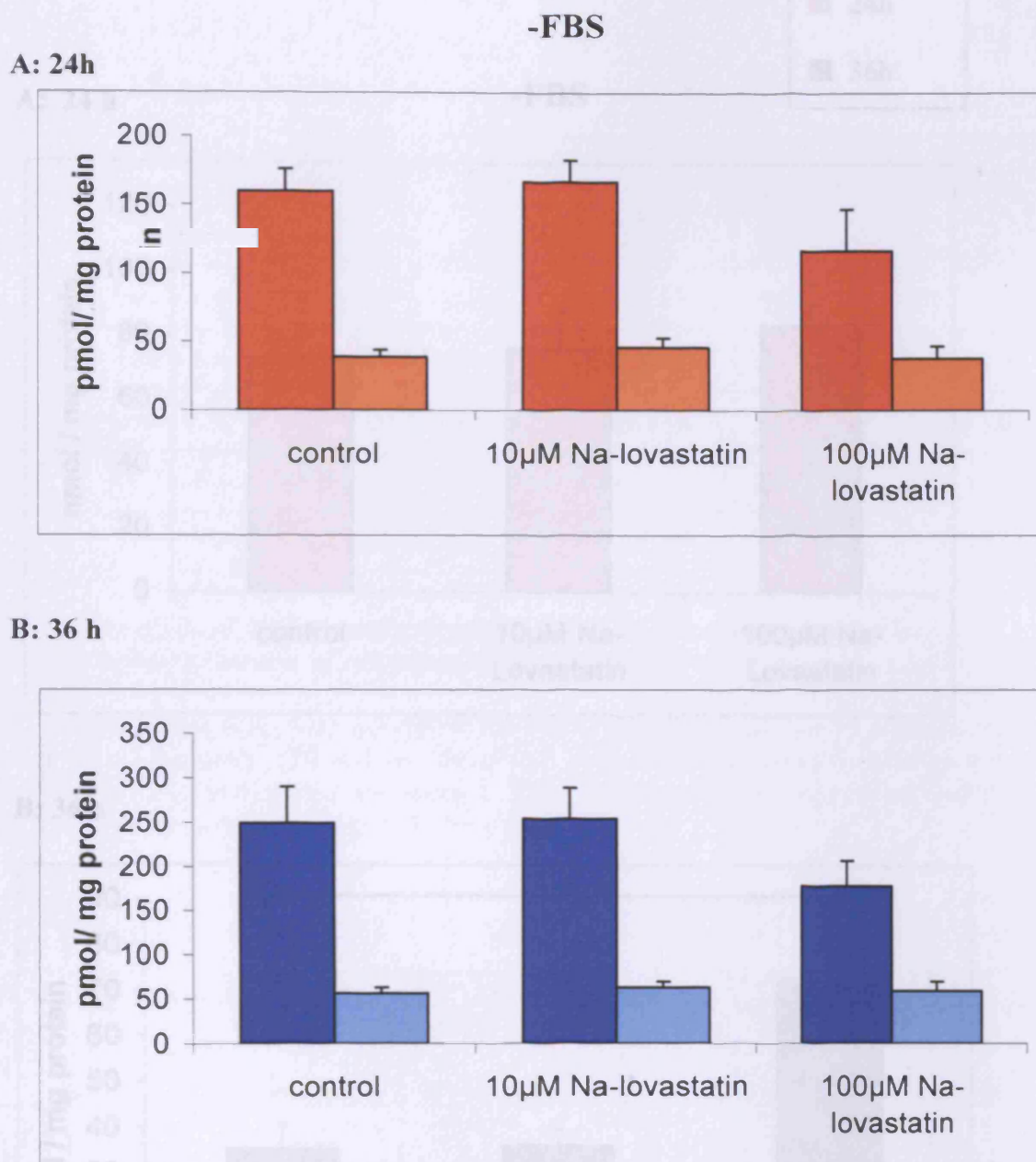


Figure 6.8. The effect of Na-lovastatin exposure upon the CoQ status of primary cultures of rat astrocytes in the absence of serum.

A: Rat astrocytes cells were incubated for 24h in 6-well culture plates in the presence of Na-lovastatin (10 µM) but in the absence of FBS as indicated (■ = CoQ₉; □ = CoQ₁₀). Data are mean ± SEM values of seven to eight independent culture preparations.

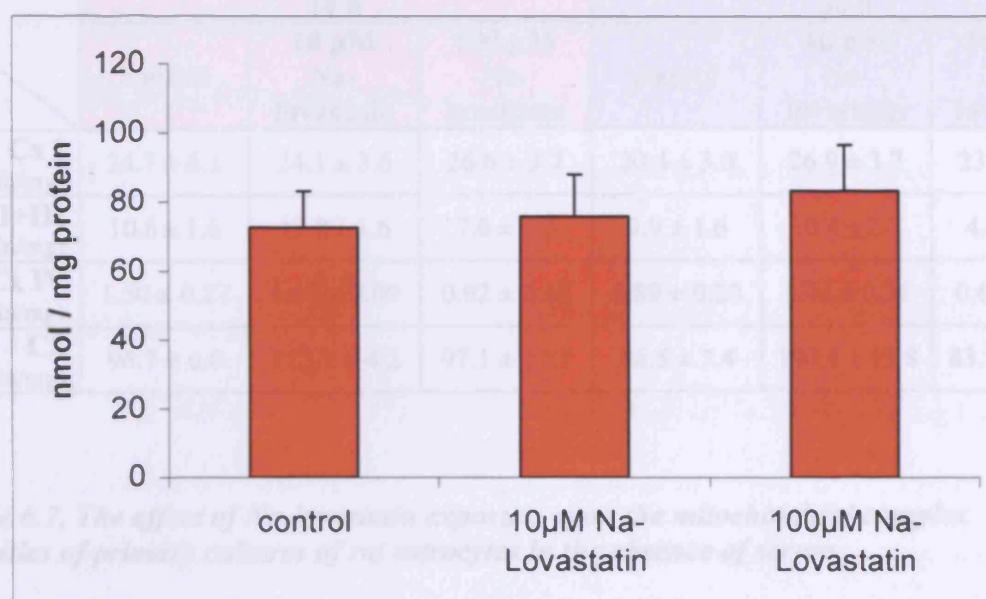
B: Rat astrocytes cells were incubated for 36h in 6-well culture plates in the presence of Na-lovastatin (10 or 100µM) and the absence of FBS as indicated (■ = CoQ₉; □ = CoQ₁₀). Data are mean ± SEM values of four to six independent culture preparations.

A: 24 h

-FBS

24h

36h



B: 36 h

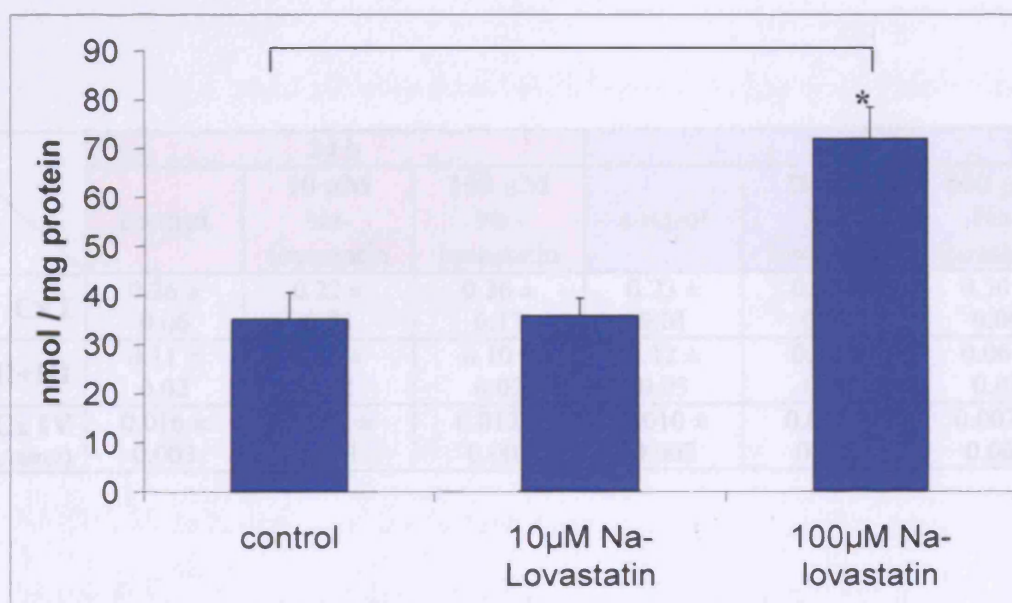


Figure 6.9. Cholesterol levels in serum - deprived astrocytes treated with Na-lovastatin

Rat astrocytes were incubated for 24h (■), or 36h (■) in 6-well culture plates in the absence of FBS as indicated. Cell culture media was supplemented as indicated, and cells harvested following 24h or 36h incubation. Data are mean \pm SEM values of three to four independent culture preparations expressed against a protein baseline.

	24 h			36 h		
	control	10 μ M Na- lovastatin	100 μ M Na- lovastatin	control	10 μ M Na- lovastatin	100 μ M Na- lovastatin
Cx I (nmol/min/mg)	24.7 \pm 6.1	24.1 \pm 3.6	26.6 \pm 3.7	20.4 \pm 3.0	26.9 \pm 3.7	23.1 \pm 1.4
Cx II+III (nmol/min/mg)	10.6 \pm 1.6	12.8 \pm 1.6	7.6 \pm 0.5	9.9 \pm 1.6	10.4 \pm 2.7	4.6 \pm 2.6
Cx IV (k/min/mg)	1.50 \pm 0.27	1.00 \pm 0.09	0.92 \pm 0.12	0.89 \pm 0.20	1.44 \pm 0.31	0.65 \pm 0.25
CS (nmol/min/mg)	96.7 \pm 6.0	112.7 \pm 4.2	97.1 \pm 12.2	86.5 \pm 7.4	100.4 \pm 12.8	83.7 \pm 17.1

Table 6.7. The effect of Na-lovastatin exposure upon the mitochondrial complex activities of primary cultures of rat astrocytes in the absence of serum.

Rat astrocytes cells were incubated for 24h or 36h in 6-well culture plates in the presence of Na-lovastatin (10 μ M or 100 μ M). Mitochondrial complex activity was determined as described. Data are mean \pm SEM values of three independent culture preparations, expressed against a protein baseline.

	24 h			36 h		
	control	10 μ M Na- lovastatin	100 μ M Na- lovastatin	control	10 μ M Na- lovastatin	100 μ M Na- lovastatin
Cx I	0.26 \pm 0.06	0.22 \pm 0.03	0.36 \pm 0.13	0.23 \pm 0.01	0.27 \pm 0.03	0.30 \pm 0.06
Cx II+III	0.11 \pm 0.02	0.11 \pm 0.02	0.10 \pm 0.03	0.12 \pm 0.03	0.10 \pm 0.02	0.06 \pm 0.03
Cx IV (k/nmol)	0.016 \pm 0.003	0.009 \pm 0.001	0.012 \pm 0.002	0.010 \pm 0.003	0.014 \pm 0.003	0.007 \pm 0.002

Table 6.8. The effect of Na-lovastatin exposure upon the mitochondrial complex activities of primary cultures of rat astrocytes in the absence of serum.

Complex activities were determined as described in the table above, and expressed as a ratio of citrate synthase activity.

6.5.4.3. LDH release

Again when cultured in the absence of serum, 10 μ M Na-lovastatin did not significantly increase LDH release. 100 μ M Na-lovastatin however, caused a statistically significant release compared to the control vehicle (control: $7.1 \pm 2.6\%$; 10 μ M Na-lovastatin: $9.7 \pm 5.6\%$; 100 μ M Na-lovastatin: $16.3 \pm 1.4\%$).

6.6. Discussion

Lovastatin treatment has previously been described as inhibiting biosynthesis of both cholesterol (Alberts *et al.*, 1980; Bradford *et al.*, 1994) and CoQ₉₊₁₀ (Maltese and Aprille, 1985). In addition, lower levels of these end-products have been described following treatment with lovastatin (Alberts *et al.*, 1980; Willis *et al.*, 1990; Folkers *et al.*, 1990). Thus primary cultures of rat astrocytes were treated with lovastatin and cholesterol, CoQ₉ and CoQ₁₀ and ETC enzyme activities measured. While plasma protein binding could possibly limit bioavailability (Selleri *et al.*, 2003; Mundy *et al.*, 2004), albumin carriage as a result of lovastatin binding to proteins in FBS could enhance uptake, or a lactonase activity of FBS could enhance conversion to the active isoform. Thus lovastatin was added in culture media in the presence or absence of FBS (10%).

As Na-lovastatin has been established as being more effective at inhibiting HMG-CoA reductase than the lactone form (Endo, *et al.*, 1976; Alberts *et al.*, 1980; Merck & Co. Inc., 2003), both lovastatin and Na-lovastatin were added to the culture medium for up to 36h in the presence or absence of FBS.

While lovastatin exposure significantly decreased CoQ₉ levels after 24h when used at a concentration of 100 μ M (Fig 6.1A), the decrease observed with Na-lovastatin under the same conditions (although still statistically significant) was markedly smaller

(Fig 6.4A). In both cases, the absence of serum resulted in smaller non-significant decreases suggesting that the presence of FBS may facilitate the entry of lovastatin to, or otherwise increase the efficacy of the drug in these primary astrocyte cultures.

A number of mammalian sera have lactonase activity (Roth *et al.*, 1967; Teiber *et al.*, 2003). In human serum, lovastatin can be converted to the activated form by serum, although the serum-dependant component accounts for only 15% of the total lovastatin conversion, which primarily occurs in the liver (Tang and Kalow, 1995). Serum lactonase activity metabolising lovastatin has been ascribed to paraoxonase 1 (PON1; EC. 3.1.8.1, formerly 3.1.1.2; Billecke *et al.*, 2000), while rabbit serum contains PON3 (Draganov *et al.*, 2000). Thus while literature searches do not confirm the presence of PON isoforms in FBS, it is possible that the 10% supplementation of culture media with FBS could convert the prodrug to the active form.

Notably, given that no changes in either CoQ₉ or CoQ₁₀ levels were observed following 10 μ M exposure to lovastatin or Na-lovastatin.

Lovastatin (100 μ M) inclusion in serum-containing media for 36h resulted in a significant decrease of in CoQ₉ but not CoQ₁₀ in comparison to control levels, mirroring the findings of the 24h experiment (Fig 6.1B). Again the absence of serum in these experiments abolished the decrease in CoQ₉ levels. However, despite the decreases in CoQ₉, CoQ₁₀ status was unaffected. Although a modest increase in CoQ₁₀ levels was observed in one case in the absence of FBS (Fig. 6.6B), the reasons for this are unclear. Taken in light of the finding of decreased CoQ₉ levels while CoQ₁₀ is maintained, these data may support the proposition of distinct metabolic pathways for synthesis of CoQ₉ and CoQ₁₀, where levels of one may be amenable to modulation whilst maintaining concentration of the other homologue.

Rather than displaying increased potency, Na-lovastatin appeared to be less effective in modulating cellular CoQ levels: the decreases observed in CoQ₉ concentration with Na-lovastatin were generally smaller in either the presence or absence of serum.

While CoQ₉ levels were seen to decrease, cholesterol levels were maintained with lovastatin treatment in the presence of serum. Cholesterol levels were elevated following Na-lovastatin treatment (100 μ M) in the presence of serum for 24h (while CoQ₉ decreased) and after 36h incubation in the absence of serum (when CoQ₉ levels did not change significantly). The reasons for this are unclear; however the increases in cholesterol may be attributable to the induction of rat HMG-CoA reductase synthesis following competitive inhibition by lovastatin, as described in animal studies by (Edwards *et al.*, 1983; Yamauchi *et al.*, 1991). As ubiquinone synthesis in rat brain slices is approximately 20-fold slower than that of cholesterol yet the half life CoQ turnover is 90h compared to approximately 4000h for cholesterol (Andersson *et al.*, 1990), it is possible such induction of HMG-CoA reductase may not be sufficient to maintain CoQ₉ levels following initial inhibition. Additionally, serum lipoprotein withdrawal has also been described as an inducer of HMG-CoA reductase activity in primary cultures of rat glia (Langan *et al.*, 1987).

It is therefore evident that decreases in CoQ₉ did not correlate to a loss of cellular cholesterol and the differential effects upon CoQ₉, CoQ₁₀ and cholesterol (which may share a common biosynthetic pathway) therefore remains to be resolved. However as the biochemistry of CoQ synthesis has yet to be fully elucidated in mammals, it is possible that distinct CoQ homologues and cholesterol, as the end products of the mevalonate pathway, are regulated independently.

While the LDH data would suggest increased membrane permeability of cultures treated with lovastatin, these findings must be treated with caution. As described by Keilhoff & Wolf (1993), increased LDH activity in cell culture medium may not necessarily correlate with decreased cell viability. These authors suggest that LDH may be better used as a marker of cell stress than cell death. Finally, the observed decreases in CoQ₉ were unlikely to be attributable to cell death given that CoQ₁₀ status did not change.

In order to gain further insight into the consequences of depletion of cellular CoQ₉ resulting from lovastatin and Na-lovastatin treatment, the activities of the ETC enzymes were determined. As can be seen, only complex IV was affected, with significant decreases in activity observed in 100 μ M lovastatin-treated cultures grown in the absence of serum for 36h and expressed against CS activity (Table 6.2). This appeared to correspond to decreased CoQ₉ levels, but not CoQ₁₀ or cholesterol. Given the antioxidant nature of CoQ, and the susceptibility of complex IV to oxidative stress and free radical-mediated inhibition (Brown and Cooper, 1994; Bolaños *et al.*, 1994; Bolaños *et al.*, 1996, reviewed in Heales *et al.*, 1999), it is conceivable that decreased antioxidant defences at the levels of either CoQ₉ or CoQ₁₀ could result in decreased complex IV activity. However a statistically significant decrease in complex IV was also observed with 24h lovastatin treatment in the absence FBS. Under these conditions no changes in CoQ₉, CoQ₁₀ or cholesterol metabolism were observed; subsequently it is unclear as to whether complex IV activity was decreased as a result of alterations in the cellular levels CoQ₉.

The complex II+III assay may be dependent upon endogenous CoQ homologues in the ETC (Clark *et al.*, 1994; Rahman *et al.*, 2001); thus a marked loss of at least one of these homologues could potentially manifest as a decreased activity of

this linked assay (Shults *et al.*, 1997; Van Maldegerm *et al.*, 2002). However, the decreases in CoQ₉ observed with 100 μ M lovastatin and 100 μ M Na-lovastatin after 24h and 36h (Figs 6.1 and 6.4A) did not translate to statistically significant decreases in complex II+III activity *in vitro*. A number of possibilities can be considered: while mitochondrial complex II+III activity was used as a putative index of CoQ₉ or CoQ₁₀ function in the inner mitochondrial membrane, this study addressed total cellular levels of these species. It may be that changes in other membranes' CoQ₉ or CoQ₁₀ status are not related to levels in the inner mitochondrial membrane. Thus alterations in mitochondrial CoQ₉ or CoQ₁₀ may not be evident in whole cell measurements. It is also possible that a much greater decrease in CoQ₉ or CoQ₁₀ may be necessary to elicit decreased levels of complex II+III activity. However, it may be important that under these conditions, CoQ₁₀ levels were maintained. Thus the possibility exists that while cellular levels of CoQ₉ are decreased, it is CoQ₁₀ which is functionally active as an electron carrier within the inner mitochondrial membrane.

6.7. Conclusion

It was found that 100 μ M lovastatin or Na-lovastatin had the ability to decrease cellular levels of CoQ₉ (but not CoQ₁₀) following 24h or 36h exposure. A lower concentration of the statin (10 μ M) did not alter CoQ status. Decreases observed in the absence of serum were less profound than those observed in the presence of serum. Thus albumin carriage may be a factor in cellular uptake of lovastatin; alternatively these effects may be attributed to lactonase activity of the FBS.

Total cellular cholesterol did not decrease under comparable conditions. In these cases, Na-lovastatin appeared to be more effective in eliciting an increase in cellular cholesterol than was lovastatin. Whether the differential effects observed on

CoQ₉ and cholesterol are due to differences in cellular turnover and biosynthetic rate of these molecules, or another mechanism remains to be elucidated.

Complex II+III activity did not correlate with the increases or decreases observed in CoQ₉ or CoQ₁₀. These findings may support the hypothesis that the major and minor isoforms of CoQ are involved in differing physiological functions in discrete subcellular locations.

**7. CoQ₉ AND CoQ₁₀ LEVELS IN PRIMARY
CULTURES OF RAT ASTROCYTES AND
NEURONS; EFFECTS OF EXPOSURE TO
NITRIC OXIDE**

7. CoQ₉ AND CoQ₁₀ LEVELS IN PRIMARY CULTURES OF RAT ASTROCYTES AND NEURONS; EFFECTS OF EXPOSURE TO NITRIC OXIDE

7.1. Introduction

With regard to the effects upon astrocytes and neurons, a number of differential effects of reactive nitrogen species (RNS) have been reported (reviewed in Heales *et al.*, 2004).

RNS acting upon the ETC have been shown to inhibit complexes II+III and complex IV in primary cultures of astrocytes (Bolaños *et al.*, 1994, Stewart *et al.*, 1998b). The neuronal ETC however, appears to be less robust (Bolaños *et al.*, 1995; Gegg *et al.*, 2003).

GSH status of such astrocytes almost doubles upon 24h exposure to DETA-NO; neurons however, exposed to the same conditions for 18h decrease their GSH content by almost 50%, (Gegg *et al.*, 2003). Moreover, while in cultured astrocytes and neurons RNS exposure does not readily inhibit complex I (Bolaños *et al.*, 1994, 1995, 1996), following GSH depletion with L-BSO, complex I becomes susceptible to RNS-mediated inhibition (Barker *et al.*, 1996).

Monocultured neurons contain approximately 70% less GSH than neurons cultured in the presence of astrocytes (Bolaños *et al.*, 1996). Induction of iNOS for 24h in these astrocytes cocultured with neurons results in significant neuronal mitochondrial damage; however, cell death does not occur at this timepoint (Stewart *et al.*, 1998b). In contrast, direct exposure of monocultured neurons to RNS causes cell death associated with mitochondrial damage (Bolaños *et al.*, 1995, 1996).

Cocultured neurons with NO-generating astrocytes increase their GSH levels, and subsequently maintain ETC activities. If the astrocytes are previously depleted of GSH, nearby neurons are unable to upregulate GSH synthesis; subsequently complex II+III and complex IV activity decreases (Gegg *et al.*, 2005).

RNS exposure does not immediately cause cell death of astrocytes (Bolaños *et al.* 1994, 1995). However, neurons have been shown to be vulnerable to RNS-mediated damage. This differential is in part due to the ability of astrocytes to maintain ATP synthesis (and thus prevent ATP hydrolysis as a reversal of the ATP synthase) by an upregulation of glycolysis (Bolaños *et al.*, 1994, Almeida *et al.*, 2004).

Although a number of differential effects resulting from RNS exposure to astrocytes and neurons have been documented, the CoQ₉ and CoQ₁₀ status under such conditions has not yet been examined. This chapter describes the effects of iNOS induction in astrocytes, and DETA-NO exposure in astrocytes and neurons with regard to cellular levels of CoQ₉ and CoQ₁₀.

7.2.Aims

- To investigate the effects of iNOS activation for up to 36h upon cellular levels of CoQ₉, and CoQ₁₀, and the activities of the enzymes of the ETC in astrocyte cultures.
- To investigate the effects of DETA-NO as an exogenous source of NO in this cell culture system.
- To characterise the CoQ₉ and CoQ₁₀ status of neurons, and their responses to exogenous NO as a result of DETA-NO addition to the culture medium.

7.3.Methods

7.3.1. Tissue culture

7.3.1.1. Primary astrocyte cultures

Primary cultures of rat astrocytes were prepared and maintained as described in section 2.2.3. On DIV 13, as described in section 2.2.6, cultures were exposed to LPS (1 µg/ ml) and IFNγ (100 U/ml) for 24h or 36h in the absence of serum to induce iNOS-mediated NO generation (Bolaños *et al.*, 1994). L-NIL (100 µM) was used as an inhibitor of iNOS (Moore *et al.*, 1994). Exogenous NO was generated in cell culture media by the addition of the NO donor DETA-NO (500 µM). Cells were collected as a pellet as described in sections 2.2.6.

7.3.1.2.Primary neuron cultures

Neuron-enriched cultures were prepared as described in section 2.2.4. On DIV 6, cultures were maintained in the absence of serum for 24h. In experiments investigating the effect of endogenous NO, DETA-NO (500 µM) or the degraded control was added to the culture medium (section 2.2.6.4).

7.3.2. CoQ measurement by HPLC

Cellular lipids were extracted as described in section 3.2.5, and the concentrations of CoQ₉ and CoQ₁₀ were measured by reverse-phase UV-HPLC as in section 3.2.3.

7.3.3. ETC enzyme assays

The activities of the enzymes of the respiratory chain were assayed in the samples as described in section 2.3

7.3.4. Lactate dehydrogenase determination

As an index of cell stress, LDH release from the astrocyte cultures was measured after 36h of growth in 6 well plates, and expressed as a percentage of the total LDH activity of the culture. This is described in section 2.5.

7.3.5. Measurement of NO_x in culture media

The generation of NO₂⁻ and NO₃⁻ (NO_x) species in the culture media was used as an index of NO generation. Determination of NO_x used the Greiss assay (based on the method of Green *et al.*, 1982); wherein a pink diazo product was formed from the reaction between naphthaethylenediamine dihydrochloride, and sulphanilamide/ H₃PO₄. This has previously been described in section 2.4.

7.3.6. Protein determination

CoQ levels in cells and ETC activities were expressed against a protein baseline. the protein content of samples was determined by the method of Lowry *et al.* (1951) as in section 2.7.

7.4. Experimental protocol

7.4.1. Exposure of astrocyte cultures to LPS + IFN γ

Primary cultures of rat astrocytes were exposed to media supplemented with LPS (1 μ g/ ml) and IFN γ (100 U/ml) for 24h or 36h. This has previously been described to induce the iNOS protein (Bolaños *et al.*, 1994), leading to NO generation and subsequent elevation of NO_x in culture medium. Control experiments used untreated cells incubated for the same time. Some experiments used L-NIL (100 μ M) in addition LPS + IFN γ to inhibit activation of iNOS.

7.4.2. Exposure of astrocyte cultures to DETA-NO

DETA-NO (500 μ M) in this astrocyte and neuron culture medium has previously been calculated to release a steady state concentration of approximately 1 μ M NO for 24h (Gegg *et al.*, 2003). This compound was used to expose astrocytes to exogenous NO. In control experiments, media was supplemented with the same concentration of degraded DETA-NO. This had been previously incubated at 37°C for 7 days. Given that the half life of DETA-NO is approximately 8h (Seccia *et al.*, 1996), negligible NO will be generated by the addition of the degraded compound to cell culture media. The CoQ status and ETC enzyme activities of astrocyte cultures exposed to NO of exogenous or endogenous origin were reported.

7.4.3. CoQ status of neuronal cultures and exposure to DETA- NO

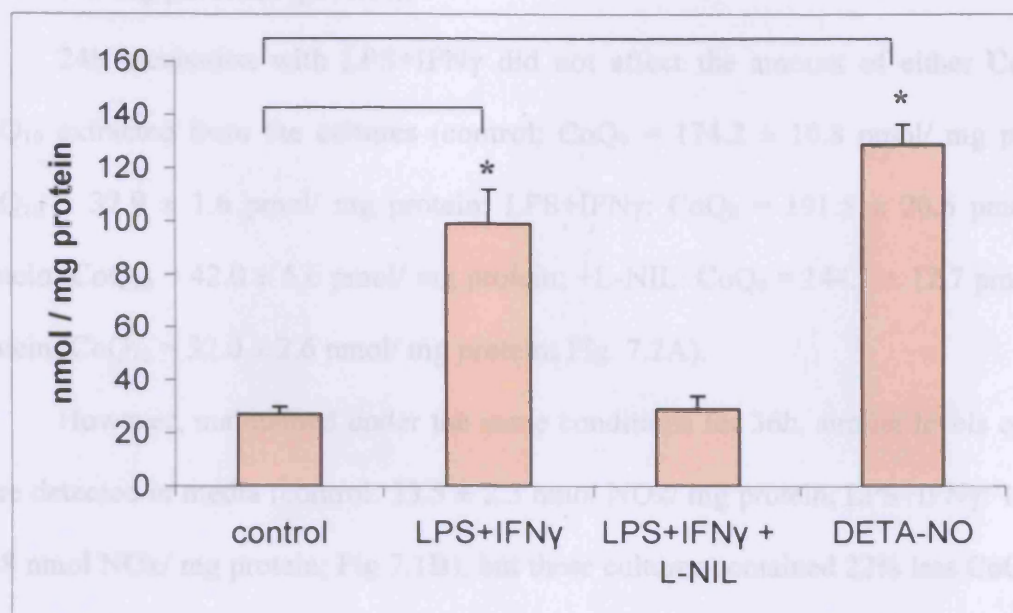
CoQ₉ and CoQ₁₀ status of these neuron-enriched cultures was determined as conducted previously with other cell types: section 3.2.5 describes the extraction and sample preparation for the determination of CoQ by UV-HPLC. CoQ₉ and CoQ₁₀ levels were measured in untreated cells and following the inclusion for 24h of either fresh DETA-NO (500 μ M) in the cell culture media, or degraded DETA-NO as a control.

7.5. Results

7.5.1. CoQ status of astrocyte cultures following LPS + IFN γ exposure

Incubation of astrocytes with LPS + IFN γ for 24h generated significant amounts of NO in the culture media as witnessed by the measurement of NO_x (Fig. 7.1A). This was abolished by the use of the inhibitor of iNOS, L-NIL (control: 26.8 \pm 3.2 nmol

A:



B:

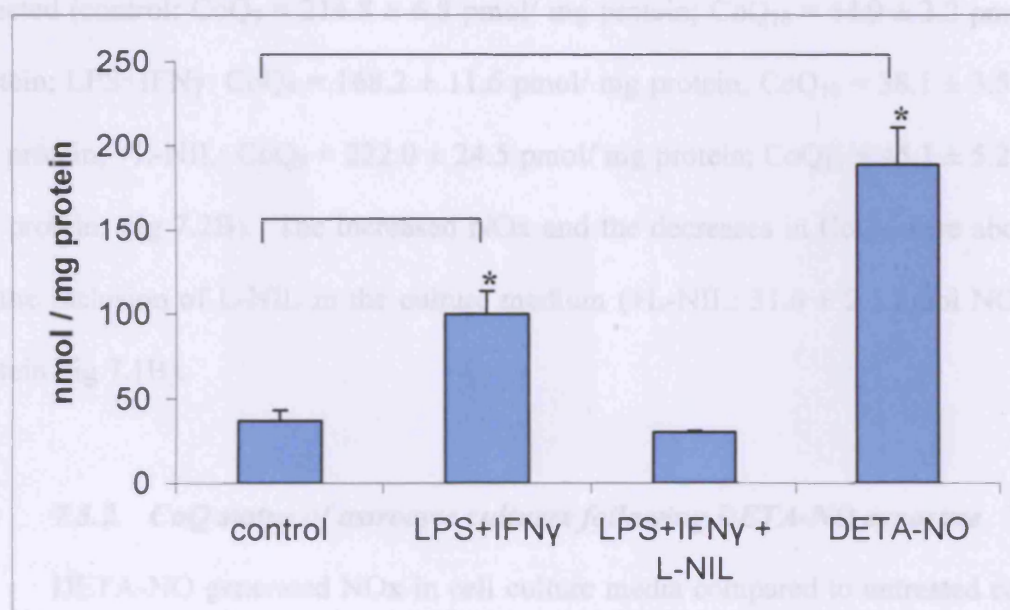


Fig 7.1 NOx levels in culture media from rat primary astrocytes

Rat primary astrocytes were incubated for 24h (A: ■) or 36h (B: ■) in 6-well culture plates in the absence (control) or presence of LPS (1 μ g/ml) and IFN γ (100 U/ml), with and without the inhibitor of iNOS L-NIL (100 μ M) or alternatively DETA-NO (500 μ M) as indicated. Data are mean \pm SEM values of three to four independent culture preparations. * signifies $p < 0.05$ compared to control values following analysis by one-way ANOVA.

NOx/ mg protein; LPS+IFN γ : 99.1 ± 12.5 nmol NOx/ mg protein; +L-NIL: 28.9 ± 5.2 nmol NOx/ mg protein; Fig. 7.1A).

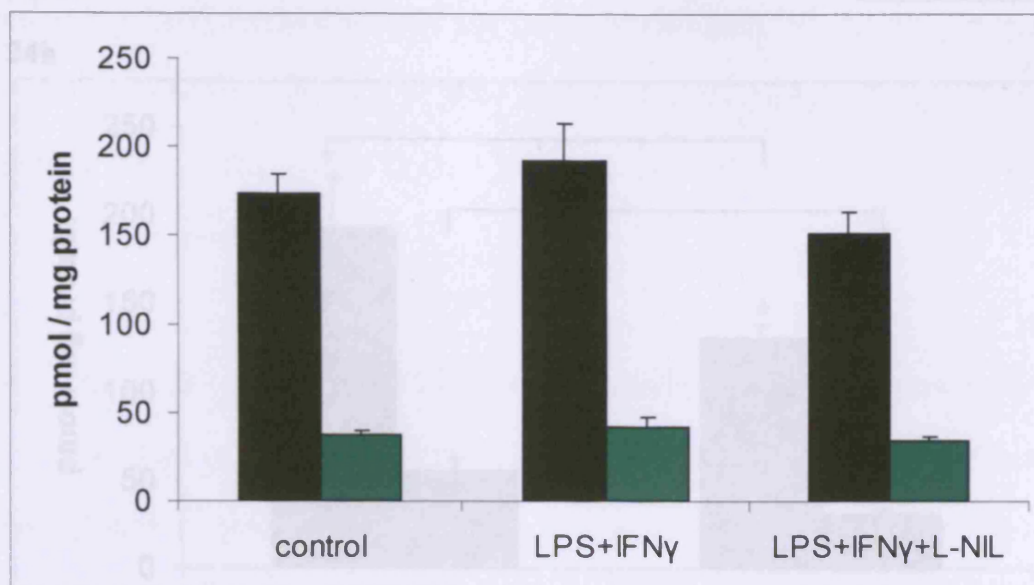
24h incubation with LPS+IFN γ did not affect the amount of either CoQ $_9$ or CoQ $_{10}$ extracted from the cultures (control: CoQ $_9$ = 174.2 ± 10.8 pmol/ mg protein; CoQ $_{10}$ = 37.9 ± 1.6 pmol/ mg protein; LPS+IFN γ : CoQ $_9$ = 191.5 ± 20.6 pmol/ mg protein; CoQ $_{10}$ = 42.0 ± 5.6 pmol/ mg protein; +L-NIL: CoQ $_9$ = 144.1 ± 12.7 pmol/ mg protein; CoQ $_{10}$ = 32.0 ± 2.6 pmol/ mg protein; Fig. 7.2A).

However, maintained under the same conditions for 36h, similar levels of NOx were detected in media (control: 33.5 ± 2.3 nmol NOx/ mg protein; LPS+IFN γ : 100.1 ± 13.8 nmol NOx/ mg protein; Fig 7.1B), but these cultures contained 22% less CoQ $_9$ ($p = 0.05$) than controls. Under the same conditions, CoQ $_{10}$ levels were not significantly affected (control: CoQ $_9$ = 214.8 ± 6.8 pmol/ mg protein; CoQ $_{10}$ = 44.9 ± 3.2 pmol/ mg protein; LPS+IFN γ : CoQ $_9$ = 168.2 ± 11.6 pmol/ mg protein; CoQ $_{10}$ = 38.1 ± 3.5 pmol/ mg protein; +L-NIL: CoQ $_9$ = 222.0 ± 24.5 pmol/ mg protein; CoQ $_{10}$ = 45.1 ± 5.2 pmol/ mg protein; Fig 7.2B). The increased NOx and the decreases in CoQ $_9$ were abolished by the inclusion of L-NIL in the culture medium (+L-NIL: 31.6 ± 2.5 nmol NOx/ mg protein Fig 7.1B).

7.5.2. CoQ status of astrocyte cultures following DETA-NO exposure

DETA-NO generated NOx in cell culture media compared to untreated controls (DETA-NO: 128.6 ± 7.5 nmol NOx/ mg protein; Fig 7.1). After 24h, this resulted in CoQ $_9$ and CoQ $_{10}$ levels which were significantly decreased compared to controls (control: CoQ $_9$ = 193.3 ± 28.2 pmol/ mg protein; CoQ $_{10}$ = 55.3 ± 7.1 pmol/ mg protein; DETA-NO: CoQ $_9$ = 130.5 ± 7.0 pmol/ mg protein; CoQ $_{10}$ = 31.2 ± 3.1 pmol/ mg protein; Fig 7.3A). However, extension of this incubation with DETA-NO to 36h while

A: 24h



B: 36h

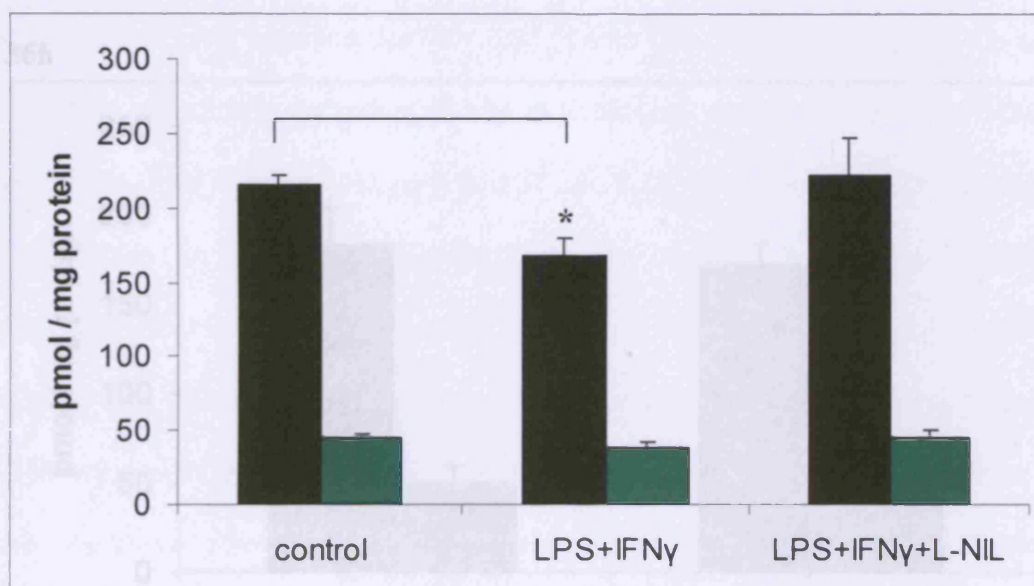
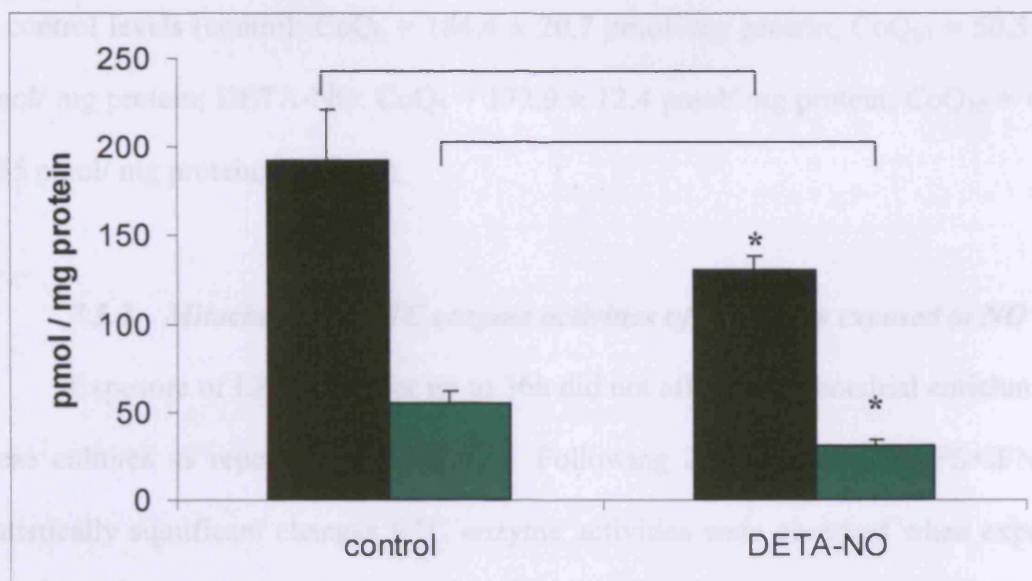


Figure 7.2. The effect of LPS+IFN γ upon the CoQ status of primary cultures of rat astrocytes.

A: Rat astrocytes were incubated for 24h in 6-well culture plates as indicated. Data are mean \pm SEM values of between seven and twelve independent culture preparations.

B: Rat astrocytes were incubated for 36h in 6-well culture plates as indicated. Data are mean \pm SEM values of five or six independent culture preparations (* signifies $p = 0.05$).

A: 24h



B: 36h

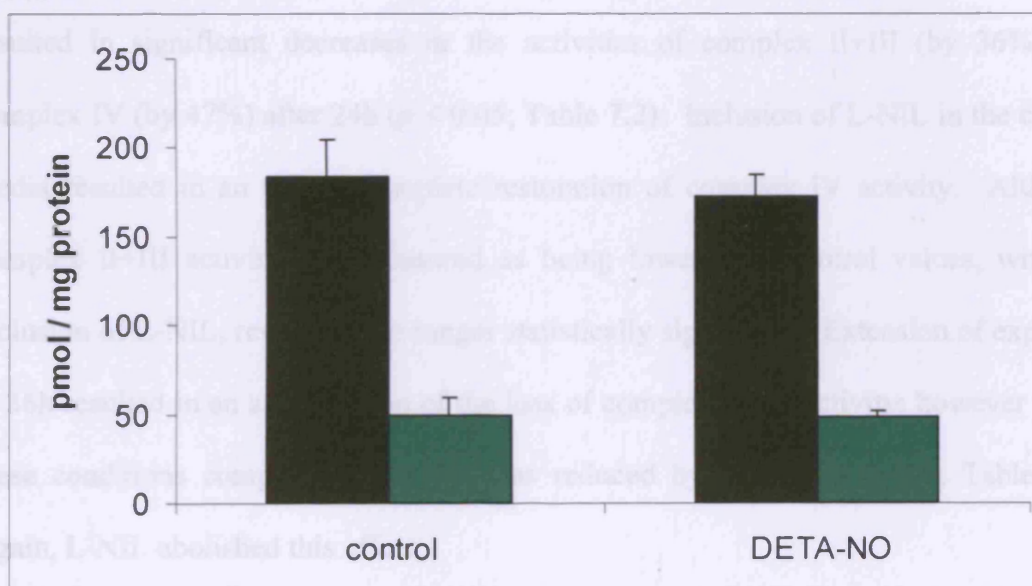


Figure 7.3. The effect of DETA-NO upon CoQ status of rat primary astrocyte cultures

Rat astrocytes were incubated for 24h (A) or 36h (B) in 6-well culture plates as indicated. DETA-NO (500 μ M) was added as a source of exogenous NO; degraded DETA-NO was used as a control. Data are mean \pm SEM values of between three and five independent culture preparations. (* signifies $p = 0.05$).

greater levels of NO_x in culture media (DETA-NO: 189.2 ± 21.7 nmol NO_x/ mg protein; Fig 7.1B), resulted in CoQ₉ and CoQ₁₀ levels which were unchanged compared to control levels (control: CoQ₉ = 184.4 ± 20.7 pmol/ mg protein; CoQ₁₀ = 50.5 ± 9.2 pmol/ mg protein; DETA-NO: CoQ₉ = 172.9 ± 12.4 pmol/ mg protein; CoQ₁₀ = 48.7 ± 2.55 pmol/ mg protein; Fig 7.3B).

7.5.3. Mitochondrial ETC enzyme activities of astrocytes exposed to NO

Exposure of LPS+IFN γ for up to 36h did not affect mitochondrial enrichment of these cultures as reported in Table 7.1. Following 24h exposure to LPS+IFN γ , no statistically significant changes ETC enzyme activities were observed when expressed against a protein baseline (Table 7.1). Following 36h exposure a 60% decrease in complex IV activity was recorded ($p < 0.05$; Table 7.1). Expression against CS activity resulted in significant decreases in the activities of complex II+III (by 36%) and complex IV (by 47%) after 24h ($p < 0.05$; Table 7.2). Inclusion of L-NIL in the culture media resulted in an almost complete restoration of complex IV activity. Although complex II+III activity was measured as being lower than control values, with the inclusion of L-NIL, result was no longer statistically significant. Extension of exposure to 36h resulted in an amelioration of the loss of complex II+III activity; however under these conditions complex IV activity was reduced by 60% ($p < 0.001$; Table 7.2). Again, L-NIL abolished this effect.

DETA-NO was used to generate exogenous NO in the culture medium, and this did not affect CS activity in these samples (Table 7.3). However, complex IV activity after 24h exposure was decreased by 57% ($p < 0.001$) and 43% lower after 36h ($p < 0.05$), following expression against a protein baseline (Table 7.3).

	24 h			36 h		
	control	LPS + IFN γ	LPS+IFN γ +L-NIL	control	LPS + IFN γ	LPS+IFN γ +L-NIL
Cx I (nmol/min/mg)	25.0 \pm 4.15	29.2 \pm 2.2	27.3 \pm 6.1	17.5 \pm 3.3	24.4 \pm 1.8	28.8 \pm 5.0
Cx II+III (nmol/min/mg)	15.9 \pm 1.6	13.0 \pm 3.5	20.6 \pm 1.7	9.0 \pm 1.3	9.1 \pm 2.6	12.3 \pm 1.4
Cx IV (k/min/mg)	1.78 \pm 0.34	1.03 \pm 0.063	1.54 \pm 0.141	1.03 \pm 0.17	0.41 \pm 0.11	1.16 \pm 0.16
CS (nmol/min/mg)	111.5 \pm 3.5	120.9 \pm 6.2	103.5 \pm 2.2	95.3 \pm 17.3	105.8 \pm 19.9	100.2 \pm 5.6

Table 7.1. The effect of LPS+IFN γ exposure upon the mitochondrial complex activities of primary cultures of rat astrocytes.

Rat astrocytes cells were incubated for 24h or 36h in 6-well culture plates in the presence of absence (control) or presence of LPS+IFN γ (1 μ g/ ml and 100 U/ml respectively). The inhibitor of iNOS L-NIL was also included in some experiments. Mitochondrial complex activity was determined as described. Data are mean \pm SEM values of three to four independent culture preparations, expressed against a protein baseline. Yellow highlighting represents a statistically significant difference compared to control values ($p < 0.05$).

	24 h			36 h		
	control	LPS + IFN γ	LPS+IFN γ +L-NIL	control	LPS + IFN γ	LPS+IFN γ +L-NIL
Cx I	0.23 \pm 0.04	0.26 \pm 0.02	0.27 \pm 0.05	0.19 \pm 0.04	0.24 \pm 0.03	0.26 \pm 0.05
Cx II+III	0.14 \pm 0.02	0.09 \pm 0.01	0.11 \pm 0.01	0.11 \pm 0.03	0.08 \pm 0.01	0.11 \pm 0.01
Cx IV (k/nmol)	0.016 \pm 0.004	0.009 \pm 0.001	0.015 \pm 0.002	0.011 \pm 0.001	0.004 \pm 0.001	0.011 \pm 0.001

Table 7.2. The effect of LPS+IFN γ exposure upon the mitochondrial complex activities of primary cultures of rat astrocytes.

Complex activities were determined as described in the table above, and expressed as a ratio of citrate synthase activity. Highlighting represents a statistically significant difference compared to control values (yellow = $p < 0.05$; green = $p < 0.001$).

	24 h		36 h	
	control	DETA-NO	control	DETA-NO
Cx I (nmol/min/mg)	21.9 ± 2.9	21.0 ± 2.9	24.3 ± 3.9	28.8 ± 3.6
Cx II+III (nmol/min/mg)	8.6 ± 1.5	7.5 ± 0.6	7.2 ± 1.1	7.3 ± 1.3
Cx IV (k/min/mg)	1.27 ± 0.08	0.55 ± 0.07	0.87 ± 0.17	0.50 ± 0.09
CS (nmol/min/mg)	99.5 ± 14.4	100.2 ± 5.6	95.9 ± 12.9	110.3 ± 2.0

Table 7.3. The effect of NO exposure upon the mitochondrial complex activities of primary cultures of rat astrocytes.

Rat astrocytes cells were incubated for 24h or 36h in 6-well culture plates in the presence of DETA-NO (500 μ M). Degraded DETA-NO was added at the same concentration as a control. Mitochondrial complex activity was determined as described. Data are mean \pm SEM values of three to five independent culture preparations, expressed against a protein baseline. Highlighting represents a statistically significant difference compared to control values (yellow = $p < 0.05$; green = $p < 0.001$).

	24 h		36 h	
	control	DETA-NO	control	DETA-NO
Cx I	0.27 ± 0.09	0.24 ± 0.04	0.27 ± 0.06	0.26 ± 0.03
Cx II+III	0.09 ± 0.01	0.09 ± 0.01	0.07 ± 0.01	0.06 ± 0.01
Cx IV (k/nmol)	0.011 ± 0.001	0.006 ± 0.001	0.012 ± 0.005	0.005 ± 0.001

Table 7.4. The effect of NO exposure upon the mitochondrial complex activities of primary cultures of rat astrocytes.

Complex activities were determined as described in the table above, and expressed as a ratio of citrate synthase activity. Yellow highlighting represents a statistically significant difference compared to control values ($p < 0.05$).

Against CS activity, decreases in complex IV activity were also evident: 42% after 24h and 62% after 36h ($p < 0.05$; Table 7.4). None of the other respiratory complex activities were significantly altered following exposure to DETA-NO.

7.5.4. The effect of LPS+IFN γ and DETA-NO on lactate dehydrogenase levels from primary astrocyte cultures

LDH release from those astrocyte cultures treated with LPS/IFN γ for 36h was not significantly increased compared to untreated controls (control: $3.6 \pm 0.6\%$; LPS + IFN γ : $6.5 \pm 1.9\%$). DETA-NO treatment for the same time did not significantly alter media LDH activity compared to cultures treated with the degraded NO donor (control: $4.3 \pm 1.4\%$; DETA-NO: $7.8 \pm 1.7\%$).

7.5.5. CoQ status of untreated astrocyte and neuron-enriched cultures

The CoQ $_9$ and CoQ $_{10}$ levels in untreated astrocytes are compared to that of neuron-enriched cultures under identical conditions as shown in figure 7.4A. Neuron-enriched cultures contained similar amounts of CoQ $_9$ but significantly more CoQ $_{10}$ than astrocytes (astrocyte: CoQ $_9$ = 174.2 ± 10.8 pmol/ mg protein; CoQ $_{10}$ = 37.9 ± 1.6 pmol/ mg protein; neuron: CoQ $_9$ = 183.7 ± 13.6 pmol/ mg protein; CoQ $_{10}$ = 67.9 ± 3.9 pmol/ mg protein; Fig 7.4A).

7.5.6. Q status of neuron-enriched cultures following exposure to DETA-NO

Following exposure of neuron-enriched cultures for 24h, DETA-NO (500 μ M) did not significantly alter CoQ $_9$ or CoQ $_{10}$ levels in these cultures (control: CoQ $_9$ = 202.7 ± 31.7 pmol/ mg protein; CoQ $_{10}$ = 70.6 ± 5.9 pmol/ mg protein; DETA-

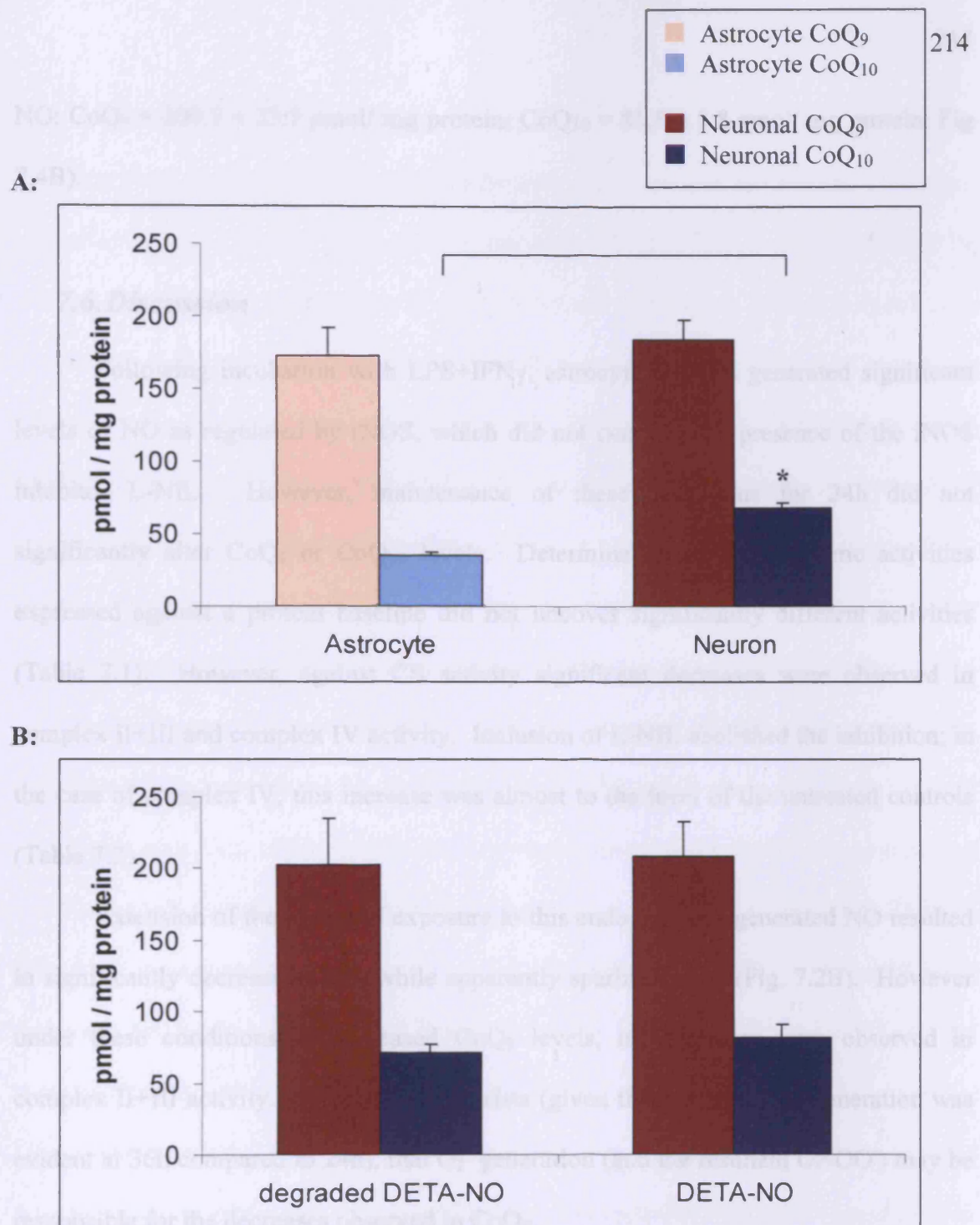


Figure 7.4. CoQ status of rat astrocyte and neuron-enriched rat primary cultures and the effect of DETA-NO.

A: Rat astrocyte and neuron-enriched cultures were incubated for 24h in 6-well culture plates. These are compared to data obtained from identically treated astrocytes. Data are mean \pm SEM values of between eight and twelve independent culture preparations.

(* signifies $p < 0.05$ following analysis by unpaired t -test)

B: Rat neuron-enriched cultures were similarly incubated for 24h with DETA-NO (500 μ M); degraded DETA-NO was added as a control. Data are mean \pm SEM values of between three and six independent culture preparations.

NO: CoQ₉ = 209.7 ± 23.7 pmol/ mg protein; CoQ₁₀ = 81.5 ± 8.8 pmol/ mg protein; Fig 7.4B).

7.6. Discussion

Following incubation with LPS+IFN γ , astrocyte cultures generated significant levels of NO as regulated by iNOS, which did not occur in the presence of the iNOS inhibitor L-NIL. However, maintenance of these conditions for 24h did not significantly alter CoQ₉ or CoQ₁₀ levels. Determination of ETC enzyme activities expressed against a protein baseline did not uncover significantly different activities (Table 7.1). However, against CS activity significant decreases were observed in complex II+III and complex IV activity. Inclusion of L-NIL abolished the inhibition; in the case of complex IV, this increase was almost to the level of the untreated controls (Table 7.2).

Extension of the period of exposure to this endogenously-generated NO resulted in significantly decreased CoQ₉ while apparently sparing CoQ₁₀ (Fig. 7.2B). However under these conditions of decreased CoQ₉ levels, no decreases were observed in complex II+III activity. The possibility exists (given that no more NO generation was evident at 36h compared to 24h), that O₂⁻ generation (and the resultant ONOO⁻) may be responsible for the decreases observed in CoQ₉.

After 36h, iNOS-mediated decreases in complex IV activity were observed against both protein and CS baselines (Tables 7.1 and 7.2). In agreement with previous works (Bolaños *et al.*, 1994, 1995; Stewart *et al.*, 2000) complex I in astrocytes appears relatively resistant to inhibition by RNS. However, Complex IV was significantly inhibited by these conditions.

Inclusion of DETA-NO in the culture media for 24h resulted in slightly higher NO_x levels than those obtained with LPS+IFN γ . Under these conditions, a decrease was observed in CoQ₉ and CoQ₁₀ levels concomitantly (Fig 7.3A). While complex IV activity was similarly decreased with LPS+IFN γ and DETA-NO (Tables 7.3 and 7.4), exogenous NO thus generated did not significantly affect any other ETC enzymes. Other studies (such as those of Gegg *et al.*, 2003) have demonstrated significant inhibition of complex II+III with DETA-NO; it is unclear as to why the data from current study did not achieve a significant decrease with the same concentration of NO donor. However, it is possible that the lack of serum in the culture medium of the current study resulted in slightly lower control values than those previous studies.

The nature of this method of NO generation resulted in higher levels of NO_x at 36h than at 24h incubation. NO generation from DETA-NO was approximately linear up to 36h: after 24h, 128.6 nmol NO_x/ mg were present in the media. Compared to a basal rate of 26.8 nmolNO_x/ mg protein, this would imply that approximately 4.25 nmol NO_x/ mg were generated per hour. After 36h, 189.2 nmolNO_x/ mg protein were present in the media. Thus in the 12h interim period, approximately 60 nmol NO_x/ mg were generated: 5 nmol NO_x / mg protein/ h.

iNOS generated NO at a slightly lower rate: approximately 3 nmol/ mg protein/ h up to 24h. However, after a further 12h, there was apparently no further generation of NO. This gives rise to the possibility of enzymatic recovery of complex II+III activity after 36h incubation with LPS+IFN γ (Table 7.2), and may explain why complex II+III activity did not decrease after 36h as described by Bolaños *et al.*, (1994). Stewart *et al.* (2000) have previously demonstrated (using cocultured neurons) that recovery of complex II+III is possible upon withdrawal of iNOS generating astrocytes.

Subsequently this data shows that recovery may be possible in astrocytes when iNOS activation does not generate NO continuously for prolonged periods of time.

Interestingly, the decreases in CoQ₉ and CoQ₁₀ after 24h exposure to DETA-NO did not occur at the 36h timepoint. Following 36h exposure, greater inhibition of complex IV was evident, although cellular levels of CoQ₉ and CoQ₁₀ were unchanged compared to controls (Fig 7.3B and tables 7.3 and 7.4). While the reasons for this apparent restoration of CoQ₉ and CoQ₁₀ levels is not clear, it may be of note that endogenous NO (i.e. iNOS-derived) did not alter CoQ₉ or CoQ₁₀ status until 36h, whereas exogenous (donor-derived) NO caused an initial decrease, but after 36h levels were unchanged when compared to control. While the mechanisms involved in this are unclear, hypothetically it is possible that NO from the extracellular environment caused an initial decrease, followed by an restoration of CoQ₉ and CoQ₁₀ status, while NO generated from by the cell in question after initial maintenance of CoQ₉ and CoQ₁₀ levels eventually elicited a decrease in these molecules.

With regard to untreated neurons, while similar levels of CoQ₉ were observed in comparison with primary cultures of rat astrocytes, a significantly higher concentration of CoQ₁₀ was found (Fig 7.4A). This may reflect the neuron's greater reliance upon OXPHOS for ATP generation. While astrocytes can upregulate the glycolytic regulatory enzyme enzyme phosphofructo-1-kinase (PFK-1), neurons do not seem to be capable of this (Almeida *et al.*, 2004). These authors found that inhibition of the ETC by NO resulted in increased glycolytic flux in astrocytes but not in neurons (Bolaños *et al.*, 1994; Almeida *et al.*, 2004). Thus the lower levels of CoQ₁₀ in astrocytes may be as a result of these cells' ability to generate ATP anaerobically. Conversely, neurons may contain higher levels of CoQ₁₀ as it is possible that the higher molecular mass isoform is more intimately involved in OXPHOS. This has been proposed by a number of groups:

Matsura *et al.* (1991), using rabbit hepatocytes found CoQ₉ to be primarily an extramitochondrial antioxidant, and proposed CoQ₁₀ to be a mitochondrial antioxidant and electron carrier. Lass *et al.* (1997) found O₂⁻ generation of sub-mitochondrial particles derived from a number of mammalian species correlated with CoQ₉ levels, and inversely with CoQ₁₀ content. The findings of Battino *et al.* (2001) using rat brain mitochondria also supported a bioenergetic role for CoQ₁₀ and antioxidant role for CoQ₉ from mitochondria which may have been older, and thus subjected to greater oxidative stress.

The neuronal response to exogenous NO was different to that of the astrocyte: following 24h exposure, astrocytic CoQ₉ and CoQ₁₀ were both decreased. However neurons maintained under the same conditions did not alter their CoQ status. The neurobiological significance of this finding is not yet clear. However in the context of antioxidant availability of astrocytes and neurons, when cultured alone, astrocytes have approximately double the amount of neuronal GSH (Bolaños *et al.*, 1995), this work shows that CoQ₁₀ levels in neurons are almost double that of astrocytes. While NO exposure increases astrocytic GSH content (Gegg *et al.*, 2003), CoQ₉ and CoQ₁₀ status appears to be compromised. Neuronal GSH decreases in response to NO, while neuronal CoQ₉ and CoQ₁₀ is maintained.

The data referring to the astrocytic ETC would suggest that CoQ₉ status may not be the most NO-susceptible factor in dictating complex II+III activity; electron transport between these complexes was not diminished as measured by the linked enzyme assay.

NO-mediated decreases in CoQ₉ or CoQ₁₀ did not correlate with decreased complex II+III activity; thus *in vitro* activity of this linked system may be sufficiently robust to be maintained despite lower availability of the major CoQ homologue.

7.7. Conclusion

Two systems were used to generate NO in cultures of rat astrocytes: LPS+IFN γ induced iNOS expression while DETA-NO liberated similar levels of NO as measured by NO $_x$ levels in culture media. Following 36h exposure to LPS+IFN γ , astrocyte levels of CoQ $_9$ (but not CoQ $_{10}$) were significantly lower; this effect was abolished by the use of L-NIL. Thus activation of iNOS was seen to decrease the CoQ status of astrocytes. Following 24h exposure to DETA-NO, both CoQ $_9$ and CoQ $_{10}$ were decreased. However, this decrease appears transient as after 36h both CoQ $_9$ and CoQ $_{10}$ status had returned close to control levels, possibly reflecting an upregulation in response to prolonged NO generation.

The decreases observed in CoQ status did not correlate with inhibition of the activity of complex II+III of the ETC. In one case, a significant decrease was observed in complex II+III activity; however under these conditions no changes in cellular CoQ status were recorded. NO derived from both endogenous and exogenous sources appeared to inhibit only complex IV against both protein and CS baselines.

Neuron-enriched cultures were also examined and exposed to DETA-NO. Determination of the CoQ status of these untreated cultures showed substantially greater amounts of CoQ $_{10}$ in neurons compared to astrocytes. Whether this reflects the reliance of neurons upon OXPHOS to maintain ATP or a possible antioxidant defence is unclear. Whereas astrocytic CoQ $_9$ and CoQ $_{10}$ status was compromised following 24h exposure to DETA-NO, neuronal levels of CoQ $_9$ and CoQ $_{10}$ under these conditions were maintained.

8. THE USE OF SHORT INTERFERING RNA TO ALTER UBIQUINONE BIOSYNTHESIS IN RAT AND HUMAN CELLS

8. THE USE OF SHORT INTERFERING RNA (siRNA) TO ALTER UBIQUINONE BIOSYNTHESIS IN RAT AND HUMAN CELLS

8.1. Introduction

RNA interference (RNAi) is a relatively recently described technique with the potential to downregulate specific gene products. It was first recognised by Fire *et al.* (1998) using *C. elegans*, that microinjection of these nematodes with double-stranded RNA (dsRNA) (but not sense or antisense injections separately) caused potent and specific knockdown of gene products. This inhibition was also carried over to the F₁ progeny. Other organisms have also been used to demonstrate effective gene silencing using ds-RNA including plants (Waterhouse *et al.*, 1998), trypanosomes (Ngo *et al.*, 1998), drosophila (Kennerdell & Carthew, 2000), fish (Wargelius *et al.*, 1999) and mice (Wianny & Zernicka-Goetz, 2000). In addition, subsequent modification of the technique now means that mammalian cell culture models are also amenable to RNA-mediated interference; this has been shown in a number of cell types including human MCF-7 cells (Brummelkamp *et al.*, 2002), human embryonic kidney and HeLa cells (Elbashir *et al.*, 2001), and recently in primary cultures such as rat astrocytes (Nicchia *et al.*, 2003).

RNA interference (RNAi) uses dsRNA homologous to the sequence of a specific gene to downregulate production of mRNA and thus the final gene product (Fire, *et al.* 1998; Elbashir *et al.* 2001). Fire *et al.* (1998) microinjected ds-RNA of length 299 to 1033 nucleotides (nt), to down-regulate a number of gene products. However, in mammalian cells, it had been noted that the introduction of ds-RNA of size greater than approximately 30-nt evoked a strong cytotoxic response and induction of interferon synthesis (Hunter *et*

al. 1975, Stark *et al.* 1998). This apparent stumbling block was eliminated by the finding by Elbashir *et al.* (2001), using 21-22-nt sequences in mammalian cells, that the cytotoxic response could be circumvented with shorter sections of RNA. Although this "short interfering RNA" (siRNA) successfully mediated strong and specific gene suppression, the effects were relatively short-lived: clearance and/ or degradation of siRNAs meant that inhibition of the endogenous mRNA was transient. However, the discovery of a number of novel vector systems around the same time has allowed stable transfection of siRNAs into mammalian cells (Paul *et al.*, 2002; Brummelkamp *et al.*, 2002; Sui *et al.*, 2002; Lee *et al.*, 2002; Miyagishi & Taira, 2002). Of these, the pSUPER vector system can show loss-of-function phenotypes up to 2 months post-transfection (Brummelkamp *et al.*, 2002). pSUPER is a mammalian expression vector able to direct siRNA synthesis in viable cells (Fig 8.1). An inserted sequence is specific for the target gene of interest and is preceded by the H1-RNA gene promoter and terminated by a following sequence of five thymidines (5T). The polymerase III H1-RNA promoter produces an RNA transcript without a polyadenosine tail, and with a 2 uridine (2U) 3' overhang (Brummelkamp *et al.*, 2002).

The ds insert is of 64-nt (Fig 8.2A), such that the predicted 49-nt transcript of RNA folds back on itself in a hairpin-like loop: a 19nt section (derived from the target transcript) is followed by a 9-nt "spacer" which is followed in turn by the antiparallel complement of the same sequence (Fig 8.2B). This "hairpin" structure is then believed to be rapidly cleaved by the Dicer enzyme (an RNase III) to form functional siRNAs (Fig 8.2C). This latter finding comes from the fact that Dicer-suppressed cells do not undergo hairpin-mediated silencing (Paddison *et al.*, 2002).

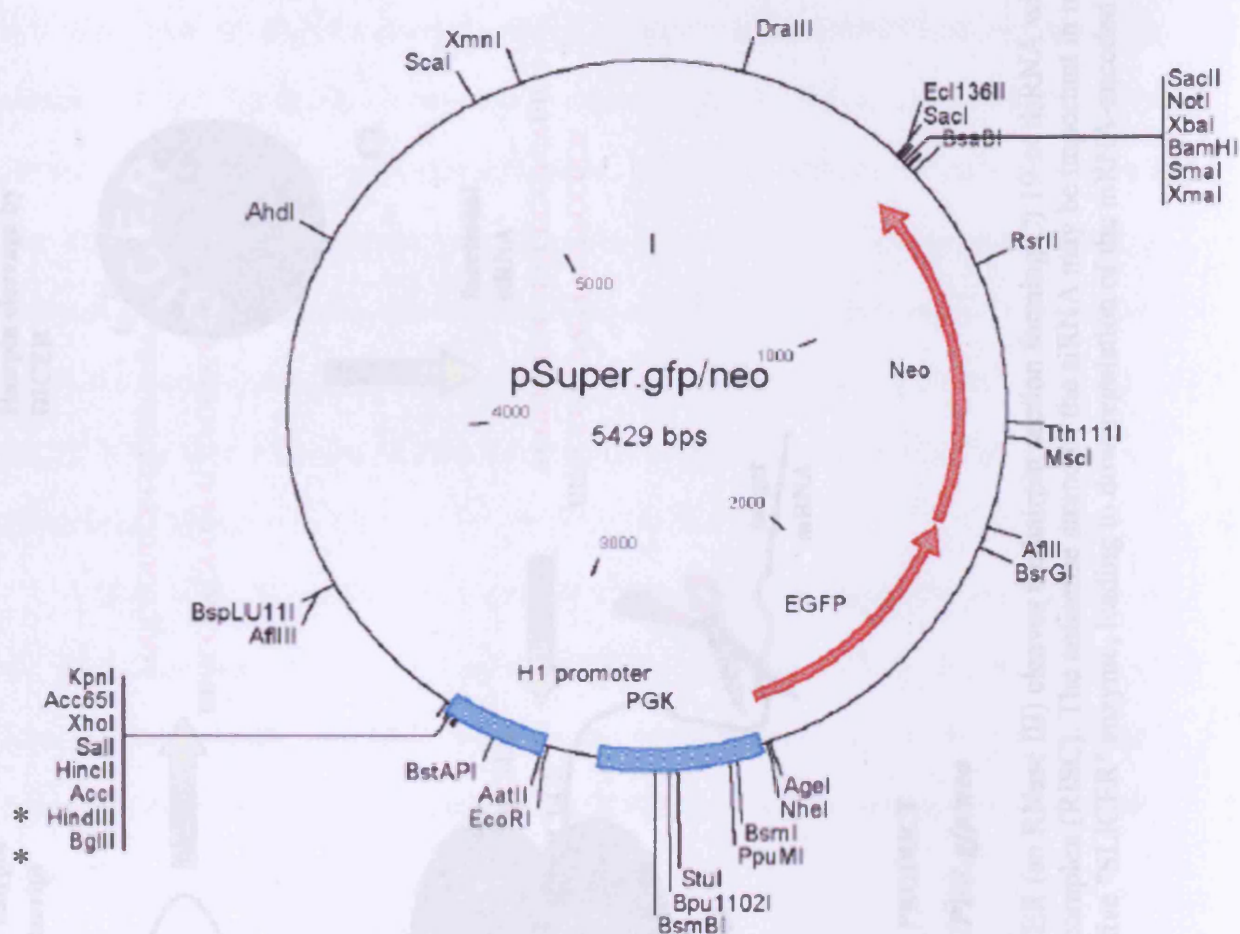


Figure 8.1. Schematic diagram of the pSUPER.gfp/neo vector.

Bgl II and Hind III site are marked with asterisks, and are used for the cloning of 64-nt inserts as described in the text. This diagram was adapted from the manufacturer's instructions for the vector, available at http://www.oligoengine.com/pSUPER_New/pSUPERdocs/Maps/Maps_PDF/pSUPERneoGFP_Map.pdf

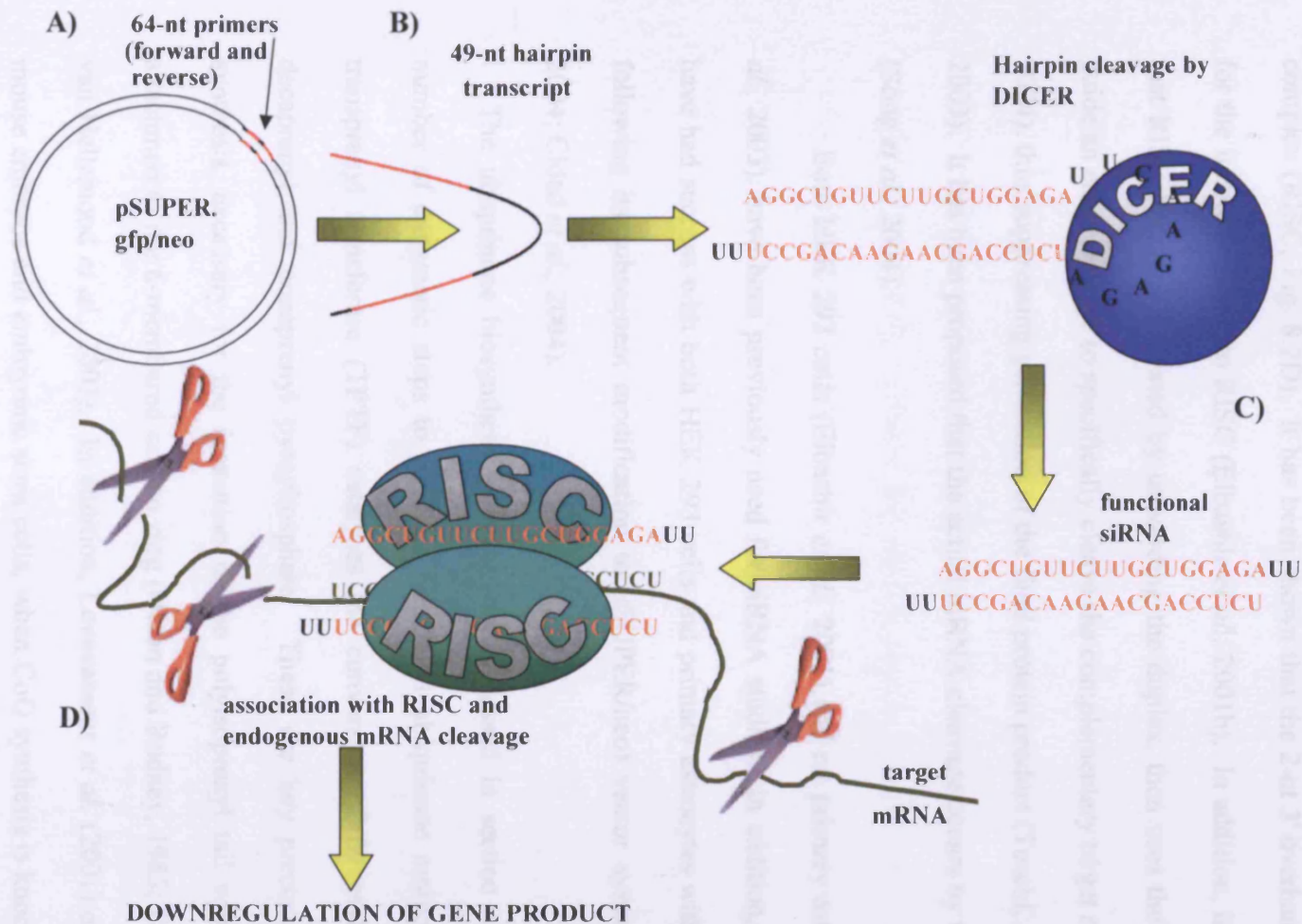


Figure 8.2. Schematic diagram of siRNA mechanism with pSUPER.gfp/neo

A) dsDNA primers generate B) ssRNA with UU at one end. DICER (an RNase III) cleaves the hairpin section forming C) 19-nt dsRNA with UU overhangs. D) This associates with the RNA-induced silencing complex (RISC). The antisense strand of the siRNA may be important in mRNA target selection by RISC. Subsequently, mRNA is cleaved by the putative "SLICER" enzyme, leading to downregulation of the mRNA-encoded product.

While the exact mechanism of action of siRNA has not been completely elucidated, it is likely that the siRNAs assemble with a putatively identified RNA-induced silencing complex (RISC; Fig. 8.2D). It has been shown that the 2-nt 3' overhangs are important in for the incorporation into RISC (Elbashir *et al.*, 2001b). In addition, it has been proposed that RISC becomes activated by unwinding the duplex, then uses the antisense strand to guide an endonuclease to specifically cleave the complementary target mRNA (Jones *et al.*, 2004), thus suppressing generation of the final protein product (Tuschl, 2002; Kurrek *et al.*, 2003). It has been proposed that the actual mRNA cleavage occurs by the "Slicer" enzyme (Song *et al.*, 2004).

Both HEK 293 cells (Elbashir *et al.*, 2001) and rat primary astrocytes (Nicchia *et al.*, 2003). have been previously used for siRNA studies. In addition, the Bolaños group have had success with both HEK 293 cells and primary astrocytes with the pSUPER (and following its subsequent modification to pSUPER/neo) vector system (Almeida *et al.*, 2004; Ciudad *et al.*, 2004).

The ubiquinone biosynthetic pathway (as discussed in section 1.4.2) relies upon a number of enzymatic steps to generate functional ubiquinone molecules. The enzyme transprenyl transferase (TPTF) catalyses the conversion of farnesyl pyrophosphate to decaprenyl and nonaprenyl pyrophosphate. These are key precursors for ubiquinone synthesis, necessary for the formation of the polyisoprenyl tail which is subsequently attached to the 6-membered carbon ring (Olson and Rudney, 1983; Turunen *et al.*, 2002; van Hellemond *et al.*, 2003). In addition, Levavasseur *et al.* (2001) demonstrated that in mouse embryos and embryonic stem cells, when CoQ synthesis is knocked out at the level of 3-methoxy-6-methyl-5-nonaprenyl-benzoquinone-hydroxylase (clk-1; the penultimate

biosynthetic enzyme) cells instead accumulate the intermediate demethoxyubiquinone (DMQ). This latter study targeted the *CLK-1* gene, which encodes a highly conserved mitochondrial protein required for CoQ synthesis, possibly a hydrolase converting DMQ into 5-hydroxy-ubiquinone (Stenmark *et al.*, 2001). However, although it was noted that these cells accumulated DMQ in the same quantities as CoQ and are deficient in CoQ, the activities of complex II+III were only modestly lower. Thus, it was concluded that although DMQ is not as efficient as CoQ as an electron carrier in the ETC, the mitochondria of such cells could still function (Levavasseur *et al.*, 2001). Thus when considering an enzyme suitable for siRNA downregulation, TPTF would exclude the possibility of "ubiquinone precursors" acting as substitute electron carriers, as was noted by Levavasseur *et al.*, (2001).

8.2.Aims

- To attempt transfection of both the HEK293T Human Embryonic Kidney cell line (Graham, *et al.*, 1977; DuBridge *et al.*, 1987) and astrocyte primary cultures with the pSUPER.gfp/neo vector with a 64-nt insert predicted to inhibit synthesis of TPTF.
- To probe any decrease in cellular levels of TPTF mRNA.
- To measure CoQ levels in such cultures directly by HPLC
- To measure the activity of mitochondrial ETC enzymes in these cultures.

8.3.Methods

All work except that described in sections 8.3.9 and 8.3.10 was carried out in the laboratory of Dr. Juan Bolaños, Universidad de Salamanca, Spain

8.3.1. Tissue Culture

Rat primary cortical astrocyte cultures were prepared as described previously in section 2.2.3. In addition, a Human Embryonic Kidney cell line (HEK293T; DuBridge *et al.*, 1987) was used in some experiments. This well characterised cell line has been used previously for siRNA studies (Elbashir *et al.*, 2001; Williams *et al.*, 2004) and is well known to accept transfection using lipophilic cations (Sandor *et al.*, 2002). These cells were grown in Dulbecco's Modified Eagle Media (DMEM; 4500mg glucose/l) supplemented with 10% (v/v) FBS, 2mM L-Glutamine and 1% (v/v) antibiotic/antimycotic.

Both the rat primary cultures and the human cell line were plated onto large (60cm²) Petri dishes, previously coated with poly-D-lysine as described in section 2.2.3. The seeding density in the plate was calculated as 1.5x10⁵ cells/cm² (primary astrocytes) or 1x10⁵ cells/cm² (HEK 293T).

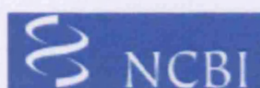
8.3.2. Small interfering RNA oligonucleotide design

In order to effect efficient gene silencing, it is necessary to determine first the mRNA sequence of the gene-product of interest, and then design a pair of 64 nucleotide (-nt) "forward" and "reverse" oligonucleotide "primers" each containing a unique and complementary 19-nt sequence which will form double stranded (ds) RNA. The primers are derived from a sequence of the target transcript. Currently, the mRNA sequence of the biosynthetic enzyme TPTF is known in the human and the mouse. These sequences are

available on the National Center for Biotechnology Information (NCBI) BLAST search engine and databases (<http://www.ncbi.nlm.nih.gov/BLAST/>), and have been assigned the NCBI gene identifier (gi) numbers: gi31980944 and gi11863164 for the mouse and human sequences respectively. The "NCBI Blast 2 sequences" facility is available at <http://www.ncbi.nlm.nih.gov/blast/bl2seq/bl2.html> and allows the user to align locally 2 given sequences (Tatusova, & Madden 1999); in this case mouse and human TPTF. A truncated screenshot from the Blast 2 website showing sequence homology of 88% between the mouse and human TPTF variants is shown in figure 8.3. The major homological sequence of the mouse and human mRNA for the gene product is shown in figure 8.4. As conservation of the sequence is high between mouse and human, it is likely also to be very similar to the TPTF sequence in the rat.

Selection of target sequences will be most likely to give strong knockdown of the gene product if a number of guidelines are followed:

- 1) The 19nt target sequence should be flanked with AA at the 5' end preferably with TT at the 3'.
- 2) The 19nt sequence should be at least 100bp from either the start or the termination of translation.
- 3) The bases guanine and cytosine (G and C respectively) should account for a minimum of 30% to 50% of the targeting sequence. This determines the annealing temperature of the 2 primers. Ideally, the annealing temperature of both primers should be similar.



Blast 2 Sequences results

PubMed

Entrez

BLAST

OMIM

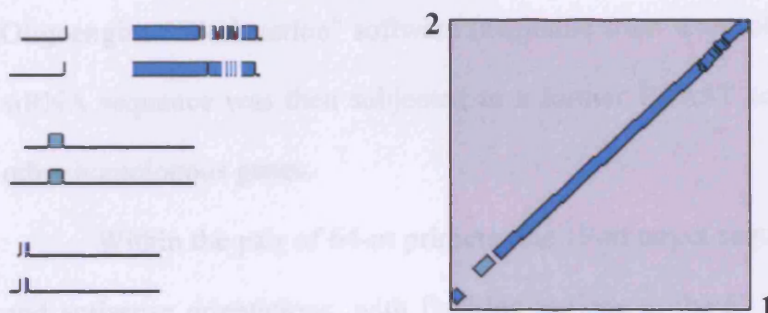
Taxonomy

Structure

BLAST 2 SEQUENCES RESULTS VERSION BLASTN 2.2.9 [May-01-2004]

Sequence gi Mus musculus trans-prenyltransferase (Tprt), Length 1552
1 [31980944](#) mRNA

Sequence gi Homo sapiens trans-prenyltransferase (TPRT), Length 1630
2 [11863164](#) mRNA



88% homology

Identities = 1158/1313 (88%), Gaps = 27/1313 (2%)

forward primer:

5' GATCCCG...TTCAGGAGA

reverse primer:

Figure 8.3. A truncated screenshot of the NCBI "Blast 2 sequences" local alignment tool

This screen shows 88% homology between the mouse (termed sequence "1") and human (sequence "2") transprenyl transferase mRNA. This sequence was used to design 19-nt sections of the forward and reverse 64-nt pSUPER primers used for the siRNA experiments, and additionally to determine the sequence of primers used later in RT-PCR.

4) When using the pSUPER vector system, it is vital that the 19-nt selection does not contain four or more adenines (AAAA) or thymines (TTTT) as this will give premature termination of the transcript.

As highlighted in orange in figure 8.4, a section of the sequence corresponding to bases 601-619 of the mouse and 661-679 of the human sequence was selected as the target by Dr. Juan Bolaños using "*Oligo 4.0*" (National Biosciences, Plymouth, MN) and Oligoengine "Workstation" software (available from www.oligoengine.com). The selected siRNA sequence was then subjected to a further BLAST search to avoid the targeting of other homologous genes.

Within the pair of 64-nt primers, the 19-nt target sequence appears in both the sense and antisense orientations, with flanking regions at the 5'- and 3'- ends. A 9-nt "spacer" sequence must also be included between the sense and antisense 19-nt specific target regions which forms the hairpin loop of the pre-siRNA molecule. When using pSUPER, the ends of the primer and the spacer section must have the sequence as follows:

forward primer:

5' GATCCCC-[sense target sequence]-TTCAAGAGA-[antisense target sequence]-TTTTTGAAA 3'

reverse primer:

3' GGG-[antisense target sequence]-AAGTTCTCT-[sense target sequence]-AAAACCTTTTCGA 5'

Having chosen a target sequence, flanking regions and the spacer were added (Fig 8.5), and the primers synthesised by Isogen Life Science (Maarssen, The Netherlands).

247 aaactcagagtgggtgagaaatacagtgatccttttaaacttggctggagagacttgaaag 306
||||| || | ||||| ||||| ||||| ||||| ||||| ||||| ||||| |||||
307 aaacacacagtggtgagaaatacaccgatcctttcaaactcggttggagagacttgaaag 366
46 K T H S G E K Y T D P F K L G W R D L K

307 gtctgtatgaagacattagaaaggagctgcacatctccaccagagaactaaaggacatgt 366
| | | | | | | | | | | | | | | | | | | | | | | |
367 gtctgtatgagggtattagaaagggaacccctcatatcaacaacagaacttaaggaaatct 426
66 G L Y E G I R K E P L I S T T E L K E I

367 ccgaataactacttcgatggcaaaggaaaagccttttagaccgattattgttggtgctaattgg 426
| | | | | | | | | | | | | | | | | | | | | |
427 ctgagtactactttgatgtaaaaggaaaagccttttagaccgattattgttggtgctaattgg 486
86 S E Y Y F D V K G K A F R P I I V V L M

427 cccgagcgtgtaatatcatcataataatgcccgagagatgcaagccagccagcgctcca 486
|||||
487 cccgagcatgcaatatcatcataacaactcccgacatgtgcaagccagccagcgcgcca 546
106 A R A C N I H H N N S R H V Q A S Q R A

487 tagccttagttgcagaaatgatccacactgctactctggttcacgatgacgttattgatg 546
|||
547 tagccttaattgcagaaatgatccacactgctagtctggttcacgatgacgttattgacg 606
126 I A L I A E M I H T A S L V H D D V I D

547 atgcaagttctcgaagaggaaaacatacagttaataaaatctggggtgagaaaaaggctg 606
 |||||
 607 atgcaagttctcgaagaggaaaacacacagttaataagatctggggtgaaaagaaggctg 666
 146 D A S S R R G K H T V N K I W G E K K A

607 **ttcttgctggaga** atttaattc ttttctgcagcgctctgtagctctggcacggattggaaaca 666
| | | | | | | | | | | | | | | | | | | | | | | | | | | |
667 **ttcttgctggaga** atttaattc ttttctgcagcatctatagctctggcacgaattggaaata 726
166V L A G D L I L S A A S I A L A R I G N

667 cagctgttgatatctatgtagcccaagtattgaagatttggcggtggaatttcctc 726
|| ||| ||| ||| ||| ||| ||| ||| ||| ||| ||| ||| ||| ||| ||| |||
727 caactgttatatctattttaaccaagtattgaagatttggcggtggaatttcctc 786
186 T T V I S I L T Q V I E D L V R G E F L

727 agctaggggtcaaaagaaaatgagaatgaaaggtttgcactaccttgagaagaccttca 786
||| ||| ||| ||| ||| ||| ||| ||| ||| ||| ||| ||| ||| ||| ||| ||| |||
787 agctcgggtcaaaagaaaatgagaatgaaagatttgcacactaccttgagaagacattca 846
206 Q L G S K E N E N E R F A H Y L E K T F

787 agaagacagccagcctgatagccaacagtgtgtaaagcagtcctctgtcctgggttgccctg 846
 |||||
847 agaagaccgccagcctgatagccaacagtgtgtaaagcagtcctctgttctaggatgtccccg 906
226 K K T A S L I A N S C K A V S V L G C P


```

847  acccagtgggtgcatgagatagcctatcagtatgggaaaaatggtggaatagcttttcagc 906
      |||||||
907  acccagtgggtgcatgagatgcctatcagtacggaaaaaatgtaggaatagcttttcagc 966
246  D P V V H E I A Y Q Y G K N V G I A F Q

907  tcatagatgatgtattggatttcacctcatgttctgaccagatgggcaagccaacatctg 966
      | |||||||
967  taatagatgatgtattggacttcacctcgtgttctgaccagatgggcaaaccaacatcag 1026
266  L I D D V L D F T S C S D Q M G K P T S

967  cagacctgaagctaggcatagccactggcctgtcttgtttgcttgccagcagttccag 1026
      | || |||||
1027  ctgatctgaagctcgggttagccactggcctgtcctgtttgcctgtcagcagttccag 1086
286  A D L K L G L A T G P V L F A C Q Q F P

1027  aaatgaatgctatgataatgagacgggttcagtttgccaggagatgtggacagagcacgac 1086
      |||||||
1087  aaatgaatgctatgatcatgcgacgggttcagtttgccctggagatgtagacagagctcgac 1146
306  E M N A M I M R R F S L P G D V D R A R

1087  agtatgtattacagagtgatggcgtgcagcaaacacctacctcgcccagcagtactgcc 1146
      |||||||
1147  agtatgtactacagagtgatggtgtgcaacaaacacctacctcgcccagcagtactgcc 1206
326  Q Y V L Q S D G V Q Q T T Y L A Q Q Y C

1147  acaaagctgtgagagagatcaggaagcttagaccatctacagaaagggacgcctcattc 1206
      | |||||
1207  atgaagcaataagagagatcagtaaacttcgaccatccccagaaagagatgcctcattc 1266
46  H E A I R E I S K L R P S P E R D A L I

1207  agctttcagaaagtgtgctcaccagagataaatgacaattcctcctcttctttctggcag 1266
      |||||
1267  agctttcagaaattgtactcacaagagataaatgacaactctttctgttctttctggcag 1326
366  Q L S E I V L T R D K ^^^

1267  ctattttaccagactgtgcctaataga-ttttgtgaaacac----tatttgcttcatgtgc 1321
      |||||
1327  ctatcttaccagactgtgcctaaagaattttgtggaatacactttgtttgcttcatgtgc 1386

1322  agaaaacaaaaatcattttaagaaataatttcaaccttattgatgggcaattt----- 1375
      |||
1387  agataacaaaaatcattttaaaagata---tcaaacttattgatgggcaatttattttt 1443

1376  --ttattggcaaag-tttttcggaaaactttttaaatgtaatt---aaaccag----- 1422
      |||||
1444  ttttattgcaaaaggtttttcagaaaactttttaaatgtaattaataaaccacctgaatc 1503

1423  tgtcattatagtcctataaattctaatacgaggtatcctgatgggttatatgtggtattgtt 1482
      |||||
1504  tgtcattctagtcctataaattataatcaaggtatcttgatgggttatatgtggtattgtt 1563

```

```

1483 tacactgttaatgccacatgtaaagccattacacaaataaataatcaacggtt 1535
      ||||| ||||| ||||| ||||| ||||| ||||| ||||| ||||| |||||
1564 tacactgttaatatccacatgtaaggccattacacaaataaataaccaatggtt 1616

```

```

      (mouse 5' direction)                                (collective orientation)
5'-GATCTCCAAAGCTTCTTCTCGACATTCAAGAGATTTCTCAGCAAGAACT-3'
  AGCTTTTCTTCAAAA-3'

```

Figure 8.4. The major homological sequence between mouse and human transprenyl transferase mRNA

The mouse sequence is shown in blue, the human sequence in green, and the amino acid sequence in black. The 19-nt sequence used to design the pSUPER primers is shown in orange between 601-619 (mouse) and 661-679 (human)

```

      (mouse 5' direction)                                (collective orientation)
5'-AGCTTTTCCAAAAAGAGCTTCTGCTCGACATTCTCTTCAATTTCTCAGCA-3'
  AA-AACAGCTTGG-3'

```

Figure 8.4 shows the major homological sequence between mouse and human transprenyl transferase mRNA. The mouse sequence is shown in blue, the human sequence in green, and the amino acid sequence in black. The 19-nt sequence used to design the pSUPER primers is shown in orange between 601-619 (mouse) and 661-679 (human).

Figure 8.5 shows the forward and reverse sequence of the 64-nt primers inserted into the pSUPER.gfp/neo vector system.

The primers were annealed and phosphorylated prior to insertion to form dsDNA as shown.

Figure 8.5 shows the forward and reverse sequence of the 64-nt primers inserted into the pSUPER.gfp/neo vector system.

The primers were annealed and phosphorylated prior to insertion to form dsDNA as shown.

Figure 8.5 shows the forward and reverse sequence of the 64-nt primers inserted into the pSUPER.gfp/neo vector system.

The primers were annealed and phosphorylated prior to insertion to form dsDNA as shown.

Figure 8.5 shows the forward and reverse sequence of the 64-nt primers inserted into the pSUPER.gfp/neo vector system.

The primers were annealed and phosphorylated prior to insertion to form dsDNA as shown.

Figure 8.5 shows the forward and reverse sequence of the 64-nt primers inserted into the pSUPER.gfp/neo vector system.

The primers were annealed and phosphorylated prior to insertion to form dsDNA as shown.

Figure 8.5 shows the forward and reverse sequence of the 64-nt primers inserted into the pSUPER.gfp/neo vector system.

The primers were annealed and phosphorylated prior to insertion to form dsDNA as shown.

Figure 8.5 shows the forward and reverse sequence of the 64-nt primers inserted into the pSUPER.gfp/neo vector system.

The primers were annealed and phosphorylated prior to insertion to form dsDNA as shown.

Figure 8.5 shows the forward and reverse sequence of the 64-nt primers inserted into the pSUPER.gfp/neo vector system.

The primers were annealed and phosphorylated prior to insertion to form dsDNA as shown.

Figure 8.5 shows the forward and reverse sequence of the 64-nt primers inserted into the pSUPER.gfp/neo vector system.

The primers were annealed and phosphorylated prior to insertion to form dsDNA as shown.

Figure 8.5 shows the forward and reverse sequence of the 64-nt primers inserted into the pSUPER.gfp/neo vector system.

The primers were annealed and phosphorylated prior to insertion to form dsDNA as shown.

Forward primer sequence:

(sense orientation) (antisense orientation)

5'-GATCCCC**AGGCTGTTCTTGCTGGAGATTCAAGAGATCTCCAGCAAGAAC**
AGCCTTTTTTGGAAA -3'

Reverse primer sequence:

(sense orientation) (antisense orientation)

5'-AGCTTTTCCAAAA**AGGCTGTTCTTGCTGGAGATCTCTTGAA****TCTCCAGC**
AAGAACAGCCTGGG -3'

Annealed and phosphorylated oligonucleotide primers ready for insertion into pSUPER

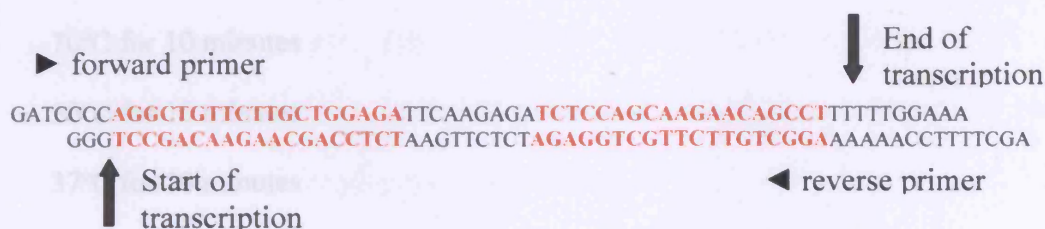


Figure 8.5. The forward and reverse sequence of the 64-nt primers inserted into the pSUPER.gfp/neo vector system.

The primers were annealed and phosphorylated prior to insertion, to form dsDNA as shown.

8.3.3. Ligation of oligonucleotides into pSuper.gfp/neo, and transformation in bacteria

8.3.3.1. Annealing of primers

Unless otherwise stated, all water used is nucleotide and nuclease free. This was accomplished by the addition of the histidine-specific alkylating agent diethyl pyrocarbonate (DEPC; 0.1%, v/v) followed by autoclaving. The two 64-nt primers were supplied separately in a lyophilised and dephosphorylated state to ensure the single stranded DNA was linear. Before insertion of the primer into pSUPER.gfp/neo, the 64-nt primers were first annealed to form double-stranded (ds)DNA and then phosphorylated to aid entry to the dephosphorylated vector.

1 µg of each primer was added to 48 µl of annealing buffer (10x; 100mM NaCl, 50 mM HEPES; pH 7.4). To anneal the 2 single strands, it was necessary to rapidly bring the mixture up to 100°C for 4 minutes, and then reduce it in a controlled, step-wise manner as follows:

70°C for 10 minutes

50°C for 10 minutes

37°C for 10 minutes

20°C for 5 minutes, then cool in ice, and the dsDNA can be stored at -20°C.

8.3.3.2. Phosphorylation of primers

Phosphorylation of the dsDNA used the polynucleotide kinase (PNK; Promega, Charbonnières, France):

2µl of the ds primers were added to 1µl T4 PNK buffer (10x; 0.5M Tris-HCl; 100mM MgCl₂, 100mM 2-mercaptoethanol, pH 7.4; Promega, Charbonnieres, France), 1 µl PNK (10 u/ml; Promega, Charbonnieres, France), ATP (1mM) is necessary as a cofactor. The total volume was made up to 10µl with water.

This mixture was incubated at 37°C for 30mins, to allow the reaction to proceed. It was then heated to 70°C for 10 mins to inactivate PNK.

8.3.3.3. Linearisation of pSUPER.gfp/neo, and purification in agarose gel

Linearisation of the pSUPER.gfp/neo vector was achieved using with Hind III and Bgl II restriction enzymes and CIP (Calf Interstitial Alkaline Phosphatase; Promega, Charbonnieres, France). 2.2 µg of pSUPER.gfp/neo was added to 1µl Hind III (Promega, Charbonnieres, France), 3µl buffer B (10x; 100mM Tris-HCl, 100mM MgCl₂, 1 mg/ ml BSA, pH 7.5; Promega, Charbonnieres, France) and 23µl of water. After incubation for 1h at 37°C, 1µl Bgl II was added, and the reaction allowed to proceed for a further 2h at 37°C. The restriction enzymes were then inactivated by incubation at 70°C for 20 min. Dephosphorylation of the vector used CIP to remove the phosphate groups from both 5' ends of the DNA, hence preventing recircularisation.

To this end, 30 µl of digestion product was added to 4 µl alkaline phosphatase reaction buffer (10x; 500 mM Tris-HCl; 10 mM MgCl₂, 1 mM ZnCl₂, 10 mM spermidine; Promega, Charbonnieres, France), 4µl CIP (0.1u/ µl) and 2µl water. The reaction was incubated at 37°C for 15mins, and CIP inactivated by incubation at 70°C for 10mins.

The plasmid was then run in a 1% agarose gel to check the size of the fragment size (5429bp), remove the fragment between Bgl II and Hind III, and to separate any undigested

circular plasmid. The band was cut from the gel, and purified using the Matrix Gel Extraction System (Marligen, Ijamsville, USA) according to the manufacturer's instructions. 350 mg of gel was dissolved in 30 μ l Gel Solubilisation Buffer (a proprietary solution containing concentrated sodium perchlorate, sodium acetate and solubiliser). 35 μ l silica resin was added, and the mixture incubated at 50°C for 20 min and vortexed regularly to ensure gel dissolution. DNA bound to the Silica resin was isolated by centrifugation at 12,000 x g for 30s. Supernatant was discarded, and the resin pellet washed with 100 μ l of Gel Solubilisation Buffer before the mixture was centrifuged at 12,000 x g and the supernatant discarded. The resin pellet was then twice resuspended in Wash Buffer (a proprietary solution containing NaCl, EDTA and Tris-HCl in ethanol), centrifuged and the supernatant discarded. The resin was then dried and DNA eluted from the resin by resuspension in 20 μ l TE buffer (10 mM Tris-HCl, 0.1 mM EDTA, pH 8.0). This was incubated at 50°C for 5 min and centrifuged at 12,000 x g for 30s. The pSUPER.gfp/neo DNA-containing supernatant was transferred to a fresh tube and stored at -20°C.

8.3.3.4. Ligation of the primers into pSUPER.gfp/neo, transformation in bacteria and plasmid extraction

Ligation of the phosphorylated dsDNA into the pSUPER.gfp/neo vector required DNA ligase (MBI Fermentas GmbH, St. Leon-Rot, Germany). 2 μ l of the annealed phosphorylated primers were added to 1 μ l T4 DNA ligase (1 Weiss unit/ μ l; 200 cohesive end ligation units/ μ l; MBI Fermentas, St Leon-Rot, Germany) and 1 μ l of ligase buffer (10x; 660 mM Tris, 50 mM magnesium chloride, 10 mM dithiothreitol, 10 mM ATP; pH

7.5; MBI Fermentas, St Leon-Rot, Germany). 1 µl of pSUPER.gfp/neo (digested with Bgl II and Hind III, and CIP-treated) was added, and the mixture incubated overnight at 16°C.

The pSUPER.gfp/neo both with and without the TPTF primer insert was then transformed in *E. coli* DH5α bacteria. 10 µl of each plasmid (pSUPER.gfp/neo and pSUPER.gfp/neo+TPTF; between 1 and 10 ng/ µl) were incubated separately with 100 µl competent bacteria. This was done on ice, and mixed gently for 30mins, whereupon the tubes were transferred to a 42°C waterbath for exactly 45s. They were then returned to ice for at least 2mins.

100 µl SOB media (20g/L Bactotryptone, 5g/L yeast extract, 10mM NaCl, 2.5 mM KCl, 10mM MgCl₂, 10mM MgSO₄ 20mM glucose) was added to each tube, and the mixture incubated while shaking for 1h at 37°C. Between 50 and 100 µl was added to each LB agar plate and colonies grown overnight in LB agar plates (10g/L bactotryptone, 5g/L yeast extract, 250 mM NaCl; 15g/L agar; pH 7.5). Ampicillin was added at 0.05g/L; resistance was conferred only to the transfected bacteria. The transformation of the bacteria was confirmed by re-seeding the colonies with 2XYT media overnight.

The GenElute Plasmid Miniprep kit (Sigma-Aldrich Quimica SA, Madrid, Spain) was used to isolate the plasmid DNA from the bacterial cultures. Bacterial cells were harvested via centrifugation (5000 x g), and then alkaline lysed. When loaded onto the supplied column, the DNA becomes bound to silica. The column was washed to remove contaminants and the purified DNA was eluted in water. Digestion with Eco RI and Hind III was used to confirm insertion of the primers into the vector (the Bgl II site of pSUPER.gfp/neo is lost following insertion of the 64-nt insert) prior to electrophoresis in an agarose gel (1%). This

effectively allowed visualisation of the insert: following digestion the empty vector has a size of around 240 bp. With the insert, this is increased to approximately 300 bp.

Plasmid extraction was effected using the Promega "Wizard *Plus* Midipreps" Kit (Promega, Charbonnieres, France) in accordance with the manufacturer's instructions. In summary, the following steps were followed. Initially, the vector-containing bacteria were centrifuged to form a pellet. Then, following resuspension in 3ml "Cell Resuspension Solution", 3ml "Cell Lysis Solution" is used in alkaline lysis of the cells. A further 3ml of "Neutralisation Solution" was added, the mixture centrifuged and the supernatant decanted. In order to purify the plasmid DNA, it was necessary to mix 10ml of the proprietary DNA Purification Resin to the lysate and transfer to the Midicolumn. A vacuum was applied to pull the mixture into the column until all had passed through. The DNA was left on the resin, which subsequently needed washing twice with 15ml of column wash solution and the column dried by pulling air through for 30s. The Midicolumn was then spun at 10,000 x g for 2 minutes to remove any residual Column Wash Solution. Following transfer of the column to new tube, 300µl of nuclease-free water preheated to 65°C was added to the column. DNA was eluted from the column by a spin at 10,000 x g for 20s. In order to remove fine particulate matter from the eluate, the sample is spun a final time at 10,000 x g to pellet the fines. The DNA-containing supernatant was carefully removed and transferred to a clean microcentrifuge tube. The extracted pSUPER vector DNA both with the inserted 64-mer (pSUPER.gfp/neo+TPTF) and the control without (pSUPER.gfp/neo) were stored in water at -20°C.

8.3.4. Transfection of cells with pSuper.gfp/neo and transprenyl transferase knockdown siRNA

Cells were transfected using Lipofectamine 2000 (Invitrogen S.A., Barcelona, Spain). For transfection of a single 60cm² plate, 30µg of pSUPER.gfp/neo vector was dissolved in 1.5ml Opti-MEM transfection medium without antibiotic (Invitrogen S.A., Barcelona, Spain). 30µl of Lipofectamine 2000 was dissolved, again in 1.5ml Opti-MEM in another tube. After 5 minutes at room temperature, the 2 tubes were combined, gently mixed and incubated at room temperature for 20 mins to allow the siRNA:Lipofectamine 2000 complexes to form. The 3ml total was then added to the plate. Cells were transfected with both control vector (pSUPER.gfp/neo) and the proposed TPTF knockdown (pSUPER.gfp/neo+TPTF) in parallel experiments.

8.3.5. Imaging of cell cultures for transfection efficiency

Expression of the vector (and thus the siRNA hairpin) was confirmed by checking the presence of the GFP tag when viewing the cultures using fluorescence microscopy. Blue light ($\lambda_{\text{max}}=488$) was directed at the cultures from a Leica DM IRB microscope causing GFP emission at $\lambda_{\text{max}}=507$ and the images captured using a Leica DC100 digital camera.

8.3.6. RNA extraction and isolation from cultures followed by spectrophotometric determination and agarose gel electrophoresis

Following transfection with control pSUPER.gfp/neo and pSUPER.gfp/neo+TPTF, RNA was extracted from the cells in order to perform RT-PCR to visualise the amount of

TPTF mRNA in cultures as a result of pSUPER.gfp/neo+TPTF-mediated siRNA production. In order to extract total RNA, the GenElute Mammalian Total RNA Kit (Sigma-Aldrich Quimica SA, Madrid, Spain) was used, and the manufacturer's protocol followed. Briefly, all RNases were inactivated with 2-mercaptoethanol, cells are lysed and homogenised. Following addition of lysate to the filtration column, RNA was bound to the silica membrane, and following washing was eluted for RT-PCR.

Culture medium was removed and the cells were rapidly and thoroughly disrupted with 500 µl Lysis Solution (a proprietary formulation containing guanidine thiocyanate) supplemented with 2-mercaptoethanol (1% v/v), to inactivate RNase enzymes. A cell scraper was used to thoroughly ensure disruption. Lysed cells were transferred to the GenElute Filtration Column, spun at 16,000 x g to remove cellular debris and shear DNA. The column was discarded, and 500 µl ethanol (70% (v/v)) added to the filtrate before being thoroughly vortexed and loaded into the GenElute Binding Column. This was spun in a microcentrifuge at 16,000 x g for 15s. The flow-through was discarded, and 500 µl Wash Solution 1 (proprietary) added to the column before another 16,000 x g 15s spin. 500 µl of Wash Solution 2 (a proprietary solution containing ethanol) was loaded onto the column and centrifuged at 16,000 x g for 15s. Filtrate was again discarded, before a second 500 µl addition of Wash Solution 2 was added and the spin extended to 2 mins to dry the column. In order to elute the isolated RNA, the GenElute Binding Column insert was transferred to a fresh tube, 50 µl of the proprietary Elution Solution added, and spun at 16,000 x g for 1 minute. Purified RNA was contained in the eluate. Purity and concentration of RNA was determined by spectrophotometric analysis. A 1% (w/v) agarose denaturing gel stained with ethidium bromide (EtBr) was prepared and

electrophoresis conducted to ensure the amount of DNA in the sample was low and the RNA harvested was not degraded (Srivastava and Schlessinger, 1991). This is shown in Figure 8.6. Storage was at -70°C.

8.3.7. Reverse Transcription and Polymerase Chain Reaction

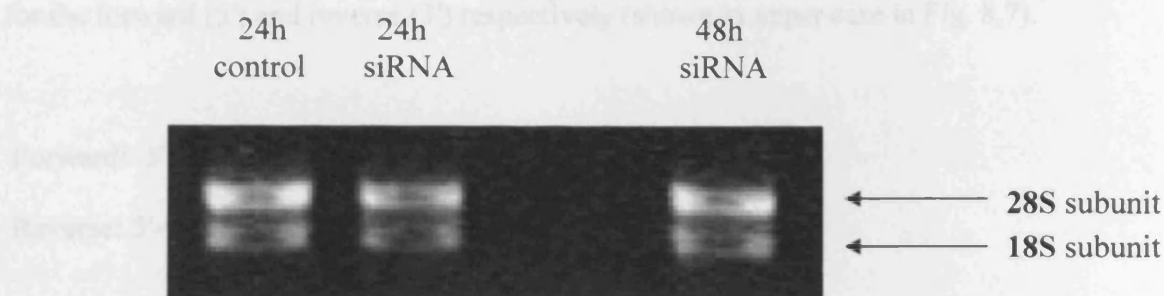
In order to visualise the amount of TPTF mRNA in these cells, it was necessary to employ Reverse Transcriptase (RT) to convert the RNA to DNA, and then amplify this with the Polymerase Chain Reaction (PCR; Mullis *et al.*, 1986). The Reverse Transcription System Kit (Promega, Charbonnieres, France) contains avian myeloblastis virus (AMV) RT which was used to perform the RT reaction. DNA Polymerase and PCR buffers were supplied by Biotools.

8.3.7.1. Reverse Transcription

1 µg of total RNA was added to 1 µg of the 3' primer, and the final volume made up to 10 µl with nuclease-free water. This was allowed to incubate at 70°C for 10 min to allow the primer to bind to the straight, denatured RNA. Rapid cooling in ice ensured the structure of the RNA remained straight. Then 9 µl of the cooled RNA+3' primer was added to 4 µl of MgCl₂ (25mM), 2 µl of RT buffer (10x; 100 mM Tris-HCl, 500 mM KCl, 1% (v/v) Triton X-100; pH 9.0), 2 µl of deoxynucleotide mix (dNTP mix) (10mM), 25 units RNasin Ribonuclease Inhibitor, 15 units AMV RT. The volume was made up to 20 µl with the nuclease-free water supplied, and the reaction incubated at 42°C for 60 min, 95°C for 5 minutes, followed by rapid cooling on ice. The last two temperature steps inactivate AMV RT and prevent it binding cDNA.

8.3.3.2 The Poly(A) Tail Reaction

PCR primers were designed by Dr. Jeroen Deinum, University of Salamanca, corresponding to the mouse TPTF sequence (nt 740 to 723 and the outparallel nt 825 to 801 for the forward and reverse primers, respectively) (which appear in Fig. 8.7).



These primers would produce a PCR product of size 123 nt as shown in black in Fig. 8.7 and were synthesized by Invitrogen (Leiden, Netherlands).

50 µl of RT product was added to 5 µl DNA Polymerase buffer (14x; 750 mM Gcs, 100 mM Tris-HCl, 20 mM MgCl₂, 50 mM KCl, 200 mM (NH₄)₂SO₄, pH 9; Biotools), 1 µl 5' primer (50 µM), 1 µl 3' primer (50 µM), 1 µl of dNTP mix (10 mM; Promega), 0.5 µl DNA Polymerase (1 unit/µl; Biotools). Thermocycling was as follows:

- 90°C for 5 min (initial denaturing cycle)
- 94°C for 15 sec denaturing
- 56°C for 30 sec annealing
- 72°C for 60 sec extension
- 72°C for 5 min final extension

Figure 8.6 Total RNA as extracted from rat astrocytes transfected with *pSUPER.gfp/neo* and *pSUPER.gfp/neo* + TPTF.

Following transfection, RNA was extracted as described in the text. Electrophoresis was conducted in a EtBr-stained 1% agarose gel. The 28S and the 18S ribosomal subunits are evident and 28S:18S intensity is approximately = 2 confirming isolation of intact RNA.

8.3.7.2. *The Polymerase Chain Reaction*

PCR primers were designed by Dr. Juan Bolaños, Universidad de Salamanca, corresponding to the mouse TPTF sequence nt's 705 to 725 and the antiparallel of nt's 825 to 801 for the forward (5') and reverse (3') respectively (shown in upper case in Fig. 8.7).

Forward: 5'-TTG GTG CGT GGT GAA TTT CTT-3'

Reverse: 5'-CTG CTT TAC AAC TGT TGG CTA TCA G-3'

These primers would predict a PCR product of size 121-nt as shown in black in Fig 8.7 and were synthesised by Isogen Bioscience (Maarsen, Netherlands)

9µl of RT product was added to 5 µl DNA Polymerase buffer (10x; 750 mM Tris HCl, 20mM MgCl₂, 500mM KCl, 200mM (NH₄)₂SO₄, pH 9; Biotools), 1 µl 3' primer (50 µM), 1 µl 5' primer (50µM), 1 µl of dNTP mix (10mM, Promega), 0.5 µl DNA Polymerase (1unit/ µl; Biotools). Thermocycling was as follows:

94°C for 5 mins initial denaturing cycle

→ 94°C for 15 secs denaturing

56°C for 30 secs annealing

72°C for 60 secs synthesis

72°C for 5 mins final extension

The PCR product was stored at 4°C.

A number of different cycles were used in an attempt to visualise knockdown of the PCR product. At first, 35 cycles was used as this is likely to be saturating (i.e. no more product generated with an increasing number of cycles), but this was later reduced in order

486

486

546

606

666

726

786

846

The sequence used to design the primers for pSUPER is shown in orange.

to reduce the amount to product formed. This form of semi-quantitative RT was used in conjunction with Northern blotting for the TPTF mRNA directly.

8.3.8. Northern Blotting

Northern blotting allows visualisation of RNA for a protein of interest. RNA was first separated by electrophoresis, then transferred to a nitrocellulose membrane. After transfer, the membrane was hybridised with a complementary radiolabeled ^{32}P probe specific for the RNA of interest. The radiolabeled probe bound to the RNA on the membrane could thus be visualised following exposure of the photographic film whereupon relative size and abundance were observed.

8.3.8.1. Radiolabeling the probe

The RT-PCR product of 2 μg RNA was electrophoresed in an agarose gel. When pouring the gel, 5 wells were taped together to make a single large well. This dsDNA was used to make the radiolabeled probe, the gel is shown in Fig 8.8. The band was excised, and the DNA extracted as previously with the Marligen Gel Extraction kit (Marligen, Ijamsville, USA) as in section 8.3.3.3. 20ng of 5' DNA was denatured by boiling for 10 mins, and rapidly cooled to uncoil the DNA. To the sides of the tube were added 1 μl of each dATP, dGTP, and dTTP (all 10mM), 2 μl of "Hexanucleotide Reaction Mix" (10x, a mixture of random hexanucleotides in reaction buffer, Roche Farma, Madrid, Spain). In a designated radioactive area, 2 μl ^{32}P -dCTP (3000 Ci/mmol) and 1 μl Klenow enzyme (2units/ μl , Roche Farma, Madrid, Spain) were added. The latter is responsible for the synthesis of the probe as it catalyses the addition of mononucleotides (including

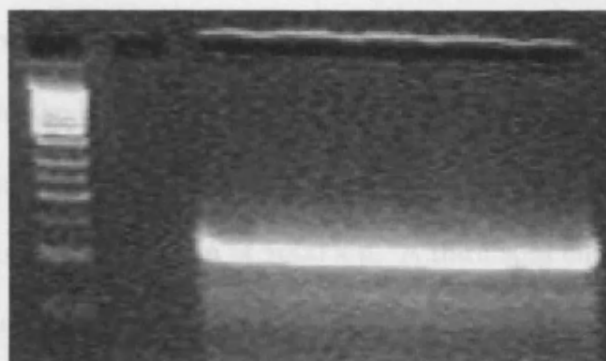


Figure 8.8 Large scale RT-PCR and gel electrophoresis to make a probe for Northern blotting

5 wells of the comb were taped together before pouring the gel and a large amount of DNA purified by excising the band, and the radioactive probe synthesised using ^{32}P labelled cytosine.

15 μg RNA was added to precleaved spin-column tubes and freeze-dried for approximately 30 mins. 40 μl of the following "loading mixture" was added to each sample:

radiolabeled dCPT) complementary the PCR product (i.e. TPTF). This was then mixed and incubated at 37°C for 30 mins. The Klenow enzyme was inactivated by the addition of 60µl TE buffer, giving a final volume of 80 µl.

Purification of the probe was with a sepharose column, made with an eppendorf tube with a pinhole in the bottom, packed with glass wool. Sepharose (previously mixed) was added to the glass wool in the tube, and spun briefly at 5000 x g. 1 ml of TE buffer was added and the column spun again at 5000 x g. A third spin eliminated all TE from the column. The column was placed inside a fresh eppendorf tube and 80µl of impure probe was added to the column and centrifuged at 5000 x g for 1 min. When checking with a Geiger counter, the radioactive count of the eluted pure probe was approximately equal to that remaining in the column. The probe was stored at -20°C.

8.3.8.2.RNA electrophoresis

A 2% agarose gel was prepared using nuclease-free water with 2.2% formaldehyde and MOPS: in 100 ml, 6ml folmaldehyde (37%) and 10 ml 3-(N-Morpholino)propanesulfonic acid (MOPS 10x: 20.9g MOPS, 8,3ml 3M sodium acetate and 10ml 0.5M EDTA made up to 500 ml; pH 7, autoclaved; Sigma-Aldrich Quimica SA, Madrid, Spain). The running buffer in this case was MOPS 1x made up with nuclease-free water.

8.3.8.3.Sample preparation

15µg RNA was added to autoclaved eppendorf tubes and freeze-dried for approximately 30 mins. 40µl of the following "loading mixture" was added to each sample:

80 µl MOPS 10x, 400 µl formamide, 120µl formaldehyde, 120µl water, 80µl RNA loading buffer (10x; comprising glycerol (50%, v/v), bromphenol blue (0.4%, v/v) xylene cyanol (0.4%, v/v). The reaction mixture was incubated at 65°C for 10 mins, and cooled rapidly on ice. After a final spin, 35µl was loaded onto the gel. Electrophoresis was conducted at approximately 40v for 6h.

8.3.8.4. Transfer of RNA to the membrane

Following electrophoresis, the RNA was transferred to the "GeneScreen Plus" membrane (NEN Life Sciences, New England, USA) by capillary action, assisted by the fact that the membrane was placed into firm contact with the gel. A bath of SSC (10x; 1.5M NaCl, 0.15M sodium citrate) was used as the blotting solution, and the transfer allowed to run overnight. The set up is shown in the schematic diagram in figure 8.9. Upon removal of the newly transferred membrane, the RNA was immediately cross-linked using a Hoefer UVC500 Crosslinker set to 254 nm. The membrane was dried at room temperature overnight.

8.3.8.5. Hybridisation of the membrane and exposure of the film

The membrane was wetted first with water then 2x SSC for 10 min. It was then carefully placed in a hybridisation tube, with the RNA-coated side innermost. 10ml prehybridisation solution (1% SDS, 1M NaCl, 10% dextran sulphate) was added and the tube placed in a hybridisation oven set to 65°C and 4 rpm. After 10minutes, the radiolabeled probe was added, and the hybridisation allowed to proceed overnight.

A number of washes were then conducted in the hybridisation oven to remove any non-bound probe which would otherwise cloud the photographic plate:

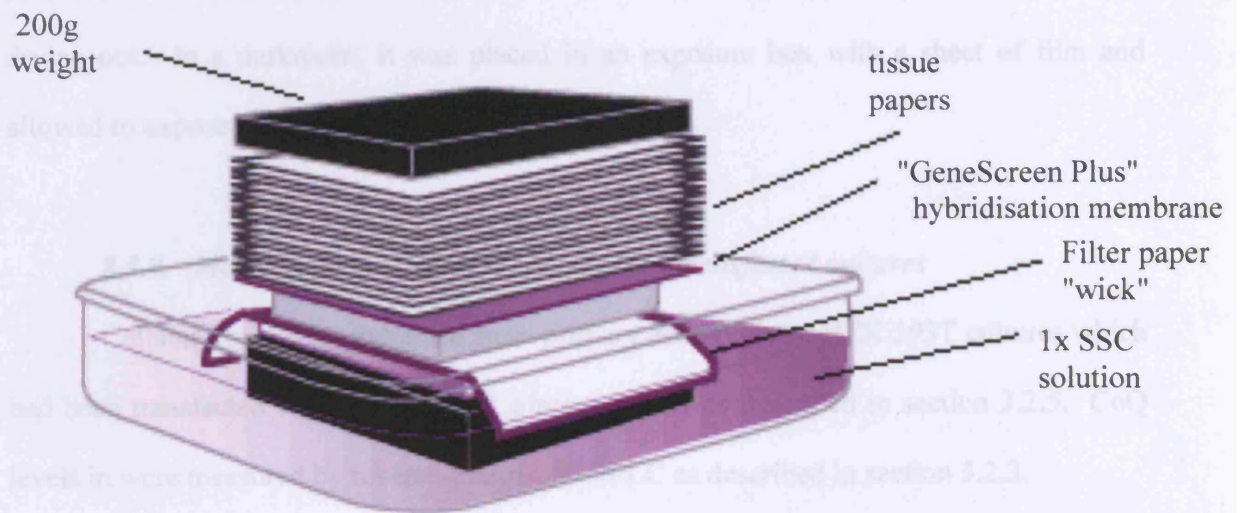


Figure 8.9. A schematic diagram of the apparatus used to transfer RNA from the gel to the hybridisation membrane

Details of the method used to generate the Northern Blot are given in the text. Capillary action draws NaCl/sodium citrate solution (SSC) from the reservoir. Image reproduced and adapted from the Dept. of Biochemistry, University of Arizona website (<http://www.biochem.arizona.edu/classes/bioc471/pages/Lecture2/AMG1.14-North.gif>)

One wash with 2x SSC with 1% SDS at 65°C for 5 min

2 washes with 2x SSC with 1% SDS at 65°C for 30 min each

One wash with 0.1x SSC at room temperature. The background count of the membrane was at this point low. The membrane was wrapped in cling film to prevent it drying out. In a darkroom, it was placed in an exposure box with a sheet of film and allowed to expose the film for 48h at -80°C.

8.3.9. Measurement of ubiquinone levels in transfected cultures

Cellular lipids were extracted from primary astrocyte and HEK 293T cultures which had been transfected with the pSUPER.gfp/neo vector as described in section 3.2.5. CoQ levels in were measured by reverse-phase UV-HPLC as described in section 3.2.3.

8.3.10. Determination of ETC activity in transfected cultures

Following transfection, with both pSUPER.gfp/neo and pSUPER.gfp/neo+TPTF, respiratory chain enzyme activities were determined in both cell types as described in section 2.3.

8.4. Experimental Protocols

Rat primary astrocyte cultures and immortalised human embryonic kidney (HEK293T) cultures were plated as described in section 8.3.1. Both cell types were transfected with the pSUPER.gfp/neo vector and following media replacement, allowed to remain in the plate for up to 48h (HEK 293T) or 72h (astrocytes) post-transfection. In some cases the vector was "empty" (i.e. control experiments), while other cultures

received the vector with an additional ds 64-nt insert. Intracellular generation of siRNA molecules could potentially interfere with ubiquinone biosynthesis. This was examined in a number of ways:

Visualising any downregulation of TPTF mRNA as a product of RT-PCR

Northern Blotting for TPTF mRNA

Measurement of CoQ directly in transfected cultures

Determination of the activity of complex II+III in such cultures

8.5. Results

8.5.1. Visualising Green Fluorescent Protein as a marker of cellular transfection

Following transfection, with pSUPER.gfp/neo and pSUPER.gfp/neo+TPTF, the same visual field of the cultures were photographed in both phase contrast, and under violet (visible) light. Figure 8.10A shows a control culture of HEK 293T 48h post-transfection. Figure 8.10B shows acceptable transfection of the same cell line and time point with the siRNA insert. Having obtained favourable results with the cell line model, Figure 8.11 shows rat primary astrocytes 72h after transfection with pSUPER.gfp/neo+TPTF.

8.5.2. Confirmation of RT-PCR product as TPTF

Following transfection, RNA was extracted from primary astrocyte cultures as described in section 8.3.6 after 24h and 48h. The reverse transcriptase reaction was performed in both the presence and absence of the reverse transcriptase enzyme to ensure any subsequent amplification during PCR was not due to DNA contamination, and the product was RT- dependant. In this case, 35 PCR cycles used was likely to be saturating as

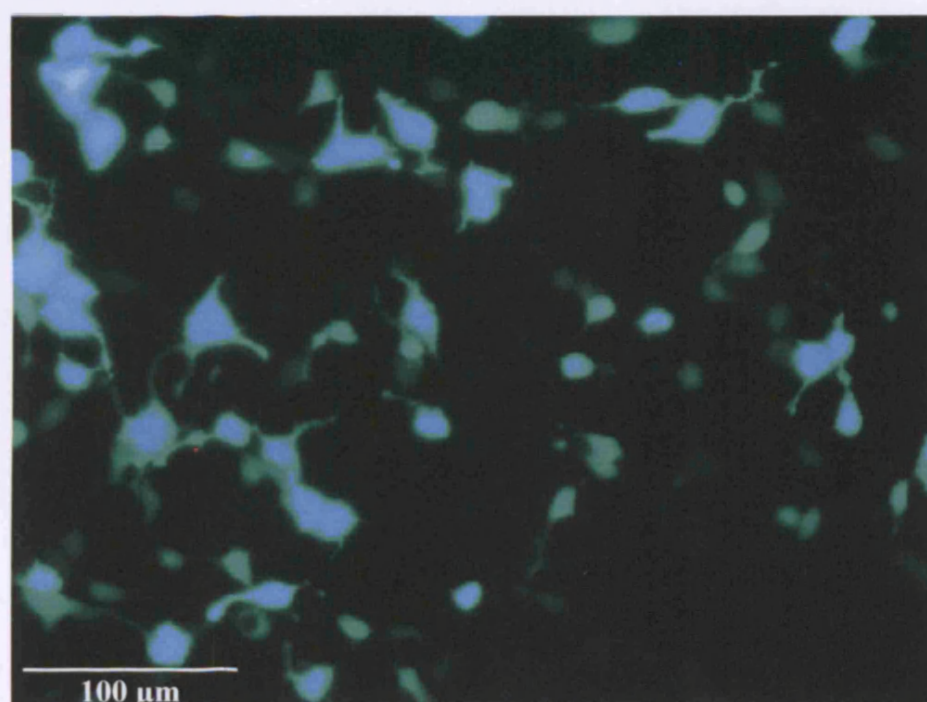
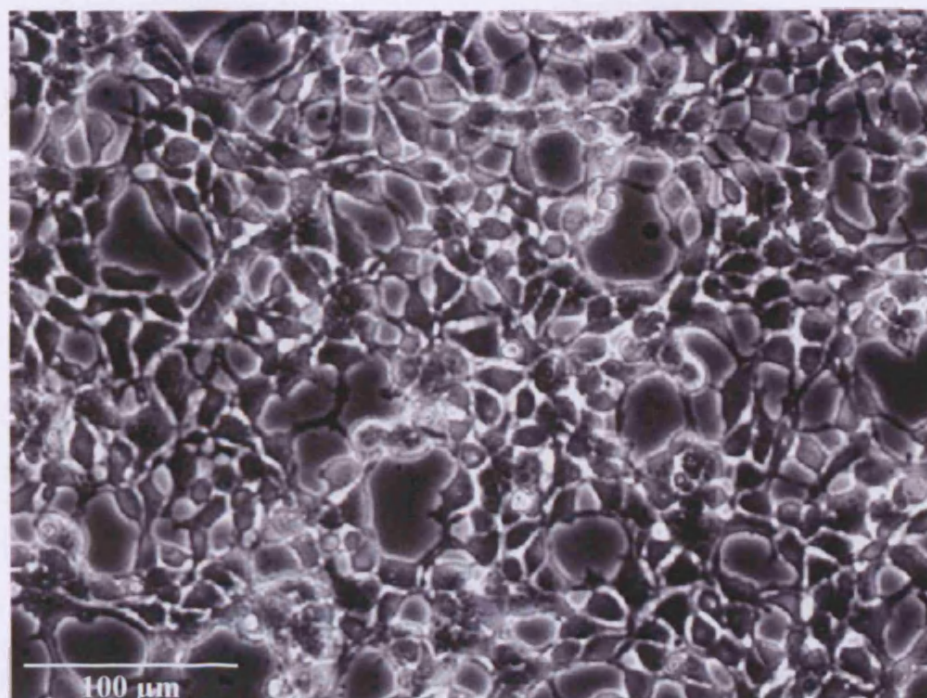


Figure 8.10. HEK 293T cells photographed 48h after transfection with *pSUPER.gfp/neo*

Cultures were transfected with the empty *pSUPER.gfp/neo* vector, and the culture maintained for 48h. The same visual field was photographed A) in phase contrast with a light microscope and B) under UV exposure to show GFP-expressing cells.

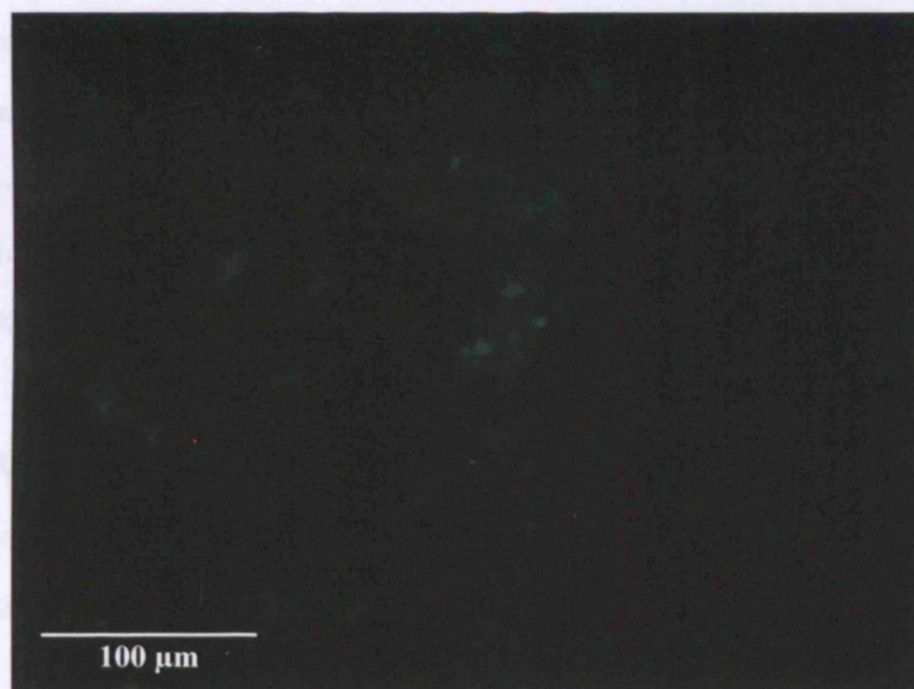


Figure 8.11. Rat primary astrocytes photographed 72h after transfection with pSUPER.gfp/neo +TPTF

Cultures were transfected with pSUPER.gfp/neo +TPTF, and the culture maintained for 72h. The same visual field was photographed A) in phase contrast with a light microscope and B) under UV exposure to show GFP-expressing cells.

is shown in figure 8.12. Extension of the time post-transfection to 72h, as well as a reduction in the number of PCR cycles to 28 (as shown in figure 8.13) appeared to show little difference when compared to a 48h incubation with 35 PCR cycles.

Subsequently, in order to visualise any TPTF knockdown, the semi-quantitative PCR performed is shown in Figure 8.14. Rat primary astrocytes were transfected with both the empty control vector and the vector + TPT-specific insert. 72h later, RNA was harvested, and a number of separate PCRs with differing numbers of cycles from (5 to 25 cycles) performed. Only at 25 cycles is the TPTF band just visible, and it is not clear if there is substantially less TPTF DNA in the siRNA-treated cells.

8.5.3. Northern Blotting for TPTF mRNA

mRNA for TPTF was visualised by a Northern blot. Astrocytes were treated for up to 72h, and HEK 293T cells for up to 48h. Following hybridisation of the membrane with the ^{32}P -labelled probe and exposure of the photographic film to the radioactive nitrocellulose membrane, the results were as shown in figure 8.15. Again in both astrocytes and HEK 293T cultures, there would appear to be little effect upon TPTF mRNA levels.

8.5.4. Measurement of CoQ in siRNA transfected cultures

CoQ levels were measured as in previous chapters, by lipid extraction from the harvested culture (section 3.2.5) followed by reverse-phase HPLC coupled to a UV detector (section 3.2.3).

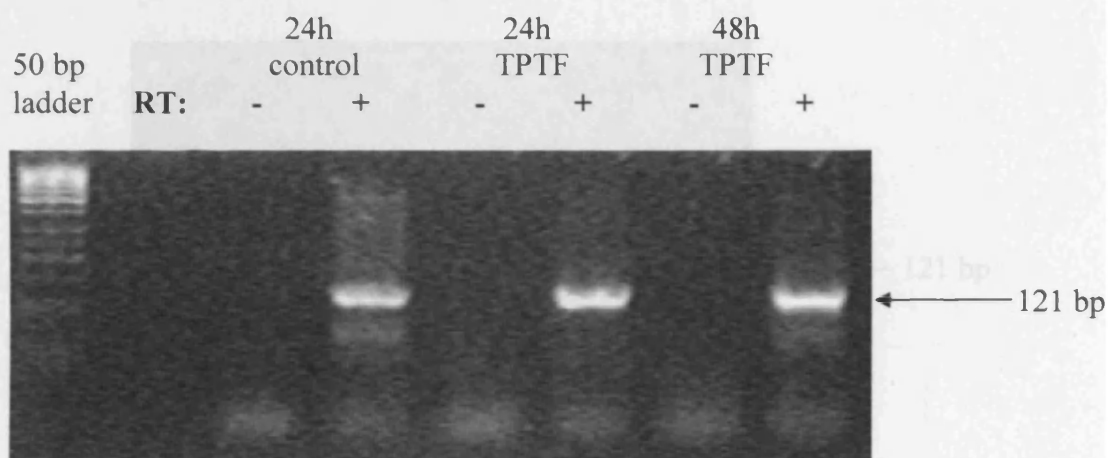


Figure 8.12. Electrophoresis of the astrocyte RT-PCR product.

The cDNA product of the RT-PCR performed as described in the text was shown to be RT dependant and to give a band of the predicted size at 121 bp. RNA was extracted from astrocytes following maintenance for 24h after transfection with the control vector and 24h and 48h after transfection with pSUPER.gfp/neo+TPTF. RT-PCR was performed using 35 cycles to ensure maximum possible amplification.

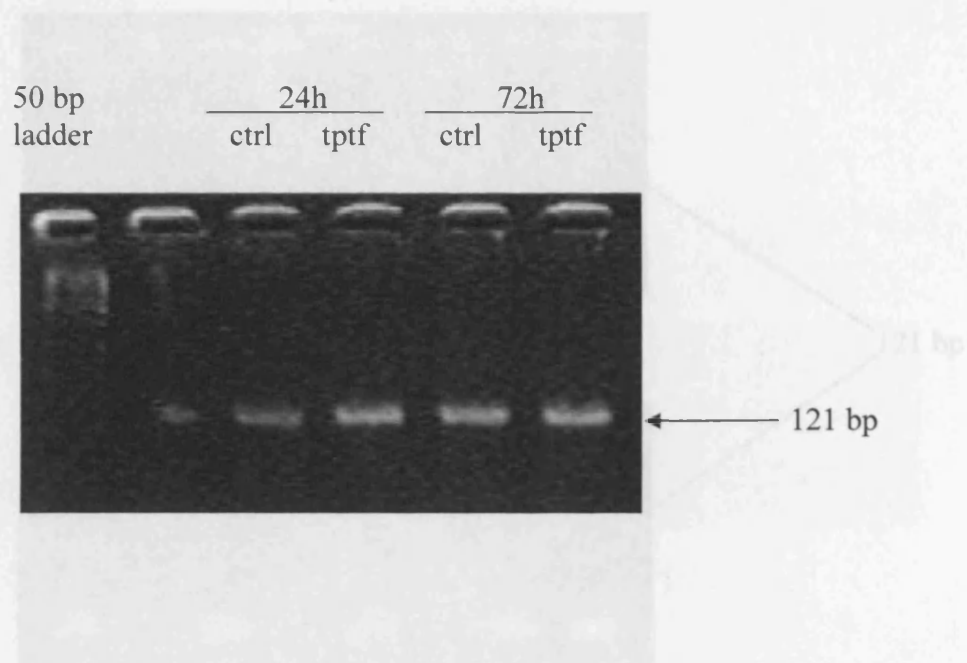


Figure 8.13. Astrocyte RT-PCR product following 28 PCR cycles

Astrocytes were transfected with both control and TPTF siRNA vectors. RNA was extracted after being maintained in culture for 24h and 72h, and RT-PCR performed. Following 28 PCR cycles, the cDNA was visualised in a EtBr agarose gel.

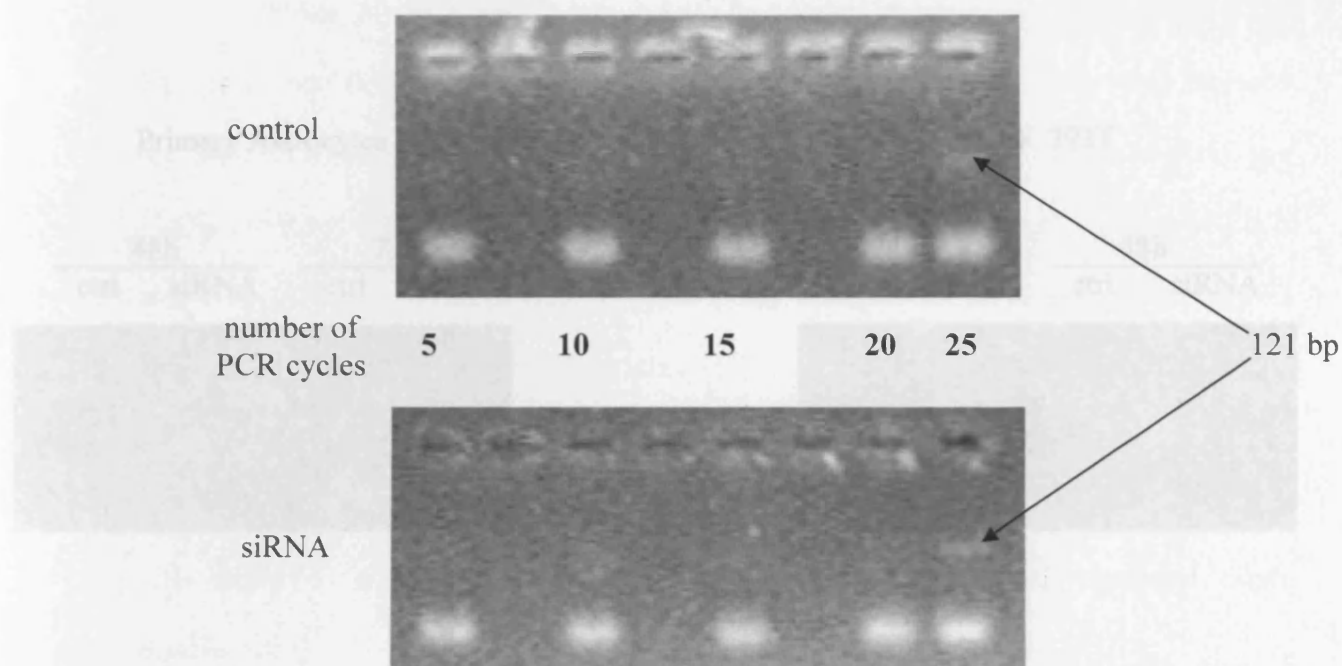


Figure 8.14. Semiquantitative RT-PCR using an increasing number of cycles to aid visualisation of possible TPTF knockdown

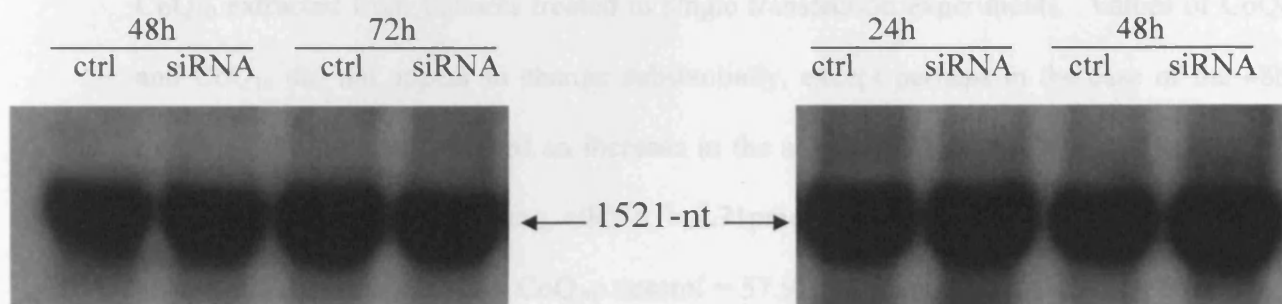
Astrocytes were transfected with both control (upper image) and TPTF siRNA (lower image) vectors. RNA was extracted after being maintained in culture for 72h, and RT-PCR performed. The number of PCR cycles employed is as indicated and cDNA was visualised in a EtBr agarose gel. Only after 25 cycles is there sufficient product to be visualised.

8.5.4.1 HEK 293T cultures

Cultures of HEK 293T cells were transfected as described in section 8.3.4. Following incubation in the transfection media for 6h, the media was completely replaced with fresh DMEM supplemented with 10% FBS. Cells were harvested at 24h or 48h post-transfection. Figure 8.16 shows the levels of CoQ₁₀ and TPTF mRNA in HEK 293T cells transfected with either control or siRNA.

Primary Astrocytes

HEK 293T



48h control = 50.03 pmol/mg, siRNA = 50.41 pmol/mg (data represent single transfection).

8.5.4.2 Primary astrocyte cultures

Identical experimental methods were used to treat the primary astrocyte cultures. In addition, the post-transfection incubation was extended to 72h. The data are shown in figure 8.17. In this case, CoQ₁₀ are lower in the siRNA-transfected cells; the most profound decrease was observed after 72h. After 24h and 48h, there were moderate decreases (5% and 8% respectively). However, 72h post-transfection, a 23% decrease was observed in CoQ₁₀ levels compared to control values. CoQ₁₀ levels decreased 5% after 24h, and 8% after 48h. TPTF mRNA levels were not significantly affected by siRNA treatment. (24h CoQ₁₀ control = 222.71 pmol/mg, siRNA = 205.93 pmol/mg, 48h CoQ₁₀ control = 222.71 pmol/mg, siRNA = 205.93 pmol/mg, 72h CoQ₁₀ control = 222.71 pmol/mg, siRNA = 205.93 pmol/mg).

Figure 8.15. Northern Blot for TPTF mRNA in primary astrocyte and HEK 293T cultures.

Following the procedure as detailed in the text, after being maintained post-transfection with either the control or the siRNA vector for a maximum of 72h (astrocytes) or 48h (HEK 293T), RNA was isolated from the cultures. Equal amounts were loaded into a 2% agarose gel prior to electrolysis, transfer, probe hybridisation and subsequent exposure of the photographic film.

8.5.4.1. HEK 293T cultures

Cultures of HEK 293T cells were transfected as described in section 8.3.4. Following incubation in the transfection media for 6h, the media was completely replaced and the cells cultured for a further 24h or 48h. Figure 8.16 shows the amounts of CoQ₉ and CoQ₁₀ extracted from cultures treated in single transfection experiments. Values of CoQ₉ and CoQ₁₀ did not appear to change substantially, except perhaps in the case of the 48h treatment group which showed an increase in the amount of both CoQ₉ and CoQ₁₀. (24h CoQ₉: control = 3.93 pmol/ mg, siRNA = 4.71pmol/ mg; 48h control = 4.50 pmol/ mg, siRNA = 8.31pmol/ mg. 24h CoQ₁₀: control = 57.92 pmol/ mg, siRNA = 60.68 pmol/ mg; 48h control = 60.03 pmol/ mg, siRNA = 80.41 pmol/ mg [data represent single transfections]).

8.5.4.2. Primary astrocyte cultures

Identical experimental methods were used to treat rat primary astrocyte cultures. In addition, the post-transfection time-point was extended to 72h. These data are shown in figure 8.17. In each case, CoQ₉ are lower in the siRNA-transfected cells; the most profound decrease was observed after 72h. After 24h and 48h, these decreases were moderate (6% and 8% respectively). However, 72h post-transfection, a 25% decrease was observed in CoQ₉ levels compared to control values. CoQ₁₀ levels decreased 5% after 24h, and 8% following 48h transfection. In the case of 72h post-transfection, CoQ₁₀ levels appeared to increase by 7%. (24h CoQ₉: control = 222.71 pmol/ mg, siRNA = 205.95 pmol/ mg; 48h control = 259.82 pmol/ mg, siRNA = 244.63 pmol/ mg; 72h control = 317.45 pmol/ mg, siRNA = 236.6 pmol/ mg. 24h CoQ₁₀: control = 67.52 pmol/ mg, siRNA

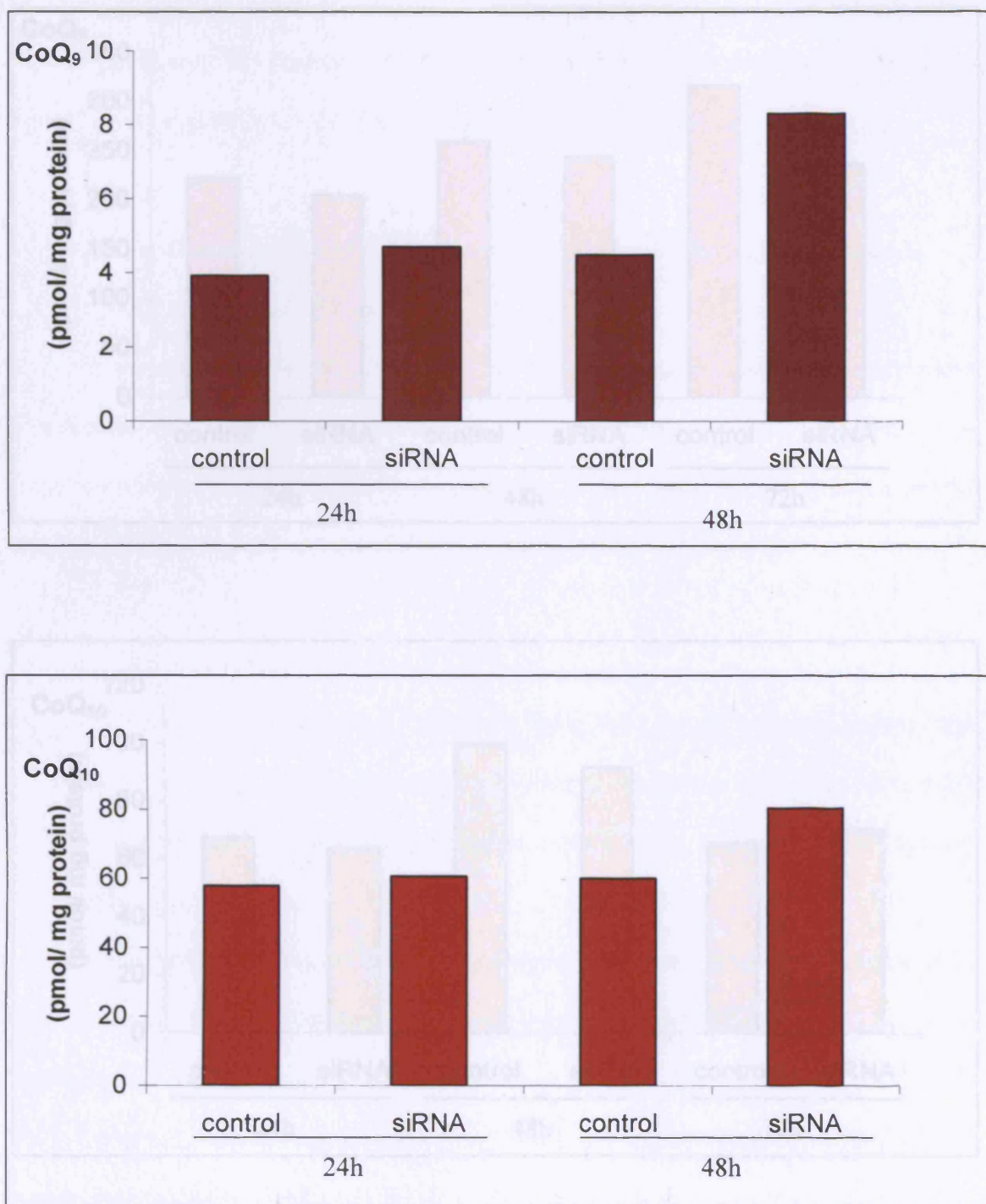


Figure 8.16. Ubiquinone levels in HEK 293T cultures following transfection

Cultures were transfected with either control (empty) vector, or the same vector containing the TPTF-knockdown primers. Following maintenance in culture for either 24h or 48h, lipid extraction was performed on these cells and CoQ₉ and CoQ₁₀ levels measured by UV-HPLC. Data are the product of single culture preparations expressed against a protein baseline.

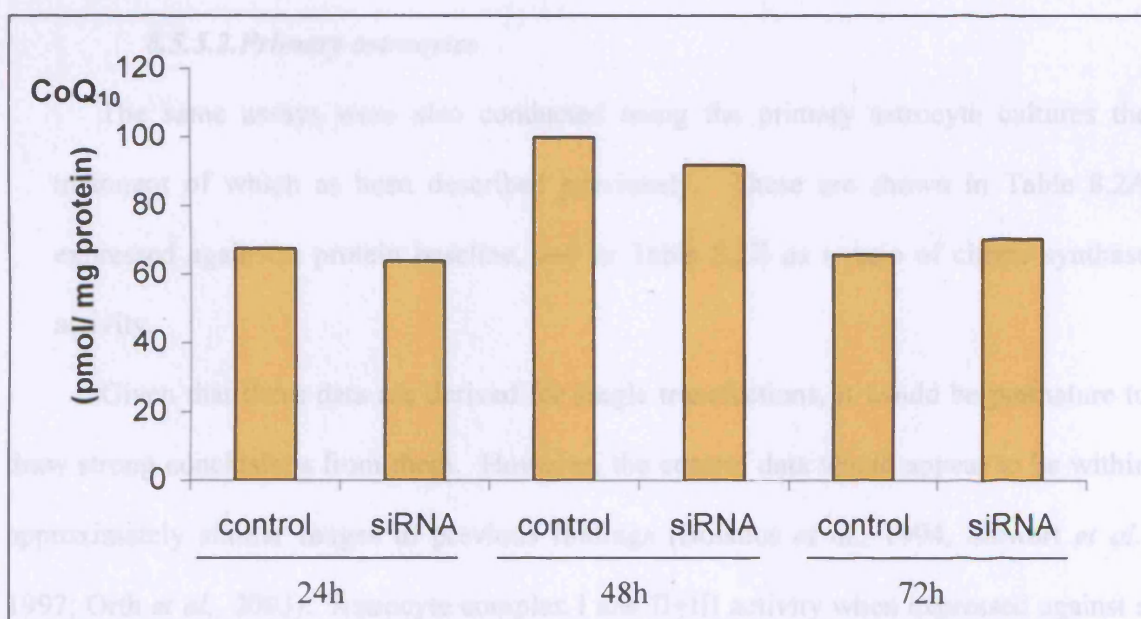
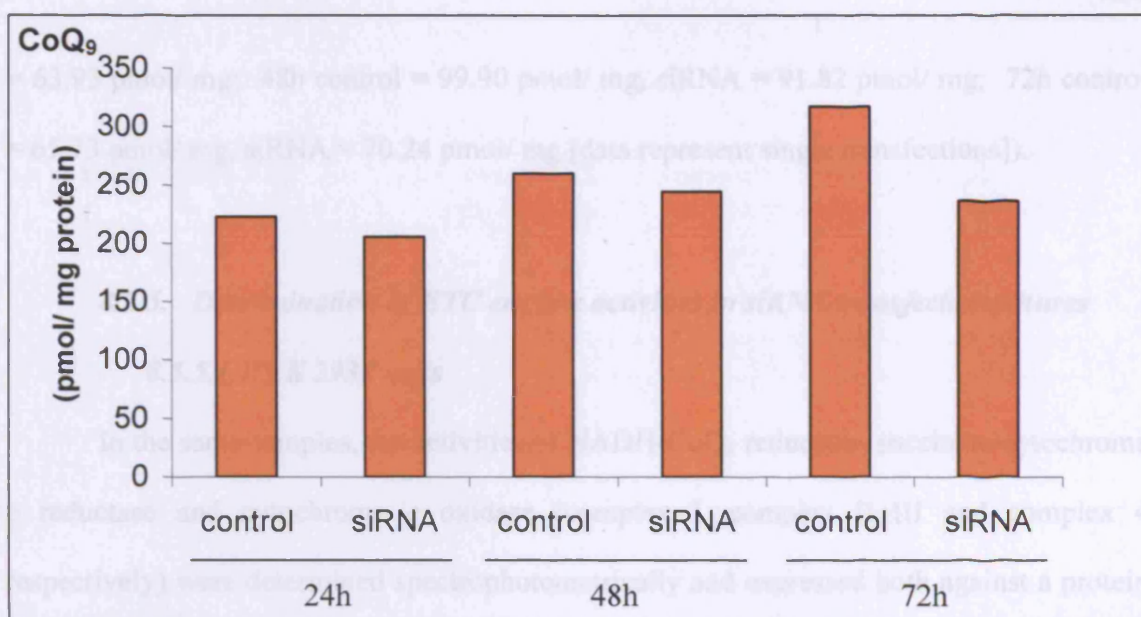


Figure 8.17. Ubiquinone levels in primary astrocyte cultures following transfection.

Cultures were transfected with either control (empty) vector, or the same vector containing the TPTF-knockdown primers. Following maintenance in culture for 24h, 48h, or 72h lipid extraction was performed on these cells and CoQ₉ and CoQ₁₀ levels measured by UV-HPLC. Data are the product of single culture preparations expressed against a protein baseline.

= 63.93 pmol/ mg; 48h control = 99.90 pmol/ mg, siRNA = 91.82 pmol/ mg; 72h control = 65.73 pmol/ mg, siRNA = 70.24 pmol/ mg [data represent single transfections]).

8.5.5. Determination of ETC enzyme activities in siRNA transfected cultures

8.5.5.1. HEK 293T cells

In the same samples, the activities of NADH-CoQ₁ reductase, succinate-cytochrome *c* reductase and cytochrome *c* oxidase (complex I, complex II+III and complex 4 respectively) were determined spectrophotometrically and expressed both against a protein baseline (Table 8.1A) and as ratio of citrate synthase activity (Table 8.1B).

8.5.5.2. Primary astrocytes

The same assays were also conducted using the primary astrocyte cultures the treatment of which as been described previously. These are shown in Table 8.2A expressed against a protein baseline, and in Table 8.2B as a ratio of citrate synthase activity.

Given that these data are derived for single transfections, it would be premature to draw strong conclusions from them. However, the control data would appear to be within approximately similar ranges to previous findings (Bolaños *et al.*, 1994, Stewart *et al.*, 1997; Orth *et al.*, 2003). Astrocyte complex I and II+III activity when expressed against a protein baseline, seem higher than previous findings. However, when expressed as a ratio of citrate synthase activity, these data do not appear to be outwith previous finding from this and other laboratories (Bolaños *et al.*, 1994, Vasquez *et al.*, 2001).

A

HEK 293T		complex I (nmol/min/mg)	complex II+III (nmol/min/mg)	complex IV (k/min/mg)
24h	control	17.7	11.9	0.62
	siRNA	13.7	12.1	0.61
48h	Control	28.8	7.6	0.48
	siRNA	56.6	5.8	0.56

B

HEK 293T		complex I	complex II+III	complex IV
24h	control	0.14	0.09	0.0049
	siRNA	0.12	0.10	0.0052
48h	Control	0.21	0.06	0.0035
	siRNA	0.42	0.04	0.0041

Table 8.1. Mitochondrial complex activities in HEK 293T cultures following transfection.

Cultures were transfected with either control (empty) vector, or the same vector containing the TPTF-knockdown primers. Following maintenance in culture for 24h or 48h, cells were trypsinised and harvested as described previously. Data are expressed A) against a protein baseline and B) as a ratio to citrate synthase activity. Data are the product of single culture preparations expressed against a protein baseline.

A

Primary astrocytes		complex I (nmol/min/mg)	complex II+III (nmol/min/mg)	complex IV (k/min/mg)
24h	control	55.3	36.4	2.14
	siRNA	61.3	28.96	2.43
48h	control	122.2	49.54	3.72
	siRNA	47.7	44.8	4.04
72h	control	289.7	32.3	2.58
	siRNA	192.6	34.1	1.14

B

Primary astrocytes		complex I	complex II+III	complex IV
24h	control	0.27	0.18	0.010
	siRNA	0.32	0.15	0.013
48h	control	0.49	0.20	0.015
	siRNA	0.19	0.18	0.016
72h	control	0.79	0.16	0.013
	siRNA	0.65	0.16	0.006

Table 8.2. Mitochondrial complex activities in primary astrocyte cultures following transfection.

Cultures were transfected with either control (empty) vector, or the same vector containing the TPTF-knockdown primers. Following maintenance in culture for 24h, 48h or 72h, cells were trypsinised and harvested as described previously. Data are expressed A) against a protein baseline and B) as a ratio to citrate synthase activity. Data are the product of single culture preparations expressed against a protein baseline.

8.6. Discussion

During the course of this investigation, a number of techniques were applied to cells previously transfected with a vector for the expression of siRNA molecules in mammalian cells. A primary aim of this work was to decrease in CoQ synthesis as the result of siRNAs targeted against mRNA encoding the biosynthetic enzyme transprenyl transferase (TPTF).

Successful transfection with control (pSUPER.gfp/neo) and siRNA (pSUPER.gfp/neo+TPTF) vectors was achieved using the human HEK 293T cell line. This was confirmed by expression of GFP in at least 50% of these cells (Fig 8.10). In primary cultures of rat astrocytes, the number of cells expressing GFP was approximately 20%, and GFP was visually less abundant in such cells (fig. 8.11). However GFP visualisation was still possible in every culture so treated. The problems associated with transfecting primary cultures has been previously observed (Spänkuch-Schmitt *et al.*, 2002) and it is known that transfection of primary cultures results in a much lower efficiency of transfection than with cell lines (Almeida *et al.*, 2004). However, in neither cell line did the presence of the TPTF insert in the vector did not appear to strongly influence GFP expression.

Having confirmed entry and expression of the vector into the host cells (albeit at a lower level in the primary cultures), RT-PCR was performed upon RNA isolated from primary cultures. The predicted product (121 bp) was obtained (Fig, 8.12), and basic semi-quantitative PCR (between 5 and 35 cycles) used to visualise any possible knockdown of TPTF. In control cells, the band intensity showed dependence upon the number of cycles; it was just possible to visualise a faint band at 25 cycles, but not below. The band was stronger at 28 and stronger still at 35 cycles. Knockdown of a gene product would be supported under these conditions by the presence of the control band at a lower cycle

number than that at which the siRNA-transfected cultures appears. This did not happen when semi-quantitative RT-PCR was performed using RNA extracted from these cultures.

In order to visualise the mRNA levels directly, a Northern blot was performed. A radiolabelled probe was synthesised from the RT-PCR product to hybridise TPTF mRNA following electrophoresis. The relative abundance of TPTF mRNA in both the rat primary and the human cell line cultures is shown in figure 8.15. Post-transfection time prior to RNA isolation was up to 48h in HEK 293T cells and up to 72h in primary cultures. However, no evidence (either from RT-PCR or from the Northern blot) was found to support strong knockdown of TPTF.

Analysis of CoQ status and ETC complex activity was performed in cells harvested from single experiments. While 24h incubation did not markedly alter CoQ₉ or CoQ₁₀ status, 48h siRNA treatment of HEK 293T cultures showed an increase in both CoQ₉ and CoQ₁₀. Under these conditions, complex II+III activity in these cells did not change substantially. Although it is not possible to draw strong conclusions from data derived from single observations, CoQ₉ levels in astrocyte cultures appeared to decrease following transfection; this was greatest following 72h culture post-transfection, whereupon decrease in the region of 25% was observed. As previously observed, basal levels of CoQ₉ in control cultures show an increasing trend with time in culture. This increase may be inhibited by the presence of siRNA in these cells. In addition, as the half life for CoQ turnover is estimated to be 90h in rat brain (Andersson *et al.*, 1990), it is possible that decreases in cellular levels of CoQ₉ (or CoQ₁₀) may not become evident until later time-points. While profoundly decreased mRNA levels were not evident, it is unknown as to the degree of inhibition of TPTF expression necessary to invoke CoQ downregulation.

However, as in previous chapters, the activity of complex II+III did not reflect alterations observed in CoQ₉ status.

siRNA is a relatively novel technique, the mechanisms of which are not yet completely understood. However, there are an abundance of studies within the literature demonstrating that it can be extremely specific and efficacious with regard to gene silencing and with a number of applications (Hannon, 2002; Kurreck, 2003; Jones *et al.*, 2004). A number of reasons can be proposed for a lack of effect with regard to gene product knock-down. However, some possibilities can be ruled out. The 64-nt pSUPER.gfp/neo primers are likely to be specific for TPTF, given the extensive electronic database comparisons. Although the Blast 2 sequences search compared mouse and human, TPTF sequences, the study examined rat primary cultures, and transformed human cultures. In addition, primer efficacy is by no means guaranteed, and it is likely that most siRNA studies use a number of possible primer sequences with differing results (Brummelkamp *et al.*, 2002; Devroe and Silver 2003; Davies *et al* 2004). Ideally, rather than rely on a single proposed sequence, this study could have used a number of similar primers, with slight discrete alterations of the sequence. Unfortunately this was outside the scope of the current study. Since this work was undertaken, more has appeared within the literature on the subject of siRNA sequence design; Reynolds *et al.* (2004) have described novel "rules" for optimal sequence design. In this work, they suggest that a low C/G content, and some sense-strand base preferences may allow for more efficacious sequence selection. Perhaps alternative and better sequences could have been could have been selected if this information were available at the time.

Transfection efficiency was relatively low in the astrocyte study; however abundant expression of GFP in the HEK 293T cell line would suggest that low transfection is not responsible for the lack of knockdown in these cultures. However, it is likely that in both cell types transfection efficiency could be optimised with regard to exposure time to the vector-containing liposomal media and cell density.

Finally, if TPTF protein turnover were shown to be extremely low then it is possible that longer time between transfection and RNA isolation may be necessary before any down-regulation becomes evident. A similar study (Nicchia *et al.*, 2003) was able to show protein knockdown after 2 days, but levels were much lower after 4 days. The 25% decrease in cellular CoQ₉ observed in rat primary cultures 72h post-transfection may thus further decrease with increasing incubation time.

8.7. Conclusion

Rat primary astrocytes and HEK 293T cells were transfected with the pSUPER.gfp/neo vector containing inserts which may be specific for the knockdown of TPTF. Vector expression in both cell types was confirmed by the visualisation of the GFP tag associated with the vector. However, abundant expression of GFP in the HEK 293T cells would suggest higher transfection efficiency than in the primary cultures. Semi quantitative PCR for TPTF cDNA did not reveal any noticeable difference in the amount of TPTF mRNA between the control and siRNA cultures. Northern blotting for mRNA encoding TPTF confirmed this finding. In addition, as in previous chapters, determination of the activities of mitochondrial respiratory chain enzymes (in particular complex II+III) did not indicate that ETC function had been compromised over the time frame of this study.

Measurement of CoQ levels in the HEK 293T cultures up to 48h post-transfection did not show lower abundance of CoQ₉ or CoQ₁₀. In rat primary astrocyte cultures, lower levels of CoQ₉ may have been evident at 72h post-transfection; under these conditions CoQ₁₀ levels showed a small increase. It is possible that the decrease in CoQ₉ levels would become greater with further increasing the time in culture post-transfection.

9. GENERAL DISCUSSION AND SUGGESTED FURTHER WORK

9. GENERAL DISCUSSION AND SUGGESTED FURTHER WORK

This thesis described the establishment of an HPLC method, employing an internal standard, to detect CoQ₉ and CoQ₁₀ in a number of cell culture systems. Subsequently, aims included characterisation of the CoQ status of these cultures, assessing the effects of NO exposure, and investigation of potential pharmacological and molecular biological mechanisms for inhibition of the CoQ biosynthetic pathway.

9.1. HPLC Method

The conjugated nature of the 6-membered ring with oxygen atoms at positions 1 and 4 gives ubiquinone distinct redox properties, and allows detection due to a λ_{max} of absorption at 275 nm. This is exploited in the HPLC method described in this thesis. Similarly the length of the hydrophobic tail determines the elution time from the column. With regard to an internal standard, previous studies have used CoQ homologues which do not predominate in the species being examined; i.e. CoQ₉ as an internal standard for bacterial (Santos Ocaña *et al.*, 2002) and human (Okamoto *et al.*, 1985; Ogashara *et al.*, 1989) studies, and CoQ₆ in rodent studies (Thelin *et al.*, 1992; Tang *et al.*, 2004). However the presence of small quantities of such analogues as a result of dietary intake or synthesis by gut flora may affect quantification of the internal standard. The synthesis of a non-physiological analogue of CoQ₁₀ (diethoxy-CoQ₁₀) allowed accurate determination of losses occurring due to the lipid extraction process. Based on a modification of

the methods of Edlund (1988) and subsequently Eaton *et al.* (2000), this has been used for the successful determination of both rodent and human CoQ status. The method displayed good recovery and acceptable inter and intra assay variability (Table 9.1).

Recovery		107 ± 2 %
Variability	inter-assay	6.5 %
	intra-assay	4.8 %

Table 9.1 Recovery and variability of HPLC method

These were determined as described in sections 3.3.2 and 3.4.3

9.2. Human and rodent cell line responses to lovastatin and iNOS activation

Human and rat brain cell line cultures responded differently to exposure to 10 µM lovastatin. While the human astrocytoma required the prodrug's conversion to the active form to decrease CoQ₉ levels (Fig. 4.6), rat glioma cells (which have higher basal total ubiquinone levels than the human astrocytoma cell line) decreased CoQ₉ status with both the prodrug and activated form by approximately 33% (Fig. 4.8). This may suggest that whereas the rat glioma cell line has a paraoxonase isoform (lactonase) to hydrolyse the lactone ring of lovastatin, the human astrocytoma cells did not.

Additionally human astrocytoma cultures also appeared relatively resistant to the effects of LPS+IFN γ ; in contrast, rat glioma cells significantly increased CoQ₉ levels by 55% under the same conditions (Fig. 4.2). This was likely to be due to

iNOS activation (but not NO as the increase was not accompanied by an increase in NO_x in the culture media; Fig. 4.3) and was abolished by L-NIL. However, it is necessary to consider that basal levels of NO_x generated by these systems were approaching the limit of detection of the Greiss assay. Thus it is possible that NO was being generated in such small quantities that it could not be detected by this assay. Nonetheless, iNOS has been described as a system capable of O₂⁻ generation under certain conditions (Heinzel *et al.*, 1992; Consentino *et al.*, 2001); thus these cultures may increase CoQ₉ status in response to O₂⁻. The simultaneous presence of NO in the rat glioma media (generated from DETA-NO) abolished this increase; this may be attributed to the clearance of O₂⁻ due to its reaction with NO (Fig. 4.14). DETA-NO itself did not alter the status of CoQ₉ or CoQ₁₀ in these cells.

9.3. CoQ status of primary astrocytes and neurons

Differing roles of CoQ₉ and CoQ₁₀ with regard to electron transport, antioxidant function and superoxide generation have been previously suggested in a number of studies (Kagan *et al.*, 1990; Matsura 1991, 1992; Lass *et al.*, 1997; Battino *et al.*, 2001).

Kagan *et al.* (1990) and Matsura *et al.* (1992) proposed CoQ₉ to be a more potent inhibitor of lipid peroxidation than CoQ₁₀, an action possibly attributed to relative partitioning of the two molecules in biological membranes. In hepatocytes, different roles for the two isoforms were considered by Matsura *et al.* (1991) : CoQ₉, found to be largely extra-mitochondrial, was suggested to function as an antioxidant,

while CoQ₁₀ which was mainly localised in mitochondria was ascribed roles as both an antioxidant and as a carrier within the electron transport system.

In this study primary cultures enriched with neurons contain the same amount of CoQ₉ as primary cultures of astrocytes. However, the neuron-enriched cultures contained almost twice as much CoQ₁₀ as the astrocytes (Fig 7.4, Table 9.2). This may be a reflection of the greater dependence of the neuron for mitochondrial OXPHOS. When compared to astrocytes, neurons appear unable to upregulate glycolysis in the face of inhibition of the mitochondrial ETC (Bolaños *et al.*, 1994; Almeida *et al.*, 2004), suggesting a particular reliance by neurons for OXPHOS. This dependence may be reflected in the greater CoQ₁₀ level of neurons and possibly suggests that CoQ₉ and CoQ₁₀ perform distinct metabolic roles.

9.4. Cellular dependence on OXPHOS and differences in CoQ₉ and CoQ₁₀ levels

It is of note that both the CoQ₉ and CoQ₁₀ status in the transformed glial cell lines was lower than that of the primary astrocyte cultures examined. This may be a result of the “Warburg effect”, a shift in cancer cells’ primary energy production from OXPHOS to glycolysis (Warburg 1930, 1956; reviewed in Gatenby and Gillies, 2004). Thus the lower dependence of transformed cells for mitochondrial OXPHOS may manifest as a relative lower abundance of cellular ubiquinone. As described, and shown subsequently in table 9.2, neurons are almost entirely dependant upon OXPHOS for ATP generation; these cells display higher levels of both CoQ₉ and CoQ₁₀ than either the transformed cell lines or the primary cultures.

Thus as OXPHOS dependancy increases, not only does the total CoQ₉ + CoQ₁₀ increase, but the percentage of CoQ₁₀ in total CoQ₉ + CoQ₁₀ also increases. This may again reflect a role CoQ₁₀ over CoQ₉ in mitochondrial electron transport.

	CoQ ₉	CoQ ₁₀	% CoQ ₁₀
Rat C6 glioma	114.3 ± 15.7	17.8 ± 3.3	13%
Primary astrocytes	174.2 ± 10.8	37.9 ± 1.6	18%
Primary neurons	183.7 ± 13.6	67.9 ± 3.9	27%

Table 9.2 CoQ₉ and CoQ₁₀ status of different rat cell types

As the cell types' dependence upon OXPHOS increases, note that not only does total cellular CoQ increase, CoQ₁₀ increases disproportionately

9.5. Influence of serum-withdrawal on astrocyte CoQ availability

Withdrawal of serum from cell cultures has been reported to increase oxidative stress (Barroso, 1997; Palazzotti *et al.*, 1999), possibly via the direct or indirect promotion of cellular O₂⁻ generation (Menzies *et al.*, 2002; Maestre *et al.*, 2003). The resultant oxidative stress has also been reported to increase CoQ levels, possibly as a protective antioxidant response in cultures of human promyelocytic HL-60 cells (Barroso *et al.*, 1997; Gomez-Diaz *et al.* 2003).

The current work has shown that serum withdrawal from astrocyte cultures for 36h resulted in significant increases by approximately 20% in both CoQ₉ and

CoQ₁₀ (Fig. 5.1). While this may be due to increased biosynthesis in response to removal of exogenous CoQ₉ or CoQ₁₀ from culture media, oxidative stress may also be implicated (Huertas *et al.*, 1991). Mataix, *et al.* (1997) suggested that increased oxidative stress in rats elevated CoQ₉ levels in the mitochondrial membrane. Additionally, increased antioxidant defence at the level of manganese superoxide dismutase (MnSOD) was described by Palazzotti *et al.* (1999) following serum deprivation. Primary glial cultures also increase synthesis of the mitochondrial antioxidant GSH in response to oxidative or nitrosative stress (Iwata-Ichikawa *et al.*, 1999; Gegg *et al.*, 2003). Thus serum-withdrawal-mediated ROS generation in the primary cultures described in this thesis may have resulted in elevated CoQ status.

9.6. Influence of lovastatin on CoQ availability of primary astrocyte cultures

In contrast to the rat glial cell lines discussed earlier, the CoQ status of primary cultures of rat astrocytes was unchanged following exposure to 10 μ M lovastatin; however, 100 μ M lovastatin elicited a decrease of up to 50% in CoQ₉ following 24h exposure. Again CoQ₁₀ levels were unaffected (Fig. 6.2).

In the primary astrocyte cultures, it was not necessary to hydrolyse lovastatin to the β -hydroxy acid to affect CoQ status; however, the effects were abolished in the absence of FBS. As serum withdrawal alone increased CoQ levels; this could otherwise mask the direct effects of lovastatin. Alternatively, albumin in the serum may be necessary to transport lovastatin into the cell (Peters, 1985; Nagasawa *et al.*, 2004). Thirdly, lactonase activity due to PON isoenzymes has been reported in the sera of a number of species including rat, rabbit and human; if present in FBS, this

may be shown to result in more effective conversion of the prodrug to the active isoform (Roth *et al.*, 1967; Billecke, *et al.*, 2000; Teiber *et al.*, 2003).

9.7. Influence of iNOS and NO on CoQ availability

In primary astrocytes, following 24h activation of iNOS, no alteration in CoQ status was observed. Extension of incubation to 36h demonstrated a statistically significant decrease in CoQ₉ with no change in CoQ₁₀ levels (Fig 7.2).

Bolaños *et al.* (1994) showed using cultured astrocytes that maintenance of iNOS activation for 36h resulted in an inhibition of complex II+III which did not occur after 18h (Bolaños *et al.*, 1994). ONOO⁻ has also been demonstrated to directly oxidise short-chain ubiquinol to the semiquinone form (Schöpfer *et al.*, 2000). The possibility therefore exists that the deleterious effects of RNS upon CoQ may be responsible for the inhibition of this linked enzyme system. While it is possible that the findings of Bolaños *et al.* (1994) could be attributed to decreased CoQ availability, under the conditions described here, no significant decreases in complex II+III were detected. It is possible that the absence of serum from the cell culture media of the current study resulted in the absence of complex II+III inhibition. This work has shown that serum withdrawal for 36h increased cellular CoQ status. Subsequently, this may either confer additional antioxidant protection against the RNS-mediated inhibition of complex II+III activity, or allow maintenance of electron transport at the levels of complex II+III in the face of inhibition of the ETC. In keeping with the findings of Bolaños *et al.*, (1994), complex IV was the particularly susceptible to RNS-mediated inhibition.

Exposure of similar astrocyte cultures to NO from an exogenous source (i.e. DETA-NO) resulted in an initial decrease in both CoQ₉ and CoQ₁₀; however, extended exposure resulted in an apparent restoration of CoQ levels. Given the greater levels of NO_x generated by DETA-NO compared to LPS + IFN γ after 36h, this may represent a mechanism whereby cellular antioxidant status can be upregulated in times of prolonged or severe oxidative / nitrosative stress. Such mechanisms have previously been described for CoQ (Huertas *et al.*, 1991; Barroso *et al.*, 1997; Gomez-Diaz *et al.* 2003), GSH (Gegg *et al.*, 2003), MnSOD (Palazzotti *et al.*, 1999), catalase (Treichel *et al.*, 2004) and ascorbate (reviewed in Rice *et al.*, 2002).

9.8. Differential effects of DETA-NO on astrocytes and neurons

As previously discussed, basal levels of CoQ₉ between astrocyte and neuron-enriched cultures are the same, but neuron-enriched cultures contain 1.8-fold more CoQ₁₀, possibly as a result of their higher dependence on OXPHOS. However, the astrocytic and neuronal response to DETA-NO was also different. While astrocyte cultures decrease CoQ₉ and CoQ₁₀ by approximately 32% and 44% respectively after 24h exposure to DETA-NO; neuronal levels of CoQ₉ and CoQ₁₀ were unchanged. The full implications of this finding have not yet been elucidated; however it is possible that while the astrocyte can utilise glycolysis to generate ATP following ETC inhibition, the preservation of CoQ₉ and CoQ₁₀ by the neuron represents a response to maintain sufficient electron transport in the face of RNS-mediated inhibition.

In addition, these findings may become clearer in light of existing knowledge of another cellular and mitochondrial antioxidant, GSH. Monocultures of astrocytes have approximately double the amount of GSH than that of neurons (Bolaños *et al.*, 1995). The present study shows almost double the amount of CoQ₁₀ in neurons compared to astrocytes. Furthermore, Gegg *et al.* (2003) have shown that exposure of astrocytes to DETA-NO causes an increase in GSH content; both CoQ₉ and CoQ₁₀ decrease under these conditions. It would appear however that neuronal loss of GSH in response to NO (Gegg *et al.*, 2003) may be counteracted by the maintenance of CoQ₉ and CoQ₁₀ in these cells. This gives rise to the possibility of a compensatory effect, i.e. the upregulation of one antioxidant in response to the decrease of another.

9.9. CoQ status and ETC activity

The complex II+III assay requires endogenous CoQ, and it has been proposed that CoQ availability may be limiting for this assay (Clark *et al.*, 1994; Rahman *et al.*, 2001). Thus to gain insight into the effects of CoQ depletion upon the ETC, the respiratory chain enzyme activities of the primary cultures of rat astrocytes were determined.

Although CoQ₉ levels decreased by up to 50% following treatment with lovastatin (100 µM), no decrease in the activity of the linked II+III assay was observed (Tables 6.10 and 6.11). Similarly, neither NO generated from iNOS nor DETA-NO were seen to inhibit complex II+III activity even though CoQ₉ levels had decreased by 22% with LPS+IFN γ and 32% with DETA-NO (Table 7.6). It is

possible that these overall findings of complex II+III activity which appears not to be limited by CoQ status may suggest that a threshold of depletion necessary for CoQ₉ to inhibit complex II+III activity was not reached. These data would suggest that such a threshold would have to represent depletion of CoQ₉ of at least 32% in rat primary astrocyte cultures. Alternatively, a decrease in cellular CoQ may not necessarily reflect a decrease in CoQ in the inner mitochondrial membrane. Given the maintenance of CoQ₁₀ levels under these conditions, it is also possible that complex II+III activity in these cells relies more heavily upon the availability of CoQ₁₀ than CoQ₉ for electron transport. In support of this last hypothesis, consideration of the complex II+III activity of the human astrocytoma cell line and the rat primary astrocyte cultures may be important. Although the present study did not measure the ETC activities of the cell lines, this has previously been done by Stewart *et al.* (1998). These authors describe very similar values for complex II+II activity (11.7 ± 1.2 and 13.9 ± 2.4 nmol/min/mg protein for primary rat astrocytes and human astrocytoma cultures respectively). The current work has shown that while CoQ₉ status of these cultures differs by > 50-fold, CoQ₁₀ levels are almost identical (35.4 ± 2.7 and 33.8 ± 7.6 pmol/mg protein for primary rat astrocytes and human astrocytoma cultures respectively). Thus availability of CoQ₁₀ rather than CoQ₉ may be particularly important in determining activity of complex II+III.

9.10. siRNA study

The use of siRNA directed against transprenyl transferase a key biosynthetic enzyme was examined (Fire, *et al.* 1998; Elbashir *et al.* 2001). Following

confirmation of efficient siRNA transfection with immortalised HEK 293T cultures, rat primary astrocytes notably expressed lower levels of the GFP tag associated with the pSUPER.gfp/neo vector (noted in Spänkuch-Schmitt *et al.*, 2002). Thus it is possible that siRNA transfection efficiency could be improved in primary astrocytes (as achieved by Nicchia *et al.*, 2003 and Almeida *et al.*, 2004) and to lesser degree HEK 293T cells.

Semiquantitative RT-PCR for the transprenyl transferase mRNA did not show decreased levels (Fig. 8.14); similarly Northern blotting did not display markedly lower values of mRNA (Fig 8.15). However, while the HEK 293T cells did not show decreases in cellular CoQ₉ or CoQ₁₀, levels of particularly CoQ₉ were decreased by 25% 72h post-transfection. Given that the half life in turnover of CoQ in rat brain has been postulated as being in the region of 90h, it is possible that a longer period in culture post-transfection would have mediated a more profound decrease in CoQ₉ levels. As described in previous chapters, measurement of ETC complex activities did not indicate inhibition complex II+III activity under these conditions. While it is possible that more effective gene silencing could have been effected with alternative primers, and a number of protocols and observations have allowed more accurate and efficient design, it is still unknown as to why some primers give better gene product downregulation than others (Reynolds *et al.*, 2004). For this reason, siRNA studies generally trial a number of primers in parallel before the selection of one as the most effective at mediating knockdown of the gene product of interest (Brummelkamp *et al.*, 2002; Devroe and Silver, 2003).

9.11. Conclusions and potential implications of research

The effects observed in the models described were predominantly upon CoQ₉ with an apparent sparing of CoQ₁₀. It has been proposed that an interconversion between CoQ₉ and CoQ₁₀ can occur: studies administering dietary CoQ₁₀ to rodents, have reported increased levels of both CoQ₉ and CoQ₁₀ in a number of tissues (Lönnrot *et al.*, 1998; Kwong *et al.*, 2002) and in mitochondrial membranes (Lass *et al.*, 1999). Thus *in vivo*, CoQ₉ may be synthesised from CoQ₁₀ and *vice versa*. Indeed it has been suggested that the addition of a final isopentenyl pyrophosphate to nonaprenyl pyrophosphate is a rate limiting step in CoQ₁₀ biosynthesis (Yamamoto *et al.*, 1989).

Transformation of cells involves a lowered reliance on OXPHOS; this may account for the lower CoQ₉ and CoQ₁₀ levels in the rat glioma than the corresponding primary astrocyte cultures. Similarly, the higher CoQ₁₀ levels in primary rat neurons compared to astrocytes may be a reflection of their relative reliance on functional mitochondria. Given that complex II+III activity did not decrease under conditions where CoQ₉ availability was compromised (and CoQ₁₀ levels were maintained), a body of evidence is accumulating which may support the role of CoQ₁₀ as the primary electron carrier in the mitochondrial ETC. The similarity in the documented complex II+III activities of human astrocytoma cells and rat primary astrocytes (Stewart *et al.*, 1998), and the current finding of near-identical CoQ₁₀ levels (although vastly different CoQ₉ status) may provide circumstantial evidence to support this.

Exposure to DETA-NO for 24h caused a lowering of both CoQ₉ and CoQ₁₀ in astrocytes. However, following 36h exposure, these levels had returned almost to control values. These findings could have implications for oxidative / nitrosative stress studies in that CoQ₉ and CoQ₁₀ levels in astrocytes may increase following prolonged oxidative insult (i.e. 36h withdrawal of serum) or recover after an initial decrease following prolonged nitrosative stress (36h DETA-NO exposure).

While 36h exposure to LPS + IFN γ caused a significant decrease in CoQ₉ but not CoQ₁₀, in contrast to previous works (such as that of Bolaños *et al.*, 1994) complex II+III activity did not decrease. However, it is possible that the lack of serum in the cell culture medium of the current study may have prompted cellular upregulation of CoQ₉ and or CoQ₁₀ leading to the maintenance of complex II+III activity.

Expression of siRNA in primary astrocytes for 72h has shown a 25% decrease in CoQ₉ levels compared to control values. As the predicted half life of turnover of CoQ in rat brain (Andersson *et al.*, 1990), this initial finding may represent a method to decrease cellular levels of CoQ₉ in rat tissue.

Finally, the apparently higher sensitivity of the CoQ biosynthetic pathway to lovastatin in rat glioma and human astrocytoma cells when compared to rat primary astrocyte cultures may support the proposed anti-tumourogenic properties of the statin drugs. Lovastatin and other HMG-CoA reductase inhibitors have been shown to have the potential to trigger apoptosis in some tumour-derived cells both *in vitro* (Dimitroulakos and Yeger, 1996; Dimitroulakos *et al.*, 1999; Wong *et al.*, 2001) and *in vivo* (Minden *et al.*, 2001). An epidemiological study has also reported a

decreased risk of cancer in statin users (Blais *et al.*, 2000). Specifically, the potential for statin drugs in the treatment of CNS malignancies has been investigated *in vitro* (Soma *et al.*, 1992; Prasanna *et al.*, 1996; Dimitroulakos and Yeger, 1996) and using animal models (Soma *et al.*, 1995; Kikuchi *et al.*, 1997). Thus the statin class of drugs may have antiproliferative, proapoptotic, anti-invasive and radiosensitising properties and have been proposed as potential chemotherapeutic agents (reviewed in Chan *et al.*, 2003).

SUGGESTED FUTURE WORK

- As this work has found little evidence that disruption of cellular CoQ₉ status affects mitochondrial electron transport, it is recommended that future studies address mitochondrial CoQ₁₀ status. This could be achieved by subcellular fractionation using the method of Almeida and Medina (1998) prior to CoQ₁₀ determination. Subsequently this could be dissected into the response of CoQ₁₀ in mitochondria extracted from primary astrocytic and neuronal cultures. Preliminary data has been obtained describing the CoQ₉ and CoQ₁₀ content of rat brain non-synaptic mitochondria isolated using the method of Lai and Clark (1979), shown in Table 9.3.

	(pmol/ mg protein)
CoQ ₉	32.3
CoQ ₁₀	14.2

Table 9.3 Preliminary findings examining CoQ₉ and CoQ₁₀ content of non-synaptic mitochondria from rat brain (n=2)

- It has been observed that CoQ₉ levels in primary cultures can decrease by 50% following incubation with lovastatin. Thus it would be of interest to administer lovastatin to animals in order to assess whether such a situation may exist in the brain or other tissues following lovastatin treatment.

- CoQ-deficient states resulting from inborn errors of metabolism have been identified in human patients. Oral administration of CoQ₁₀ or idebenone (the CoQ analogue which crosses the blood-brain barrier) has been beneficial in the treatment of such conditions. If lovastatin-mediated cellular CoQ depletion were observed *in vivo* in experimental animals, the potential for oral CoQ and / or idebenone administration in the therapeutic intervention of such a state would also be of clinical interest.

- With regard to the siRNA study, although it was not possible to conclusively demonstrate “knock-down” of TPTF mRNA or protein, CoQ₉ levels appeared to decrease by 25% in primary rat astrocyte cultures. Extension of time in culture post transfection may show further decreases in cellular CoQ₉ or CoQ₁₀. As proof of principle with regard to transfection, RT-PCR and Northern blot probes has been achieved, further investigation is warranted. Initially, such a study could continue to investigate the HEK 293T cell line and primary cultures of rat astrocytes (and subsequently neurons) at extended time points. Additional work with a number of different primers for the same enzyme may produce an siRNA sequence more effective in lowering TPTF mRNA and protein levels.

- The apparent sensitivity to lovastatin of rat glioma cells compared to primary astrocytes may merit the treatment of experimental glioma-type tumours in

animals with this drug. The inhibitor of GSH biosynthesis L-BSO has been shown to increase the sensitivity of human cancer cells to radiation possibly as a result of the decreased antioxidant capacity of the tumour cells (Lippitz *et al.*, 1990; Kato *et al.*, 2000); radiosensitisation has also been hypothesised following lovastatin treatment (Chan *et al.*, 2003), an effect which may also represent a targeted decrease in the antioxidant capacity of such cells. Given that increased susceptibility of tumour cells over healthy tissue is a major goal of current cancer therapy, the findings of this current work merit further study with regard to the therapeutic potential of the statin drugs as anticancer agents.

REFERENCES

REFERENCES

- Åberg, F., Appelkvist, E-L., Dallner, G. and Ernster, L. (1992) Distribution and redox state of ubiquinones in rat and human tissues. *Arch. Biochim. Biophys.* **295**, 230-234
- Abrahams, J.P., Leslie, A.G.W., Lutter, R. and Walker, J.E. Structure at 2.8 Å resolution of F₁-ATPase from bovine heart mitochondria. *Nature* **370**, 621-628
- Albano, C. B., Muralikrishnan, D. and Ebadi, M. (2002) Distribution of coenzyme Q homologues in brain. *Neurochem. Res.* **27**, 359-368
- Alberts, A. W., Chen, J., Kuron, G., Hunt, V., Huff, J., Hoffman, C., Rothrock, J., Lopez, M., Joshua, H., Harris, E., Patchett, A., Monaghan, R., Currie, S., Stapley, E., Albers-Schonberg, G., Hensens, O., Hirshfield, K., Hoogsteen, K., Liesch, J. and Springer, J. (1980) Mevinolin: a highly potent competitive inhibitor of hydroxymethylglutaryl-coenzyme A reductase and a cholesterol-lowering agent. *Biochemistry*, **77**, 3957-3961
- Alderton, W.K., Cooper, C.E. and Knowles, R.G. (2001) Nitric oxide synthases: structure, function and inhibition. *Biochem. J.* **357**, 593-615
- Almeida, A. and Medina, J.M. (1998) A rapid method for the isolation of metabolically active mitochondria from rat neurons and astrocytes in primary culture. *Brain Res. Prot.* **2**, 209-214

Almeida, A. and Bolaños, J. P. (2001) A transient inhibition of mitochondrial ATP synthesis by nitric oxide synthase activation triggered apoptosis in primary cortical neurons. *J. Neurochem.* **77**, 676-690

Almeida, A., Moncada, S. and Bolaños, J.P. (2004) Nitric Oxide switches on glycolysis through the AMP protein kinase and 6-phosphofructo-2-kinase pathway. *Nat. Cell Biol.* **6**, 45-51

Anderson, S., Banhier, A.T., Barrel, B.G., DeBruijn, M.H.L., Coulson, A.R., Drouin, J., Eperton, I.C., Mierlich, D.P., Roc, B.A., Sanger, F., Schreier, P.H., Smith, A.J.R., Standen, R. and Young, I.G. (1981) Sequence and organisation of the human mitochondrial genome. *Nature* **290**, 457-465

Andersson, M., Elmberger, P.G., Edlund, C., Kristensson, K. and Dallner, G. (1990) Rates of cholesterol, ubiquinone, dolichol and dolichol-P biosynthesis in rat brain slices. *FEBS Lett.* **269**, 15-18

Anggard, E. (1994) Nitric oxide: mediator, murderer, and medicine. *Lancet* **343**, 1199-1206

Armstrong, J.S., Whiteman, M., Rose, P. and Jones D.P. (2003) The Coenzyme Q10 analog decylubiquinone inhibits the redox-activated mitochondrial permeability transition: role of mitochondrial complex III. *J. Biol. Chem.* **278**, 49079-79084

Babcock, G.T. and Wikström, M. (1992) Oxygen activation and the conservation of energy in cell respiration. *Nature*, **356**, 301-309

Barja, G., Herrero, A.J. (1998) Localization at complex I and mechanism of the higher free radical production of brain nonsynaptic mitochondria in the short-lived rat than in the longevous pigeon. *J. Bioenerg. Biomembr.* **30**, 235-243

Barker, J., E., Bolaños, J.P., Land, J.M., Clark, J.B. and Heales, S.J.R. (1996) Glutathione protects astrocytes from peroxynitrite-mediated mitochondrial damage: implications for neuronal/astrocyte trafficking and neurodegeneration. *Dev. Neurosci.*, **18**, 391-396

Barth, R. L. (1998) Rat brain tumor models in experimental neuro-oncology: The 9L, C6, F98, RG2 (D74), RT-2 and CNS-1 Gliomas. *J. Neurooncol.* **36**, 91-102

Barroso, M.P., Gomez-Diaz, C., Villalba, J.M., Buron, M.I., Lopez-Lluch, G. and Navas, P. (1997) Plasma membrane ubiquinone controls ceramide production and prevents cell death induced by serum withdrawal. *J. Bioenerg. Biomembr.* **29**, 259-267

Bates, T.E., Loesch, A., Burnstock, G. and Clark, J.B. (1995) Immunocytochemical evidence for a mitochondrially located nitric oxide synthase in brain and liver. *Biophys. Biochem. Res. Commun.* **218**, 40-44

Bates, T.E., Loesch, A., Burnstoch, G. and Clark, J.B. (1996) Mitochondrial nitric oxide synthase: a physiological regulator of oxidative phosphorylation? *Biophys. Biochem. Res. Commun.* **213**, 896-900

Battino, M., Gorini, A., Villa, R.F., Genova, M.L., Bovina, C., Sassi, S., Littaru, G.P. and Lenaz, G. (1995) Coenzyme Q content in synaptic and non-synaptic mitochondria from differing brain regions in the aging rat. *Mech. Aging Dev.* **78**, 173-187

Battino, M., Bompadre, S., Leone, L., Villa, R.F., Gorini, A. (2001) Coenzymes Q₉ and Q₁₀, vitamin E and peroxidation in rat synaptic and non-synaptic occipital cerebral cortex mitochondria during ageing. *Biol. Chem.* **382**, 925-931

Beal M. F. and Matthews, R. T. (1997) Coenzyme Q₁₀ in the central nervous system and its potential usefulness in the the treatment of neurodegenerative diseases. *Molec. Aspects Med.* **18**, s169-s179

Beal, M.F. (1999) Coenzyme Q₁₀ administration and its potential for treatment of neurodegenerative diseases. *Biofactors* **9**, 261-266

Beckmann, J.D., and Frerman F.E. (1985) Electron-transfer flavoprotein-ubiquinone oxidoreductase from pig liver : purification and molecular, redox, and catalytic properties. *Biochemistry* **24**, 3913-3921

- Belogrudov, G.I., Lee, P.T., Johanssen, T., Hsu, A.Y., Gin, P. and Clarke, C.F. (2001) Yeast COQ4 encodes a mitochondrial protein required for coenzyme Q synthesis. *Arch. Biochem. Biophys.* **392**, 48-58
- Bentinger, M., Dallner, G., Chojnacki, T. and Swiesewska, E. (2003) Distribution and breakdown of labeled coenzyme Q₁₀ in rat. *Free Rad. Biol. Med.* **34**, 563-575
- Bignami, A., Eng, L.F., Dahl, D. and Uyeda, C.Y. (1972) Localization of the glial fibrillary acidic protein in astrocytes by immunofluorescence. *Brain Res.* **43**, 429-435
- Bilheimer, D.W., Grundy, S.M., Brown, M.S. and Goldstein, J.L. (1983) Mevinolin stimulates receptor-mediated clearance of low density lipoprotein from plasma in familial hypercholesterolaemia heterozygotes. *Proc. Natl. Acad. Sci. USA.* **113**, 387-392
- Billecke, S., Draganov, D., Counsell, R., Stetson, P., Watson, C., Hsu, C. and La Du, B.N. (2000) Human serum paraoxonase (PON1) isoenzymes Q and R hydrolyze lactones and cyclic carbonate esters. *Drug Metab. Dispos.* **28**, 1335-1342
- Blais L., Desgagne, A. and LeLorier J. (2000) 3-hydroxy-3-methylglutaryl coenzyme A reductase inhibitors and the risk of cancer: a nested case-controlled study. *Arch. Int. Med.* **160**, 2363-2368

Boitier, E., Degoul, F., Desguerre, I., Charpentier, C., François, D., Ponsot, G., Diry, M., Rustin, P. and Marsac, C. (1998) A case of mitochondrial encephalomyopathy associated with a muscle coenzyme Q₁₀ deficiency. *J. Neurol. Sci.* **156**, 14-46

Bolaños, J.P., Peuchen, S., Heales, S. J. R., Land, J.M. and Clark, J. B. (1994) Nitric oxide-mediated inhibition of the mitochondrial respiratory chain in cultured astrocytes. *J. Neurochem.* **63**, 910-916

Bolaños, J.P., Heales, S. J. R., Land, J.M., and Clark, J.B. (1995) Effect of peroxynitrite on the mitochondrial respiratory chain: differential susceptibility of neurones and astrocytes in primary culture. *J. Neurochem.* **64**, 1965-1972

Bolaños, J. P., Heales, S. J. R., Peuchen, S., Barker, J. E., Land, J. M. and Clark, J. B. (1996) Nitric oxide mediated mitochondrial damage: a potential neuroprotective role for glutathione. *Fr. Rad. Biol. Med.* **21**, 995-1001

Borst, P. (1963) Hydrogen transport and transport metabolites. In: Funktionelle und morphologische Organisation der Zelle. (Karlson, P., ed.) Springer, Berlin

Boveris, A. and Chance, B. (1973) The mitochondrial generation of hydrogen peroxide. General properties and effect of hyperbaric oxygen. *Biochem. J.* **134**, 707-716

Boveris, A., Cadanas, E. and Stoppani, A.O.M. (1976) Role of ubiquinone in the mitochondrial generation of hydrogen peroxide. *Biochem. J.* **156**, 435-444

Boyer, P.D. (1997) The ATP synthase – a splendid molecular machine. *Ann. Rev. Biochem.* **66**, 717-749

Bradford RH, Shear CL, Chremos AN, Dujovne CA, Franklin FA, Grillo RB, Higgins J, Langendorfer A, Nash DT, Pool JL, et al. (1994) Expanded clinical evaluation of lovastatin (EXCEL) study results: a two-year efficacy and safety follow-up. *Am. J. Cardiol.* **74**, 667-673

Bredt DS, Snyder SH. (1990) Isolation of nitric oxide synthetase, a calmodulin-requiring enzyme. *Proc Natl Acad Sci U S A.* **87**, 682-685.

Breda, P., Lightbody, J., Sato, G., Levine, L. and Sweet, W. (1968) Differentiated rat glial cell strain in tissue culture. *Science* **26**, 370-371

Brismar, T, (1995) Physiology of transformed glial cells *Glia*, **15**, 231-243

Brivet, M., Boutron, A., Slama, A., Costa, C., Thuillier, L., Demaugre, F., Rabier, D., Saudbray, J.M/ and Bonnefont, J.P. (1999) Defects in activation and transport of fatty acids *J. Inher. Metab. Dis.* **22**, 428-441

Brookes, P. S., Land, J. M., Clark, J. B. and Heales, S. J. R. (1998) Peroxynitrite and brain mitochondria: evidence for increased proton leak. *J. Neurochem.* **70**, 2195-2202

Brown, G.C. and Cooper, C.E. (1994) Nanomolar concentrations of nitric oxide reversibly inhibit synaptosomal respiration by competing with oxygen at cytochrome oxidase. *FEBS Lett.* **356**, 295-298

Brown, G.C. and Borutaite, V. (2004) Inhibition of mitochondrial respiratory complex I by nitric oxide, peroxynitrite and S-nitrosothiols. *Biochim. Biophys. Acta.* **1658**, 44-49

Brown, M.S. and Goldstein, J.L. (2004) A tribute to Akira Endo, discoverer of a “penicillin” for cholesterol *Atheroscler. Suppl.* **5**, 13-16

Brudvig, G.W.; Stevens, T.H.; Chan, S.I. (1980) Reactions of nitric oxide with cytochrome c oxidase. *Biochemistry* **19**: 5275-5285

Brummelkamp, T. R., Bernards, R. and Agami, R. (2002) A system for stable expression of short interfering RNAs in mammalian cells. *Science* **296**, 550-553

Buga GM, Gold ME, Fukuto JM, Ignarro LJ. (1991) Shear stress-induced release of nitric oxide from endothelial cells grown on beads. *Hypertension.* **17**, 187-93.

Cammer, W. (2002) Protection of cultured oligodendrocytes against tumour necrosis factor- α by the antioxidants coenzyme Q₁₀ and *N*-acetyl cysteine. *Brain. Res. Bull.* **6**, 587-592

Canevari, L., Clark, J.B. and Bates, T. E. (1999) Beta-amyloid fragment 25-35 selectively decreases complex IV activity in isolated mitochondria. *FEBS Lett.* **457**, 131-134

Canevari, L., Casley, C.S., Sharpe, M.A., and Land, J.M. (2001) Amyloid β peptide inhibits mitochondrial enzymes and function. *J. Neurochem.* **76**, (suppl. 1) 30

Cao, B-J. and Reith M. E. A. (2002) Nitric oxide inhibits uptake of dopamine and N-methyl-4-phenylpyridinium (MPP(+)) but not release of MPP(+) in rat C6 glioma cells expressing human dopamine transporter. *Br. J. Pharm.* **137**, 1155-1162

Casley, C.S., Sharpe, M.A., Land, J.M., Clark, J.B. and Canevari, L. (2001) β -Amyloid causes loss of neuronal mitochondrial function. *J. Neurochem.* **76**, (suppl. 1): 12

Casley, C.S., Canevari, L., Land, J.M., Clark, J.B. and Sharpe, M.A. (2002) β -Amyloid inhibits integrated mitochondrial respiration and key enzyme activities. *J. Neurochem.* **80**, 91-100

Cassina, A. and Radi, R. (1996) Differential inhibitory action of nitric oxide and peroxynitrite on mitochondrial electron transport. *Arch. Biochem. Biophys.* **328**, 309-316

Chan, K.K.W., Oza, A. and Sui, L.L. (2003) The statins as anticancer agents. *Clin. Cancer Res.* **9**, 10-19

Chen, L., Haught, W.H., Yang, B., Saldeen, T.G., Parathasarathy, S. and Mehta, J.L. (1997) Preservation of endogenous antioxidant activity and inhibition of lipid peroxidation as common mechanisms of antiatherosclerotic effects of vitamin E, lovastatin and amlodipine. *J. Am. Coll. Cardiol.* **30**, 569-75.

Chen, Q., Vazquez, E.J., Moghaddas, S., Hoppel, C.L. and Lesnefsky, E.J. (2003) Production of reactive oxygen species by mitochondria. Central role of complex III. *J. Biol. Chem.* **278**, 36027-36031

Cho, H.J., Xie, Q.W., Calaycay, J., Mumford, R.A., Swiderek, K.M., Lee, T.D. and Nathan, C. (1992) Calmodulin is a subunit of nitric oxide synthase from macrophages. *J. Exp. Med.* **176**, 599-604.

Cidad, P., Almeida, A. and Bolaños, J.P. Inhibition of mitochondrial respiration by nitric oxide rapidly stimulates cytoprotective Glut3-mediated glucose uptake through 5'-AMP activated protein kinase. *Biochem. J.* [in press]

Clark, J. B., Bates, T. E., Boakye, P., Kuimov, A. and Land, J. M. (1994) Investigation of mitochondrial defects in brain and skeletal muscle. In: Turner A. J., Bachelard, H. S., eds. *Neurochemistry: a practical approach*. 2nd ed. Oxford University Press: Oxford, 151-174

Cleeter, M.W., Cooper, J.M. and Schapira, A.H.V. (1992) Irreversible inhibition of mitochondrial complex I by 1-methyl-4-phenylpyridinium: evidence for free radical involvement. *J. Neurochem.* **58**, 786-789

Cleeter, M.J.W., Cooper, J.M., Darley-Usmar, V.M, Moncada, S. and Schapira, A.H.V. (1994) Reversible inhibition of cytochrome c oxidase the terminal enzyme of the mitochondrial respiratory chain by nitric oxide. Implications for neurodegenerative diseases. *FEBS Lett.* **345**, 50-54

Clementi, E., Brown, G.C., Feelisch, M. and Moncada, S. (1998) Persistent inhibition of cell respiration by nitric oxide: crucial role of S-nitrosylation of mitochondrial complex I and protective role of glutathione. *Proc. Natl. Acad. Sci.* **95**, 7631-7636

Consentino, F., Barker, J.E., Brand, M.P., Heales, S.J., Werenner, E. R., Tippins, J.R., West, N., Channon, K.M., Volpe, M., and Luscher, T.F. (2001) Reactive oxygen species mediate endothelium-dependant relaxations in tetrahydrobiopterin deficient mice. *Arterioscler. Thromb. Vasc. Biol.* **21**, 496-502

Constantinescu, A., McGuire, J.J., and Packer L. (1994) Interaction between ubiquinones and vitamins in membranes and cells. *Mol. Aspects Med.* **15**, s57-65

Coon M.J., Hoeven, T.A., Kaschnitz, R.M. and Strobel, H.W. (1973) Biochemical studies on cytochrome P-450 solubilized from liver microsomes: partial purification and mechanism of catalysis. *Ann. N. Y. Acad. Sci.* **212**, 449-457.

Crane, D.I. and Beinert, H. (1956) On the mechanism of dehydrogenation of fatty acyl derivatives of coenzyme A II. The electron transferring flavoprotein. *J. Biol. Chem.* **218**, 717-731

Crane, F.L., Hatefi, Y., Lester, R.L. and Widmer, C. (1957) Isolation of a quinone from beef heart mitochondria. *Biochim. Biophys. Acta.* **25**, 220-221

Crane, F.L. (2001) Biochemical functions of coenzyme Q10. *J. Am. Coll. Nutr.* **20**, 591-598

Crofts, A.R. (2004) The cytochrome *bc*₁ complex: function in the context of structure. *Annu. Rev. Physiol.* **66**, 689-733

Crompton, M. and Costi A. (1988) Kinetic evidence for a heart mitochondrial pore activated by Ca²⁺, inorganic phosphate and oxidative stress. A potential mechanism for mitochondrial dysfunction during cellular Ca²⁺ overload. *Eur. J. Biochem.* **178**, 489-501

Crompton, M. (1999) The mitochondrial permeability transition pore and its role in cell death. *Biochem. J.* **341**, 233-249

Cucchiara, B. and Kasner, S.E. (2001) Use of statins in CNS disorders. *J. Neurol. Sci.* **187**, 81-89

Dahl, D. and Bignami, A. (1977) Preparation of antisera to neurofilament protein from chicken brain and human sciatic nerve. *J. Comp. Neurol.* **176**, 645-658

Dallner, G. and Sindelar, P. J. (2000) Regulation of ubiquinone metabolism. *Free Radic. Biol. Med.* **29**, 285-294

Davey, G. P., Canevari, L. and Clark, J. B. (1997) Threshold effects in synaptosomal and nonsynaptic mitochondria from hippocampal CA1 and paramedian neocortex brain regions. *J. Neurochem.* **69**, 2564-2570

Davey, G.P., Peuchen, S. and Clark, J.B. (1998) Energy thresholds on brain mitochondria. *J. Biol. Chem.* **273**, 12753-12757

Davies, J.A., Lodomery, M., Hohenstein, P., Michael, L., Shafe, A., Spraggon, L. and Hastoe, N. (2004) Development of an siRNA-based method for repressing specific genes in renal organ culture and its use to show that the Wt1 tumour suppressor is required for nephron differentiation. *Hum. Mol. Genet.* **13**, 235-246

Dawson, V. L., Dawson, T. M., London, E.D., Bredt, D. S. and Snyder, S.H (1991) Nitric oxide mediates glutamate neurotoxicity in primary cortical cultures. *Proc. Natl. Acad. Sci. USA* **11**, 6368-6371

Dawson, V. L. and Dawson, T. M. (1996) Nitric oxide neurotoxicity. *J. Chem. Neuroanat.* **10**, 179-190

Devroe, E. and Silver, P.A. (2002) Retrovirus-delivered siRNA. *BMC Biotechnology* **2**; 15
<http://www.biomedcentral.com/1472-6750/2/15>

Di Giovanni, S., Mirabella, M., Spinazzola, A., Crociani, P., Silvestri, G., Broccolini, A., Tonali, P., Di Mauro, S. and Servidei, S. (1997) Coenzyme Q₁₀ reverses pathological phenotype and reduces apoptosis in familial CoQ₁₀ deficiency *Neurology* **57**, 515-518

Dimitroulakos J. and Yeger, H. (1996) HMG-CoA reductase mediates the biological effects of retinoic acid on human neuroblastoma cells: lovastatin specifically targets P-glycoprotein-expressing cells. *Nat. Med.* **2**, 326-333

Dimitroulakos, J., Hohynek, D., Backway, K.L., Hedley, D.W., Yeger, H., Freedman, M.H., Minden, M.D. and Penn L.Z. (1999) Increased sensitivity of acute myeloid leukemias to lovastatin-induced apoptosis: a potential therapeutic approach. *Blood* **93**, 1308-1318

Dorheim, M.A.; Tracey, W.R.; Pollock, J.S.; Grammas, P. (1994) Nitric oxide synthase activation is elevated in brain microvessels in Alzheimer's disease. *Biochem. Biophys. Res. Commun.* **205**, 659-665

Draganov, D.I., Stetson, P.I., Watson, C.E., Billecke, S.S. and La Du, B.N. (2000) Rabbit serum paraoxonase 3 (PON3) is a high density lipoprotein-associated lactonase and protects low density lipoprotein against oxidation. *J. Biol. Chem.* **43**, 33435-33442

DuBridge, R.B., Tang, P., Hsia, H.C., Leong, P-M., Miller, J.H., Calos, M.P. (1987) Analysis of mutation in human cells by using an Epstein-Barr virus shuttle system. *Mol. Cell. Biol.* **7**, 379-387

Duncan, A.J. and Heales, S.J.R. (2005) Nitric oxide and neurological disorders *Mol. Aspects Med.* **26**, 67-96

Eaton, S., Skinner, R., Hale, J.P., Pourfarzam, M., Roberts, A., Price, L. and Bartlett, K. (2000) Plasma coenzyme Q₁₀ in children and adolescents undergoing doxorubicin therapy. *Clin. Chim. Acta* **302**, 1-9

Echtay, K.S., Winkler, E. and Klingenberg, M. (2000) Coenzyme Q is an obligatory cofactor for uncoupling protein function. *Nature* **408**, 609-613

Echtay, K.S., Winkler, E. Frischmuth, K. and Klingenberg, M. (2001) Uncoupling proteins 2 and 3 are highly active H⁺ transporters and highly nucleotide sensitive when activated by coenzyme Q (ubiquinone). *Proc. Natl. Acad. Sci. USA.* **98**, 1416-1421

Echtay, K.S., Roussel, D., St-Pierre, J., Jekabsens, M.B., Cadenas. S. Stuart, J.A., Harper, J.A., Roebuck, S.J., Morrison, A., Pickering, S., Clapham, J.C. and Brand, M. (2002a) Superoxide activates mitochondrial uncoupling proteins *Nature* **415**, 96-99

Echtay, K.S., Murphy, M.P., Smith, R.A.J., Talbot, D.A. and Brand, M.D. (2002b) Superoxide activates mitochondrial uncoupling protein 2 from the matrix side. *J. Biol. Chem.* **49**, 47129-47135

Edlund, C., Holmberg, K., Dallner, G., Norrby, E. and Kristensson, K. (1994) Ubiquinone-10 protects neurons from virus-induced degeneration. *J. Neurochem.* **63**, 634-639

Edlund, P. O. (1988) Determination of Coenzyme Q₁₀, α-tocopherol and cholesterol in biological samples by coupled column liquid chromatography with coulometric and ultraviolet detection. *J. Chromatogr.* **425**, 87-97

Edwards, P.A., Lan, S.-F. and Fogelman, A.M. (1983) Alterations in the rates of synthesis and degradation of rat liver 3-hydroxy-3-methylglutaryl coenzyme A reductase produced by cholestyramine and mevinolin. *J. Biol. Chem.* **258**, 10219-10222

Elbashir, S.M., Harborth, J., Lendeckel, W., Yalcin, A., Weber, K., and Tuschl, T. (2001) Duplexes of 21-nucleotide RNAs mediate RNA interference in cultured mammalian cells. *Nature*, **411**, 494-498

Elbashir, S.M., Martinez, J., Patkaniowska, A., Lendeckel, W., and Tuschl, T. (2001b) Functional anatomy of siRNAs for mediating efficient RNAi in *Drosophila melanogaster* embryo lysate. *EMBO J.* **20**, 6877-6888

Endo, A., Kuroda, M. and Tazawa, K. (1976) Competitive inhibition of 3-hydroxy-3-methylglutaryl coenzyme A reductase by ML-236A and ML-236B fungal metabolites, having hypocholesterolemic activity. *FEBS Lett.* **72**, 323-326

Ernster, L. and Dallner, G. (1995) Biochemical, physiological and medical aspects of ubiquinone function. *Biochim. Biophys. Acta* **1271**, 195-204

Fernandez-Ayala, D.J.M., Lopez-Lluch, G., Garcia-Valdes, M., Arroyo, A. and Navas, P. (2005) Specificity of coenzyme Q₁₀ for a balanced function of respiratory chain and endogenous ubiquinone synthesis in human cells. *Biochim. Biophys. Acta* **1706**, 174-183

Festenstein, G.N., Heaton, F.W., Lowe, J.S. and Morton, R. A. (1955) A constituent of the unsaponifiable portion of the animal tissues lipids (λ_{max} 272 mμ) *Biochem. J.* **59**, 558-566

Feinstein, D. L., Galea, E., Roberts, S., Berquist, H., Wang, H. and Reis, D. J. (1994) Induction of nitric oxide synthase in rat C6 glioma cells. *J. Neurochem.*, **62**, 315-321

Fire, A., Xu, S., Montgomery, M.K., Kostas, S.A., Driver, S.E., and Mello, C.C. (1998) Potent and specific genetic interference by double-stranded RNA in *Caenorhabditis elegans*. *Nature*, **391**, 806-811

Folkers, K., Langsjoen, P., Willis, R., Richardson, P., Xia, L-J. and Ye, C-Q (1990) Lovastatin decreases coenzyme Q levels in humans. *Proc. Natl. Acad. Sci. USA* **87**, 8931-8934

Foster, S. J. and Perkins, J. P. (1977) Glucocorticoids increase the responsiveness of cells in culture to prostaglandin E₁. *Proc. Natl. Acad. Sci. USA* **74**, 4716-4820

Frey, T. G. and Mannella, C. A. (2000) The internal structure of mitochondria. *Trends Biochem. Sci.* **25**, 319-324

Friedrich, T., van Heek, P., Leif, H., Ohnishi, T., Forche, E., Kunze, B., Jansen, R., Trowitsch-Keinast W., Hofle, G., Reichbach, H. *et al.* (1994) Two binding sites of inhibitors in NADH: ubiquinone oxidoreductase (complex I). Relationship of one site with the ubiquinone-binding site of bacterial glucose: ubiquinone oxidoreductase. *Eur. J. Biochem.* **219**, 691-698

Friedrich, T. and Böttcher, B. (2004) The gross structure of the respiratory complex I: a Lego system. *Biochim. Biophys. Acta.* **1608**, 1-9

Galea, E., Feinstein, D. L. and Reis, D. J. (1992) Induction of calcium-independent nitric oxide synthase activity in primary rat glial cultures. *Proc. Natl. Acad. Sci. USA* **89**, 10945-10949

Gao, X., Wen, X., Esser, L., Quinn, B., Yu, L., Yu, C-A. and Xia, D. (2003) Structural basis for the quinone reduction in the bc_1 complex: a comparative analysis of crystal structures of mitochondrial cytochrome bc_1 with bound substrate and inhibitors at the Q_1 site. *Biochemistry.* **42**, 9067-9080

Gatenby, R.A. and Gillies, R.J. (2004) Why do cancers have high aerobic glycolysis? *Nat. Rev. Cancer*, **4**, 891-899

Gegg, M. E., Beltran, B., Salas-Pino, S., Bolaños, J. P., Clark, J. B., Moncada, S. and Heales, S. J. R. (2003) Differential effect of nitric oxide on glutathione metabolism and mitochondrial function in astrocytes and neurones: implications for neuroprotection /neurodegeneration? *J. Neurochem.* **86**, 228-237 .

Gegg, M.E. (2003) PhD Thesis University of London

Gegg, M.E., Clark, J.B. and Heales, S.J.R. (2005) Co-culture of neurones with glutathione deficient astrocytes leads to increased neuronal susceptibility to nitric oxide and increased glutamate-cysteine ligase activity. *Brain Res.* **1036**, 1-6

Gerson, R.J., MacDonald, J.S., Alberts, A.W., Kornbrust, D.J., Majka, J.A., Stubbs, R.J. and Bokelman, D.L. (1989) Animal safety and toxicology of simvastatin and related hydroxy-methylglutaryl-coenzyme A reductase inhibitors. *Am. J. Med.* **87**, 28S-36S

Giason, B.I., Duda, J.E., Murray, I. V. J., Chen, Q. P., Souza, J. M., Hurtig, H. I., Ischiropoulos, H., Trojanowski, J., Q. and Lee, V. M. Y. (2000) Oxidative damage linked to neurodegeneration by selective α -synuclein nitration in synucleinopathy. *Science* **290**, 985-989

Gillespie, J.S., Liu, X.R. and Martin, W. (1989) The effects of L-arginine and N^G-monomethyl L-arginine on the response of the rat anococcygeus muscle to NANC nerve stimulation. *Br. J. Pharmacol.* **98**, 1080-1082

Girard, J., Ferre, P., Pegorier, J.P. and Duee P.H. (1992) Adaptations of glucose and fatty acid metabolism during perinatal period and suckling-weaning transition. *Physiol. Rev.* **72**, 507-62

Glinka, Y., Tipton, K.F. and Youdim, M.B. (1996) Nature of inhibition of mitochondrial respiratory complex I by 6-Hydroxydopamine. *J. Neurochem.* **66**, 2004-2010.

Gluck, M.R., Youngster, S.K., Ramsay, R.R., Singer, T.P. and Nicklas WJ. (1994) Studies on the characterization of the inhibitory mechanism of 4'-alkylated 1-methyl-4-phenylpyridinium and phenylpyridine analogues in mitochondria and electron transport particles. *J. Neurochem.* **63**, 655-661.

Gluck M, Ehrhart J, Jayatilleke E, Zeevalk GD. (2002) Inhibition of brain mitochondrial respiration by dopamine: involvement of H₂O₂ and hydroxyl radicals but not glutathione-protein-mixed disulfides. *J. Neurochem.* **82**, 66-74.

Gomez-Diaz, C., Bello, R.I., Lopez-Lluch, G., Forthoffer, N., Navas, P. and Villalba, J.M. (2003) Antioxidant response induced by serum withdrawal protects HL-60 cells against inhibition of NAD(P)H;quinone oxidoreductase 1. *Biofactors* **18**, 219-228

Gomez-Diaz, C, Burón, M.I., Alcaín, F.J., González-Ojeda, R., González-Reyes, J.A., Bello, R.I., Herman, M.D., Navas, P and Villalba, J.M. (2003b) Effect of dietary coenzyme Q and fatty acids on the antioxidant status of rat tissues. *Protoplasma* **221**, 11-17

Good, P.F., Hsu, A., Werner, P., Perl, D.P. and Olanov, C.W. (1998) Protein nitration in Parkinson's disease. *J. Neuropathol. Exp. Neurol.* **57**, 338-342

Götz, M. E., Gerstner, A., Harth, R., Dirr, A., Janetzky, B., Kuhn, W., Riederer, P. and Gerlach, M. (2000) Altered redox state of platelet coenzyme Q₁₀ in Parkinson's disease. *J. Neural Trans.* **107**, 41-48

Graham, F.L., Smiley, J., Russell, W.C., Nairn, R. (1977) Characteristics of a human cell line transformed by DNA from human adenovirus type 5. *J. Gen. Virol.* **36**, 59-74

Green, L.C., Wagner, D.A., Glogowski, J., Skipper, P.L., Wishnock, J.S. and Tannenbaum, S.P. (1982) Analysis of nitrate, nitrite and [N- ¹⁵N]-labelled nitrate in biological fluids. *Anal. Biochem.* **126**, 131-138

Gresser, M.J., Myers, J.A. and Boyer, P.D. (1982) Catalytic site cooperativity of beef heart mitochondrial F₁ adenosine triphosphatase. Correlations of initial velocity, bound intermediate, and oxygen exchange measurements with an alternating three-site model. *J. Biol. Chem.* **257**, 12030-12038

Grigorieff, N. (1998) Three-dimensional structure of bovine NADH : ubiquinone oxidoreductase (complex I) at 22Å in ice. *J. Mol. Biol.* **277**, 1033-1046

Guénebaut, V., Vincentelli, R., Mills, D., Weiss, H. and Leonard, K.R. (1997) Three-dimensional structure of NADH-dehydrogenase from *Neurospora crassa* by electron microscopy and conical tilt reconstruction. *J. Mol. Biol.* **265**, 409-418

Haltia, T., Finel, M., Harms, N., Nakari, T., Raitio, Wilkström, M and Sraste, M. (1989) Deletion of the gene for subunit III leads to defective assembly of bacterial cytochrome oxidase. *EMBO J* **8**, 3571-3578

Halliwell, B, and Gutteridge, J.M.C. (1999) Free Radicals in Biology and Medicine. 3rd edition. Oxford University Press, Oxford.

Han, S., Ching Y.C. and Eousseau, D.L. (1990) Ferryl and hydroxy intermediates in the reaction of oxygen with reduced cytochrome c oxidase. *Nature*, **348**, 89-90

Han. D., Williams, E. and Cadenas, E. (2001) Mitochondrial respiratory chain-dependent generation of superoxide anion and its release into the intermembrane space. *Biochem. J.* **353**, 411-416

Hannon, G.J. (2002) RNA interference. *Nature* **418**, 244-251

Haslam, G., Wyatt, D. and Kitos, P.A. (2000) Estimating the number of viable animal cells in multi-well cultures based on their lactate dehydrogenase activities. *Cytotechnology* **32**, 63-75

Haynes, V., Elfering, S.L., Squires, R.J., Traaseth, N., Solien, J., Ettl, A. and Giulivi C. (2004) Mitochondrial nitric-oxide synthase: role in pathophysiology *IUBMB Life* **55**, 599-603

Heales, S. J. R., Hargreaves, I. P., Olpin, S. E., Guthrie, P., Bonham, J. R., Morris, A. A. M., Clark, J. B. and Land, J. M. (1995) Diagnosis of mitochondrial electron transport chain defects in small muscle biopsies. *J. Inher. Metab. Dis.* **19**, (Suppl. 1), p76

Heales, S. J. R., Bolaños, J. P., Stewart, V. C., Brookes, P., S., Land, J. M. and Clark, J.B. (1999) Nitric oxide, mitochondria and neurological disease. *Biochim. Biophys. Acta* **1410**, 215-228

Heales, S. J. R., Gegg, M. E. and Clark, J. B. (2002) Oxidative phosphorylation: structure, function and intermediary metabolism. *Int. Rev. Neurobiol.* **53**, 25-56

Heales, S.J.R., Lam, A.A.J., Duncan, A.J. and Land J.M. (2004) Neurodegeneration or neuroprotection: the pivotal role of astrocytes. *Neurochem. Res.* **29**, 513-519

Heinzel, B., John, M., Klatt, P. and Meyer, B. (1992) Ca^{2+} /calmodulin-dependant formation of hydrogen peroxide by brain nitric oxide synthase. *Biochem J.* **281**, 627-630

Hibbs, J.B. Jr, Taintor, R.R., Vavrin, Z. and Rachlin, E.M.. (1988) Nitric oxide: a cytotoxic activated macrophage effector molecule. *Biochem. Biophys. Res. Commun.* **157**, 87-94.

Hirawake, H., Taniwaki, M., Tamura, A., Amino, H., Tomitsuka, E. and Kita, K. (1999) Characterisation of the human SDHD gene encoding the small subunit of cytochrome b

(cybS) in mitochondrial succinate-ubiquinone oxidoreductase. *Biochim. Biophys. Acta*, **1412**, 295-300

Horsefield, R., Yankovskaya, V., Törnroth, S., Luna-Chavez- C., Stambouli, E., Barber, J., Byrne, B., Cecchini, G. and Iwata, S. (2003) Using rational screening and electron microscopy to optimize the crysallisation of succinate: ubiquinone oxidoreductase from *Escherichia coli*. *Acta. Cryst.* **D59**, 600-602

Huang, K.C., Chen, C.W., Chen, J.C. and Lin W.W. (2003) HMG-CoA reductase inhibitors inhibit inducible nitric oxide synthase gene expression in macrophages. *J. Biomed. Sci.* **10**, 396-405

Huertas, J.R., Battino, M., Lenaz, G. and Mataix F.J. (1991) Changes in mitochondrial and microsomal rat liver coenzyme Q₉ and Q₁₀ content induced by dietary fat and exogenous lipid peroxidation. *FEBS Lett.* **287**, 89-92

Hunot S, Boissiere F, Faucheux B, Brugg B, Mouatt-Prigent A, Agid Y, Hirsch EC. (1996) Nitric oxide synthase and neuronal vulnerability in Parkinson's disease. *Neuroscience* **72**, 355-363.

Hunter, T., Hunt, T. and Jackson, R.J. (1975) The characteristics of inhibition of protein synthesis by double-stranded ribonucleic acid in reticulocyte lysates. *J. Biol/ Chem.* **250**, 409-417

Huntingdon Study Group (2001) A randomised, placebo-controlled trial of coenzyme Q₁₀ and remacemide in Huntington's disease. *Neurology* **57**, 397-403

Ignarro, L. J., Fukuto, J. M., Griscavage, J. M., Rogers, N. E., and Burns, R. E. (1993) Oxidation of nitric oxide in aqueous solution to nitrite but not nitrate: comparison with enzymatically formed nitric oxide from L-arginine. *Proc. Natl. Acad. Sci. USA* **90**, 8103-8107

IUPAC-IUB Commission on Biochemical Nomenclature (1975) The nomenclature of lipids. *Eur. J. Biochem.* **53**, 15-18

Ikeda, U., Shimpo, M., Ikeda, M., Minota, S., and Shimada, K. (2001) Lipophilic statins augment inducible nitric oxide synthase expression in cytokine-stimulated cardiac myocytes. *J. Cardiovasc. Pharm.* **38**, 69-77

Ishizaki, Y., Cheng, L., Mudge, A.W. and Raff, M.C. (1995) Programmed cell death by default in embryonic cells, fibroblasts and cancer cells. *Mol. Biol. Cell.* **6**, 1443-1458

Iverson, T.M., Luna-Chavez, C., Cecchini G. and Rees, D.C. (1999) Structure of the *Escherichia coli* fumarate reductase respiratory complex. *Science* **284**, 1969

Iwata-Ichikawa, E., Kondo, Y., Miyazaki, I., Asanuma, M. and Ogawa, N. (1999) Glial cells protect neurons against oxidative stress via transcriptional up-regulation of the glutathione synthesis. *J. Neurochem.* **72**, 2334-44

Jekabsone, A., Ivanoviene, L., Brown, G.C. and Borutaite, V. (2003) Nitric oxide and calcium together inactivate mitochondrial complex I and induce cytochrome *c* release. *J. Mol. Cell. Cardiol.* **35**, 803-809

Jenner, P., Dexter, D.T., Sian, J., Schapira, A.H.V. and Marsden, C.D. (1992) Oxidative stress as a cause of nigral cell death in Parkinson's Disease and incidental Lewy Body Disease. *Ann. Neurology* **32**, S82-S87

Jick, H., Zornberg, G.L., Jick, S.S. Seshadri, S. and Drachman, D.A (2000) Statins and the risk of dementia. *The Lancet*, **356**, 1627-1631

Jimenez-Jimenez, F. J., Molina, J. A., de Bustos F., Garcia-Redondo, A., Gomez-Escalonilla, C., Martinez-Salio, A., Berbel, A., Camacho, A., Zurdo, M., Barcenilla, B., Enriquez de Salamanca, R. and Arenas, J. (2000) Serum levels of coenzyme Q₁₀ in patients with Parkinson's disease. *J. Neural. Transm.* **107**, 177-181

Johanssen, T. and Clarke, T.F. (2000) Isolation and functional expression of human COQ3, a gene encoding a methyltransferase required for ubiquinone biosynthesis. *J. Biol. Chem.* **275**, 12381-12387

Jones, S.W., de Souza, P. and Lindsay, M.A. (2004) siRNA for gene silencing: a route to drug target discovery. *Curr. Opin. Pharmacology* **4**, 522-527

Kagan, V.E., Serbinova, E. A, Koynova, G. M., Kitanova, S. A., Tyurin, V. A., Stoytchev, T. S., Quinn, P. J and Packer, L. (1990) Antioxidant action of ubiquinol homologues with different isoprenoid chain lengths in biomembranes. *Free Radic. Biol. Med.* **9**, 117-126

Kalen, A., Appelkvist, E.L. and Dallner, G. (1989) Age-related changes in the lipid compositions of rat and human tissues. *Lipids* **24**, 579-584

Kanai AJ, Pearce LL, Clemens PR, Birder LA, VanBibber MM, Choi SY, de Groat WC, Peterson J. (2001) Identification of a neuronal nitric oxide synthase in isolated cardiac mitochondria using electrochemical detection. *Proc. Natl. Acad. Sci. USA.* **98**, 14126-1431.

Kanai A, Epperly M, Pearce L, Birder L, Zeidel M, Meyers S, Greenberger J, de Groat W, Apodaca G, Peterson J. (2003) Differing roles of mitochondrial nitric oxide synthase in cardiomyocytes and urothelial cells *Am. J. Physiol. Heart Circ. Physiol.* **286**, H13-21.

Kato, T., Duffey, D.C., Ondrey, F.G., Dong, G., Chen, Z., Cook, J.A., Mitchell, J.B., and Van Waes, C. (2000) Cisplatin and radiation sensitivity in human head and neck squamous carcinomas are independently modulated by glutathione and transcription factor NF- κ B. *Head Neck* **22**, 748-759

Kamzalov, S., Sumien, N., Forster, M.J. and Sohal R.S. (2003) Coenzyme Q intake elevates the mitochondrial and tissue levels of Coenzyme Q and α -tocopherol in young mice. *J. Nutr.* **133**, 3175-3180

Keilin, D. and Hartree, H.F. (1939) Cytochrome and cytochrome oxidase. *Proc. Royal Soc. London Series B. Biol. Sci.* **127**, 167-191

Keilhoff, G., and Wolf, G. (1993) Comparison of double fluorescence staining and LDH-test for monitoring cell viability in vitro. *Neuroreport* **18**, 125-132

Kennerdell J.R. and Carthew, R.W. (2000) Heritable gene silencing in *Drosophila* using double stranded RNA. *Nat. Biotechnology* **18**, 896-898

Kikuchi, T., Nagata, Y. and Abe, T. (1997) *In vitro* and *in vivo* antiproliferative effects of simvastatin, an HMG-CoA reductase inhibitor, on human glioma cells. *J. Neurooncol.* **34**, 233-239

King, T.S. (1967) Preparations of succinate-cytochrome c reductase and the cytochrome b-c₁ particle, and reconstitution of succinate-cytochrome c reductase. *Meth.s Enzymol.* **10**, 217-235

Kish, S.J., Bergeron, C., Rajput, A., Dozic, S., Mastrogiacomo, F., Chang, L., Wilson, J.M., DiStefano, J.N., and Nobrega, J.N. (1992) Brain cytochrome oxidase in Alzheimers disease. *J. Neurochem.* **59**, 776-779

Klingenberg, M., Winkler, E. and Echtay, K. (2001) Uncoupling protein, H⁺ transport and regulation. *Biochem. Soc. Trans.* **29**, 806-811

Knowles, R.G., Palacios, M., Palmer, R.M. and Moncada S. (1989) Formation of nitric oxide from L-arginine in the central nervous system: a transduction mechanism for stimulation of the soluble guanylate cyclase. *Proc. Natl. Acad. Sci. USA.* **86**, 5159-5162.

Koh, J.Y. & Choi D.W. (1987) Quantitative determination of glutamate-mediated cortical neuronal injury in cell culture by lactate dehydrogenase efflux assay. *J. Neurosci. Methods* **20**, 83-90

Koshimura, K., Murakami, Y., Tanaka, J. and Kato, Y. (2000) The role of 6R-tetrahydrobiopterin in the nervous system. *Prog. Neurobiol.* **61**, 415-438

Krebs, H. A. and Henseleit, K. (1932) Untersuchungen über die Harnstoffbildung im Tierkörper. [Hoppe-Seyler's] Zeitschrift für physiologische Chemie, **210**, 33-46.

Krebs, H.A. and Johnson W.A. (1937) The role of citric acid in intermediate metabolism in animal tissues. *Enzymologica*, **4**, 148-156. Subsequently reprinted: (1980) *FEBS. Lett.* **117(Suppl.)**, K2-K10

Kröger A. and Klingenberg, M. (1973) The kinetics of the redox reactions of ubiquinone related to the electron-transport activity in the respiratory chain. *Eur. J. Biochem.* **34**, 358-368

Kuroda, M., Tsujita Y., Tanzawa, K. and Endo, A. (1979) Hypolipidemic effects in monkeys of ML-236B, a competitive inhibitor of 3-hydroxy-3-methylglutaryl coenzyme A reductase. *Lipids* **14**, 585-589

Kurreck, J. (2003) Antisense technologies. *Eur J. Biochem.* **270**, 1628-1644

Kwong, L. K., Kamzalov, S., Rebrin, I., Bayne, A-C. V., Jana C. K., Morris, P., Forster, M. J. and Sohal, R. S. (2002) Effects of Coenzyme Q₁₀ administration on its tissue concentrations, mitochondrial oxidant generation and oxidative stress in the rat. *Fr. Rad. Biol. Med.* **33**, 627-638

Lacza, Z., Snipes, J.A., Zhang, J., Horvath, E.M., Figueroa, J.P., Szabo, C. and Busija, D.W. (2003) Mitochondrial nitric oxide synthase is not eNOS, nNOS or iNOS. *Free Radic. Biol. Med.* **35**, 1217-1228.

Lacza, Z., Horn, T.F., Snipes, J.A., Zhang, J., Roychowdhury, S., Horvath, E.M., Figueroa, J.P., Kollai, M., Szabo, C, and Busija, D.W. (2004) Lack of mitochondrial nitric oxide production in the mouse brain. *J. Neurochem.* **90**, 942-951.

Lai, J., C. and Clark, J.B. (1979) Preparation of synaptic and non-synaptic mitochondria from mammalian brain. *Methods Enzymol.* **55**, 51-60

Lam, A.J. (2004) PhD Thesis; University of London

Lancaster CR, Kröger A, Auer M, Michel H. (1999) Structure of fumarate reductase from *Wolinella succinogenes* at 2.2 Å resolution. *Nature* **402**, 377-85.

Langan, T.J., Iimori, Y., White, G. and Volpe, J.J. (1987) Regulation of sterol synthesis and 3-hydroxy-3-methylglutaryl coenzyme A reductase by lipoproteins in glial cells in primary culture. *J. Neurosci. Res.* **17**, 361-366

Lass, A., Agrawal, S. and Sohal, R. S. (1997) Mitochondrial ubiquinone homologues, superoxide radical generation, and longevity in different mammalian species. *J. Biol. Chem.* **272**, 19199-19204

Lass, A. and Sohal R. S. (1999) Comparisons of coenzyme Q bound to mitochondrial membrane proteins among different mammalian species. *Fr. Rad. Biol. Med.* **27**, 220-226

Laufts, U. La Fata, V., Plutzky, J. and Liao, J.K. (1998) Upregulation of endothelial nitric oxide synthase by HMG CoA reductase inhibitors. *Circulation* **97**, 1129-1135

Lee, N.S., Dohjima, T., Bauer, G., Li, H., Li, M-J. Ehsani, A., Salvaterra, P. and Rossi, J. (2002) Expression of small interfering RNAs targeted against HIV-1 *Rev* transcripts in human cells. *Nat. Biotechnol.* **20**, 500-505

Lehninger, A.L. (2000) "Principles of Biochemistry"; 3rd edition; Nelson, D.L. and Cox, M.M (eds.). Worth Publishers; New York

Lenaz, G. (2001) A critical appraisal of the mitochondrial coenzyme Q pool. *FEBS. Lett.* **509**, 151-155

Levavasseur, F., Miyadera, H., Sirois, J., Tremblay, M.L., Kita, K., Shoubridge, E, and Hekimi, S. (2001) Ubiquinone is necessary for mouse embryonic development but is not essential for mitochondrial respiration

Li, P., Nijhawan, D. Budihardjo, I., Srinivasula, S.M., Ahmad, M., Alnemri, E.S. and Wang, X. (1997) Cytochrome *c* and dATP dependant formation of Apaf-1/caspase-9 complex initiate an apoptotic protease cascade. *Cell* **91**, 479-489

Lincoln, J., Hoyle, C.H.V. and Burnstock, G. (1997). Nitric oxide in health and disease, 1st ed. Cambridge, Cambridge University Press

Lippitz BE, Halperin EC, Griffith OW, Colvin OM, Honore G, Ostertag CB, Bigner DD, Friedman HS. (1990) L-buthionine-sulfoximine-mediated radiosensitization in experimental interstitial radiotherapy of intracerebral D-54 MG glioma xenografts in athymic mice. *Neurosurgery* **26**, 255-260

Liu, X., Kim, C.N., Yang, J., Jemmerson, R. and Wang, X. (1996) Induction of apoptotic program in cell-free extracts: requirement for dATP and cytochrome *c*. *Cell* **86**, 147-157

Liu, Y., Fiskum, G. and Schubert, D. (2002) Generation of reactive oxygen species by the mitochondrial electron transport chain. *J. Neurochem.* **80**, 780-787

Lönnrot K., Holm, P., Lagerstedt, A., Huhtala, H. and Alho, H. (1988) The effects of lifelong ubiquinone supplementation on the Q₉ and Q₁₀ tissue concentrations and life span of male rats and mice. *Biochem. Mol. Biol. Int.* **44**, 727-737

Lowry, O.H., Rosebrough, N.J., Farr, A.L. and Randall, R.J. (1951) Protein measurement with the Folin phenol reagent. *J. Biol. Chem* **193**, 265-275

Liu, X., Budihardjo, I., Zou, H., Slaughter, C. and Wang X. (1998) Bid, a Bcl2 interacting protein, mediates cytochrome c release from mitochondria in response to activation of cell surface death receptors. *Cell* **94**, 481-490

MacMicking J., Xie, Q.W. and Nathan, C. (1997) Nitric oxide and macrophage function. *Ann. Rev. Immunol.* **15**, 323-350

McCord J.M. and Fridovich, I. Superoxide dismutase. An enzymic function for erythrocuprein (hemocuprein) *J.Biol. Chem.* **244**, 6049-6055

MacIntyre, E. H., Ponten, J. and Vatter, A. E. (1972) The ultrastructure of human and murine astrocytes and of human fibroblasts in culture. *Acta. Pathol. Microbiol. Scanda.* **80**, 267-283

Maestre, I., Joradan, J., Calvo, S., Reig, J.A., Ceña, V., Soria, B., Prentki, M. and Roche, E. (2003) Mitochondrial dysfunction is involved in apoptosis induced by serum withdrawal and fatty acids in the β -cell line INS-1. **144**, 335-345

Maltese, W. A. and Aprille, J.R. (1985) Relation of mevalonate synthesis to mitochondrial ubiquinone content and respiratory function in cultured neuroblastoma cells. *J. Biol. Chem.* **260**, 11524-11529

Maranga, L., Coroadinha, A.S. and Corrondo, M.J.T. (2002) Insect cell culture medium supplementation with fetal bovine serum and bovine serum albumin: effects on baculovirus adsorption and infection kinetics. *Biotechnol. Prog.* **18**, 855-861

Marbois, B.N. and Clarke, C.F. (1996) The COQ7 gene encodes a protein in *Saccharomyces cerevisiae* necessary for ubiquinone biosynthesis. *J. Biol. Chem.* **271**, 2995-3004

Margulis, L. (1981) "Symbiosis in Cell Evolution". W. H. Freeman and Company, San Francisco

Marletta, M.A., Yoon, P.S., Iyengar, R., Leaf, C.D. and Wishnok, J.S. (1988) Macrophage oxidation of L-arginine to nitrite and nitrate: nitric oxide is an intermediate. *Biochemistry* **27**, 8706-8711.

Martinou, J.C. and Green, D.R. (2001) Breaking the mitochondrial barrier. *Nat. Rev. Mol. Cell. Biol.* **2**, 63-67

Marzo, I., Brenner, C., Zamzami, N., Jurgensmeier, J.M., Susin, S.A., Vieira, H.L., Prevost, M.C., Xie, Z., Matsuyama, S., Reed, J.C., Kroemer, G. (1998) Bax and adenine nucleotide translocator cooperate in the mitochondrial control of apoptosis. *Science* **281**, 2027-2031

Mataix, J., Mañas, M., Quiles, J., Battino, M., Lopez-Frias, M. and Huertas, J.R. (1997) Coenzyme Q content depends upon oxidative stress and dietary fat saturation. *Molec. Aspects Med.* **18**, s129-s135

Matsubara, T., Azuma, T., Yoshida, S. and Yamagami, T. (1991) Serum coenzyme Q₁₀ level in Parkinson syndrome. In: Folkers, K., Littarru, G.P., and Yamagami, T. (eds.). *Biomedical and clinical aspects of coenzyme Q*. Elsevier Science, Amsterdam, pp159-166

Matsura, T., Yamada, K. and Kawasaki, T. (1991) Changes in the content and intracellular distribution of coenzyme Q homologs in rabbit liver during growth. *Biochim. Biophys. Acta* **1083**, 277-282

Matsura, T., Yamada, K. and Kawasaki, T. (1992) Difference in antioxidant activity between reduced coenzyme Q₉ and reduced coenzyme Q₁₀ in the cell: studies with isolated rat and guinea pig hepatocytes treated with a water-soluble radical initiator. *Biochim. Biophys. Acta* **1123**, 309-315

Matthews, R. T., Yang, L., Browne, S., Baik, M. and Beal, M. F (1998) Coenzyme Q₁₀ administration increases brain mitochondrial concentrations and exerts neuroprotective effects. *Proc. Natl. Acad. Sci. USA* **95**, 8892-8897

Maurer, H.R. (1986) Towards chemically-defined, serum-free media for mammalian cell culture. In *Animal cell culture -a practical approach*, Freshney, R. I. (ed.) IRL Press, Oxford, Washington DC, pp13-31

Merck & Co. Inc. (2003) MerckFrosst MEVACOR Product monograph (August 2003).

Viewed online on 23rd August 2004 at:

http://www.merckfrosst.ca/e/products/monographs/MEVACOR_879-a_10_03-E.pdf

Menzies, F.M., Cookson, M.R., Taylor, R.W., Turnbull, D.M., Chrzanowska-Lightowlers, Z.M.A., Dong, L., Figlewicz, D.A. and Shaw, P.J. (2002) Mitochondrial dysfunction in a cell culture model of familial amyotrophic lateral sclerosis. *Brain*, **125**, 1522-1533

Michel, H. (1998) The mechanism of proton pumping by cytochrome c oxidase. *Proc. Natl. Acad. Sci.* **95**, 12819-12824

Minden, M.D., Dimitroulakos, J., Nohynek, D. and Penn, L.Z. (2001) Lovastatin induced control of blast cell growth in an elderly patient with acute myeloblastic leukemia. *Leuk. Lymphoma*, **40**, 659-662

Mitchell, G.A., Kassovska-Bratinova, S., Boukaftane, Y., Robert, M.F., Wang, S.P., Ashmarina, L., Lambert, M., Lapierre, P. and Potier, E. (1995) Medical aspects of ketone body metabolism. *Clin. Invest. Med.* **18**, 193-216.

Mitchell P. (1961) Coupling of phosphorylation to hydrogen and electron transfer by a chemiosmotic type mechanism. *Nature* **191**, 144-148

Mitchell, P. and Moyle, J. (1969) Translocation of some anions, cations and some acids in rat liver mitochondria. *Eur. J. Biochem.* **9**, 149-155

Mitchell, P. (1975) The protonmotive Q cycle: a general formulation. *FEBS Lett.* **59**, 137-139

Mitrovic, B., Ignarro, L.J., Montestruque, S., Smoll, A. and Merrill, J.E. (1994) Nitric oxide as a potential pathological mechanism in demyelination: its differential effects on primary glial cells *in vitro*. *Neuroscience* **61**, 575-585

Miyadera, H., Amino, H., Hiraishi, A., Taka, H., Murayama, K., Miyoshi, H., Sakamoto, K., Ishii, N., Hekimi, S. and Kita K. (2001) Altered quinone biosynthesis in the long-lived *clk-1* mutants of *caenorhabditis elegans*. *J. Biol. Chem.* **276**, 7713-7716

Miyagishi, M. and Taira, K. (2002) U6 promoter-driven siRNAs with four uridine 3' overhangs efficiently suppress targeted gene expression in mammalian cells. *Nat. Biotechnol.* **20**, 497-500

Miyoshi, H. Probing the ubiquinone reduction site in bovine mitochondrial complex I using a series of synthetic ubiquinones and inhibitors. *J. Bioenerg. Biomem.* **33**, 223-231

Molina, J. A., de Bustos, F., Jimenez-Jimenez, F. J., Gomez-Escalonilla, C., Garcia-Redondo, A., Esteban, J., Guerrero-Sola, A., del Hoyo, P., Martinez-Salio, A., Ramirez-

Ramos, C., Indurain, G. R. and Arenas, J. (2000) Serum levels of coenzyme Q₁₀ in patients with amyotrophic lateral sclerosis. *J. Neural Transm.* **107**, 1021-1026

Molina, J. A., de Bustos, F., Ortiz, S., Del Ser, T., Seijo, M., Benito-Léon, J., Oliva, J. M. and Manzanares, J. (2002) Serum levels of coenzyme Q in patients with Lewy body disease. *J. Neural Transm.* **109**, 1195-1201

Mollace, V., Colasanti, M., Rodino, P., Massoud, R., Lauro, G.M., and Nistico, G. (1993) Cytokine induced nitric oxide generation by cultured astrocytoma celss involves a Ca²⁺-independent NO-synthase. *Biochem. Biophys. Res. Commun.* **191**, 327-334

Moncada, S., Palmer R.M.J. and Higgs, E.A. (1991) Nitric oxide: physiology pathophysiology and pharmacology. *Pharmacol. Rev.* **43**, 109-142

Moore, W. M., Webber, R. K., Jerome, G. M., Tjoeng, F. S., Misko, T. P. and Currie, M. G. (1994) L-N6-(l-iminoethyl)lysine: A selective inhibitor of inducible nitric oxide synthase. *J. Med. Chem.* **37**, 3886-3888

Mueller, D.M. (2000) Partial assembly of the yeast mitochondrial ATP synthase. *J. Bioenerg. Biomem.* **32**, 391-400

Mullis, K., Faloona, S., Scharf, S., Saiki, R., Horn, G. and Erlich, H. (1986) Specific enzymatic amplification of DNA in vitro: the polymerase chain reaction. *Cold Spring Harbor Symposia on Quantitative Biology*.

Mundy, W.R., Freudenrich, T.M., Crofton, K.M. and DeVito, M.J. (2004) Accumulation of PBDE-47 in primary cultures of rat neocortical cells. *Toxicol. Sci.* **82**, 164-169

Murphy, S., Simmons, M.L., Agullo, L., Garcia, A., Feinstein, D.L., Galea, E., Reis, D.J., Minc-Golomb, D., and Schwartz, J.P. (1993) Synthesis of nitric oxide in CNS glial cells. *Trends Neurosci.* **16**, 323-8.

Nagasawa, K., Muraki, Y., Matsuda, T., Ohnishi, N. and Yokoyama, T. (2000) Inhibitory effect of statins on fetal bovine serum-induced proliferation of rat cultured mesangial cells and correlation between their inhibitory effects and transport characteristics. *J. Pharm. Sci.* **89**, 1594-1604

Nazareth, W., Yafei, N. and Crompton, M. (1991) Inhibition of anoxia-induced injury in heart myocytes by cyclosporin A. *J. Mol. Cell. Cardiol.* **23**, 1351-1354

Nicchia, G.P., Frigeri, A., Liuzzi, G.M. and Svelto, M. (2003) Inhibition of AQP4 expression in astrocytes by RNAi determines alterations in cell morphology, growth and water transport and induces changes in ischemia-related genes. *FASEB J.* **17**, 1508-1510

Nohl, H. and Jordan, W. (1986) The mitochondrial site of superoxide formation. *Biochem. Biophys. Res. Commun.* **138**, 533–539

Ogashara, S., Nishikawa, Y., Yorifuji, S., Soga, F., Nakamura, Y., Takahashi, M., Hashimoto, S., Kono, N. and Tarui, S. (1986) Treatment of Kearns-Sayre syndrome with coenzyme Q₁₀. *Neurology* **36**, 45-53

Ogashara, S., Engel, A.G., Frens, D. and Mack, D. (1989) Muscle coenzyme Q deficiency in familial mitochondrial encephalomyopathy. *Proc. Natl. Acad. Sci. USA.* **86**, 2379-2382

Oury TD, Ho YS, Piantadosi CA, Crapo JD. (1992) Extracellular superoxide dismutase, nitric oxide, and central nervous system O₂ toxicity. *Proc. Natl. Acad. Sci. USA.* **89**, 9715-9719.

Ngo, H., Tschudi, K., Gull, K., and Ullu, E. (1998) Double-stranded RNA induces mRNA degradation in *Trypanosoma brucei*. *Proc. Natl. Acad. Sci.* **95**, 14687-14692

Ogashara, S., Engel, A. G., Frens, D. and Mack, D. (1989) Muscle coenzyme Q deficiency in familial mitochondrial encephalomyopathy. *Proc. Nat. Acad. Sci.* **86**, 2379-2382

Ogilvie, I., Aggeler, R. and Capaldi, R.A. (1997) Cross linking of the δ subunit to one of the three α subunits has no effect on functioning, as expected if δ is part of the stator that

links the F_1 and F_0 parts of the *Escherichia coli* ATP synthase. *J. Biol. Chem.* **26**, 16652-16656

Okamoto, T., Fukui, K., Nakamoto, M., Kishi, T., Okishio, T., Yamagami, T., Kanamori, N., Kishi, H. and Hiraoka E. (1985) High-performance liquid chromatography of coenzyme Q-related compounds and its application to biological materials. *J. Chromatogr.* **342**, 35-46

Olson R.E. and Rudney H. (1983) Biosynthesis of ubiquinone. *Vitam. Horm.* **40**, 1-43

Orth, M., Tabrizi, S.J., Schapira, A.H.V., Cooper, J.M. (2003) α -synuclein expression in HEK293 cells enhances the mitochondrial sensitivity to rotenone. *Neurosci. Lett.* **351**, 29-32

Ostrowski, R.P. (2000) Effect of coenzyme Q₁₀ on biochemical and morphological changes in experimental ischemia in the rat brain. *Brain Res. Bull.* **4**, 399-407

Paddison, P.J., Caudy, A.A., Bernstein, E., Hannon, G.J. and Conklin DS (2002) Short hairpin RNAs (shRNAs) induce sequence-specific silencing in mammalian cells. *Genes Dev.* **16**, 948-58.

Pahan, K., Sheikh, F. G., Namboodiri, A. M. S., and Singh, I. (1997) Lovastatin and phenylacetate inhibit the induction of nitric oxide synthase and cytokines in rat primary astrocytes, microglia and macrophages. *J. Clin. Invest.* **100**, 2971-2679

Palazzotti, B., Pani, G., Colavitti, R., De Leo, M.E., Bedogni, B., Borrello, S. and Galeotti, T. (1999) Increased growth capacity of cervical-carcinoma cells over-expression manganous superoxide dismutase. *Int. J. Cancer* **82**, 145-150

Papucci, L., Schiavone, N., Witort, E., Donnini, M., Lapucci, A., Tempestini, A., Formigli, L., Zecchi-Orlandini, S., Orlandini, G., Carella, G., Brancato, R. and Capaccioli, S. (2003) Coenzyme q10 prevents apoptosis by inhibiting mitochondrial depolarization independently of its free radical scavenging property. *J. Biol. Chem.* **278**, 28220-28228

Paul, C.P., Good, P.D., Winer, I., Engelke, D.R. (2002) Effective expression of small interfering RNA in human cells. *Nat. Biotechnol.* **20**, 505-508

Peters, T Jr. (1985) Serum albumin. *Adv. Prot. Chem.* **37**, 161-245

Poderoso, J.J., Carreras, M.C., Lisdero, C.L., Riobo, N.A., Schopfer, F., Boveris, A.D. (1996) Nitric oxide inhibits electron transfer and increases superoxide radical production in rat heart mitochondria and submitochondrial particles. *Arch. Biochem. Biophys.* **328**: 85-92

Poseroso, J. J., Carreras, M C., Schöpfer, F., Lisdero, C, L., Riobo, N. A., Guilivi, C., Boveris, A. D., Boveris, A., Cadenas, E. (1999) The reaction of nitric oxide with ubiquinol: kinetic properties and biological significance. *Fr. Rad. Biol. Med.* **26**, 925-935

Ponten, J. and MacIntyre E. H. (1968) Long term culture of normal and neoplastic human glia. *Acta Pathol. Microbiol. Scand.* **74**, 465-486

Prasanna, P., Thibault, A., Liu, L. and Samid, D. (1996) Lipid metabolism as a target for brain cancer therapy: synergistic activity of lovastatin and sodium phenylacetate against human glioma cells. *J. Neurochem.* **66**, 710-716

Quereshi, G.A., Baia, S.M. and Parvez, S. (1998) Neurotoxicity and possible roles of aspartic acid, glutamic acid and GABA in some neurological disorders. *Biogenic Amines* **13**, 565-578

Quesney-Huneus, V., Wiley, M.H. and Siperstein, M.D. (1979) Essential role for mevalonate synthesis in DNA replication. *Proc. Natl. Acad. Sci.* **76**, 5056-5060

Radi, R., Rodriguez, M., Castro, L. and Telleri, R. (1994) Inhibition of mitochondrial electron transport by peroxynitrite. *Arch. Biochem. Biophys.* **308**, 89-95

Raff, M.C., Miller, R.H. and Noble, M. (1983) A glial progenitor cell that develops in vitro into an astrocyte or an oligodendrocyte depending on culture medium. *Nature* **303**, 390-396

Rahman, S., Hargreaves, I., Clayton, P. and Heales, S. (2001) Neonatal presentation of coenzyme Q₁₀ deficiency. *J. Pediatr.* **139**, 456-458

Ragan, C.I., Wilson, M.T., Darley-USmar, V.M. and Lowe, P.N. (1987) Subfractionation of mitochondria and isolation of the proteins of oxidative phosphorylation, in "Mitochondria, a practical approach". (Darley-USmar, V.M., Rickwood, D., and Wilson, M.T. eds) pp 79-112 IRL Press, London

Ramasara, T. (1985) Coenzyme Q Biochemistry bioenergetics and clinical applications of ubiquinone. In: Lenaz, G pp68-81: Coenzyme Q-10, Wiley, New York

Ramsay, R.R., Youngster, S.K., Nicklas, W.J., McKeown, K.A., Jin, Y.Z., Heikkila, R.E. and Singer, P.T. (1989) Structural dependence of the inhibition of mitochondrial respiration and of NADH oxidase by 1-methyl-4-phenylpyridium (MPP⁺) analogs and their energized accumulation by mitochondria. *Proc. Natl. Acad. Sci.* **86**, 9168-9172

Rattan, R., Giri, S., Singh A.K., and Singh, I. (2003) Rho A negatively regulates cytokine-mediated inducible nitric oxide synthase expression in brain-derived transformed cell lines: negative regulation of IKK α *Free Radic. Biol. Med.* **9**, 1037-1050

Reynolds, A., Leake, D., Boese, Q., Scaringe, S., Marshall, W.S. and Khvorova, A. (2004) Rational siRNA design and RNA interference. *Nat. Biotech.* **22**, 326-330

Richter, O.-M.H. and Ludwig, B. (2003) Cytochrome *c* oxidase- structure, function, and physiology of a redox-driven molecular machine. *Rev. Physiol. Biochem. Pharmacol.* **147**, 47-74

Rice, M.E., Forman, R.E., Chen, B.T., Avshalimov, M.V., Cragg, S.J. and Drew, K.L. (2002) Brain antioxidant regulation in mammals and anoxia-tolerant reptiles: balanced for neuroprotection and neuromodulation. *Comp. Biochem. Physiol. C.* **133**, 515-525

Richmond, W. (1973) [Preparation and properties of a of a cholesterol oxidase from *Nocardia sp.* and its application to the enzymatic assay of total cholesterol *Clin. Chem.*, **19**, 1350-1356

Rigoulet, M., Aguilaniu, H., Averet, N., Bunoust, O., Camougrand, N., Grandier-Vazeille, X., Larsson, C., Pahlman, I.L., Manon, S. and Gustafsson, L. (2004) Organization and regulation of the cytosolic NADH metabolism in the yeast *Saccharomyces cerevisiae*. *Mol. Cell. Biochem.* **256-257**, 73-81.

Rodwell, V. W., Nordstrom, J. L. and Mitschelen, J. J. (1976) Regulation of HMG-CoA reductase. *Adv. Lipid Res.* **14**, 1-74

Roe, C.R. and Coates, P.M. (1995) Mitochondrial fatty acid oxidation disorders. In "The metabolic and molecular basis of inherited disease." (Scriver, C.R., Beaudet, A.L., Sly, W.S., Valle, D. eds) McGraw-Hill, New York

Rössler, O.G., Bauer, I., Chung, H-Y. and Thiel, G. (2004) Glutamate-induced cell death of immortalized murine hippocampal neurons: neuroprotective activity of heme oxygenase-1, heat shock protein 70 and sodium selenite. *Neurosci. Lett.* **362**, 253-257

Roth, R.H., Levy, R. and Giarman N.J. (1967) Dependence of rat serum lactonase upon calcium. *Biochem. Pharmacol.* **16**, 596-598

Rotig, A. Appelkvist, E. L., Geromel, V., Chretien, D., Kadhon, N., Edery, P., Leblond, M., Dallner, G., Munnich, A., Ernster, L. and Rustin P. (2000) Quinone-responsive multiple respiratory-chain dysfunction due to widespread coenzyme Q₁₀ deficiency. *Lancet*, **356**, 391-395

Sandor, M., Mehta, S., Harris, J., Thanos, C., Weston, P., Marshall, J. and Methiowitz, J. (2002). Transfection of HEK cells with DNA-loaded PLGA and P(FASA) nanospheres. *J. Drug Target.* **10**, 497-506

Sandu, J. K., Pandey, S., Ribocco-Lutkiewicz, M., Monette, R., Borowy-Borowski, H., Walker, P. R. and Sikorska, M. (2003) Molecular mechanisms of glutamate neurotoxicity of NT2-derived neurons and astrocytes: protective effects of Coenzyme Q₁₀. *J. Neurosci. Res.* **72**, 691-703

Santos-Ocaña, C., Do, T.Q., Padilla, S., Navas, P. and Clarke, C.F. (2002) Uptake of exogenous Coenzyme Q and transport to mitochondria is required for bc_1 complex stability in yeast *coq* mutants. *J. Biol. Chem.* **277**, 10973-10981

Schägger, H., and Pfiffer, K. (2001) The ratio of oxidative phosphorylation complexes I-V in bovine heart mitochondria and the composition of the respiratory chain supercomplexes. *J. Biol. Chem.* **276**, 37861-37867

Schapira, A.H.V., Cooper, J.M., Dexter, D., Clark, J. B., Jenner, P. and Marsden, C.D. (1990) Mitochondrial complex I deficiency in Parkinson's disease. *J. Neurochem.* **54**, 823-827

Scheffler, I.E. (1999). "Mitochondria". Wiley-Liss, New York

Schöpfer, F., Riobo, N., Carreras, M. C., Alvarez, B., Radi, R., Boveris, A., Cadenas, E., and Poderoso, J. J. (2000) Oxidation of ubiquinol by peroxynitrite: implications for protection of mitochondria against nitrosative damage. *Biochem. J.* **349**, 35-42

Seccia, M., Perugini, C., Albano, E. and Bellomo, G. (1996) Inhibition of Cu^{2+} -induced LDL oxidation by nitric oxide: a study using donors with different half-time of NO release. *Biochem. Biophys. Res.* **220**, 306-309

Selleri, C., Maciejewski, J.P., Montouri, N., Ricci., Visconte, V., Serio, B., Luciano, L. and Rotoli, B. (2003) Involvement of nitric oxide in farnesyl transferase inhibitor-mediated apoptosis in myeloid leukemia cells. *Blood* **102**, 1490-1498

Sharpe, M.A. and Cooper, C.E. (1998) Interaction of peroxynitrite with mitochondrial cytochrome oxidase. *J. Biol. Chem.* **273**, 30961-30972

Shepherd J.A., and Garland, P.B. (1969) The kinetic properties of citrate synthase from rat liver mitochondria. *Biochem J.* **114**, 597-610

Shergill, J.K., Cammack, R., Cooper, C.E., Cooper, J.M., Mann, V.M. and Schapira AH. (1996) Detection of nitrosyl complexes in human substantia nigra, in relation to Parkinson's disease. *Biochem. Biophys. Res. Commun.* **228**, 298-305

Shults, C. W., Haas, R. H., Passov, D. and Beal, M. F. (1997) Coenzyme Q₁₀ levels correlate with the activities of complexes I and I/III in mitochondria from parkinsonian and nonparkinsonian subjects. *Ann. Neurol.* **42**, 261-264

Shults, C. W., Oakes, D., Kieburtz, K., Beal, M. F., Haas, R., Plumb, S., Juncos, J. L., Nutt, J., Shoulson, I., Carter, J., Komoliti, K., Perlmutter, J. S., Reich, S., Watts, R. L., Kurlan, R., Molho, E., Harrison, M., Lew, M., and the Parkinson Study Group (2002) Effects of coenzyme Q₁₀ in early Parkinson disease. *Arch. Neurol.* **59**, 1541-1550

Simmons M.L and Murphy, S. (1992) Induction of nitric oxide synthase in glial cells. *J. Neurochem.* **59**, 897-905.

Simons M, Schwarzler F, Lutjohann D, von Bergmann K, Beyreuther K, Dichgans J, Wormstall H, Hartmann T, Schulz JB. (2002) Treatment with simvastatin in normocholesterolemic patients with Alzheimer's disease: A 26-week randomized, placebo-controlled, double-blind trial. *Ann. Neurol.* **52**, 346-350.

Skulachev, V.P. (1996) Why are mitochondria involved in apoptosis? Permeability transition pores and apoptosis as selective mechanisms to eliminate superoxide-producing mitochondria and cell. *FEBS Lett.* **397**, 7-10

Smith, M. A., Harris, P.L.R., Sayre, L.M., Beckman, J.S. and Perry G. (1997) Widespread peroxynitrite-mediated damage in Alzheimer's disease. *J. Neurosci. Res.* **17**, 2653-2657

Söderberg, M., Edlund, C., Alafuzoff, I., Kristensson, K., and Dallner, G. (1992) Lipid composition in different regions of the brain in Alzheimer's disease/ senile dementia of Alzheimer's type. *J. Neurochem.* **59**, 1646-1653

Soma MR, Pagliarini P, Butti G, Paoletti R, Paoletti P, Fumagalli R. (1992) Simvastatin, an inhibitor of cholesterol biosynthesis, shows a synergistic effect with N,N'-bis(2-chloroethyl)-N-nitrosourea and beta-interferon on human glioma cells. *Cancer Res.* **52**, 4348-4355

Soma MR, Baetta R, De Renzis MR, Mazzini G, Davegna C, Magrassi L, Butti G, Pezzotta S, Paoletti R, Fumagalli R. (1995) In vivo enhanced antitumor activity of carmustine [N,N'-bis(2-chloroethyl)-N-nitrosourea] by simvastatin. *Cancer Res.* **55**, 597-602.

Song, J-J., Smith, S.K., Hannon, G.J. and Josua-Tor, L. (2004) Crystal structure for Argonaut and its implications for RISC Slicer activity. *Science*, **305**, 1434-1437

Spänkuch-Schmitt, B., Bereiter-Hahn, J., Kaufmann, M. and Strebhardt, K. (2002) Effect of RNA silencing of Polio-like kinase-1 (PLK-1) on apoptosis and spindle formation in human cancer cells. *J. Natl. Cancer Inst.* **94**, 1863-1877

Srinivasula SM, Ahmad M, Fernandes-Alnemri T, Alnemri ES. (1998) Autoactivation of procaspase-9 by Apaf-1-mediated oligomerization. *Mol. Cell.* **1**, 949-57.

Srivastava, A.K. and Schlessinger, D. (1991) Structure and organisation of ribosomal RNA. *Biochimie*, **73**, 631-638

Stadler, J., Billiar, T.R., Curran, R.D., Stuehr, D.J., Ochoa, J.B. and Simmons RL. (1991) Effect of exogenous and endogenous nitric oxide on mitochondrial respiration of rat hepatocytes. *Am. J. Physiol.* **260**, C910-6.

Stanislaus, R., Singh, A.K. and Singh, I. (2001) Lovastatin treatment decreases mononuclear cell infiltration into the CNS of Lewis rats with experimental allergic encephalomyelitis. *J. Neurosci. Res.* **66**, 155-162

Stark, G.R., Kerr, I.M., Williams, B.R., Silverman, R.H. and Schreiber, R.D (1998). How cells respond to interferons. *Annu. Rev. Biochem.* **67**, 227-264

Stenmark, P., Grünler, Mattsson, J., Sindelar, P.J., Nordlund, P. and Berthold, D.A. (2001) A new member of the family of di-iron carboxylate proteins. *J. Biol. Chem.* **276**, 33297-33300

Stewart, V.C., Giovannoni, G., Land, J. M., McDonald, W. I., Clark, J.B. and Heales, S.J.R. (1997) Pretreatment of astrocytes interferon- α/β impairs interferon- γ induction of nitric oxide synthase. *J. Neurochem.* **68**, 2547-2551

Stewart, V. C., Land, J. M., Clark, J. B. and Heales, S. J. R. (1998) Comparison of mitochondrial respiratory chain enzyme activities in rodent astrocytes and neurones and a human astrocytoma cell line. *Neurosci. Lett.* **247**, 201-203

Stewart, V.C., Land, J.M., Clark, J.B. and Heales S.J.R. (1998b) Pretreatment of astrocytes with interferon α/β prevents neuronal respiratory chain damage. *J. Neurochem.* **70**, 432-434

Stewart, V.C., Sharpe, M.A., Clark, J.B. and Heales, S.J.R. (2000) Astrocyte-derived nitric oxide causes both reversible and irreversible damage to the neuronal mitochondrial respiratory chain. *J. Neurochem.* **75**, 694-700

Stewart, V. C., Stone, R., Gegg, M. E., Sharpe, M. A., Hurst, R. D., Clark, J. B., and Heales, S. J. R. (2002a) Preservation of extracellular glutathione by an astrocyte derived factor with properties comparable to extracellular superoxide dismutase. *J. Neurochem.* **83**, 984-991

Stewart, V.C. and Heales, S.J.R. (2003) Nitric oxide-induced mitochondrial dysfunction: implications for neurodegeneration. *Free Radic. Biol. Med.* **34**, 287-303

Stone, R. (2001) PhD Thesis University of London

Sui, G., Soohoo, C., Affar, E.B., Gay, F., Shi, Y., Forrester, W.C. and Shi, Y. (2002) A DNA vector-based RNAi technology to suppress gene expression in mammalian cells. *Proc. Natl. Acad. Sci. USA* **99**, 5515-5520

Szabo, I and Zarotti, M. (1991) The giant channel of the inner membrane is inhibited by cyclosporin A. *J. Biol. Chem.* **266**, 3376-3379

Szelenyi, Z. (1998) Neuroglia: possible role in thermogenesis and body temperature control. *Med. Hypotheses* **50**, 191-197

Szkopinska, A. (2000) Ubiquinone. Biosynthesis of quinone ring and its isoprenoid side chain. Intracellular localisation. *Acta Biochimica Polonica* **47**, 469-480

Tabernero, A., Bolaños, J. P. and Medina, J. M. (1993) Lipogenesis from lactate in rat neurons and astrocytes in primary culture. *Biochem. J.* **294**, 635-638

Takada, M., Ikenoya, S., Yuzuriha, T., and Katayama, K. (1982) Studies of reduced and oxidised coenzyme Q (ubiquinones). II. The determination of oxidation-reduction levels of coenzyme Q in mitochondria, microsomes and plasma by high-performance liquid chromatography. *Biochim. Biophys. Acta.* **679**, 308-314

Tang, B.K. and Kalow, W. (1995) Variable activation of lovastatin by hydrolytic enzymes in human plasma and liver. *Eur. J. Clin. Pharmacol.* **47**, 449-451

Tang, P, Miles, M., Miles, L., Quinlan, J., Wong, B., Wenisch, A. and Bove, K. (2004) Measurement of reduced and oxidised coenzyme Q₉ and coenzyme Q₁₀ levels in mouse tissues by HPLC with coulometric detection. *Clinica Chimica Acta.* **341**, 173-184

Tatoyan, A. and Giulivi, C. (1998) Purification and characterization of a nitric-oxide synthase from rat liver mitochondria. *J. Biol. Chem.* **273**, 11044-11048

Tatusova, T.A. and Madden, T.L. (1999) BLAST 2 SEQUENCES, a new tool for comparing protein and nucleotide sequences. *FEMS Microbiology Lett.* **174**, 247-250

Tay, Y.M.S., Lim, K.S., Sheu, F-S., Jenner, A., Whiteman, A., Wong, K.P. and Halliwell, B. (2004) Do mitochondria make nitric oxide? No? *Free Rad. Res.* **38**, 591-599

Teeter, M.E., Baginsky, M.L. and Hatefi, Y. (1969) Ectopic inhibition of the complexes of the electron transport system by rotenone, piercidin A, demerol and antimycin, A. *Biochim. Biophys. Acta.* **172**, 331-333

Teiber, J.F., Draganov, D.I., La Du, B.N. (2003) Lactonase and lactonizing activities of human serum paraoxonase (PON1) and rabbit PON3. *Biochem. Pharmacol.* **66**, 887-896

Thelin, A., Schedin, S., and Dallner, G. (1992) Half life of ubiquinone-9 in rat tissues. *FEBS Lett.* **313**, 118-120

Tormo, J.R. and Estornell, E. (2000) New evidence of the multiplicity of ubiquinone- and inhibitor- binding sites in the mitochondrial complex I. *Arch. Biochem. Biophys.* **381**, 241-246

Treichel, J.L., Henry, M.M., Skumatz, C.M.B., Eells, J.T. and Burke, J.M. (2004) Antioxidants and ocular cell type differences in cytoprotection from formic acid toxicity in vitro. *Toxicol. Sci.* **82**, 183-192

Tsuji, A., Saheki, A., Tamai, I. and Terasaki T (1993) Transport mechanism of 3-hydroxy-3-methylglutaryl coenzyme A reductase inhibitors at the blood-brain barrier. *J. Pharmacol Exp Ther.* **267**, 1085-1090

Tsujita Y, Kuroda M, Tanzawa K, Kitano N, Endo A. (1979) Hypolipidemic effects in dogs of ML-236B, a competitive inhibitor of 3-hydroxy-3-methylglutaryl coenzyme A reductase. *Atherosclerosis* **32**, 307-13.

Tsukihara, T., Aoyama, H., Yamashita, E., Tomizaki, T., Yamaguchi, H., Shinzawa-Itoh, K. Hakashima, R., Yaono, R. and Yoshikawa, S. (1996) The whole structure of the 13-subunit oxidised cytochrome *c* oxidase at 2.8 Å *Science*, **272**, 1136-1144

Tsukihara, T. (1998) Redox coupled crystal structural changes in bovine heart cytochrome *c* oxidase. *Science*, **280**, 1723-1729

Turrens, J.F. (2003) Mitochondrial formation of reactive oxygen species. *J. Physiol.* **552**, 335-344

Turrens, J.F. and Boveris, A. (1980) Generation of superoxide anion by the NADH dehydrogenase of bovine heart mitochondria. *Biochem. J.* **191**, 421-427

Turrens JF, Freeman BA, Levitt JG, Crapo JD. (1982) The effect of hyperoxia on superoxide production by lung submitochondrial particles. *Arch. Biochem. Biophys.* **217**, 401-410

Turunen, M. Appelkvist, E.L., Sindelar, P. and Dallner, G. (1999) Blood concentration of coenzyme Q₁₀ increases in rat when esterified forms are administered. *J. Nutr.* **129**, 2113-2118

Turunen, M., Swiezewska, E., Chojnacki, P. and Dallner, G (2002) Regulatory aspects of CoQ metabolism *Free Rad. Res.* **36**, 437-443

Turnunen, M., Olssen, J. and Dallner, G. (2004) Metabolism and function of Coenzyme Q. *Biochim. Biophys. Acta.* **1660**, 171-199

Tuschl, T. (2002) Expanding small RNA interference. *Nat. Biotechnol.* **20**, 446-448

Vajo Z, King LM, Jonassen T, Wilkin DJ, Ho N, Munnich A, Clarke CF, Francomano CA. (1999) Conservation of the *Caenorhabditis elegans* timing gene *clk-1* from yeast to human: a gene required for ubiquinone biosynthesis with potential implications for aging. *Mamm. Genome* **10**, 1000-1004

Van Hellemond, J.J., van der Klei, A., van Weelden, W.H., Tielens, A.G.M. (2003) Biochemical and evolutionary aspects of anaerobically functioning mitochondria. *Phil. Trans. R. Soc. Lond.* **358**, 205-215

Van Maldergem, L., Trijbels, F., DiMauro, S., Sindelar, P. J., Musumeci, O., Janssen, A., Delberghe, X., Martin, J-J., and Gillerot, Y. (2002) Coenzyme Q-responsive Leigh's encephalomyopathy in two sisters. *Ann. Neurol.* **52**, 750-754

Vasquez, O.L., Almeida, A. and Bloaños J.P. (2001) Depletion of glutathione up-regulates mitochondrial complex I expression in glial cells. *J. Neurochem.* **76**, 1593-1596

Vassault, A. (1983) L-lactate dehydrogenase. UV method with pyruvate and NADH, in *Methods in Enzymic Analysis, Vol. 3* (Bergmeyer, J. and Grassl, M., eds) pp 118-126. Verlag Chemie GmbH, Weinheim

Vaughan C.J. and Delanty, N. (1999) Neuroprotective properties of statins in cerebral ischemia and stroke. *Stroke* **30**, 1969-1973

Vicario, C., Tabernero, A. and Medina, J.M. (1993) Regulation of lactate metabolism by albumin in rat neurons and astrocytes from primary culture. *Pediatr. Res.* **34**, 709-715

Vigne, P., Damais, C. and Frelin, C. (1993) IL-1 and TNF- α induce cGMP formation in C6 astrocytoma cells via the nitridergic pathway. *Brain Res.* **606**, 332-334

Villalba, J.M., Navarro, F., Cordoba, F., Serrano, A., Arroyo, A., Crane, F.L. and Navas, P. (1995) Coenzyme Q reductase from liver plasma membrane: purification and role in trans-plasma-membrane electron transport. *Proc Natl Acad Sci USA.* **92**, 4887-4891

Wallace, D. C. (1999) Mitochondrial diseases in man and mouse. *Science* **283**, 1482-1488

Walter, L., Nogueira, V., Leverage, X., Heitz, M.P., Bernardi, P. and Fontaine E (2000) Three classes of ubiquinone analogs regulate the mitochondrial permeability transition pore through a common site. *J. Biol. Chem.* **275**, 29521-29527.

Wanders, R.J.A., Vrekenn, P., Den Boer, M.E.J., Wijburg, F.A., Van Gennip, A.H. and Ijlist, L. (1999) Disorders of mitochondrial fatty acid CoA β -oxidation. *J. Inher. Metab. Dis.* **22**, 442-487

Warburg, O. (1930) *Über den stoffwechsel der tumoren* [The metabolism of tumours]. Constable and Co. London

Warburg, O. (1956) On the origin of cancer cells. *Science*, **123**, 309-314

Wargelius, A., Ellingsen, S. and Fjose, A. (1999) Double-stranded RNA induces specific developmental defects in zebrafish embryos. *Biochem. Biophys. Res. Commun.* **263**, 156-161

Waterhouse, P.M., Graham, M.W. and Wang, M.B. (1998) Virus resistance and gene-silencing in plants can be induced by simultaneous expression of sense and antisense RNA. *Proc. Natl. Acad. Sci.* **95**, 13959-13964

Wharton, D.C. and Tzagoloff, A. (1967) Cytochrome oxidase from beef heart mitochondria. *Meth. Enzymol.* **10**, 245-250

Wianny, F. and Zernicka-Goetz, M. (2000) Specific interference with gene function by double-stranded RNA in early mouse development. *Nat. Cell Biol.* **21**, 70-75

Wilkens, S. and Capaldi, R.A. (1998) ATP synthase's second stalk comes into focus. *Nature*, **393**, 29

Wikström, M.K. (1977) Proton pump coupled to cytochrome c in mitochondria. *Nature* **266**, 271-273

Williams, S.E., Wootton, P., Mason, H.S., Iles, D.E. Peers, C. and Kemp, P. J. (2004) siRNA knock-down of γ -glutamyl transpeptidase does not affect hypoxic K⁺ channel inhibition. *Biochem. Biophys. Res. Comm.* **314**, 63-68

Willis, R. A., Folkers, K., Tucker, J. L., Ye, C-Q., Xia, L-J., and Tamagawa H. (1990) Lovastatin decreases coenzyme Q levels in rats. *Proc. Natl. Acad. Sci. USA* **87**, 8928-8930

Witt, H., Wittershagen, A., Bill, E., Kolbesen, B.O. and Ludwig, B. (1997) Asp-193 and Glu 218 of subunit II are involved in the Mn^{2+} binding of *Paracoccus denitrificans* cytochrome c oxidase. *FEBS Lett.* **409**, 128-130

Wolf, D. E., Hoffman, C. H., Trenner, N. R., Arison, B. H., Shunk, C.H., Linn, B.O., McPherson, J.F. and Folkers, K. (1958) Coenzyme Q. Structure studies on the coenzyme Q group. *J. Am. Chem. Soc.* **80**, 4752

Wolozin, B., Kellman, W., Ruosseau, P., Celesia, G.G. and Siegel, G. (2000) Decreased prevalence of Alzheimer disease associated with 3-hydroxy-3-methylglutaryl coenzyme A reductase inhibitors. *Arch. Neurol.* **57**, 1439-1443.

Wong, W. W-L., Tan, M.M., Xia, Z. Dimitroulakos, J., Minden, M.D. and Penn, L.Z. (2001) Cerivastatin triggers tumor-specific apoptosis with higher efficacy than lovastatin. *Clin. Cancer Res.* **7**, 2067-2075

Xia, D., Yu, C-A., Kim, H., Xia J-Z, Kachurin, A.M *et al.*, (1997) Chrystal structure of the cytochrome bc_1 complex from bovine heart mitochondria. *Science* **277**, 60-66

Xie, J., Wang, Y., Lipton, H., Cai, B., Nelson, S., Kolls, J., Summer, W.R. and Greenberg, S.S. (1993) Tumor necrosis factor inhibits stimulated but not basal release of nitric oxide. *Am. Rev. Respir. Dis.* **148**, 627-636

Yamamoto, T., Shimizu, S., Sugawara, H., Momose, K. and Rudney, H. (1989) Identification of regulatory sites in the biosynthesis of ubiquinone in the perfused rat heart. *Arch. Biochim. Biophys.* **269**, 86-92

Yamamoto, T., Maruyama, W., Kato, Y., Yi, H., Shamoto-Nagai, M., Tanaka, M., Sato, Y. and Naoi M. (2002) Selective nitration of mitochondrial complex I by peroxynitrite: involvement in mitochondria dysfunction and cell death of dopaminergic SH-SY5Y cells. *J. Neural. Transm.* **109**, 1-13.

Yamauchi, S., Linscheer, W. and Beach, D. (1991) Increase in serum and bile cholesterol and HMG CoQ reductase by lovastatin in rats. *Am. J. Physiol.* **260**, G625-G630

Yankovskaya, V., Horsefield, R., Törnrother, S., Luna-Chavez, C., Miyoshi, H., Léger, C., Byrne, B., Cecchini, G. and Iwata, S. (2003) Architecture of succinate dehydrogenase and reactive oxygen species generation. *Science*, **299**, 700-704

Yoshikawa, S., Shinzawa-Itoh, K., Nakashima, R., Yaono, R., Yamashita, E., Inoue, N., Yao, M., Fei, M.J., Peters-Liebeu, C., Mizushima, T., Yamaguchi, H., Tomizaki, T. and

Tsukihara, T. (1998) Redox coupled crystal structure changes in bovine heart cytochrome *c* oxidase *Science*, **280**, 1723-1729

Zhang, Z., Huang, L-S., Schulmeister, V.M., Kim, K-K., *et al.*, (1998) Electron transfer by domain movement in cytochrome *bc*₁. *Nature* **392**, 677-684

Zhang Y, Marcillat O, Giulivi C, Ernster L, Davies KJ. (1990) The oxidative inactivation of mitochondrial electron transport chain components and ATPase. *J. Biol. Chem.* **265**, 16330-16336.

Zoratti, M. and Szabo, I. (1995) The mitochondrial permeability transition. *Biochim. Biophys. Acta.* **1241**, 139-176

APPENDIX I
AN INVESTIGATION INTO A POSSIBLE CASE OF UBIQUINONE
DEFICIENCY

APPENDIX I: AN INVESTIGATION INTO A POSSIBLE CASE OF HUMAN UBIQUINONE DEFICIENCY

A.1 Introduction

As described in the main introduction, human ubiquinone deficiency can give rise to mitochondrial encephelomyopathies. Usually these occur as a result of an inborn error of metabolism. The Neurometabolic Unit of the National Hospital for Neurology and Neurosurgery, Queen Square, London, UK routinely assesses the mitochondrial function of patients suspected to be suffering from mitochondrial encephelomyopathies.

A muscle biopsy was received from a patient for analysis of mitochondrial function. The boy was the second child of unrelated parents of Norwegian origin. He presented at 4 months with severe hypotonia, feeding difficulties, and had developed apnoeic spells. After an initial muscle biopsy was taken at 6 months, the patient was given carnitine, riboflavin and oral CoQ₁₀, until his death at 10 months, possibly due to pneumonia complicating his primary condition. Permission was obtained for a post-mortem muscle biopsy.

Prior to death, the patient underwent various clinical metabolic investigations, and on several occasions displayed increased lactate in blood and CSF. While both muscle samples appeared to be histologically normal, analysis of the initial biopsy revealed complex I+III activity was decreased, and complex II+III activity was almost abolished. The post-mortem sample however, showed that (possibly due to CoQ₁₀ supplementation)

these enzyme activities had increased. Consequently, in order to clarify this, CoQ₁₀ levels in both biopsies were determined.

A.2 Methods

The biopsy was homogenised on ice using a pre-chilled teflon: glass hand held homogeniser. Tissue was homogenised to 10% (w/v) in ice-cold muscle isolation buffer (320 mM sucrose; 10 mM Tris; 1 mM EDTA dipotassium salt; pH 7.4). CoQ₁₀ content of these homogenates was determined by HPLC, as described in Chapter 3. DiethoxyCoQ₁₀ was employed as an internal standard. CoQ₁₀ in the pre-supplementation and the post-mortem muscle samples was determined, and the findings expressed against a protein baseline as shown in table A.1.

	Pre-CoQ ₁₀ supplementation	Post-CoQ ₁₀ supplementation	Reference Range*
CoQ ₁₀ levels (pmol/mg protein)	414	300	140 - 580

Table A.1. Patient muscle ubiquinone concentration and the paediatric reference range (* from Rahman et al., 2001)

A.3 Results

From these data, there was no evidence of a CoQ₁₀ deficiency, with levels in both the pre- and post-mortem samples falling clearly inside the paediatric reference range (from Rahman *et al.*, 2001). It can also be seen that oral supplementation did not increase CoQ₁₀ concentration in muscle homogenate.

A.4 Conclusions

The fact that in this case CoQ₁₀ appeared to *decrease*, following supplementation would suggest that CoQ was not taken up to any part of the cellular fraction, possibly due to lipid membrane saturation. This may support the proposal outlined by Turunen *et al.*, (1999) that appropriate tissue uptake of dietary CoQ probably only occurs in deficient states.

However evidence for this is equivocal and it remains a topic of debate within the literature (Matthews *et al.*, 1998; Dallner & Sindelar, 2000; Beal & Mathews, 1997; Kwong *et al.*, 2002). As yet, it is also unresolved how mitochondrial levels are affected by oral ubiquinone therapy, if at all.

Thus it is unclear as to why in this case the activities of complex I+III and complex II+III linked assays appear to be sub-normal. The possibility exists that impairment of the membrane-bound complexes may be responsible for the clinical symptoms. If the activity of complex III were found to be diminished, this may explain the observed inhibition of the I+III and II+III assays. However, as ubiquinone levels in this patient were normal, the

increased activities of the complex I+III and complex II+III assays following CoQ supplementation introduce the possibility of a more subtle complex III mutation. A K_m mutant of the ubiquinol : cytochrome *c* reductase complex may have a reduced affinity for ubiquinol (i.e. an increased K_m). Although the post-mortem sample would suggest that CoQ₁₀ status did not increase in skeletal muscle homogenate, as the amount of ubiquinone in the mitochondrial inner membrane has not been determined, the possibility of this patient expressing a K_m mutant complex III cannot be excluded. Alternatively it is also possible increased ETC enzyme activity may have occurred as a result of an antioxidant effect of CoQ₁₀ administration.

APPENDIX II

PUBLICATIONS

PUBLICATIONS

Full Papers:

Hargreaves, I.P., **Duncan, A.J.**, Heales, S.J.R. and Land, J.M. The effect of HMG-CoA reductase inhibitors on coenzyme Q₁₀ availability: possible biochemical/ clinical implications. *Drug Safety (in press)*

Duncan, A.J. and Heales, S.J.R. Nitric Oxide and Neurological Disorders. (2005) *Mol. Aspects Med.* **26**, 67-96

Heales, S.J.R., Lam, A.A.J., **Duncan, A.J.** and Land, J.M. (2004). Neurodegeneration or neuroprotection: the pivotal role of astrocytes. *Neurochem. Res.* **29**, 513-519.

Abstracts:

Duncan, A.J., Hargreaves, I.P., Clark, J.B. and Heales, S.J.R. (2002) Ubiquinone status in nitric oxide generating astrocytes. Handbook of the 3rd Conference of the International Coenzyme Q₁₀ Association.

Duncan, A.J., Hargreaves, I.P., Clark, J.B. and Heales, S.J.R. (2003) Nitric oxide increases ubiquinone synthesis in the rat C6 glioma cell line *J. Neurochem.* **87**, (s1), 155

Duncan, A.J., Clark, J.B. and Heales, S.J.R. (2004) Ubiquinone status of astrocytes and neurons. *Fr. Rad. Biol. Med.* **36**, Supp. 1, S103